Silicon-delivering cellularized biomaterials for dental repair

Daline Mbitta Akoa

Sorbonne Université

Ecole doctorale 397 – Physique et Chimie des Matériaux

Laboratoire de Chimie de la Matière Condensée de Paris

Laboratoire UR 2496 Pathologies, Imagerie et Biothérapie Orofaciales

Silicon-delivering cellularized biomaterials for dental repair

Par Daline Mbitta Akoa

Thèse de doctorat de Physique et Chimie des Matériaux

Présentée et soutenue publiquement le 04 Juillet 2024

Devant un jury composé de :

Catherine CHAUSSAIN	Professeure des universités – praticien hospitalier	Présidente du jury
Jean Christophe FARGES	Professeur des universités – praticien hospitalier	Rapporteur
Halima KERDJOUJ	Professeure des universités	Rapportrice
Jean-Marie NEDELEC	Professeur	Examinateur
Thibaud CORADIN	Directeur de recherche CNRS	Directeur de thèse
Anne POLIARD	Professeure émérite	Co-encadrante de thèse

Acknowledgments

Completing this PhD thesis has been a challenging but immensely rewarding journey, and it would not have been possible without the support, guidance, and encouragement of many people. I would like to take this opportunity to express my sincere gratitude to everyone who has contributed to this work and supported me throughout my doctoral studies.

First and foremost, I would like to extend my deepest appreciation to my supervisor, Thibaud Coradin. Your unwavering support, insightful guidance, and continuous encouragement have been invaluable throughout this process. Your expertise, patience, and constructive feedback have significantly shaped this research, and I am profoundly grateful for the opportunities you have provided me.

I am also immensely thankful to Anne Poliard, for graciously accepting to collaborate with us in this project. Your involvement has greatly enriched this work and I am immensely thankful for your valuable contributions.

I would like to acknowledge the invaluable support of the members of my thesis committee: Jean Christophe Farges, Halima Kerdjoudj, Jean-Marie Nedelec, Catherine Chaussain, Anne Poliard and Thibaud Coradin. Your feedback and suggestions in the reviewing of this research will be instrumental in refining and improving this work. I am grateful for your time, efforts, and insightful discussions that will surely enrich this manuscript.

Special thanks to Sorbonne University for providing the resources, facilities, and an intellectually stimulating environment that made this research possible. I am grateful to the administrative staff and librarians for their assistance and support throughout my journey there.

I want to thank: a) our lab directors – Christian Bonhomme and François Ribot – for their dedication to the normal lab running and the safe and comfortable working environment; b) administrative staff in LCMCP: Corinne Pozzo Di Borgo, Hélène Gervais, Diana Lesieur, Nora Abdoul-Aribi for their help that makes my stay at the laboratory easy to go. c) Simon Dadoun for his help to solve the computer-related problem. d)All the LCMCP lab members.

It was a pleasure for me to conduct this research within the MATBIO team of the LCMCP. I particularly valued the teamwork spirit within the group, and the interest of each member in

advancing everyone's projects, regardless of their direct involvement in them. Furthermore, the positive atmosphere and camaraderie within the group helped me feel comfortable and enabled me to maintain a balanced personal and research life. Without your willingness to share your experiences, insights, and time, this work would not have been possible. Your contributions are deeply appreciated. A special thanks to Christophe Helary for his involvement in the biological characterisations in this work.

I would like to express my gratitude to the BRIO laboratory. A special thanks to Catherine Chaussain for granting the opportunity to collaborate on this project with your laboratory. I also thank Anne, Coralie, Asma, Ludovic for the trainings in the biological field and good suggestions about this thesis projects.

I am also immensely grateful to my office members and colleagues who have become close friends over the years. Thank you for the countless hours spent discussing ideas, troubleshooting problems, and supporting each other through the highs and lows of this journey. Your collaboration and companionship have made this experience all the more enriching and enjoyable.

On a personal note, I would like to express my deepest gratitude to my family and friends. To my parents, thank you for your unconditional love, support, and for instilling in me the value of education and perseverance. Your belief in me has been a constant source of strength. To my siblings, thank you for your encouragement, the joy you bring into my life, and for always being there for me. To my friends, thank you for being present in my life, your support, and friendship.

A special thank you to my husband. Your love, patience, and unwavering support have been my anchor throughout this journey. Thank you for your understanding, for the countless sacrifices you have made, and for always believing in me even when I doubted myself.

Finally, I would like to acknowledge the countless individuals whose names may not appear here but who have, in one way or another, contributed to this thesis and my academic journey. Your support, encouragement, and kindness have been greatly appreciated.

This thesis is dedicated to all of you. Thank you for being a part of this journey and for making it possible.

Daline

Table of contents

General introduction

The study of biomaterials for dental repair has attracted considerable attention in recent years, particularly in the context of the increasing regenerative capacity of stem cells from the dental pulp.[1,2] This growing interest focuses largely on the repair of dentin, the bulk of the tooth, that surrounds the dental pulp. Damage to dentin caused by external factors such as deep caries, trauma, attritions, etc. can lead to dental hypersensitivity, dentinal sclerosis and even high risk of infection. In extreme cases, these events can lead to the exposure of the pulp, thus compromising its structural integrity.

Various methods have been developed to address dental pulp injuries/wounds, including direct pulp capping, which involves placing a biologically active material directly on the exposed pulp.[3,4] This material triggers a pulp response that promotes the formation of a reparative dentin bridge, thereby preserving the vitality of the dental pulp, essential for the long-term survival of the tooth.[5] Pulp capping materials incorporating silicon have proved to be more effective in inducing such a pulp response than their silicon-free equivalents.[6,7] In this respect, silicon, recognized as an essential trace element for bone tissue regeneration[8–10], holds great promise for modulating the fate of stem cells from the dental pulp due to its osteogenic and angiogenic properties. However, the specific effects of silicon on pulp cells behavior remain relatively unexplored in the scientific literature.

Dentin is composed of an apatite-like mineral phase and an organic phase rich in collagen.[11] Its formation is initiated by pulp stem cells, which differentiate and synthesize an extracellular matrix (ECM) rich in type I collagen that subsequently mineralizes.[12] Mimicking this collagenous ECM is therefore a foundational approach for studying the mineralization processes of dentin and even bone. Existing research indicates that collagen gels prepared by plastic compression can achieve a collagen fibrillar density comparable to that of the native dentin ECM and can be seeded with cells prior to gelation to produce cellularized gels.[13–15] However, the variability of protocols found in the literature - such as differences in the concentrations of acetic acid solutions used to solubilize collagen, the concentrations of sodium hydroxide used to adjust acidic collagen solutions, and the sufficient number of cells to induce mineralization - necessitated to develop an adapted formulation suitable for the pulp stem cells used in this study.[14,16–18] In our **first study**, we optimized the formulation of collagen hydrogels to create 3D dense gels, and analyzed their physical and mechanical properties. Then, these gels were seeded with pulp stem cells derived from deciduous and adult teeth to assess their response

to the gel microenvironment. Ultimately, human dental pulp stem cells (hDPSCs) were chosen for further investigations.

In the next steps, this research project attempts to fill the gaps existing in the understanding of the impact of silicon on hDPSCs. Literature provides sufficient evidence that silicon in its bioavailable form, silicic acid ($Si(OH)_4$), has a beneficial effect on bone[8,19,20], which shares similar characteristics to dentin.[21] These beneficial effects are even more pronounced in osteoporotic patients, where an increase in bone volume has been observed following varying durations of oral ingestion and doses of $Si(OH)_4$.[22,23] The direct effect of silicon on bone cells has also been demonstrated *in vitro*, showing improved osteoblastic differentiation and mineralization in the presence of $Si(OH)_4$.[24–26] However, the reported effective doses in the literature vary depending on the cells, and there is no consensus on the effective dose of $Si(OH)_4$ to promote beneficial effect. In our **second study**, we assessed the impact of soluble silicon on hDPSCs within 3D dense collagen gels optimized in the first study. To achieve this, we evaluated the viability, cell differentiation, and mineralization in the presence of physiological (10 µM, similar to blood levels[27]) and supraphysiological (100 µM) concentrations of silicic acid.

Most dental pulp capping materials contain silica particles (SiO_2) often coupled with calcium oxides (CaO). [28–30] Understanding the role of silicon in these products also involves studying the effects of silica-based nanoparticles (NPs), as found in commercial products. Here, we set out to compare two forms of NPs: pure silica (SiO_2) and bioglasses (SiO_2-CaO). Similar to silicic acid, these nanomaterials have shown beneficial effects in bone tissue mineralization. By integrating them into the collagen matrix, our goal was to elucidate their impact on the fate and function of dental pulp stem cells, which constituted **our third and final study**. For this purpose, characterization tests of the synthesized NPs were conducted, and when incorporated into collagen matrices, we studied the cell viability and resulting mineralization *in vitro*.

This interdisciplinary project stems from the collaboration between two partners: (1) laboratory of condensed matter chemistry in Paris, specializing in material chemistry and characterization, and its MATBIO team, recognized for its expertise in collagen extraction coupled with collagen material preparation, and (2) the BRIO laboratory, focused on biology, pathologies, and malformations of the oro-cranio-facial sphere and mineralized tissues in particular. The latter has developed expertise in extracting stem cells from dental pulp and histological characterization of tissues in recent years.

The combination of this set of skills has enabled the development of a methodological and rigorous approach that provides insights into the role of silicon in the formation of dental tissues, particularly dentin, thus expanding the scope of knowledge in the field of dental tissue regeneration/reparation.

This project focus on two main goals: (1) the optimization of the formulation of collagen gels and (2) the understanding of the complex interaction between silicon (soluble form and nanoparticles) and dental pulp stem cells in a collagenous hydrogel, designed to mimic the dentin native ECM.

This thesis manuscript comprises four chapters:

- Chapter 1: Literature review on dentin structure, composition, and formation, as well as the role of silica-based materials in dentin repair, and the existing knowledge on the relationship between silicon and bone,
- Chapter 2: Study of the impact of fibrillogenesis conditions and cell density on the mineralization of plastically-compressed collagen hydrogels by human dental pulp stem cells (**first study**),
- Chapter 3: Effects of soluble silicon on the mineralization of plastically-compressed collagen hydrogels by human dental pulp stem cells (**second study**),
- Chapter 4: Effects of silicon-releasing nanoparticles on the mineralization of plastically-compressed collagen hydrogels by human dental pulp stem cells (**third study**).

References

(1) Shah, P.; Aghazadeh, M.; Rajasingh, S.; Dixon, D.; Jain, V.; Rajasingh, J. Stem Cells in Regenerative Dentistry: Current Understanding and Future Directions. *Journal of Oral Biosciences* **2024**, S1349007924000197. https://doi.org/10.1016/j.job.2024.02.006.

(2) Morsczeck, C.; Reichert, T. E. Dental Stem Cells in Tooth Regeneration and Repair in the Future. *Expert Opinion on Biological Therapy* **2018**, *18* (2), 187–196. https://doi.org/10.1080/14712598.2018.1402004.

(3) Zhang, W.; Yelick, P. C. Vital Pulp Therapy—Current Progress of Dental Pulp Regeneration and Revascularization. *International Journal of Dentistry* **2010**, *2010*, 1–9. https://doi.org/10.1155/2010/856087.

(4) Cohenca, N.; Paranjpe, A.; Berg, J. Vital Pulp Therapy. *Dental Clinics of North America* **2013**, *57* (1), 59–73. https://doi.org/10.1016/j.cden.2012.09.004.

(5) Nie, E.; Yu, J.; Jiang, R.; Liu, X.; Li, X.; Islam, R.; Alam, M. K. Effectiveness of Direct Pulp Capping Bioactive Materials in Dentin Regeneration: A Systematic Review. *Materials* **2021**, *14* (22), 6811. https://doi.org/10.3390/ma14226811.

(6) Li, Z.; Cao, L.; Fan, M.; Xu, Q. Direct Pulp Capping with Calcium Hydroxide or Mineral Trioxide Aggregate: A Meta-Analysis. *Journal of Endodontics* **2015**, *41* (9), 1412–1417. https://doi.org/10.1016/j.joen.2015.04.012.

(7) Cushley, S.; Duncan, H. F.; Lappin, M. J.; Chua, P.; Elamin, A. D.; Clarke, M.; El-Karim, I. A. Efficacy of Direct Pulp Capping for Management of Cariously Exposed Pulps in Permanent Teeth: A Systematic Review and Meta-analysis. *Int Endodontic J* **2021**, *54* (4), 556–571. https://doi.org/10.1111/iej.13449.

(8) Jugdaohsingh, R. Silicon and Bone Health. *J Nutr Health Aging* **2007**, *11* (2), 99–110.

(9) Rodella, L. F.; Bonazza, V.; Labanca, M.; Lonati, C.; Rezzani, R. A Review of the Effects of Dietary Silicon Intake on Bone Homeostasis and Regeneration. *The Journal of nutrition, health and aging* **2014**, *18* (9), 820–826. https://doi.org/10.1007/s12603-014-0555-8.

(10) Rondanelli, M.; Faliva, M. A.; Peroni, G.; Gasparri, C.; Perna, S.; Riva, A.; Petrangolini, G.; Tartara, A. Silicon: A Neglected Micronutrient Essential for Bone Health. *Exp Biol Med (Maywood)* **2021**, *246* (13), 1500–1511. https://doi.org/10.1177/1535370221997072.

(11) Goldberg, M. Dentin Structure Composition and Mineralization. *Front Biosci* **2011**, *E3* (2), 711–735. https://doi.org/10.2741/e281.

(12) Linde, A.; Goldberg, M. Dentinogenesis. *Critical Reviews in Oral Biology & Medicine* **1993**, *4* (5), 679–728. https://doi.org/10.1177/10454411930040050301.

(13) Brown, R. A.; Wiseman, M.; Chuo, C. -B.; Cheema, U.; Nazhat, S. N. Ultrarapid Engineering of Biomimetic Materials and Tissues: Fabrication of Nano- and Microstructures by Plastic Compression. *Adv Funct Materials* **2005**, *15* (11), 1762–1770. https://doi.org/10.1002/adfm.200500042.

(14) Coyac, B. R.; Chicatun, F.; Hoac, B.; Nelea, V.; Chaussain, C.; Nazhat, S. N.; McKee, M. D. Mineralization of Dense Collagen Hydrogel Scaffolds by Human Pulp Cells. *J Dent Res* **2013**, *92* (7), 648–654. https://doi.org/10.1177/0022034513488599.

(15) Cheema, U.; Brown, R. A. Rapid Fabrication of Living Tissue Models by Collagen Plastic Compression: Understanding Three-Dimensional Cell Matrix Repair *In Vitro*. *Advances in Wound Care* **2013**, *2* (4), 176–184. https://doi.org/10.1089/wound.2012.0392.

(16) Chamieh, F.; Collignon, A.-M.; Coyac, B. R.; Lesieur, J.; Ribes, S.; Sadoine, J.; Llorens, A.; Nicoletti, A.; Letourneur, D.; Colombier, M.-L.; Nazhat, S. N.; Bouchard, P.; Chaussain, C.; Rochefort, G. Y. Accelerated Craniofacial Bone Regeneration through Dense Collagen Gel Scaffolds Seeded with Dental Pulp Stem Cells. *Sci Rep* **2016**, *6* (1), 38814. https://doi.org/10.1038/srep38814.

(17) Ajalloueian, F.; Nikogeorgos, N.; Ajalloueian, A.; Fossum, M.; Lee, S.; Chronakis, I. S. Compressed Collagen Constructs with Optimized Mechanical Properties and Cell Interactions for Tissue Engineering Applications. *International Journal of Biological Macromolecules* **2018**, *108*, 158–166. https://doi.org/10.1016/j.ijbiomac.2017.11.117.

(18) Marelli, B.; Ghezzi, C. E.; Barralet, J. E.; Nazhat, S. N. Collagen Gel Fibrillar Density Dictates the Extent of Mineralization in Vitro. *Soft Matter* **2011**, *7* (21), 9898. https://doi.org/10.1039/c1sm06027a.

(19) Jugdaohsingh, R.; Anderson, S. H.; Tucker, K. L.; Elliott, H.; Kiel, D. P.; Thompson, R. P.; Powell, J. J. Dietary Silicon Intake and Absorption. *The American Journal of Clinical Nutrition* **2002**, *75* (5), 887–893. https://doi.org/10.1093/ajcn/75.5.887.

(20) Martin, K. R. Silicon: The Health Benefits of a Metalloid. In *Interrelations between Essential Metal Ions and Human Diseases*; Sigel, A., Sigel, H., Sigel, R. K. O., Eds.; Metal Ions in Life Sciences; Springer Netherlands: Dordrecht, 2013; Vol. 13, pp 451–473. https://doi.org/10.1007/978-94-007-7500-8_14.

(21) MacDougall, M. J.; Javed, A. Dentin and Bone: Similar Collagenous Mineralized Tissues. In *Bone and Development*; Bronner, F., Farach-Carson, M. C., Roach, H. I. (Trudy), Eds.;

Springer London: London, 2010; pp 183–200. https://doi.org/10.1007/978-1-84882-822-3_11.

(22) Schröder, H. C.; Wiens, M.; Wang, X.; Schloßmacher, U.; Müller, W. E. G. Biosilica-Based Strategies for Treatment of Osteoporosis and Other Bone Diseases. In *Molecular Biomineralization*; Müller, W. E. G., Ed.; Progress in Molecular and Subcellular Biology; Springer Berlin Heidelberg: Berlin, Heidelberg, 2011; Vol. 52, pp 283–312. https://doi.org/10.1007/978-3-642-21230-7_10.

(23) Spector, T. D.; Calomme, M. R.; Anderson, S. H.; Clement, G.; Bevan, L.; Demeester, N.; Swaminathan, R.; Jugdaohsingh, R.; Berghe, D. A. V.; Powell, J. J. Choline-Stabilized Orthosilicic Acid Supplementation as an Adjunct to Calcium/Vitamin D3 Stimulates Markers of Bone Formation in Osteopenic Females: A Randomized, Placebo-Controlled Trial. *BMC Musculoskelet Disord* **2008**, *9* (1), 85. https://doi.org/10.1186/1471-2474-9-85.

(24) Reffitt, D. M.; Ogston, N.; Jugdaohsingh, R.; Cheung, H. F. J.; Evans, B. A. J.; Thompson, R. P. H.; Powell, J. J.; Hampson, G. N. Orthosilicic Acid Stimulates Collagen Type 1 Synthesis and Osteoblastic Differentiation in Human Osteoblast-like Cells in Vitro. *Bone* **2003**, *32* (2), 127–135. https://doi.org/10.1016/S8756-3282(02)00950-X.

(25) Kim, E.-J.; Bu, S.-Y.; Sung, M.-K.; Choi, M.-K. Effects of Silicon on Osteoblast Activity and Bone Mineralization of MC3T3-E1 Cells. *Biol Trace Elem Res* **2013**, *152* (1), 105–112. https://doi.org/10.1007/s12011-012-9593-4.

(26) Han, P.; Wu, C.; Xiao, Y. The Effect of Silicate Ions on Proliferation, Osteogenic Differentiation and Cell Signalling Pathways (WNT and SHH) of Bone Marrow Stromal Cells. *Biomater. Sci.* **2013**, *1* (4), 379–392. https://doi.org/10.1039/C2BM00108J.

(27) Bissé, E.; Epting, T.; Beil, A.; Lindinger, G.; Lang, H.; Wieland, H. Reference Values for Serum Silicon in Adults. *Analytical Biochemistry* **2005**, *337* (1), 130–135. https://doi.org/10.1016/j.ab.2004.10.034.

(28) Parirokh, M.; Torabinejad, M. Mineral Trioxide Aggregate: A Comprehensive Literature Review—Part I: Chemical, Physical, and Antibacterial Properties. *Journal of Endodontics* **2010**, *36* (1), 16–27. https://doi.org/10.1016/j.joen.2009.09.006.

(29) Komabayashi, T.; Zhu, Q.; Eberhart, R.; Imai, Y. Current Status of Direct Pulp-Capping Materials for Permanent Teeth. *Dental Materials Journal* **2016**, *35* (1), 1–12. https://doi.org/10.4012/dmj.2015-013.

(30) Lührs, A.-K.; Geurtsen, W. The Application of Silicon and Silicates in Dentistry: A Review. In *Biosilica in Evolution, Morphogenesis, and Nanobiotechnology*; Müller, W.

E. G., Grachev, M. A., Eds.; Progress in Molecular and Subcellular Biology; Springer Berlin Heidelberg: Berlin, Heidelberg, 2009; Vol. 47, pp 359–380. https://doi.org/10.1007/978-3-540-88552-8_16.

Chapter I

Context and state of the art

I.1. Dentin-pulp complex histophysiology

Tooth is formed of three mineralized tissues, enamel, dentin and cementum, surrounding a non-mineralized soft tissue, the dental pulp:[1] Dentin, the bulk of the tooth, protects the pulp, which itself ensures the "vitality" of the dental organ.[2] The interdependent development of dentin and pulp, their anatomical proximity, and their closely coupled/integrated function throughout the life of the tooth, account for the concept of the dentin-pulp complex.[2–5]

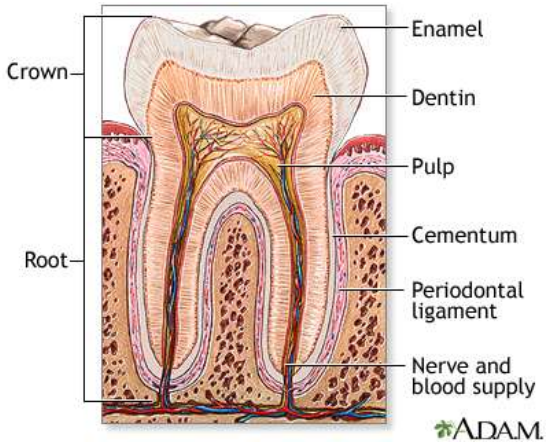

Figure I.1: Structures of the tooth [6]

I.1.1. Dentin

I.1.1.1. Extracellular matrix composition

Dentin is a complex, heterogenous, porous, and avascular biocomposite material with unique elastic properties (compressive elasticity modulus 18-24 GPa), providing essential support to the tooth.[4,7] Physically and chemically, dentin bears as strong resemblance to bone. It is made up of 70 w-% (50 vol-%) inorganic matter and 20 w-% (30% vol-%) organic matrix, the remaining fraction being water. [2,5,8–10]

The inorganic (mineral) phase consists of nanometer-sized plate crystals of a carbonate-substituted hydroxyapatite ($Ca_{10}(PO_4)_{6-x}(OH)_{2-y})(CO_3)_{x+y}$, where $0 \leq x \leq 6$, $0 \leq y \leq 2$).[5] The organic component is about 90% collagen (mainly type I), and 10% non-collagenous proteins (NCPs) including different proteoglycans, growth factors, enzymes, and phospholipids.[8,9]

Table I.1: Cells and extracellular matrix (ECM) components in dentin and pulp[1,10,11]

	Dentin	**Pulp**
Cells	Only odontoblats (cytoplasmic processes)	Fibroblasts (pulpoplasts), Dental pulp stem/progenitor cells, vascular cells, pericytes, neural cells, histiocytes, macrophages, dendritic cells, lymphocytes, mast cells
Collagens (90%)	Type I (98%) (+Type III, V)	Type I (56%) Type III (41%) associated with fibronectin (+Types V, VI) Fibrillin-containing microfibrils
Form		Thin fibrils – 100nm periodicity
Non-collagenous proteins (10%)		
Phosphorylated matrix proteins: the SIBLINGs family (Small Integrin-Binding Ligand N-linked Glycoproteins)	Dentin sialophosphoprotein (DSPP) cleaved into Dentin sialoprotein (DSP) and Dentin phosphoprotein (DPP) Dentin matrix protein-1 (DMP-1) Bone sialoprotein (BSP) /integrin-binding sialoprotein (IBSP) Osteopontin (OPN) Matrix extracellular phosphoglycoprotein (MEPE)	DSPP > DSP, DPP DMP-1 BSP OPN MEPE
Others		Nestin
Non phosphorylated matrix proteins	*Vitamin K-dependent glycoproteins* : Osteocalcin (OCN), Matrix GLA protein MGP	OCN
	Secretory calcium-binding phosphoprotein (SCPP) family: Osteonectin (secreted protein, acidic and rich in cysteine-SPARC)	Osteonectin
		Tenascin Fibronectin
Proteoglycans and glycoamino-glycans	Sulfated GAGs: *small leucine-rich proteoglycans (SLRP) family*:	
	Class I: Chondrotin sulfate/ dermatan sulfate (CS/DS) PGs - Decorin, biglycan	Class I: CS/DS PGs - Decorin, biglycan
	Class II: Keratan sulfate (KS) PGs- lumican, fibromodulin, osteoadherin	Class II: KSPGs - lumican, fibromodulin, osteoadherin Class III: CS/DS/KS PGs - epiphycan and mimecan: osteoglycin
	Large aggregating PGs:	Versican
	Non sulfated GAGs: -/-	Hyaluronic acid
Also expressed in ameloblats	Amelogenin 5-7kDa	

Growth factors	Transforming growth factor-beta (TGF-β) Bone morphogenetic Protein-2 (BMP-2) Fibroblast growth factor (FGF-2) Insulin-like growth factor (ILGF-I and -II) Vascular endothelial growth factor (VEGF) Platelet-dervied growth factor (PDGF)	TGF-β1 BMP-2 FGF-2 Tumor necrosis factor α (TNF- α) Hepatocyte growth factor (HGF) Lymphocyte enhancer-binding factor 1 (LEF1)
Matrix proteinases	*Enzymes:* Alkaline phosphatase (ALP) Acid phosphatases Serine proteases *Metalloproteinases (MMPs)* Collagenases: MMP-1, -8, -13 Gelatinases A: MMP-2, B: MMP-9 Stromelysin 1: MMP-3 Membrane-type MMPs: MT1-MMP Enamelysine: MMP-20 ADAMs and ADAMTS Thrombospondin1 *Collagenase inhibitors:* Tissue Inhibitors of MMPs (TIMP-1 to -3)	 ALP (nonspecific ALP, TNAP) Acid phosphatases Collagenases: MMP-1, -8, -13 Disintegrin and MMP-28 (ADAM28) Cysteine cathepsin Dipeptidyl peptidase II PMN elastase TIMPs
Serum proteins	αHS_2-glycoprotein, albumin, lipoproteins	Fibronectin of serum origin
Phospholipids	Membrane and extracellular-mineral-associated phospholipids	Membrane and ECM phospholipids

I.1.1.2. Structure of dentin

Structurally, dentin consists of three layers: the outer mantle dentin, adjacent to enamel; the inner circumpulpal dentin, predominantly composed of inter- and peri-tubular dentin, forming the bulk of the tooth; and predentin at the pulp interface.

Mantle dentin is a 5 to 30 µm thick layer, with an organic matrix apparently devoid of phosphoproteins and less regular in the structure than the rest of the dentin.[2,8,12,13] It also lacks large dentinal tubules; instead, there are multiple thin ramifications of tubules in their matrix. Unlike the rest of dentin, mantle organic matrix contains collagen fibrils type III (von Korff fibers) with a minor portion of type I.[14] Mineralized globular structures, around 2 µm in diameter, isolated or in groups, are present within the mantle dentin network.[2]

Dentin tubules and (inter- and peri-) tubular dentin. From the dentino-enamel junction (DEJ) cementum at the root to the predentin at the junction with the pulp chamber, dentin is traversed by canals or tubules (dentinal tubules) (**Figure I.2 A**) housing odontoblastic processes

for all or part of their course, and fluid, making it highly permeable.[4,10,15–17] Tubular number density is approximatively 18 000 to 28 000 dentinal tubules per mm.[2] [18,19] They are more numerous and larger in the inner layer of dentin than in the outer layer.[18] Each tubule is lined with a 0.5 to 1 µm cuff thick hypermineralized peritubular dentin (**Figure I.2 B**).[7,17] Several studies have concluded that peritubular dentin mostly contains apatite crystals with little organic matrix (no collagen).[17,20,21] The tubules are embedded and separated from each other in a mineralized type I collagen matrix (intertubular dentin), which constitutes the major part of dentin. Most of the collagen fibers in the intertubular dentin are arranged randomly in a plane perpendicular to the dentinal tubules and interweave in a mesh/lattice (**Figure I.2 B**).[5] The number of odontoblasts corresponds to the number of dentinal tubules.[5] Amounts of inter- and peritubular dentin vary considerably within the tooth. Whereas the volume of peritubular dentin volume increases from the DEJ towards the pulp, intertubular dentin volume decreases.[4] Nonetheless, peritubular dentin represents only a small proportion of the total dentin in human teeth, which contains mainly intertubular dentin.[3] These changes within the tooth may explain the differences in hardness observed in dentine, since peritubular dentine is much harder than intertubular dentine.[5] Dentin is harder in its center than near the pulp and at its periphery.

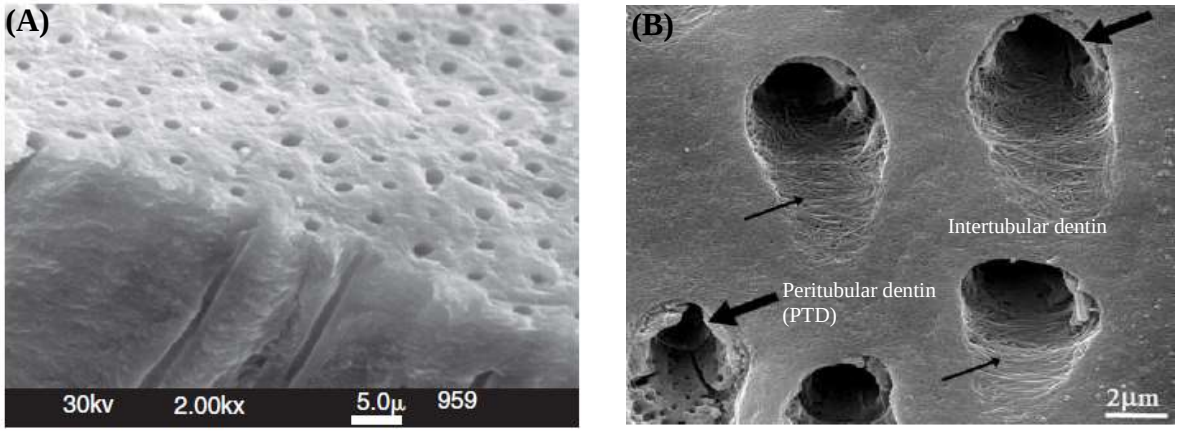

Figure I.2: SEM images of dentin. (A) Longitudinal view showing dentinal tubules [7]. (B) Cross section of dentin. Non fibrillar, spongy and porous peritubular (or intratubular) dentin around each tubule (large arrows). The internal surfaces (intertubular dentin) exposed by the fragmentation of the PTD are clearly collagen fibrils (thin arrows).[17]

Predentin and mineralization front [2,5,9,22]

Predentin is a 10-30 µm unmineralized layer secreted by odontoblasts and located at the dentin pulp interface between odontoblast cell bodies and mineralized dentin. It consists principally of type I collagen, which acts as a scaffold for mineralization. Whereas predentin gradually mineralizes into intertubular dentin at the mineralization front under the control of non-collagenous proteins (glycoproteins, proteoglycans, and enzymes), its thickness remains constant, as the calcified amount is balanced by the secretion of a new, unmineralized matrix. Peritubular dentin is absent from the predentin and starts at a certain distance from the mineralization front. The mineralization front is irregular and displays globular mineralized protuberances known as calcospherites. This protein-rich layer is present during dentinogenesis and throughout the lifetime of the tooth.

I.1.1.3. Cells : odontoblasts and odontoblastic processes [1,2,11,23]

Odontoblasts are highly specialized, polarised cells derived from the neural crest. They are post-mitotic cells (i.e. lost the ability to divide) and their primary function is to secrete dentin during dentinogenesis. Functional odontoblasts are made up of two distinct parts: a cell body and its extension, the odontoblastic process. The cell bodies are in the pulp, outside the mineralized tissue whereas the odontoblastic processes pass through the predentin and rest inside the dentinal tubules. The process consists of one main trunk with numerous lateral branches along its length. These lateral branches lie inside the canaliculi and interconnect the tubules, enabling cell-cell and cell-matrix communication. The process begins at the collar of the cells, i.e. just above the apical junctional complex where the cell gradually begins to narrow as it enters predentin. This transition between the cell body and the process is also marked by cytological changes. The cytoskeleton of the processes lacks major organelles but is full of microtubules and filaments (actin, vimentin, tubulin, nestin) arranged in a linear pattern along their length. Secretory granules, coated vesicles and pits can also be seen in the processes, suggestive of pinocytotic activity along the cell membrane. Synthesis of the predentin/dentin components occurs in the cell bodies, whereas only secretion and reabsorption occur at the processes.

I.1.2. Pulp

The pulp tissue is a loose connective tissue that occupies the central part of the tooth, known as the pulp cavity. This cavity is divided into a coronal part, termed the pulp chamber, and a

radicular part, termed the root canal. The pulp extends longitudinally along the pulp cavity from the pulp chamber to the termination of the root canal at the apical foramen, where it connects/communicates with the periodontal ligament. Nerves, blood vessels, and lymphatic vessels enter and exit the tooth through the apical foramen. Additional connections between the pulp and the periodontal tissues may also be present via the lateral canals along the lateral surface of the root. These communications between the pulpal portion of the tooth and the periodontium tissue provide nutrition for the pulp but may also be routes for the extension of disease from one tissue to another. Like other connective tissues, the dental pulp consists of three main components: pulp cells, collagens fibers, and ground substance rich in proteoglycans and glycoproteins with large amounts of water.[5,22] **(Table I.1)**

I.1.2.1. Pulp ECM composition [1,5,11,24,25]

The pulp has a soft, gelatinous consistency, reflecting a high-water content (75% in weight and 80% in volume) and the remainder being organic matter. Healthy pulp does not contain any mineral components. Both fibers and ground substance make up the ECM. The ground substance contains mainly chondroitin sulfates, hyaluronates and proteoglycans, and interstitial fluid. These proteoglycans contribute to high tissue pressure of the pulp and help in cell migration (hyaluronan) and cell adhesion (syndecan). Although also found in dentin, there are differences in the distribution of proteins in the two tissues. Fibronectin, for example, is more prevalent in the pulp (both pulp and serum origins) and has been visualised in abundance between the lateral aspects of the odontoblastic cell bodies, around the blood vessels and in the core of the pulp.[26] When it comes to collagenous proteins, type I collagen and type III are prominent in the pulp, in contrast to the predominantly type I in dentin. The presence of type V, VI and fibrillin have also been reported.

I.1.2.2. Cellular composition of the pulp

An outer layer of odontoblasts lines the pulp cavity, followed by a cell-free layer and then a cell-rich zone comprising fibroblasts, progenitors (stem cells), as well as vascular, neuronal and immune system cells [1]. (**Figure I.3)**

Odontoblast cell bodies [1,11,24,25,27]

The odontoblastic layer, subjacent to predentin, consists of odontoblastic cell bodies grouped in four to five rows lining the peripheral wall of the pulp. Odontoblast cell bodies are columnar

(in the crown) and around 50 μm high, with large nuclei lying on the basement membrane. Immediately near to the nucleus basically, are well-developed rough endoplasmic reticulum (RER), mitochondria, and Golgi apparatus. The RER contributes to the ECM synthesis, and the golgi apparatus and multivesicular bodies (at the central part) to the terminal steps of ECM synthesis and in the control of degradation after the re-internalization of molecules cleaved by metalloproteases (MMPs). In the distal cell body, the RER is abruptly interrupted, and small mitochondria are present at the junction between the cell body and the process. Many cells display cilia that may play a role in the response of odontoblasts to external stimuli.[28] The morphology of odontoblasts reflects their functional activity and ranges from an active synthetic phase (elongated, basal nucleus, dispersed chromatin, basophilic cytoplasm, prominent golgi zone) to a quiescent phase (stubby, apical and hematoxophilic nucleus, condensed chromatin, little cytoplasm). The odontoblast cell bodies are linked distally near the predentin by junctional complexes. As previously mentioned, the odontoblast layer acts as a protective barrier, restricting the passage of materials along the extracellular pathway. This is due the nature of junctions, mostly desmosomes and gap junctions, and a few occluding (tight) junctions.

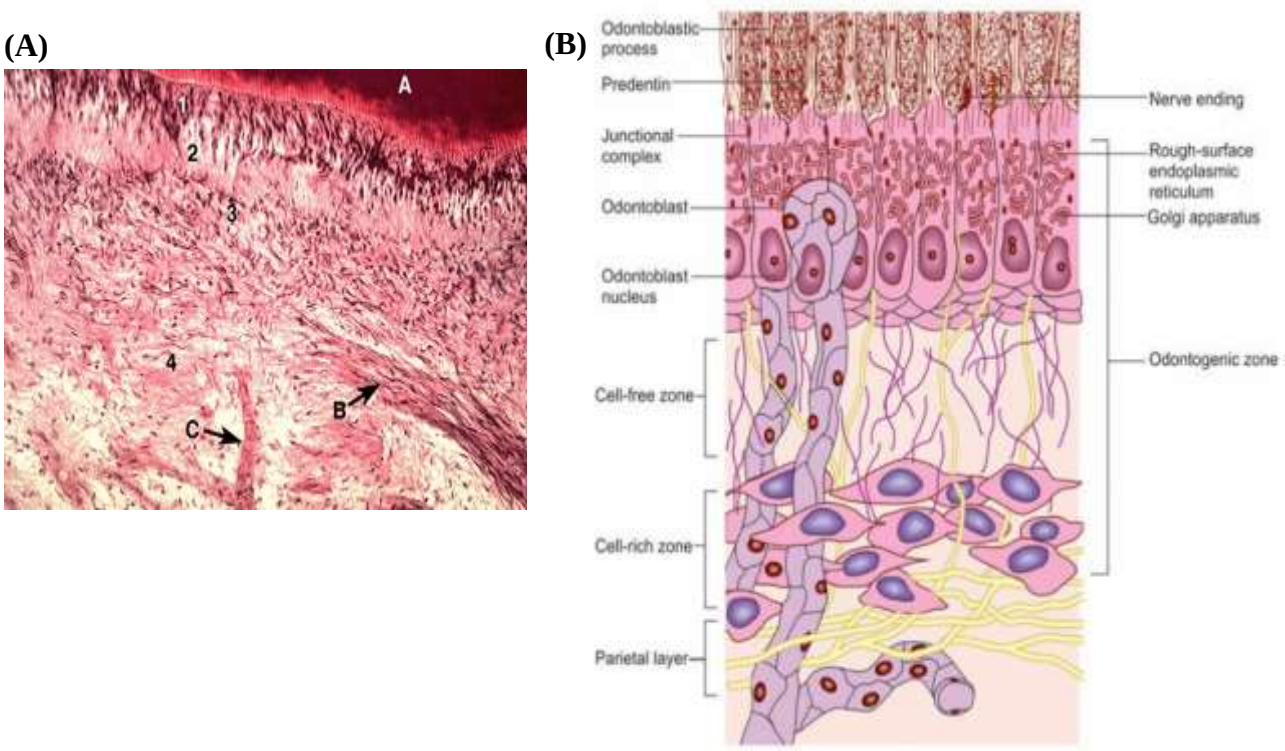

Figure I.3: Zones of the pulp. (A) Histological cross-section of the pulp. 1-odontoblast zone, 2-cell-free zone, 3-cell-rich zone, 4-pulp core, A-dentin, B-nerve, C-blood vessel.[29] (B) Diagram of odontogenic zone illustrating odontoblast, cell-free, and cell-rich zones, with blood vessels and nonmyelinated nerves among odontoblasts.[27]

Dental stem cells derived from the dental pulp are undifferentiated mesenchymal stem cells (MSCs) resident in the dental pulp. They are normally in close contact with blood vessels, and isolated populations of progenitor cells include dental pulp stem cells (DPSC) within permanent tooth pulp[30] and, when isolated from the pulp of temporary tooth, human exfoliated deciduous teeth stem cells (SHED).[31] They display a fibroblast-like morphology, plastic adherence, and express MSC and embryonic cell markers such as Oct4, Nanog, Sox-2 and SSEA, without expressing hematopoietic surface markers (CD14, CD45, CD34).[30,32–36] Like other MSCs, they can self-renew and differentiate into several lineages, including odontogenic, osteogenic, adipogenic, muscular and neuronal cells when given the proper signals.[37–39] In addition, they have the advantage of being highly proliferative. However, it is important to note that, similar to other MSCs, dental progenitor cells are an heterogeneous population of cells featuring major differences in the expression of MSC-associated markers, proliferation rates, and differentiation potential.[40–44] Thus, depending on their characteristics - multipotent or unipotent, with a high or low proliferation capacity - their contribution to cell-based therapies and regenerative approaches is likely to be quite different. [45,46] Stem cells sourced from dental pulp offer a simpler harvesting process compared to those from bone marrow, traditionally recognized

as the primary postnatal MSC source. This accessibility highlights dental pulp as a valuable reservoir of stem cells, holding significant scientific interest for various clinical applications.[47]

I.2. Dentin formation and mineralization process

I.2.1. Dentin formation – dentinogenesis

I.2.1.1. Initial dentin formation

Dentin formation involves a complex interplay between the differentiation of odontoblasts and the biomineralization process. Odontoblasts, specialized cells located at the periphery of the pulp tissue, differentiate from dental papilla mesenchymal cells and migrate towards the dentin-pulp interface during tooth development.[48] As odontoblasts mature, they begin to synthesize and secrete extracellular matrix components, primarily type I collagen, which form the organic matrix of dentin. This process occurs in two main stages: (i) the secretion of predentin, a non-mineralized matrix precursor, followed by (ii) the deposition of hydroxyapatite crystals onto the predentin matrix, leading to mineralization and the formation of mature dentin [2,10,11] (**Figure I.4**). Unlike other mineralized tissues like bone, cementum or mantle dentin where matrix vesicles (MVs) play a crucial role in mineral nucleation, odontoblasts do not release MVs for the biomineralization of circumpulpal predentin.[49] Rather, they secrete phosphorylated proteins, lipids, and other factors necessary for appositional calcification at the mineralization front. It is worth noting that MVs have been implicated in the mineralization of reparative dentin under injury.[50,51]

Pattern of mineralization. Histologically, there are two patterns of dentin mineralization - globular and linear calcification. Globular (or calcospheric) calcification involves crystal deposition in distinct areas of the matrix, forming globular masses that eventually merge into a single calcified mass. This pattern is prominent in mantle dentin, where MVs initiate mineralization foci that grow radially and fuse. In circumpulpal dentin, mineralization can occur in either globular or linear patterns. The size of the globules is related to the rate of dentin deposition, with faster deposition resulting in larger globules. Slower deposition leads to a more uniform mineralization front, characterized as linear. Despite some crystal growth as dentin matures, the final crystal size remains small, about 3 nm thick and 100 nm long. Apatite crystals in dentin resemble those in bone and cementum but are 300 times smaller than those found in enamel.[5,27]

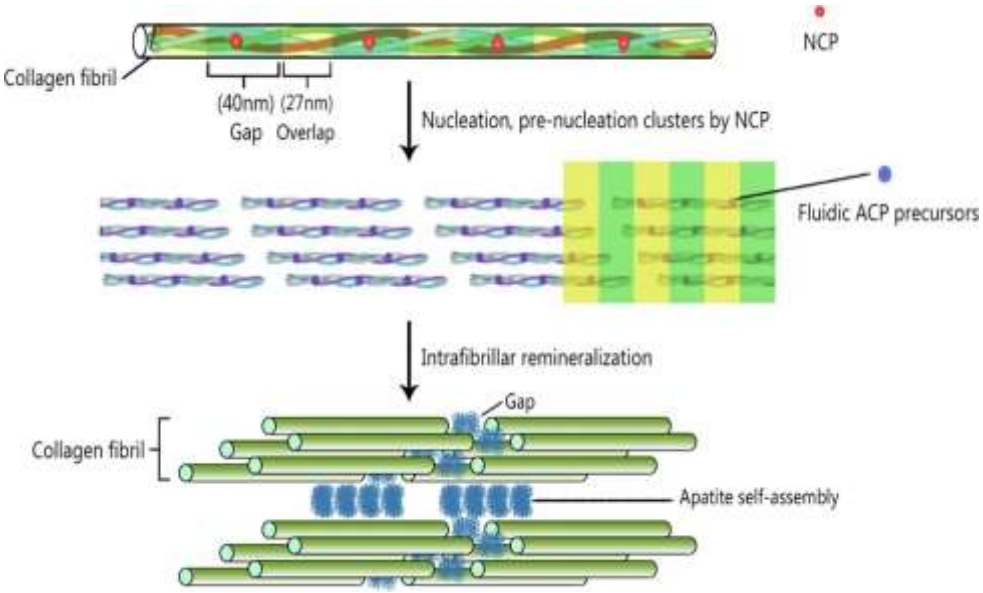

Figure I.4: Biomineralization process: nucleation and growth of hydroxyapatite crystals within the collagen fibrils of the extracellular matrix. ACP=Amorphous calcium phosphate.[52]

I.2.1.2. Functions of dentin matrix proteins in the mineralization process

Dentin non-collagenous proteins (NCPs) mainly consist of phosphorylated proteins of the SIBLING (i.e. small integrin-binding ligand N-linked glycoproteins) family, including dentin sialoprotein (DSP), dentin phosphoprotein (DPP), bone sialoprotein (BSP), dentine matrix protein-1 (DMP-1), osteopontin (OPN), and matrix extracellular phosphoglycoprotein (MEPE). Their coding genes are located on human chromosome 4 and their Arg-Gly-Asp (RGD) motif functions in signalling and acts as a nucleation factor for the mineralization process by regulating the formation of hydroxyapatite (HAP) crystals.[53–59]

DMP1 is expressed in differentiating odontoblasts and can influence the fate of stem cells, directing them towards dentin-producing cells. [60,61] It can bind to calcium ions and initiate HAP nucleation.[53] DSPP (i.e. dentin sialophosphoprotein) is processed into DPP, DSP and DGP.[5] DPP is the most expressed NCP in dentin matrix.[58,62] It is highly anionic and have a high affinity for calcium, transports it to the mineralization front and controls the growth of apatite crystals.[63–65] It also possesses a signal transduction function and can initiate mesenchymal stem cell lineage-specific dental differentiation.[66–68] DSP acts as a ligand in an RGD-independent manner and is involved in intracellular signalling via interaction with integrin β6. Moreover,

the DSP domain regulates DSPP expression and odontoblast homeostasis via a positive feedback loop.[69] A study showed that DSP has limited effects on *in vitro* apatite formation and growth.[70] Recent studies showed that BSP is not highly expressed in odontoblast or dentin in developing teeth, while it is highly expressed in osteoblast and cementoblast at early stage of differentiation.[71,72] Instead, BSP is strongly expressed during reparative dentinogenesis.[71,73] OPN can bind calcium ions, cause HAP nucleation and promote matrix mineralization by controlling the shape and size of HAP crystals.[74–78] Some data indicate that this molecule has an inhibitory effect on HAP formation and growth.[79,80] MEPE expression is expressed in odontoblast during tooth formation [81] and has also been reported to have inhibitory effects on mineralization.[82–84] Thus, SIBLING molecules probably interact to balance mineralization promotion and inhibition.

Other ECM molecules found in dentin, such as osteocalcin (OC) and small leucine-rich proteoglycans (SLRP) like decorin and biglycan, play an important role in the regulation of mineralization.[85] OC is the most NCP in bone [86] but has also been detected in smaller amounts in the cell bodies and processes of odontoblasts, reaching the dentino-enamel junction where it is believed to influence the maturation of adjacent enamel.[87,88] SLRPs present in predentin are widely considered essential in collagen fibril formation and arrangement[89,90] and play a role in mineralisation events via their ability to bind calcium.[91,92]

I.2.2. Types of dentinogenesis [1,2,5,9,27]

There are many approaches in the literature to classify the different forms of dentinogenesis. Here, we propose the following: (i) based on time of formation - primary dentinogenesis and secondary dentinogenesis, and (ii) based on external stimulus - tertiary dentinogenesis. During the life of the tooth, physiological factors, aging and disease are likely to have an impact on the type of dentin formed.[7,93]

I.2.2.1. Primary dentinogenesis

Primary dentinogenesis takes place during tooth development. It leads to the formation of the very first physiological dentin and includes both mantle and circumpulpal dentins. The deposition rate of primary dentin is 4 µm/day.

I.2.2.2. Secondary dentinogenesis

After primary dentinogenesis, i.e. once the root is complete for some, or the tooth appears in the dental arch for others, dentin formation continues in the form of secondary dentin. Secondary dentin secretion is four times slower than primary dentin, as the secreting odontoblast seems to have fallen into a semi-inactive, semi-active form. However, the chemical composition and structural organization of primary and secondary dentin are identical. The process occurs regularly all over the life of tooth, but not uniformly. More secondary dentin formation is seen on the roof and floor of the pulp chamber, causing progressive reduction in its size and asymmetric decrease in the root canal volume/space. It is physiologic and in no way pathologic. Secondary dentin also includes circumpulpal dentin.

I.2.2.3. Tertiary dentinogenesis: pulp response to external agression

The tertiary dentine is secreted in response to an aggression (caries, abrasion, erosion, restorative procedure…) to protect the underlying pulp. Such stimulation switches the cells from their inactive phase to an active phase. In contrast to physiological secondary dentin, tertiary dentin is deposited on the pulpal surface of dentin only in the affected area (**Figure I.5)**.

Reactionary dentin. In the case of low to moderate aggression (without destruction of odontoblasts), an innate defense mechanism is initiated by preexisting odontoblasts, i.e. odontoblasts that have originally differentiated during the development of the tooth germ, to secrete reactionary dentin. Its structure is more or less similar to the physiological dentin.

Reparative dentin. When the damage is significant and the odontoblastic layer is altered, a reparative dentin is produced by newly odontoblast-like cells that have differentiated from a pool of dental mesenchymal pulp stem cells. The dentinal healing process starts by the migration of dental stem cells to the site of injury where they differentiate into odontoblasts. Dental stem cells differentiation is associated with the release of sequestered TGF-β following physical damage and activation of Wnt signalling.[94–96] Thus, the presence of TGF-β in dentin tubules assists in the formation of reparative dentin. These signalling molecules not only contribute to the mineralization process but also promote the migration and pro-inflammatory activation of immune system cells.[97] Reparative dentin is usually in the form of a thin dentinal bridge occluding the exposure site, or a bone-like structure (osteo-dentin) filling partially or totally the pulp.

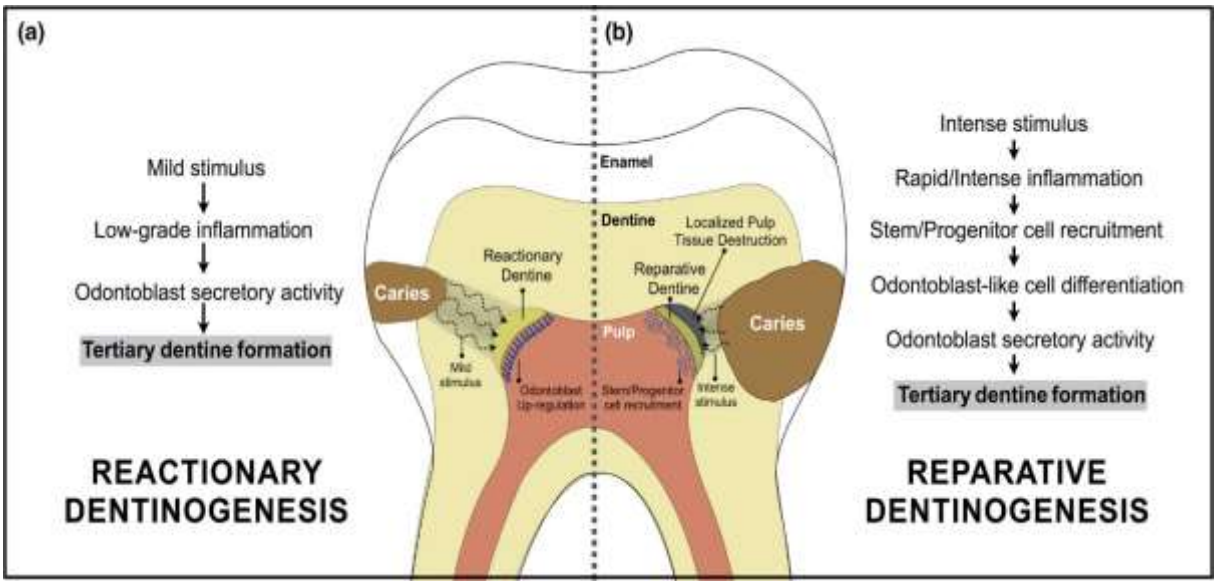

Figure I.5: Two types of tertiary dentine formation. (a) reactionary dentinogenesis following moderate dentin injury if primary odontoblasts are present to secrete dentine, and (b) reparative dentinogenesis if odontoblasts have been damaged or destroyed and if the formation of tertiary dentine is performed after stem/progenitor cell recruitment by odontoblast-like cells.[98]

I.3. A therapeutic application of the regeneration potential of dentin pulp-complex: direct pulp capping

Preserving the vitality of the dental pulp is a necessity for the long-term survival of the tooth in the oral cavity. Pulpless teeth lose their ability to perceive and respond to environmental stimuli, as well as their capacity to produce dentin. As a result, they are no longer able to detect the progression of caries and are more vulnerable to the forces of mastication.[99–101] In cases of pulp exposure following trauma or injury, direct pulp capping is often recommended as the treatment of choice.[99,102,103] This approach involves the placement of a bioactive material directly over the exposed (wounded) pulp to stimulate the dentinogenic potential of pulp stem cells so as to produce reparative dentin.[102,104] A successful pulp capping material relies of its ability to promote the formation of a long-term sealed protective barrier and maintain pulp tissue vitality.[102,104,105] This well-established technique has been the subject of extensive research, with early reports of mediocre success rates (using materials such as calcium hydroxide - $Ca(OH)_2$) due to the failure to control bacterial contamination, thereby raising concerns about its clinical efficacy.[106–109] However, recent investigations utilizing biocompatible products with superior sealing capabilities, such as mineral trioxide aggregate (MTA), Biodentine, and other calcium silicate cements, have been associated with significantly higher success rates in the management of both traumatic and cariously exposed teeth.[110–112]

I.3.1. Calcium silicates materials used for dental pulp capping

I.3.1.1. 1st generation: MTA

ProRoot MTA White, launched in the 1990's by Dentsply Sirona (York, PA, USA), comprises tri- and di- calcium silicates, tricalcium aluminate, bismuth oxide and gypsum. Other variations like ProRoot MTA Gray, MTA Angelus (Angelus, Londrina, Brazil), Grey MTA Plus (Avalon Biomed, Bradenton, FL, USA), EndoCem MTA (Maruchi, Gangwon-do, Korea) and Ortho MTA (BioMTA, Daejeon, Korea), among others, are available, with MTA White being the most prevalent.[105] Bismuth oxide and calcium sulfate serve as the radiopacifier and setting modifier, respectively. Its advantages include sealing ability, biocompatibility, bioactivity and dentin bridge formation with little inflammation and necrosis of the pulp.[113–115] However, its antibacterial effect is debated.[116] MTA showed an antibacterial effect on some of the facultative

bacteria but no effect on any of the strictly anaerobic bacteria.[117] Drawbacks include long setting times, poor handling, and potential tooth discoloration.[115,118,119] Reported initial setting times vary from 50 and 70 min.[119,120] Handling properties are influenced by the particles size (1 to 40 μm), their wide distribution, and low to middle circularity.[121] Tooth discoloration is linked to both gray and white MTA, possibly influenced by factors like blood contamination and exposure to light and oxygen.[122,123] However, animal and human studies generally favour MTA over $Ca(OH)_2$ for pulp healing, attributing its success to the formation of a quality hard-tissue barrier subjacent to MTA.[107,110,111,124]

I.3.1.2. 2nd generation: Biodentine

Biodentine, introduced in 2009 by Septodont (Saint-Maur-des-Fossés, France), comprises tri- and di- calcium silicates, calcium carbonate and oxide, iron oxide and zirconium oxide (as a radiopacifier) in its powder.[105] Unlike traditional mixing with water, it is mixed with a calcium chloride solution containing modified polycarboxylates. This unique combination reduces initial setting time to 10-12 minutes. Calcium chloride speeds up hydration, while polycarboxylates maintain proper consistency, easing handling. Calcium carbonate acts as a nucleation site, enhancing hydration for faster setting. Biodentine's finer particles, with a specific surface area about 2.8 times larger than MTA Angelus White, further expedite setting.[125] Studies indicate that its efficacy is comparable to that of MTA in the direct capping of exposed molar pulps, with a favourable pulp response and the formation of a complete dentine bridge.[126,127]

Table I.2: Properties of two pulp capping agents, adapted from[128]

	MTA (ProRooT MTA White)	**Biodentine**
Composition	***Powder***: Portland cement (tricalcium silicate, dicalcium silicate, tricalcium aluminate) 75%, bismuth oxide 20%, calcium sulfate dihydrate (gypsum) 5% ***Liquid***: water	***Powder***: tricalcium silicate, dicalcium silicate, calcium oxide, calcium carbonate, zirconium oxide, iron oxide ***Liquid***: calcium chloride, water-soluble polymer, water
Setting reaction	MTA + water → calcium hydroxide + calcium silicate hydrate $2[3CaO.SiO_2]+6H_2O \rightarrow 3CaO.2SiO_2.3H_2O+3Ca(OH)_2$ $2[2CaO.SiO_2]+4H_2O \rightarrow 3CaO.2SiO_2.3H_2O+Ca(OH)_2$	Biodentine + water → hydrated calcium silicate gel + calcium hydroxide $2[3CaO.SiO_2]+6H_2O \rightarrow 3CaO.2SiO_2.3H_2O + 3Ca(OH)_2$
Final Setting time (min)	261 ± 21 [129] 228.33 ± 2.88 [130]	45.0 [131] 85.66 ± 6.03 [130]

Consistency	Granular, « sandy » mixture	Uniform, putty-like
Handling	+	++
Bond strength to dentin (After 7/14 days)	0.85 ± 1.42 / 4.96 ± 4.54 [132]	9.75 ± 2.19 / 9.34 ± 1.01 [132]
Solubility at 24h (%)	1.28 ± 0.02 [120] ; 10.89 ± 0.48 [133]	11.83 ± 0.52 [133]
Initial/Endpoint pH	12.48/11.56 [134] ; 10.99/7.20 [133]	11.98/11.16 [135] ; 11.63/9.21 [133]
Ca release (ppm)	15.7 – 27.4 [133]	18.0 – 95.3 [133]
Tooth discoloration	+	-
Seal to dentin	Chemical and/or micromechanical adhesion, penetration in dentinal tubules	

I.3.2. Healing potential after pulp exposure

I.3.2.1. Inflammatory response

Upon exposure/damage of the dental pulp, an inflammatory reaction is initiated in the remaining healthy pulp tissue. This reaction is characterized by an accumulation of inflammatory cells, which release host pro-inflammatory cytokines, such as IL-6-8-1α, and tumor necrosis factor-alpha (TNF-α).[47,97,136] These proinflammatory mediators can have both detrimental and beneficial effects on pulp tissue, depending on their concentrations.[137] High levels of cytokines such as TNF-α can lead to pulp tissue degradation events to the point of causing pulp cell death and impaired stem cell differentiation.[138] On the other hand, pro-inflammatory cytokine TNF-α and reactive oxygen species (ROS) can also stimulate pro-regenerative/reparative signalling, notably via activation of p38 MAPK pathway, leading to odontoblast-like differentiation of pulp stem cells with increased dentin phosphoprotein (DPP) and dentin sialoprotein (DSP) expression and tertiary dentinogenesis.[139] Other studies have also shown the beneficial impact of the immune system on reparative processes, highlighting how cytokines release from immunocompetent cells like macrophages and dendritic cells can promote odontoblast differentiation.[140,141] Such molecular switching highlights the potential interplay between inflammatory and regenerative events. Thus, if conditions are conducive to repair, i.e. with low levels of pro-inflammatory cytokines, the pulp's response to injury results in increased synthetic and secretory activities of differentiated pulp stem cells along with dentin deposition.[137,142]

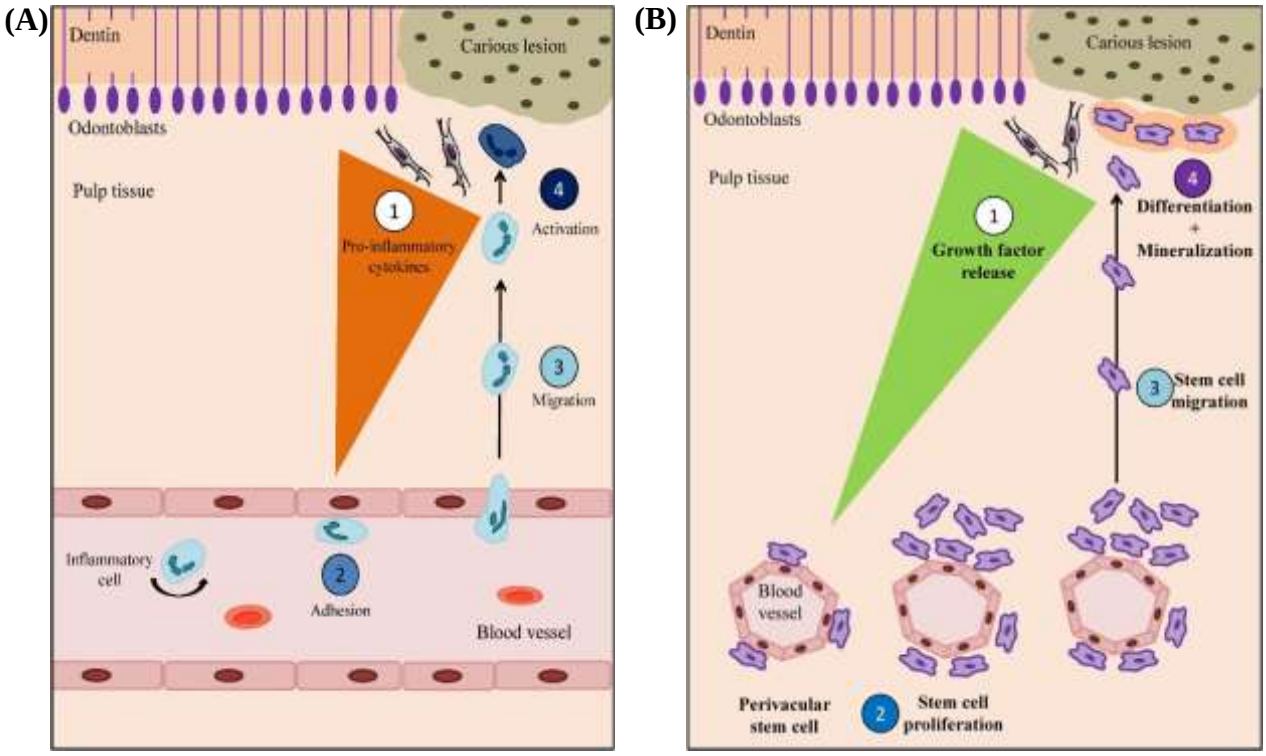

Figure I.6: (A) Initial steps of pulp inflammation following a carious/traumatic pulp lesion. secretion of pro-inflammatory cytokines by pulp fibroblasts, 2-adhesion of circulating inflammatory cells on the activated vascular endothelium, 3-migration to the injured site, 4- activation as macrophage-like cells. (B) Initial steps of dentin-pulp regeneration following a carious/traumatic pulp lesion. 1-secretion growth factors by dental pulp cells, 2-creation of a gradient by growth factors leading to stem cell proliferation, 3-migration of stem cells to the injured site and, 4-differentiation of stem cells into odontoblasts-like cells and secretion of mineralized matrix. [142]

I.3.2.2. Impact of dental pulp capping on inflammation

Given that severe pulp inflammation is detrimental to clinical outcome, pulp capping materials that reduce the inflammatory process are of particular interest.[142] Application of calcium silicates materials on injured pulp contribute to attenuate tissue inflammation during the repair phase.[110,143–145] For instance, Kang *et al*[144] found that ProRoot®MTA and Ortho®MTA led to a complete calcific dentin barrier formation after 8 weeks of direct pulp capping, while Endocem®MTA produced a partially discontinuous dentin calcific barrier presenting tunnel defects. The latter was associated with a greater inflammatory reaction than the other two MTA. In another study, the dentinal bridges in teeth that were capped with Biodentine were thicker and more continuous with less pulpal inflammation in comparison to $Ca(OH)_2$ within 45 days of treatment.[145] Similarly, other investigations suggest that a chronic inflammatory response of mild to moderate intensity may prevent the deposition of hard tissue bridges.[106,107]

Several *in vitro* studies have shed light on the underlying processes by which pulp capping materials shift the balance from inflammation towards regeneration. For example, the pro-inflammatory cytokine TNF-α has been demonstrated to trigger the expression of Transient Receptor Potential Ankyrin 1 (TRPA1), which is involved in nociception and neurogenic inflammation. Interestingly, Biodentine can reduce TNF-α-induced TRPA1 expression and functional activity.[143] In line with the inflammation-reducing effect, Biodentine and MTA promote regenerative processes by increasing TGF-1 and FGF-2 secretion by fibroblasts in the injured pulp.[146,147] TGF-1 growth factor is known to promote odontoblastic differentiation contributing as such to dentin-bridge formation.[73,95]

I.3.3. Mechanisms of action of dental pulp capping materials

The setting reaction of calcium silicate involves hydration, during which by-products are formed or released (**Figure I.7**). Most calcium silicates materials result in the formation of $Ca(OH)_2$ and the leaching of hydroxyl (OH^-) and calcium ions (Ca^{2+}), as demonstrated in MTA and Biodentine.[125,148] The released OH^- and Ca^{2+} raise the pH in the surrounding tissue, causing tissue irritation and cellular necrosis, thus creating a thin necrotic layer between the remaining vital tissue and the pulp capping agent.[107,142] The alkaline pH may also have an anti-inflammatory effect through the denaturation of proinflammatory cytokines and activation of the anti-inflammatory cytokine IL-10.[149,150] This attenuation of tissue inflammation provides a conducive environment for the formation of reparative dentin. The necrotic zone protects the underlying vital pulp cells from the material's alkaline pH, enabling them to perform healing and regeneration functions[151], while also providing antimicrobial activity.[117] Subsequent calcification of this superficial necrotic layer, together with the formation of tertiary dentin from stimulated and differentiated dental pulp stem cells, lead to the formation of a protective dentin bridge.[142] Ca^{2+} ions contribute to this process by promoting DPSC differentiation and increasing the formation of mineralized matrix nodules.[152,153] In addition, a "bioactive" surface is formed due to the nucleation of calcium phosphates and subsequent apatite formation, in a moist environment. This apatite layer is thought to stimulate cell differentiation and tissue repair.[154] Silicon species, most likely silicic acid $Si(OH)_4$ in such conditions, may also contribute to dentin-bridge formation, as their release has been shown to stimulate the formation of young bone by activating osteoblasts.[155] However, very little is known about their effect on pulp stem cells.

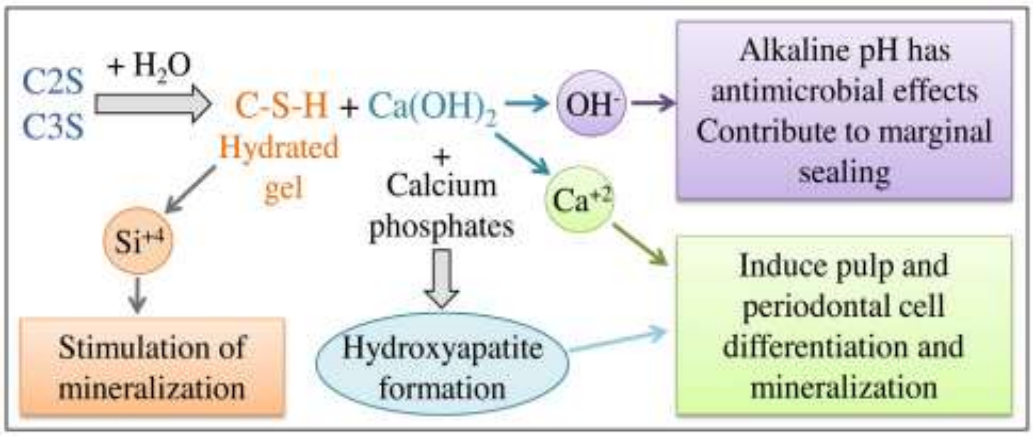

Figure I.7: Diagram illustrating the setting and biological effects of the hydration reaction of silicate-based material (C2S: dicalcium silicate, C3S: tricalcium silicates) materials. This reaction release OH^{-}, Ca^{2+}, and soluble silicon, improperly labelled "Si^{4+}".[142]

I.4. Importance of silicon in the mineralization process: the case of bone

Silicon (Si) is suggested to be essential for normal bone development and repair.[156–158] Although the bone and dentin have obvious differences (such as the absence of remodelling in dentin), they also share some common features like similarities in the composition of the ECM secreted by osteoblasts (for bone) and odontoblasts (for dentin).[2,159] In the cranial and oral spheres, both cells initially derive from cranial neural crest mesenchymal cells, with mature cells active throughout life and able to differentiate from precursors when required.[48,160] Several genetic disorders affecting bone mineralization can also manifest during dentin mineralization, including hypophosphatemic rickets and osteogenesis imperfecta, among others.[161] These parallels imply that a review of Si effects on bone cells may provide a first insight into its interactions with dental cells.

I.4.1. Silicon chemistry

Silicon, the second most abundant element in the earth's crust with an atomic weight of 28, generally exists as silica and silicates due to its strong affinity for oxygen.[162] In nature, silica (silicon dioxide, SiO_2), exists in both crystalline (such as quartz) and amorphous (such as phytoliths) phases. The water soluble forms of silicon, (ortho)silicic acid ($Si(OH)_4$) and polysilicic acids, are present in sea and running waters and exhibit high bioavailability. However silicic acid readily polymerizes at moderate concentrations (>2 mM, pH< 9), forming less bioavailable larger silica species (colloids, gels).[163–165] The human body contains 1-2 grams of Si, making it the third most abundant trace element.[156,162] Si is in the form of $Si(OH)_4$ in serum, with concentrations ranging from 0.11 to 0.31 $mg.L^{-1}$, influenced by age, sex and other factors.[166] Human exposure to Si occurs through diet and seems to offer potential health benefits, with $Si(OH)_4$ being the only bioavailable dietary form.[162,167] The main dietary sources of Si are beverages (water, coffee, beer), dietary grains (cereals, oats, barley, wheat flour, pasta, pastries, rice), and vegetables.[162,167]

I.4.2. Soluble silica role on bone formation

I.4.2.1. Animal studies

Early studies demonstrated that basal diets deficient in Si reduce overall growth in chicks and rats and produce more porous, less mineralized bone.[168,169] Similarly, supplementation of the mice diet with soluble Si (10 ppm of sodium metasilicate) and administration of Si via desalinated deep-sea water (containing 1.8 ppm of Si) resulted in increased femoral weight, bone calcium and phosphorus content, and alkaline phosphatase (ALP, bone formation marker) activity compared to the administration of desalinated surface sea water (containing 0.006 ppm of Si) or tap water.[170] In ovariectomised rats (standard model for postmenopausal bone loss), supplementation with silicon or choline-stabilized orthosilicic acid (ch-OSA) reduced bone resorption and bone loss while increasing bone formation and bone mineral density (BMD).[171–174] Results in horses also showed that Si supplementation increased BMD and mechanical strength, thereby reducing bone-related injuries.[175]

I.4.2.2. Human studies

Human studies also support the beneficial effects of Si intake on bone health. There is evidence that Si affects the increase of bone density and decrease of bone loss. In osteoporotic patients, supplementation with Si increased collagen synthesis, trabecular bone volume and femoral BMD.[176–178] Another study showed that treatment with Si is more effective in inducing a significant increase in femoral BMD than treatment with fluoride, etidronate (a bisphosphonate), and magnesium in osteoporotic women.[176] A potential beneficial effect on bone turnover and femoral BMD compared to using only calcium and vitamin D was observed in women supplemented with ch-OSA.[178,179] Compelling evidence demonstrates that dietary silicon can strengthen bones and, as a result, reduce the risk of osteoporosis.[180] Although available scientific evidence is not considered sufficiently valid to establish an adequate level of Si intake, it has been suggested that an intake of around 25 mg Si/day may be appropriate to promote positive effects on bones.[158]

I.4.2.3. Silicon and bone formation: mechanism overview

Although Si may play a role in bone formation, the precise/exact mechanism remains unclear. In vitro studies indicated that Si enhance osteoblast differentiation, extracellular matrix

synthesis, and bone mineralization.[181–183] It also increases the gene expression of osteocalcin (OCN), alkaline phosphatase (ALP) and osteopontin (OPN) in osteoblasts and MSCs[181,183–185], and it boosts their metabolic activity and proliferation.[181,186]

Interestingly, Si inhibits macrophage and osteoclast activity.[187,188] A study showed that $Si(OH)_4$ promotes osteogenesis by inhibiting the activity of nuclear factor kappa-light-chain-enhancer of activated B cells (NF-κB), a factor known to hinder osteoblastic bone formation and stimulate osteoclastic resorption.[189] Similarly, Si nanoparticles have shown inhibitory effects on osteoclasts and stimulatory effects on osteoblasts by increasing the serum levels of OCN both in vitro and in vivo.[190–192] A gene expression study found that treating osteoblasts with Bioglass 45S5 leachate increased the messenger RNA levels for several genes related to osteogenic differentiation and mineralization.[193]

Studies revealed that Si is concentrated in active bone growth areas, co-localizing with Ca in areas of greatest osteoblastic activity [194,195]. Si concentrations in osteoid are 25 times greater than in surrounding areas and the Si content gradually declines as calcification occurs, indicating that Si is probably involved in the development of organic matrix and the initiation of calcification. Researchers proposed that Si plays a structural role in stabilizing collagen and glycosaminoglycans networks in the ECM.[196,197] This may provide a low solubility matrix that attracts and contains other ions, such as Ca^{2+}, at the organic-inorganic interface.[198]

Studies in rats have demonstrated that Si at physiological levels improves Ca^{2+} incorporation in bone when compared to rats that are deficient in Si.[199,200] In contrast, other experimental studies reported small reductions in bone strength when excessively high and prolonged levels of dietary Si were added to the diet, thus illustrating antagonist effects of Si.[174,201]

I.4.3. Silicon in bone repair materials

I.4.3.1. Silica nanoparticles

In addition to the positive effects of soluble Si on bone health, it has also been demonstrated that Si-based nanoparticles can be used for bone regeneration and repair of bone defects. Silica nanoparticles (SiNPs) are inorganic materials possessing adaptable physical characteristics such as shape, size, charge, and surface chemistry.[202,203] These properties may vary according to the synthesis method. The sol-gel method (Stöber method) is one of the most widely used due to its simplicity, reproducibility and effectiveness.[204–206] This method is based on the

hydrolysis of tetraethyl orthosilicate (TEOS), followed by condensation in ethanol in the presence of ammonia (as catalyst) (**Figure I.8**). It produces spherical, monodisperse silica particles that are highly dispersible in various media (alcohol, water, PBS).[192]

Silica is generally considered to have low toxicity, with size- and dose-dependent cytotoxic effects, particularly above a concentration of 25 $\mu g.mL^{-1}$.[207] Studies reported that silica particles can be internalized, dissolved intracellularly and/or excreted.[192,208,209] When studying the effects of particle size on bioactivity, it was found that small spherical SiNPs (50-150 nm) most strongly stimulate osteoblast differentiation and mineralization, while being efficiently taken up by the cells.[190,208,209] However, the small particles may be more harmful for the cells.[209] Larger SiNPs can resist lysosomal degradation, releasing less $Si(OH)_4$, which may explain why they are less harmful to cells. In contrast, 100 nm hexagonal SiNPs have no effect on osteoblastic differentiation of mesenchymal stem cells (MSCs)[210], demonstrating how subtle physical changes in particles have a direct impact on cellular responses.[211]

Besides all inorganic materials, efforts have been directed towards developing biohybrid or bionanocomposite materials integrating silica with biological systems, including functional biomolecules, structural biopolymers, or living cells.[212–214] A number of studies focused on the combination of collagen-based materials with SiNPs demonstrated their efficacy for bone repair applications.[215–217] Noticeably, silica does not exhibit bioactivity, i.e. bone induction property, per se. However, when mixed with collagen, it does induce hydroxyapatite in vitro.[218]

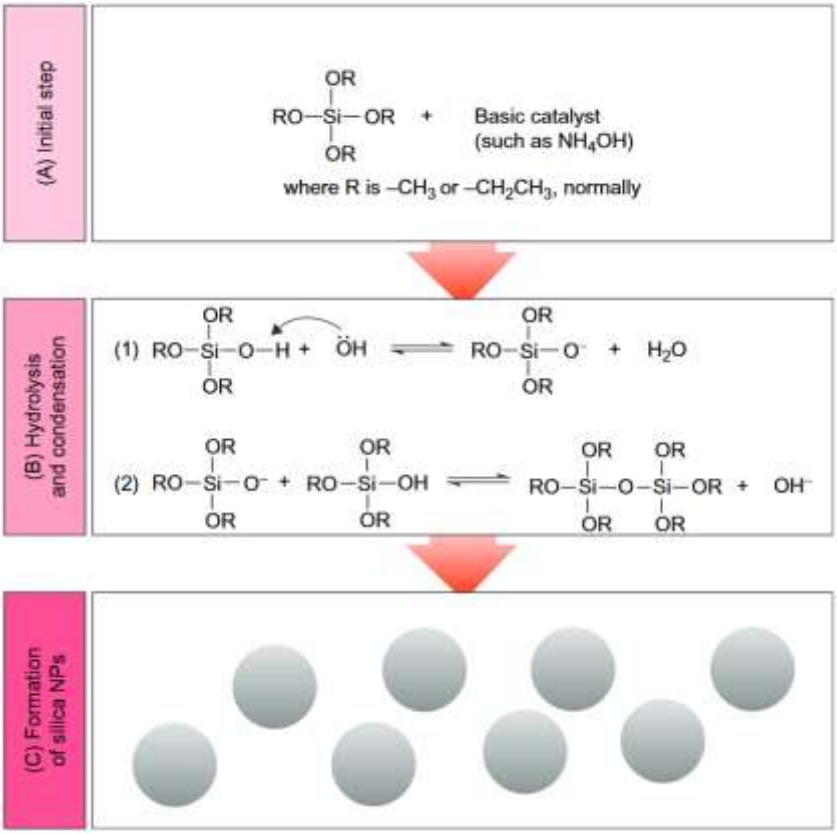

Figure I.8: General synthesis of silica nanoparticles. (A) silica precursor and catalyst are added in an alcoholic solution, if R is an ethyl group, the precursor is TEOS. (B) The precursor is then hydrolysed by a hydroxyl ion (hydrolysis, B1) and the activated precursor is condensed with another activated precursor or precursor (condensation, B2). (C) As a result of hydrolysis and condensation, silica nanoparticles are generated. [219]

I.4.3.2. Bioactive glasses

Bioactive glasses (BG) are amorphous materials whose main component is SiO_2. The best-known BG in the biomedical field is 45S5 Bioglass, which features a bioactive, biodegradable silicate composition (46,1% SiO_2 – 24,4% Na_2O – 26,9% CaO – 2,6% P_2O_5).[220] Since their first discovery 40 years ago, numerous BGs and glass-ceramics (fusion-derived or sol-gel) have been introduced for bone repair and grafting.[221–224] These glasses have the unique ability to form a bone-like apatite layer on their surface upon contact with physiological body fluid, which enables them to bond firmly with living bone and tissue.[225] The sequence of reactions on the surface of BG is illustrated in **Figure I.9**. Additionally, the dissolved $Si(OH)_4$ from BGs have been found to stimulate osteoblasts, regulating the expression of several genes, including key osteoblastic markers and extracellular matrix proteins.[193]

Although bioglasses are mostly used as microparticles, their elaboration at the nanoscale has also been achieved.[226] Composite materials associating Bioglass particles with collagen have been widely described.[227] Besides improvement of the mechanical properties of the collagen network, bioglasses confer bioactivity to the materials.

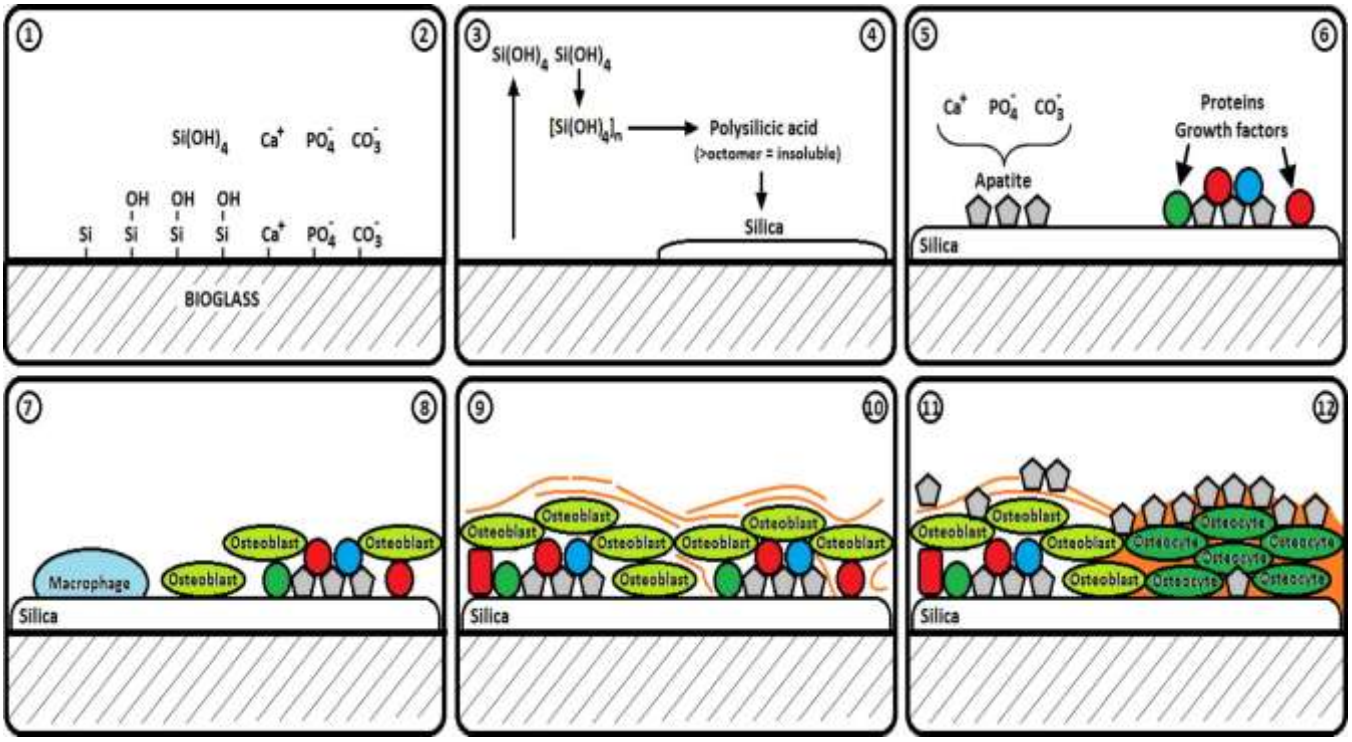

Figure I.9: The 12 stages of bone bonding by bioglass. Reaction of silica in the glass with the surrounding body fluid, forming $Si(OH)_4$ (1), diffusion of Ca^{2+}, PO^{-}_4 and CO^{-}_3 into the interface (2), polycondensation of $Si(OH)_4$ into larger polysilicic acids (3), precipitation of polysilicic acids onto the Bioglass surface forming a silica layer (4) acting as nucleation bed for apatite formation (5). Adsorption of proteins from the surrounding tissue fluid (6) assists in the recruitment of macrophages (7) and osteoblasts (8), that attach to the silica and apatite substrate. Osteoblasts proliferate (9) and produce osteoid (10), which becomes mineralized (11), finally encasing the cells in bone which prompts their differentiation into osteocytes or apoptosis (12).[222]

I.4.3.3. Silicon-containing cements

Silicon-containing cements have also been described.[228] The cements can be either mainly composed of calcium silicates, hence similar to pulp capping materials previously described, or contain only a minor fraction of a silicon-containing phase. Besides calcium silicates similar to pulp caping materials described in the previous section, silicon-doped calcium phosphate cements have been widely described. The presence of the silicon component can be beneficial to several chemical/physical properties of the cement such as improved injectability, slower

setting time and better mechanical property.[229] Moreover, the presence of silicon can improve the bone repair process.[230]

I.4.4. Silicon: from bone to tooth

Altogether, evidence has been accumulated of the beneficial effect of silicon on health, although the precise biological processes at stake remain largely unknown. On this basis, several kinds of biomaterials incorporating silicon have been developed that were found efficient in bone repair. However, although some dental materials, and in particular pulp capping cements, also contain and release silicon species, the response of dental tissues, or even of cells, to silicon has been only studied twice.[231,232] This finding was at the origin of this PhD project.

I.5. Collagen-based materials: a model for hard tissue repair

The *in vitro* study of cells' response to a given stimuli, being chemical, physical or biological, should preferably be performed in an environment which reproduces as much as possible their "natural" environment. However, facing the intrinsic complexity of biological tissues, it is necessary to define, a minima, features or properties of the model. In the case of hard tissues, collagen-based structures can be used as tissue-mimicking constructs, providing physiological and biomimetic environment in which cellular function can be studied.[233,234]

I.5.1. Collagen-based hydrogels: from highly hydrated to plastically compressed dense collagen hydrogels

Collagen-based scaffolds, made from acid-solubilized type I collagen, have been extensively utilized as three-dimensional (3D) constructs/models for cell culture and tissue engineering.[235–237] These hydrogel scaffolds exhibit good biocompatibility, biodegradability, and low antigenicity, creating an environment conducive to cell attachment, proliferation, and differentiation [233,238]. Indeed, when adjusted to physiological pH and temperature, acid-solubilized collagen molecules spontaneously self-assemble to form fibrillar collagen hydrogels.[239,240] Typically, these hydrogels are prepared with collagen solutions ranging from 2 to 10 mg.mL^{-1}, yielding highly hydrated hydrogels (>95% w/v fluid) that display a loose fibrillar network (collagen fibrillar density < 1%) and lack the structural organization and mechanical properties of native ECM of predentin/osteoid.[234] However, it is possible to rapidly and effectively increase collagen fibrillar density using a simple plastic compression technique.[241] This process generates dense collagen gel scaffolds (with collagen fibrillar density > 10%) resembling native predentin/osteoid matrix, with a defined meso-structure and enhanced biomechanical properties.[242,243] Another key advantage of plastic compression is that cell seeding can be integrated into the fabrication process without compromising cell viability, so that cells can grow and differentiate within the 3D scaffold.[241,244,245]

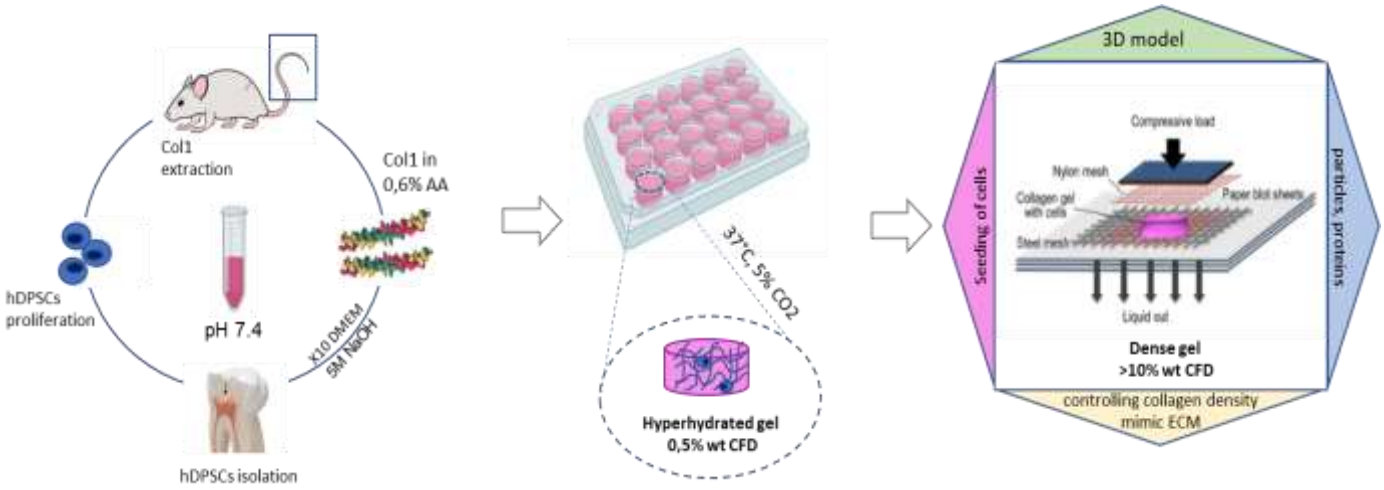

Figure I.9: Engineering 3D material model for tissue engineering by plastic compression. AA=Acetic acid, CFD=collagen fibrillar density.

I.5.2. Odontoblasts vs dental pulp stem cells

Odontoblasts are highly specialized cells that produce collagenous and non-collagenous proteins to build the dentin extracellular matrix.[1,58] Due to their postmitotic phenotype, i.e. their inability to divide and form a new secretory cell, they are difficult to culture.[23,246] Thus, in vitro studies assessing their fate once in contact with dental materials are lacking. Upon odontoblast death or removal due to severe tooth damage, another form of substitution process occurs (following the placement of a pulp capping material on the injured pulp), with new "odontoblast-like" cells differentiating from stem cells from the dental pulp to form a reparative dentin bridge.[47,247] Consequently, most studies on dental regeneration and repair are carried out using undifferentiated mesenchymal stem cells from the pulp.[248–250]

I.5.3. DPSC in combination with collagen hydrogels

The scientific literature has consistently highlighted the accessibility and plasticity of dental pulp stem cells (DPSCs) as a promising source of stem cells for regenerative medicine.[30,251–253] Their ability to expand *in vitro* and their potential to differentiate into odontogenic cells have positioned them as attractive candidates for the regeneration of the dentin-pulp complex.[248–250,254] However, as with other stem cell types, positive results depend on the precise regulation of their proliferation and differentiation in an environment that mimics *in vivo* conditions.

In this context, dense plastically compressed (PC) collagen gels have been repeatedly used by the BRIO laboratory as hosts for dental pulp stem cells (DPSCs). In a first study, they demonstrated that DPSCs immobilized in PC collagen hydrogels maintained high survival rate and mineralization ability.[245] Later on, they used these dense hydrogels to study the mineralization ability of hDPSCs from patients suffering from X-linked hypophosphatemia.[255] In parallel, the team demonstrated the efficacy of these constructs to promote bone formation in critical-size calvaria defect, highlighting the contribution of the hDPSCs to the repair process.[256–259] Noticeably, it was also demonstrated that addition of bioglass microparticles to the collagen hydrogels was an efficient strategy to promote bone repair without the need for cell addition.[260] In fact, in this case, the presence of DPSCs was detrimental to bone formation.

I.6. Objectives of the study

The present chapter exploring the current status of the topic highlights the vital role of silicon in the development and regeneration of bone tissue. This element is believed to be crucial for both bone and dentin, as they share similarities in terms of their extracellular matrix composition and the process of bone formation. In early stages of the formation of these mineralized tissues, specialized odonto/osteogenic cells produce a collagenous extracellular matrix, guiding mineralization.Therefore, it is crucial to replicate this three-dimensional (3D) extracellular matrix in order to study cell-mediated mineralization. On this basis, we decided to use the plastic compression method to fabricate dense collagen matrices incorporating human DPSCs that could be used as models to study the effect of silicon on dentin-pulp complex.

The main objective of this project is to gain an understanding of the role of silicon in dentin formation. In order to achieve this, we have divided our objective into three sub-goals:

(1) Investigate the impact of various formulations and cell culture conditions, using stem cells from dental pulp, on the preparation of plastically-compressed collagen hydrogels (Chapter 2),

(2) Study the effects of soluble silicon (silicic acid) on the viability, differentiation, and mineralization of dental pulp stem cells within collagen hydrogels (Chapter 3),

(3) Prepare collagen-based nanocomposite hydrogels containing different silicon-releasing phases (silica and bioactive glasses) and examine the behaviour of dental pulp stem cells within these nanocomposite hydrogels (Chapter 4).

References

(1) *The Dental Pulp: Biology, Pathology, and Regenerative Therapies*; Goldberg, M., Ed.; Springer Berlin Heidelberg: Berlin, Heidelberg, 2014. https://doi.org/10.1007/978-3-642-55160-4.

(2) Linde, A.; Goldberg, M. Dentinogenesis. *Critical Reviews in Oral Biology & Medicine* **1993**, *4* (5), 679–728. https://doi.org/10.1177/10454411930040050301.

(3) Goldberg, M.; Lasfargues, J.-J. Pulpo-Dentinal Complex Revisited. *Journal of Dentistry* **1995**, *23* (1), 15–20. https://doi.org/10.1016/0300-5712(95)90655-2.

(4) Pashley, D. H. Dynamics of the Pulpo-Dentin Complex. *Critical Reviews in Oral Biology & Medicine* **1996**, *7* (2), 104–133. https://doi.org/10.1177/10454411960070020101.

(5) Nanci, A.; TenCate, A. R. *Ten Cate's Oral Histology: Development, Structure, and Function*, 9th edition.; Elsevier: St. Louis, Missouri, 2018.

(6) *Tooth anatomy: MedlinePlus Medical Encyclopedia Image*. https://medlineplus.gov/ency/imagepages/1121.htm (accessed 2024-05-05).

(7) *Craig's Restorative Dental Materials*; Elsevier, 2019. https://doi.org/10.1016/C2015-0-01767-1.

(8) Tjäderhane, L.; Carrilho, M. R.; Breschi, L.; Tay, F. R.; Pashley, D. H. Dentin Basic Structure and Composition—an Overview. *Endodontic Topics* **2009**, *20* (1), 3–29. https://doi.org/10.1111/j.1601-1546.2012.00269.x.

(9) Tjäderhane, L. Dentin Basic Structure, Composition, and Function. In *The Root Canal Anatomy in Permanent Dentition*; Versiani, M. A., Basrani, B., Sousa-Neto, M. D., Eds.; Springer International Publishing: Cham, 2019; pp 17–27. https://doi.org/10.1007/978-3-319-73444-6_2.

(10) Goldberg, M. Dentin Structure Composition and Mineralization. *Front Biosci* **2011**, *E3* (2), 711–735. https://doi.org/10.2741/e281.

(11) Goldberg, M.; Smith, A. J. C ELLS AND E XTRACELLULAR M ATRICES OF D ENTIN AND P ULP: A B IOLOGICAL B ASIS FOR R EPAIR AND T ISSUE E NGINEERING. *Critical Reviews in Oral Biology & Medicine* **2004**, *15* (1), 13–27. https://doi.org/10.1177/154411130401500103.

(12) Nakamura, O.; Gohda, E.; Ozawa, M.; Senba, I.; Miyazaki, H.; Murakami, T.; Daikuhara, Y. Immunohistochemical Studies with a Monoclonal Antibody on the Distribution of Phosphophoryn in Predentin and Dentin. *Calcif Tissue Int* **1985**, *37* (5), 491–500. https://doi.org/10.1007/BF02557832.

(13) Takagi, Y.; Fujisawa, R.; Sasaki, S. Identification of Dentin Phosphophoryn Localization by Histochemical Stainings. *Connective Tissue Research* **1986**, *14* (4), 279–292. https://doi.org/10.3109/03008208609017471.

(14) Ohsaki, Y.; Nagata, K. Type III Collagen Is a Major Component of Interodontoblastic Fibers of the Developing Mouse Molar Root. *Anat. Rec.* **1994**, *240* (3), 308–313. https://doi.org/10.1002/ar.1092400303.

(15) Marshall, G. W. Dentin: Microstructure and Characterization. *Quintessence Int* **1993**, *24* (9), 606–617.

(16) Pashley, Dh. Dentin-Predentin Complex and Its Permeability: Physiologic Overviwe. *J Dent Res* **1985**, *64* (4), 613–620. https://doi.org/10.1177/00220345850640041 9.

(17) Gotliv, B.-A.; Veis, A. Peritubular Dentin, a Vertebrate Apatitic Mineralized Tissue without Collagen: Role of a Phospholipid-Proteolipid Complex. *Calcif Tissue Int* **2007**, *81* (3), 191–205. https://doi.org/10.1007/s00223-007-9053-x.

(18) Schilke, R.; Lisson, J. A.; Bauß, O.; Geurtsen, W. Comparison of the Number and Diameter of Dentinal Tubules in Human and Bovine Dentine by Scanning Electron Microscopic Investigation. *Archives of Oral Biology* **2000**, *45* (5), 355–361. https://doi.org/10.1016/S0003-9969(00)00006-6.

(19) Muendi, U.; Reiss, T.; Dursun, E.; Vennat, E. Characterization of the Dentin Microstructural Components: A FIB-SEM Analysis. In *13th International Conference on Advances in Experimental Mechanics (BSSM 2018)*; Southampton, United Kingdom, 2018.

(20) Weiner, S.; Veis, A.; Beniash, E.; Arad, T.; Dillon, J. W.; Sabsay, B.; Siddiqui, F. Peritubular Dentin Formation: Crystal Organization and the Macromolecular Constituents in Human Teeth. *Journal of Structural Biology* **1999**, *126* (1), 27–41. https://doi.org/10.1006/jsbi.1999.4096.

(21) Xu, C.; Wang, Y. Chemical Composition and Structure of Peritubular and Intertubular Human Dentine Revisited. *Archives of Oral Biology* **2012**, *57* (4), 383–391. https://doi.org/10.1016/j.archoralbio.2011.09.008.

(22) Sunkara, S. Mineralized Tissues in Oral and Craniofacial Science: Biological Principles and Clinical Correlates. *Br Dent J* **2012**, *213* (11), 583–583. https://doi.org/10.1038/sj.bdj.2012.1127.

(23) Ruch, J. V.; Lesot, H.; Bègue-Kirn, C. Odontoblast Differentiation. *Int J Dev Biol* **1995**, *39* (1), 51–68.

(24) Sloan, A. J. Biology of the Dentin-Pulp Complex. In *Stem Cell Biology and Tissue Engineering in Dental Sciences*; Elsevier, 2015; pp 371–378. https://doi.org/10.1016/B978-0-12-397157-9.00033-3.

(25) Tjäderhane, L.; Paju, S. Dentin-Pulp and Periodontal Anatomy and Physiology. In *Essential Endodontology*; Ørstavik, D., Ed.; Wiley, 2019; pp 11–58. https://doi.org/10.1002/9781119272014.ch2.

(26) Van Amerongen, J. P.; Lemmens, I. G.; Tonino, G. J. M. Immunofluorescent Localization and Extractability of Fibronectin in Human Dental Pulp. *Archives of Oral Biology* **1984**, *29* (2), 93–99. https://doi.org/10.1016/0003-9969(84)90111-0.

(27) *Orban's Oral Histology and Embryology*, 11th ed.; Orban, B. J., Bhaskar, S. N., Eds.; Mosby Year Book: St. Louis, 1991.

(28) Magloire, H.; Couble, M.; Romeas, A.; Bleicher, F. Odontoblast Primary Cilia: Facts and Hypotheses. *Cell Biology International* **2004**, *28* (2), 93–99. https://doi.org/10.1016/j.cellbi.2003.11.006.

(29) *Oral Histology Digital Lab: Dental Pulp: Zones of the Pulp (Image 4)*. https://www.uky.edu/~brmacp/oralhist/module4/lab/imgshtml/image04.htm (accessed 2024-05-05).

(30) Gronthos, S.; Mankani, M.; Brahim, J.; Robey, P. G.; Shi, S. Postnatal Human Dental Pulp Stem Cells (DPSCs) *in Vitro* and *in Vivo*. *Proc. Natl. Acad. Sci. U.S.A.* **2000**, *97* (25), 13625–13630. https://doi.org/10.1073/pnas.240309797.

(31) Miura, M.; Gronthos, S.; Zhao, M.; Lu, B.; Fisher, L. W.; Robey, P. G.; Shi, S. SHED: Stem Cells from Human Exfoliated Deciduous Teeth. *Proc. Natl. Acad. Sci. U.S.A.* **2003**, *100* (10), 5807–5812. https://doi.org/10.1073/pnas.0937635100.

(32) Kerkis, I.; Kerkis, A.; Dozortsev, D.; Stukart-Parsons, G. C.; Gomes Massironi, S. M.; Pereira, L. V.; Caplan, A. I.; Cerruti, H. F. Isolation and Characterization of a Population of Immature Dental Pulp Stem Cells Expressing OCT-4 and Other Embryonic Stem Cell Markers. *Cells Tissues Organs* **2006**, *184* (3–4), 105–116. https://doi.org/10.1159/000099617.

(33) Govindasamy, V.; Abdullah, A. N.; Sainik Ronald, V.; Musa, S.; Che Ab. Aziz, Z. A.; Zain, R. B.; Totey, S.; Bhonde, R. R.; Abu Kasim, N. H. Inherent Differential Propensity of Dental Pulp Stem Cells Derived from Human Deciduous and Permanent Teeth. *Journal of Endodontics* **2010**, *36* (9), 1504–1515. https://doi.org/10.1016/j.joen.2010.05.006.

(34) Atari, M.; Gil-Recio, C.; Fabregat, M.; García-Fernández, D. A.; Barajas, M.; Carrasco, M.; Jung, H.-S.; Hernández-Alfaro, F.; Casals, N.; Prosper, F.; Ferrés Padró, E.; Giner, L.

Dental Pulp of the Third Molar: A New Source of Pluripotent-like Stem Cells. *Journal of Cell Science* **2012**, jcs.096537. https://doi.org/10.1242/jcs.096537.

(35) Akpinar, G.; Kasap, M.; Aksoy, A.; Duruksu, G.; Gacar, G.; Karaoz, E. Phenotypic and Proteomic Characteristics of Human Dental Pulp Derived Mesenchymal Stem Cells from a Natal, an Exfoliated Deciduous, and an Impacted Third Molar Tooth. *Stem Cells International* **2014**, *2014*, e457059. https://doi.org/10.1155/2014/457059.

(36) Kolf, C. M.; Cho, E.; Tuan, R. S. Mesenchymal Stromal Cells: Biology of Adult Mesenchymal Stem Cells: Regulation of Niche, Self-Renewal and Differentiation. *Arthritis Res Ther* **2007**, *9* (1), 204. https://doi.org/10.1186/ar2116.

(37) Gronthos, S.; Brahim, J.; Li, W.; Fisher, L. W.; Cherman, N.; Boyde, A.; DenBesten, P.; Robey, P. G.; Shi, S. Stem Cell Properties of Human Dental Pulp Stem Cells. *J Dent Res* **2002**, *81* (8), 531–535. https://doi.org/10.1177/154405910208100806.

(38) Koyama, N.; Okubo, Y.; Nakao, K.; Bessho, K. Evaluation of Pluripotency in Human Dental Pulp Cells. *Journal of Oral and Maxillofacial Surgery* **2009**, *67* (3), 501–506. https://doi.org/10.1016/j.joms.2008.09.011.

(39) Huang, G. T.-J.; Yamaza, T.; Shea, L. D.; Djouad, F.; Kuhn, N. Z.; Tuan, R. S.; Shi, S. Stem/Progenitor Cell–Mediated *De Novo* Regeneration of Dental Pulp with Newly Deposited Continuous Layer of Dentin in an *In Vivo* Model. *Tissue Engineering Part A* **2010**, *16* (2), 605–615. https://doi.org/10.1089/ten.tea.2009.0518.

(40) Nel, S.; Durandt, C.; Murdoch, C.; Pepper, M. S. Determinants of Dental Pulp Stem Cell Heterogeneity. *Journal of Endodontics* **2022**, *48* (10), 1232–1240. https://doi.org/10.1016/j.joen.2022.06.013.

(41) Alraies, A.; Alaidaroos, N. Y. A.; Waddington, R. J.; Moseley, R.; Sloan, A. J. Variation in Human Dental Pulp Stem Cell Ageing Profiles Reflect Contrasting Proliferative and Regenerative Capabilities. *BMC Cell Biol* **2017**, *18* (1), 12. https://doi.org/10.1186/s12860-017-0128-x.

(42) Alraies, A.; Canetta, E.; Waddington, R. J.; Moseley, R.; Sloan, A. J. Discrimination of Dental Pulp Stem Cell Regenerative Heterogeneity by Single-Cell Raman Spectroscopy. *Tissue Engineering Part C: Methods* **2019**, *25* (8), 489–499. https://doi.org/10.1089/ten.tec.2019.0129.

(43) Kok, Z. Y.; Alaidaroos, N. Y. A.; Alraies, A.; Colombo, J. S.; Davies, L. C.; Waddington, R. J.; Sloan, A. J.; Moseley, R. Dental Pulp Stem Cell Heterogeneity: Finding Superior Quality “Needles” in a Dental Pulpal “Haystack” for Regenerative Medicine-Based

Applications. *Stem Cells International* **2022**, *2022*, 1–20. https://doi.org/10.1155/2022/9127074.

(44) Lacerda-Pinheiro, S.; Dimitrova-Nakov, S.; Harichane, Y.; Souyri, M.; Petit-Cocault, L.; Legrès, L.; Marchadier, A.; Baudry, A.; Ribes, S.; Goldberg, M.; Kellermann, O.; Poliard, A. Concomitant Multipotent and Unipotent Dental Pulp Progenitors and Their Respective Contribution to Mineralised Tissue Formation. *eCM* **2012**, *23*, 371–386. https://doi.org/10.22203/eCM.v023a29.

(45) Alraies, A.; Waddington, R. J.; Sloan, A. J.; Moseley, R. Evaluation of Dental Pulp Stem Cell Heterogeneity and Behaviour in 3D Type I Collagen Gels. *BioMed Research International* **2020**, *2020*, 1–12. https://doi.org/10.1155/2020/3034727.

(46) Dieterle, M. P.; Gross, T.; Steinberg, T.; Tomakidi, P.; Becker, K.; Vach, K.; Kremer, K.; Proksch, S. Characterization of a Stemness-Optimized Purification Method for Human Dental-Pulp Stem Cells: An Approach to Standardization. *Cells* **2022**, *11* (20), 3204. https://doi.org/10.3390/cells11203204.

(47) Simon, S.; Smith, A. J.; Lumley, P. J.; Cooper, P. R.; Berdal, A. The Pulp Healing Process: From Generation to Regeneration*. In *Oral Wound Healing*; Larjava, H., Ed.; Wiley, 2012; pp 313–332. https://doi.org/10.1002/9781118704509.ch13.

(48) Cho, S.-W. Lineage of Non-Cranial Neural Crest Cell in the Dental Mesenchyme: Using a LacZ Reporter Gene during Early Tooth Development. *Journal of Electron Microscopy* **2003**, *52* (6), 567–571. https://doi.org/10.1093/jmicro/52.6.567.

(49) Takano, Y.; Sakai, H.; Baba, O.; Terashima, T. Differential Involvement of Matrix Vesicles during the Initial and Appositional Mineralization Processes in Bone, Dentin, and Cementum. *Bone* **2000**, *26* (4), 333–339. https://doi.org/10.1016/S8756-3282(00)00243-X.

(50) Hirschfeld, Z.; Bab, I.; Ttamari, I.; Sela, J. Primary Mineralization of Dentin in Rats after Pulp Capping with Calcium-hydroxide. *J Oral Pathology Medicine* **1982**, *11* (6), 426–433. https://doi.org/10.1111/j.1600-0714.1982.tb00186.x.

(51) Sela, J.; Tamari, I.; Hirschfeld, Z.; Bab, I. Transmission Electron Microscopy of Reparative Dentin in Rat Molar Pulps. *Cells Tissues Organs* **1981**, *109* (3), 247–251. https://doi.org/10.1159/000145390.

(52) He, L.; Hao, Y.; Zhen, L.; Liu, H.; Shao, M.; Xu, X.; Liang, K.; Gao, Y.; Yuan, H.; Li, J.; Li, J.; Cheng, L.; Van Loveren, C. Biomineralization of Dentin. *Journal of Structural Biology* **2019**, *207* (2), 115–122. https://doi.org/10.1016/j.jsb.2019.05.010.

(53) He, G.; Dahl, T.; Veis, A.; George, A. Nucleation of Apatite Crystals in Vitro by Self-Assembled Dentin Matrix Protein 1. *Nature Mater* **2003**, *2* (8), 552–558. https://doi.org/10.1038/nmat945.

(54) Fisher, L. W.; Torchia, D. A.; Fohr, B.; Young, M. F.; Fedarko, N. S. Flexible Structures of SIBLING Proteins, Bone Sialoprotein, and Osteopontin. *Biochemical and Biophysical Research Communications* **2001**, *280* (2), 460–465. https://doi.org/10.1006/bbrc.2000.4146.

(55) Fisher, L. W.; Fedarko, N. S. Six Genes Expressed in Bones and Teeth Encode the Current Members of the SIBLING Family of Proteins. *Connect Tissue Res* **2003**, *44 Suppl 1*, 33–40.

(56) Hunter, G. K.; Goldberg, H. A. Nucleation of Hydroxyapatite by Bone Sialoprotein. *Proc. Natl. Acad. Sci. U.S.A.* **1993**, *90* (18), 8562–8565. https://doi.org/10.1073/pnas.90.18.8562.

(57) Goldberg, H. A.; Warner, K. J.; Stillman, M. J.; Hunter, G. K. Determination of the Hydroxyapatite-Nucleating Region of Bone Sialoprotein. *Connective Tissue Research* **1996**, *35* (1–4), 385–392. https://doi.org/10.3109/03008209609029216.

(58) Butler, W. T. Dentin Matrix Proteins. *European J Oral Sciences* **1998**, *106* (S1), 204–210. https://doi.org/10.1111/j.1600-0722.1998.tb02177.x.

(59) Smith, A. J.; Scheven, B. A.; Takahashi, Y.; Ferracane, J. L.; Shelton, R. M.; Cooper, P. R. Dentine as a Bioactive Extracellular Matrix. *Archives of Oral Biology* **2012**, *57* (2), 109–121. https://doi.org/10.1016/j.archoralbio.2011.07.008.

(60) Chaussain, C.; Eapen, A.; Huet, E.; Floris, C.; Ravindran, S.; Hao, J.; Menashi, S.; George, A. MMP2-Cleavage of DMP1 Generates a Bioactive Peptide Promoting Differentiation of Dental Pulp Stem/Progenitor Cell. *eCM* **2009**, *18*, 84–95. https://doi.org/10.22203/eCM.v018a08.

(61) Wu, H.; Teng, P.-N.; Jayaraman, T.; Onishi, S.; Li, J.; Bannon, L.; Huang, H.; Close, J.; Sfeir, C. Dentin Matrix Protein 1 (DMP1) Signals via Cell Surface Integrin. *Journal of Biological Chemistry* **2011**, *286* (34), 29462–29469. https://doi.org/10.1074/jbc.M110.194746.

(62) Yamamoto, R.; Oida, S.; Yamakoshi, Y. Dentin Sialophosphoprotein–Derived Proteins in the Dental Pulp. *J Dent Res* **2015**, *94* (8), 1120–1127. https://doi.org/10.1177/0022034515585715.

(63) Sfeir, C.; Lee, D.; Li, J.; Zhang, X.; Boskey, A. L.; Kumta, P. N. Expression of Phosphophoryn Is Sufficient for the Induction of Matrix Mineralization by Mammalian Cells. *Journal of Biological Chemistry* **2011**, *286* (23), 20228–20238. https://doi.org/10.1074/jbc.M110.209528.

(64) Villarreal-Ramirez, E.; Eliezer, D.; Garduño-Juarez, R.; Gericke, A.; Perez-Aguilar, J. M.; Boskey, A. Phosphorylation Regulates the Secondary Structure and Function of Dentin Phosphoprotein Peptides. *Bone* **2017**, *95*, 65–75. https://doi.org/10.1016/j.bone.2016.10.028.

(65) Ritchie, H. The Functional Significance of Dentin Sialoprotein-Phosphophoryn and Dentin Sialoprotein. *Int J Oral Sci* **2018**, *10* (4), 31. https://doi.org/10.1038/s41368-018-0035-9.

(66) Eapen, A.; Kulkarni, R.; Ravindran, S.; Ramachandran, A.; Sundivakkam, P.; Tiruppathi, C.; George, A. Dentin Phosphophoryn Activates Smad Protein Signaling through Ca2+-Calmodulin-Dependent Protein Kinase II in Undifferentiated Mesenchymal Cells. *Journal of Biological Chemistry* **2013**, *288* (12), 8585–8595. https://doi.org/10.1074/jbc.M112.413997.

(67) Eapen, A.; Ramachandran, A.; George, A. DPP in the Matrix Mediates Cell Adhesion but Is Not Restricted to Stickiness: A Tale of Signaling. *Cell Adhesion & Migration* **2012**, *6* (4), 307–311. https://doi.org/10.4161/cam.20627.

(68) Yang, H.; Fan, Z. The Functional Extracellular Matrix on the Regulation of Odontogenic Differentiation of Stem Cells. *Curr Med* **2022**, *1* (1), 10. https://doi.org/10.1007/s44194-022-00012-z.

(69) Wan, C.; Yuan, G.; Luo, D.; Zhang, L.; Lin, H.; Liu, H.; Chen, L.; Yang, G.; Chen, S.; Chen, Z. The Dentin Sialoprotein (DSP) Domain Regulates Dental Mesenchymal Cell Differentiation through a Novel Surface Receptor. *Sci Rep* **2016**, *6* (1), 29666. https://doi.org/10.1038/srep29666.

(70) Boskey, A.; Spevak, L.; Tan, M.; Doty, S. B.; Butler, W. T. Dentin Sialoprotein (DSP) Has Limited Effects on In Vitro Apatite Formation and Growth. *Calcif Tissue Int* **2000**, *67* (6), 472–478. https://doi.org/10.1007/s002230001169.

(71) Vijaykumar, A.; Dyrkacz, P.; Vidovic-Zdrilic, I.; Maye, P.; Mina, M. Expression of BSP-GFPtpz Transgene during Osteogenesis and Reparative Dentinogenesis. *J Dent Res* **2020**, *99* (1), 89–97. https://doi.org/10.1177/0022034519885089.

(72) Nagasaki, K.; Chavez, M. B.; Nagasaki, A.; Taylor, J. M.; Tan, M. H.; Ma, M.; Ralston, E.; Thew, M. E.; Kim, D.-G.; Somerman, M. J.; Foster, B. L. The Bone Sialoprotein RGD Domain Modulates and Maintains Periodontal Development. *J Dent Res* **2022**, *101* (10), 1238–1247. https://doi.org/10.1177/00220345221100794.

(73) Hwang, Y.-C.; Hwang, I.-N.; Oh, W.-M.; Park, J.-C.; Lee, D.-S.; Son, H.-H. Influence of TGF-B1 on the Expression of BSP, DSP, TGF-B1 Receptor I and Smad Proteins during

Reparative Dentinogenesis. *J Mol Hist* **2008**, *39* (2), 153–160. https://doi.org/10.1007/s10735-007-9148-8.

(74) Hunter, G. K. Role of Osteopontin in Modulation of Hydroxyapatite Formation. *Calcif Tissue Int* **2013**, *93* (4), 348–354. https://doi.org/10.1007/s00223-013-9698-6.

(75) Singh, A.; Gill, G.; Kaur, H.; Amhmed, M.; Jakhu, H. Role of Osteopontin in Bone Remodeling and Orthodontic Tooth Movement: A Review. *Prog Orthod.* **2018**, *19* (1), 18. https://doi.org/10.1186/s40510-018-0216-2.

(76) Icer, M. A.; Gezmen-Karadag, M. The Multiple Functions and Mechanisms of Osteopontin. *Clinical Biochemistry* **2018**, *59*, 17–24. https://doi.org/10.1016/j.clinbiochem.2018.07.003.

(77) Qiu, S. R.; Wierzbicki, A.; Orme, C. A.; Cody, A. M.; Hoyer, J. R.; Nancollas, G. H.; Zepeda, S.; De Yoreo, J. J. Molecular Modulation of Calcium Oxalate Crystallization by Osteopontin and Citrate. *Proc. Natl. Acad. Sci. U.S.A.* **2004**, *101* (7), 1811–1815. https://doi.org/10.1073/pnas.0307900100.

(78) Giachelli, C. M.; Steitz, S. Osteopontin: A Versatile Regulator of Inflammation and Biomineralization. *Matrix Biology* **2000**, *19* (7), 615–622. https://doi.org/10.1016/S0945-053X(00)00108-6.

(79) Boskey, A. L.; Spevak, L.; Paschalis, E.; Doty, S. B.; McKee, M. D. Osteopontin Deficiency Increases Mineral Content and Mineral Crystallinity in Mouse Bone. *Calcif Tissue Int* **2002**, *71* (2), 145–154. https://doi.org/10.1007/s00223-001-1121-z.

(80) Pampena, D. A.; Robertson, K. A.; Litvinova, O.; Lajoie, G.; Goldberg, H. A.; Hunter, G. K. Inhibition of Hydroxyapatite Formation by Osteopontin Phosphopeptides. *Biochemical Journal* **2004**, *378* (3), 1083–1087. https://doi.org/10.1042/bj20031150.

(81) MacDougall, M.; Simmons, D.; Gu, T. T.; Dong, J. MEPE/OF45, a New Dentin/Bone Matrix Protein and Candidate Gene for Dentin Diseases Mapping to Chromosome 4q21. *Connective Tissue Research* **2002**, *43* (2–3), 320–330. https://doi.org/10.1080/03008200290000556.

(82) Liu, H.; Li, W.; Shi, S.; Habelitz, S.; Gao, C.; DenBesten, P. MEPE Is Downregulated as Dental Pulp Stem Cells Differentiate. *Archives of Oral Biology* **2005**, *50* (11), 923–928. https://doi.org/10.1016/j.archoralbio.2005.03.003.

(83) Gullard, A.; Gluhak-Heinrich, J.; Papagerakis, S.; Sohn, P.; Unterbrink, A.; Chen, S.; MacDougall, M. MEPE Localization in the Craniofacial Complex and Function in Tooth Dentin Formation. *J Histochem Cytochem.* **2016**, *64* (4), 224–236. https://doi.org/10.1369/0022155416635569.

(84) Salmon, B.; Bardet, C.; Khaddam, M.; Naji, J.; Coyac, B. R.; Baroukh, B.; Letourneur, F.; Lesieur, J.; Decup, F.; Le Denmat, D.; Nicoletti, A.; Poliard, A.; Rowe, P. S.; Huet, E.; Vital, S. O.; Linglart, A.; McKee, M. D.; Chaussain, C. MEPE-Derived ASARM Peptide Inhibits Odontogenic Differentiation of Dental Pulp Stem Cells and Impairs Mineralization in Tooth Models of X-Linked Hypophosphatemia. *PLoS ONE* **2013**, *8* (2), e56749. https://doi.org/10.1371/journal.pone.0056749.

(85) Orsini, G.; Ruggeri, A.; Mazzoni, A.; Nato, F.; Manzoli, L.; Putignano, A.; Di Lenarda, R.; Tjäderhane, L.; Breschi, L. A Review of the Nature, Role, and Function of Dentin Non-collagenous Proteins. Part 1: Proteoglycans and Glycoproteins. *Endodontic Topics* **2009**, *21* (1), 1–18. https://doi.org/10.1111/j.1601-1546.2012.00270.x.

(86) Hauschka, P. V.; Frenkel, J.; DeMuth, R.; Gundberg, C. M. Presence of Osteocalcin and Related Higher Molecular Weight 4-Carboxyglutamic Acid-Containing Proteins in Developing Bone. *J Biol Chem* **1983**, *258* (1), 176–182.

(87) Papagerakis, P.; Berdal, A.; Mesbah, M.; Peuchmaur, M.; Malaval, L.; Nydegger, J.; Simmer, J.; Macdougall, M. Investigation of Osteocalcin, Osteonectin, and Dentin Sialophosphoprotein in Developing Human Teeth. *Bone* **2002**, *30* (2), 377–385. https://doi.org/10.1016/S8756-3282(01)00683-4.

(88) De Vries, I. G.; Coomans, D.; Wisse, E. Immunocytochemical Localization of Osteocalcin in Human and Bovine Teeth. *Calcif Tissue Int* **1988**, *43* (2), 128–130. https://doi.org/10.1007/BF02555159.

(89) Goldberg, M.; Ono, M.; Septier, D.; Bonnefoix, M.; Kilts, T. M.; Bi, Y.; Embree, M.; Ameye, L.; Young, M. F. Fibromodulin-Deficient Mice Reveal Dual Functions for Fibromodulin in Regulating Dental Tissue and Alveolar Bone Formation. *Cells Tissues Organs* **2009**, *189* (1–4), 198–202. https://doi.org/10.1159/000151370.

(90) Kalamajski, S.; Oldberg, Å. The Role of Small Leucine-Rich Proteoglycans in Collagen Fibrillogenesis. *Matrix Biology* **2010**, *29* (4), 248–253. https://doi.org/10.1016/j.matbio.2010.01.001.

(91) Embery, G.; Hall, R.; Waddington, R.; Septier, D.; Goldberg, M. Proteoglycans in Dentinogenesis. *Critical Reviews in Oral Biology & Medicine* **2001**, *12* (4), 331–349. https://doi.org/10.1177/10454411010120040401.

(92) Goldberg, M.; Rapoport, O.; Septier, D.; Palmier, K.; Hall, R.; Embery, G.; Young, M.; Ameye, L. Proteoglycans in Predentin: The Last 15 Micrometers before Mineralization. *Connect Tissue Res* **2003**, *44 Suppl 1*, 184–188.

(93) Montoya, C.; Arango-Santander, S.; Peláez-Vargas, A.; Arola, D.; Ossa, E. A. Effect of Aging on the Microstructure, Hardness and Chemical Composition of Dentin. *Archives of Oral Biology* **2015**, *60* (12), 1811–1820. https://doi.org/10.1016/j.archoralbio.2015.10.002.

(94) Zhao, S.; Sloan, A. J.; Murray, P. E.; Lumley, P. J.; Smith, A. J. Ultrastructural Localisation of TGF-β Exposure in Dentine by Chemical Treatment. *The Histochemical Journal* **2000**, *32* (8), 489–494. https://doi.org/10.1023/A:1004100518245.

(95) Magloire, H.; Romeas, A.; Melin, M.; Couble, M.-L.; Bleicher, F.; Farges, J.-C. Molecular Regulation of Odontoblast Activity under Dentin Injury. *Adv Dent Res.* **2001**, *15* (1), 46–50. https://doi.org/10.1177/08959374010150011201.

(96) Yoshioka, S.; Takahashi, Y.; Abe, M.; Michikami, I.; Imazato, S.; Wakisaka, S.; Hayashi, M.; Ebisu, S. Activation of the Wnt/ -Catenin Pathway and Tissue Inhibitor of Metalloprotease 1 during Tertiary Dentinogenesis. *Journal of Biochemistry* **2013**, *153* (1), 43–50. https://doi.org/10.1093/jb/mvs117.

(97) Neves, V. C. M.; Yianni, V.; Sharpe, P. T. Macrophage Modulation of Dental Pulp Stem Cell Activity during Tertiary Dentinogenesis. *Sci Rep* **2020**, *10* (1), 20216. https://doi.org/10.1038/s41598-020-77161-4.

(98) Da Rosa, W. L. O.; Piva, E.; Da Silva, A. F. Disclosing the Physiology of Pulp Tissue for Vital Pulp Therapy. *Int Endodontic J* **2018**, *51* (8), 829–846. https://doi.org/10.1111/iej.12906.

(99) Zhang, W.; Yelick, P. C. Vital Pulp Therapy—Current Progress of Dental Pulp Regeneration and Revascularization. *International Journal of Dentistry* **2010**, *2010*, 1–9. https://doi.org/10.1155/2010/856087.

(100) Testori, T.; Badino, M.; Castagnola, M. Vertical Root Fractures in Endodontically Treated Teeth: A Clinical Survey of 36 Cases. *Journal of Endodontics* **1993**, *19* (2), 87–90. https://doi.org/10.1016/S0099-2399(06)81202-1.

(101) Zelic, K.; Milovanovic, P.; Rakocevic, Z.; Askrabic, S.; Potocnik, J.; Popovic, M.; Djuric, M. Nano-Structural and Compositional Basis of Devitalized Tooth Fragility. *Dental Materials* **2014**, *30* (5), 476–486. https://doi.org/10.1016/j.dental.2014.01.014.

(102) Cohenca, N.; Paranjpe, A.; Berg, J. Vital Pulp Therapy. *Dental Clinics of North America* **2013**, *57* (1), 59–73. https://doi.org/10.1016/j.cden.2012.09.004.

(103) Leong, D. J. X.; Yap, A. U. Vital Pulp Therapy in Carious Pulp–Exposed Permanent Teeth: An Umbrella Review. *Clin Oral Invest* **2021**, *25* (12), 6743–6756. https://doi.org/10.1007/s00784-021-03960-2.

(104) Nie, E.; Yu, J.; Jiang, R.; Liu, X.; Li, X.; Islam, R.; Alam, M. K. Effectiveness of Direct Pulp Capping Bioactive Materials in Dentin Regeneration: A Systematic Review. *Materials* **2021**, *14* (22), 6811. https://doi.org/10.3390/ma14226811.

(105) Komabayashi, T.; Zhu, Q.; Eberhart, R.; Imai, Y. Current Status of Direct Pulp-Capping Materials for Permanent Teeth. *Dental Materials Journal* **2016**, *35* (1), 1–12. https://doi.org/10.4012/dmj.2015-013.

(106) Faraco, I. M.; Holland, R. Response of the Pulp of Dogs to Capping with Mineral Trioxide Aggregate or a Calcium Hydroxide Cement. *Dental Traumatology* **2001**, *17* (4), 163–166. https://doi.org/10.1034/j.1600-9657.2001.170405.x.

(107) Briso, A. L. F.; Rahal, V.; Mestrener, S. R.; Dezan Junior, E. Biological Response of Pulps Submitted to Different Capping Materials. *Braz. oral res.* **2006**, *20* (3), 219–225. https://doi.org/10.1590/S1806-83242006000300007.

(108) Cook, J.; Nandakumar, R.; Fouad, A. F. Molecular- and Culture-Based Comparison of the Effects of Antimicrobial Agents on Bacterial Survival in Infected Dentinal Tubules. *Journal of Endodontics* **2007**, *33* (6), 690–692. https://doi.org/10.1016/j.joen.2007.01.022.

(109) Sathorn, C.; Parashos, P.; Messer, H. Antibacterial Efficacy of Calcium Hydroxide Intracanal Dressing: A Systematic Review and Meta-analysis. *Int Endodontic J* **2007**, *40* (1), 2–10. https://doi.org/10.1111/j.1365-2591.2006.01197.x.

(110) Li, Z.; Cao, L.; Fan, M.; Xu, Q. Direct Pulp Capping with Calcium Hydroxide or Mineral Trioxide Aggregate: A Meta-Analysis. *Journal of Endodontics* **2015**, *41* (9), 1412–1417. https://doi.org/10.1016/j.joen.2015.04.012.

(111) Nair, P. N. R.; Duncan, H. F.; Pitt Ford, T. R.; Luder, H. U. Histological, Ultrastructural and Quantitative Investigations on the Response of Healthy Human Pulps to Experimental Capping with Mineral Trioxide Aggregate: A Randomized Controlled Trial. *Int Endodontic J* **2008**, *41* (2), 128–150. https://doi.org/10.1111/j.1365-2591.2007.01329.x.

(112) Cushley, S.; Duncan, H. F.; Lappin, M. J.; Chua, P.; Elamin, A. D.; Clarke, M.; El-Karim, I. A. Efficacy of Direct Pulp Capping for Management of Cariously Exposed Pulps in Permanent Teeth: A Systematic Review and Meta-analysis. *Int Endodontic J* **2021**, *54* (4), 556–571. https://doi.org/10.1111/iej.13449.

(113) Roberts, H.; Toth, J.; Berzins, D.; Charlton, D. Mineral Trioxide Aggregate Material Use in Endodontic Treatment: A Review of the Literature☆. *Dental Materials* **2008**, *24* (2), 149–164. https://doi.org/10.1016/j.dental.2007.04.007.

(114) Torabinejad, M.; Parirokh, M. Mineral Trioxide Aggregate: A Comprehensive Literature Review—Part II: Leakage and Biocompatibility Investigations. *Journal of Endodontics* **2010**, *36* (2), 190–202. https://doi.org/10.1016/j.joen.2009.09.010.

(115) Parirokh, M.; Torabinejad, M. Mineral Trioxide Aggregate: A Comprehensive Literature Review—Part III: Clinical Applications, Drawbacks, and Mechanism of Action. *Journal of Endodontics* **2010**, *36* (3), 400–413. https://doi.org/10.1016/j.joen.2009.09.009.

(116) Parirokh, M.; Torabinejad, M. Mineral Trioxide Aggregate: A Comprehensive Literature Review—Part I: Chemical, Physical, and Antibacterial Properties. *Journal of Endodontics* **2010**, *36* (1), 16–27. https://doi.org/10.1016/j.joen.2009.09.006.

(117) Torabinejad, M.; Hong, C. U.; Ford, T. R. P.; Kettering, J. D. Antibacterial Effects of Some Root End Filling Materials. *Journal of Endodontics* **1995**, *21* (8), 403–406. https://doi.org/10.1016/S0099-2399(06)80824-1.

(118) Ioannidis, K.; Mistakidis, I.; Beltes, P.; Karagiannis, V. Spectrophotometric Analysis of Coronal Discolouration Induced by Grey and White MTA. *Int Endodontic J* **2013**, *46* (2), 137–144. https://doi.org/10.1111/j.1365-2591.2012.02098.x.

(119) Kogan, P.; He, J.; Glickman, G. N.; Watanabe, I. The Effects of Various Additives on Setting Properties of MTA. *Journal of Endodontics* **2006**, *32* (6), 569–572. https://doi.org/10.1016/j.joen.2005.08.006.

(120) Chng, H. K.; Islam, I.; Yap, A. U. J.; Tong, Y. W.; Koh, E. T. Properties of a New Root-End Filling Material. *Journal of Endodontics* **2005**, *31* (9), 665–668. https://doi.org/10.1097/01.don.0000157993.89164.be.

(121) Komabayashi, T.; Spångberg, L. S. W. Comparative Analysis of the Particle Size and Shape of Commercially Available Mineral Trioxide Aggregates and Portland Cement: A Study with a Flow Particle Image Analyzer. *Journal of Endodontics* **2008**, *34* (1), 94–98. https://doi.org/10.1016/j.joen.2007.10.013.

(122) Felman, D.; Parashos, P. Coronal Tooth Discoloration and White Mineral Trioxide Aggregate. *Journal of Endodontics* **2013**, *39* (4), 484–487. https://doi.org/10.1016/j.joen.2012.11.053.

(123) Vallés, M.; Mercadé, M.; Duran-Sindreu, F.; Bourdelande, J. L.; Roig, M. Influence of Light and Oxygen on the Color Stability of Five Calcium Silicate–Based Materials. *Journal of Endodontics* **2013**, *39* (4), 525–528. https://doi.org/10.1016/j.joen.2012.12.021.

(124) Chacko, Dr. V.; Kurikose, Dr. S. Human Pulpal Response to Mineral Trioxide Aggregate (MTA): A Histologic Study. *Journal of Clinical Pediatric Dentistry* **2006**, *30* (3), 203–209. https://doi.org/10.17796/jcpd.30.3.38h13g5p84651652.

(125) Camilleri, J.; Sorrentino, F.; Damidot, D. Investigation of the Hydration and Bioactivity of Radiopacified Tricalcium Silicate Cement, Biodentine and MTA Angelus. *Dental Materials* **2013**, *29* (5), 580–593. https://doi.org/10.1016/j.dental.2013.03.007.

(126) Mahmoud, S.; El-Negoly, S.; Zaen El-Din, A.; El-Zekrid, M.; Grawish, L.; Grawish, H.; Grawish, M. Biodentine versus Mineral Trioxide Aggregate as a Direct Pulp Capping Material for Human Mature Permanent Teeth – A Systematic Review. *J Conserv Dent* **2018**, *21* (5), 466. https://doi.org/10.4103/JCD.JCD_198_18.

(127) Nowicka, A.; Lipski, M.; Parafiniuk, M.; Sporniak-Tutak, K.; Lichota, D.; Kosierkiewicz, A.; Kaczmarek, W.; Buczkowska-Radlińska, J. Response of Human Dental Pulp Capped with Biodentine and Mineral Trioxide Aggregate. *Journal of Endodontics* **2013**, *39* (6), 743–747. https://doi.org/10.1016/j.joen.2013.01.005.

(128) Kunert, M.; Lukomska-Szymanska, M. Bio-Inductive Materials in Direct and Indirect Pulp Capping—A Review Article. *Materials* **2020**, *13* (5), 1204. https://doi.org/10.3390/ma13051204.

(129) Choi, Y.; Park, S.-J.; Lee, S.-H.; Hwang, Y.-C.; Yu, M.-K.; Min, K.-S. Biological Effects and Washout Resistance of a Newly Developed Fast-Setting Pozzolan Cement. *Journal of Endodontics* **2013**, *39* (4), 467–472. https://doi.org/10.1016/j.joen.2012.11.023.

(130) Kaup, M.; Schäfer, E.; Dammaschke, T. An in Vitro Study of Different Material Properties of Biodentine Compared to ProRoot MTA. *Head Face Med* **2015**, *11* (1), 16. https://doi.org/10.1186/s13005-015-0074-9.

(131) Grech, L.; Mallia, B.; Camilleri, J. Investigation of the Physical Properties of Tricalcium Silicate Cement-Based Root-End Filling Materials. *Dental Materials* **2013**, *29* (2), e20–e28. https://doi.org/10.1016/j.dental.2012.11.007.

(132) Kaup, M.; Dammann, C. H.; Schäfer, E.; Dammaschke, T. Shear Bond Strength of Biodentine, ProRoot MTA, Glass Ionomer Cement and Composite Resin on Human Dentine Ex Vivo. *Head Face Med* **2015**, *11* (1), 14. https://doi.org/10.1186/s13005-015-0071-z.

(133) Gandolfi, M. G.; Siboni, F.; Botero, T.; Bossù, M.; Riccitiello, F.; Prati, C. Calcium Silicate and Calcium Hydroxide Materials for Pulp Capping: Biointeractivity, Porosity, Solubility and Bioactivity of Current Formulations. *Journal of Applied Biomaterials & Functional Materials* **2015**, *13* (1), 43–60. https://doi.org/10.5301/jabfm.5000201.

(134) Poggio, C.; Lombardini, M.; Colombo, M.; Beltrami, R.; Rindi, S. Solubility and PH of Direct Pulp Capping Materials: A Comparative Study. *Journal of Applied Biomaterials & Functional Materials* **2015**, *13* (2), 181–185. https://doi.org/10.5301/jabfm.5000230.

(135) Yousef, M.; Abuzeid, S.; Alothmani, O. Biodentine and Mineral Trioxide Aggregate: An Analysis of Solubility, PH Changes and Leaching Elements. **2015**, *12*, 1097–8135.

(136) Yu, C.; Abbott, P. An Overview of the Dental Pulp: Its Functions and Responses to Injury. *Australian Dental Journal* **2007**, *52* (s1). https://doi.org/10.1111/j.1834-7819.2007.tb00525.x.

(137) Cooper, P. R.; Holder, M. J.; Smith, A. J. Inflammation and Regeneration in the Dentin-Pulp Complex: A Double-Edged Sword. *Journal of Endodontics* **2014**, *40* (4), S46–S51. https://doi.org/10.1016/j.joen.2014.01.021.

(138) Bergenholtz, G. Inflammatory Response of the Dental Pulp to Bacterial Irritation. *Journal of Endodontics* **1981**, *7* (3), 100–104. https://doi.org/10.1016/S0099-2399(81)80122-7.

(139) Paula-Silva, F. W. G.; Ghosh, A.; Silva, L. A. B.; Kapila, Y. L. TNF-α Promotes an Odontoblastic Phenotype in Dental Pulp Cells. *J Dent Res* **2009**, *88* (4), 339–344. https://doi.org/10.1177/0022034509334070.

(140) Goldberg, M.; Farges, J.; Lacerdapinheiro, S.; Six, N.; Jegat, N.; Decup, F.; Septier, D.; Carrouel, F.; Durand, S.; Chaussainmiller, C. Inflammatory and Immunological Aspects of Dental Pulp Repair. *Pharmacological Research* **2008**, *58* (2), 137–147. https://doi.org/10.1016/j.phrs.2008.05.013.

(141) Saito, K.; Nakatomi, M.; Ida-Yonemochi, H.; Kenmotsu, S.; Ohshima, H. The Expression of GM-CSF and Osteopontin in Immunocompetent Cells Precedes the Odontoblast Differentiation Following Allogenic Tooth Transplantation in Mice. *J Histochem Cytochem.* **2011**, *59* (5), 518–529. https://doi.org/10.1369/0022155411403314.

(142) Giraud, T.; Jeanneau, C.; Rombouts, C.; Bakhtiar, H.; Laurent, P.; About, I. Pulp Capping Materials Modulate the Balance between Inflammation and Regeneration. *Dental Materials* **2019**, *35* (1), 24–35. https://doi.org/10.1016/j.dental.2018.09.008.

(143) El Karim, I. A.; McCrudden, M. T. C.; McGahon, M. K.; Curtis, T. M.; Jeanneau, C.; Giraud, T.; Irwin, C. R.; Linden, G. J.; Lundy, F. T.; About, I. Biodentine Reduces Tumor Necrosis Factor Alpha–Induced TRPA1 Expression in Odontoblastlike Cells. *Journal of Endodontics* **2016**, *42* (4), 589–595. https://doi.org/10.1016/j.joen.2015.12.017.

(144) Kang, C.-M.; Hwang, J.; Song, J.; Lee, J.-H.; Choi, H.-J.; Shin, Y. Effects of Three Calcium Silicate Cements on Inflammatory Response and Mineralization-Inducing Potentials in a Dog Pulpotomy Model. *Materials* **2018**, *11* (6), 899. https://doi.org/10.3390/ma11060899.

(145) Jalan, A.; Warhadpande, M.; Dakshindas, D. A Comparison of Human Dental Pulp Response to Calcium Hydroxide and Biodentine as Direct Pulp-Capping Agents. *J Conserv Dent* **2017**, *20* (2), 129. https://doi.org/10.4103/0972-0707.212247.

(146) Laurent, P.; Camps, J.; About, I. Biodentine ^{TM} Induces TGF- β 1 Release from Human Pulp Cells and Early Dental Pulp Mineralization. *Int Endodontic J* **2012**, *45* (5), 439–448. https://doi.org/10.1111/j.1365-2591.2011.01995.x.

(147) Rathinam, E.; Rajasekharan, S.; Chitturi, R. T.; Martens, L.; De Coster, P. Gene Expression Profiling and Molecular Signaling of Dental Pulp Cells in Response to Tricalcium Silicate Cements: A Systematic Review. *Journal of Endodontics* **2015**, *41* (11), 1805–1817. https://doi.org/10.1016/j.joen.2015.07.015.

(148) Natale, L. C.; Rodrigues, M. C.; Xavier, T. A.; Simões, A.; De Souza, D. N.; Braga, R. R. Ion Release and Mechanical Properties of Calcium Silicate and Calcium Hydroxide Materials Used for Pulp Capping. *Int Endodontic J* **2015**, *48* (1), 89–94. https://doi.org/10.1111/iej.12281.

(149) Khan, A. A.; Sun, X.; Hargreaves, K. M. Effect of Calcium Hydroxide on Proinflammatory Cytokines and Neuropeptides. *Journal of Endodontics* **2008**, *34* (11), 1360–1363. https://doi.org/10.1016/j.joen.2008.08.020.

(150) Reyes-Carmona, J. F.; Santos, A. R. S.; Figueiredo, C. P.; Felippe, M. S.; Felippe, W. T.; Cordeiro, M. M. In Vivo Host Interactions with Mineral Trioxide Aggregate and Calcium Hydroxide: Inflammatory Molecular Signaling Assessment. *Journal of Endodontics* **2011**, *37* (9), 1225–1235. https://doi.org/10.1016/j.joen.2011.05.031.

(151) Schröder, U. Effects of Calcium Hydroxide-Containing Pulp-Capping Agents on Pulp Cell Migration, Proliferation, and Differentiation. *J Dent Res* **1985**, *64* (4), 541–548. https://doi.org/10.1177/00220345850640040 7.

(152) An, S.; Gao, Y.; Ling, J.; Wei, X.; Xiao, Y. Calcium Ions Promote Osteogenic Differentiation and Mineralization of Human Dental Pulp Cells: Implications for Pulp Capping Materials. *J Mater Sci: Mater Med* **2012**, *23* (3), 789–795. https://doi.org/10.1007/s10856-011-4531-0.

(153) Rathinam, E.; Govindarajan, S.; Rajasekharan, S.; Declercq, H.; Elewaut, D.; De Coster, P.; Martens, L.; Leybaert, L. The Calcium Dynamics of Human Dental Pulp Stem Cells Stimulated with Tricalcium Silicate-Based Cements Determine Their Differentiation and Mineralization Outcome. *Sci Rep* **2021**, *11* (1), 645. https://doi.org/10.1038/s41598-020-80096-5.

(154) Prati, C.; Gandolfi, M. G. Calcium Silicate Bioactive Cements: Biological Perspectives and Clinical Applications. *Dental Materials* **2015**, *31* (4), 351–370. https://doi.org/10.1016/j.dental.2015.01.004.

(155) Bielby, R. C.; Christodoulou, I. S.; Pryce, R. S.; Radford, W. J. P.; Hench, L. L.; Polak, J. M. Time- and Concentration-Dependent Effects of Dissolution Products of 58S Sol–Gel Bioactive Glass on Proliferation and Differentiation of Murine and Human Osteoblasts. *Tissue Engineering* **2004**, *10* (7–8), 1018–1026. https://doi.org/10.1089/ten.2004.10.1018.

(156) Jugdaohsingh, R. Silicon and Bone Health. *J Nutr Health Aging* **2007**, *11* (2), 99–110.

(157) Rodella, L. F.; Bonazza, V.; Labanca, M.; Lonati, C.; Rezzani, R. A Review of the Effects of Dietary Silicon Intake on Bone Homeostasis and Regeneration. *The Journal of nutrition, health and aging* **2014**, *18* (9), 820–826. https://doi.org/10.1007/s12603-014-0555-8.

(158) Rondanelli, M.; Faliva, M. A.; Peroni, G.; Gasparri, C.; Perna, S.; Riva, A.; Petrangolini, G.; Tartara, A. Silicon: A Neglected Micronutrient Essential for Bone Health. *Exp Biol Med (Maywood)* **2021**, *246* (13), 1500–1511. https://doi.org/10.1177/1535370221997072.

(159) MacDougall, M. J.; Javed, A. Dentin and Bone: Similar Collagenous Mineralized Tissues. In *Bone and Development*; Bronner, F., Farach-Carson, M. C., Roach, H. I. (Trudy), Eds.; Springer London: London, 2010; pp 183–200. https://doi.org/10.1007/978-1-84882-822-3_11.

(160) Long, F. Building Strong Bones: Molecular Regulation of the Osteoblast Lineage. *Nat Rev Mol Cell Biol* **2012**, *13* (1), 27–38. https://doi.org/10.1038/nrm3254.

(161) Opsahl Vital, S.; Gaucher, C.; Bardet, C.; Rowe, P. S.; George, A.; Linglart, A.; Chaussain, C. Tooth Dentin Defects Reflect Genetic Disorders Affecting Bone Mineralization. *Bone* **2012**, *50* (4), 989–997. https://doi.org/10.1016/j.bone.2012.01.010.

(162) Martin, K. R. Silicon: The Health Benefits of a Metalloid. In *Interrelations between Essential Metal Ions and Human Diseases*; Sigel, A., Sigel, H., Sigel, R. K. O., Eds.; Metal Ions in Life Sciences; Springer Netherlands: Dordrecht, 2013; Vol. 13, pp 451–473. https://doi.org/10.1007/978-94-007-7500-8_14.

(163) Wiegmann, J. The Chemistry of Silica. Solubility, Polymerization, Colloid and Surface Properties, and Biochemistry. Von R ALPH K. I LER . New York/Chichester/Brisbane/Toronto: John Wiley & Sons 1979. XXIV, 866 S., Lwd., £ 39.50. *Acta Polymerica* **1980**, *31* (6), 406–406. https://doi.org/10.1002/actp.1980.010310623.

(164) Glasser, L. S. D.; Lachowski, E. E. Silicate Species in Solution. Part 1. Experimental Observations. *J. Chem. Soc., Dalton Trans.* **1980**, No. 3, 393. https://doi.org/10.1039/dt9800000393.

(165) Sjöberg, S. Silica in Aqueous Environments. *Journal of Non-Crystalline Solids* **1996**, *196*, 51–57. https://doi.org/10.1016/0022-3093(95)00562-5.

(166) Bissé, E.; Epting, T.; Beil, A.; Lindinger, G.; Lang, H.; Wieland, H. Reference Values for Serum Silicon in Adults. *Analytical Biochemistry* **2005**, *337* (1), 130–135. https://doi.org/10.1016/j.ab.2004.10.034.

(167) Jugdaohsingh, R.; Anderson, S. H.; Tucker, K. L.; Elliott, H.; Kiel, D. P.; Thompson, R. P.; Powell, J. J. Dietary Silicon Intake and Absorption. *The American Journal of Clinical Nutrition* **2002**, *75* (5), 887–893. https://doi.org/10.1093/ajcn/75.5.887.

(168) Carlisle, E. M. Silicon: An Essential Element for the Chick. *Science* **1972**, *178* (4061), 619–621. https://doi.org/10.1126/science.178.4061.619.

(169) Schwarz, K.; Milne, D. B. Growth-Promoting Effects of Silicon in Rats. *Nature* **1972**, *239* (5371), 333–334. https://doi.org/10.1038/239333a0.

(170) Maehira, F.; Miyagi, I.; Eguchi, Y. Effects of Calcium Sources and Soluble Silicate on Bone Metabolism and the Related Gene Expression in Mice. *Nutrition* **2009**, *25* (5), 581–589. https://doi.org/10.1016/j.nut.2008.10.023.

(171) Kalu, D. N. The Ovariectomized Rat Model of Postmenopausal Bone Loss. *Bone and Mineral* **1991**, *15* (3), 175–191. https://doi.org/10.1016/0169-6009(91)90124-I.

(172) Calomme, M.; Geusens, P.; Demeester, N.; Behets, G. J.; D'Haese, P.; Sindambiwe, J. B.; Van Hoof, V.; Berghe, D. V. Partial Prevention of Long-Term Femoral Bone Loss in Aged Ovariectomized Rats Supplemented with Choline-Stabilized Orthosilicic Acid. *Calcif Tissue Int* **2006**, *78* (4), 227–232. https://doi.org/10.1007/s00223-005-0288-0.

(173) Bae, Y.-J.; Kim, J.-Y.; Choi, M.-K.; Chung, Y.-S.; Kim, M.-H. Short-Term Administration of Water-Soluble Silicon Improves Mineral Density of the Femur and Tibia in Ovariectomized Rats. *Biol Trace Elem Res* **2008**, *124* (2), 157–163. https://doi.org/10.1007/s12011-008-8138-3.

(174) Kim, M.-H.; Bae, Y.-J.; Choi, M.-K.; Chung, Y.-S. Silicon Supplementation Improves the Bone Mineral Density of Calcium-Deficient Ovariectomized Rats by Reducing Bone Resorption. *Biol Trace Elem Res* **2009**, *128* (3), 239–247. https://doi.org/10.1007/s12011-008-8273-x.

(175) Nielsen, B. D.; Potter, G. D.; Morris, E. L.; Odom, T. W.; Senor, D. M.; Reynolds, J. A.; Smith, W. B.; Martin, M. T.; Bird, E. H. Training Distance to Failure in Young Racing Quarter Horses Fed Sodium Zeolite A. *Journal of Equine Veterinary Science* **1993**, *13* (10), 562–567. https://doi.org/10.1016/S0737-0806(06)81526-1.

(176) Eisinger, J.; Clairet, D. Effects of Silicon, Fluoride, Etidronate and Magnesium on Bone Mineral Density: A Retrospective Study. *Magnes Res* **1993**, *6* (3), 247–249.

(177) Schiano, A.; Eisinger, F.; Detolle, P.; Laponche, A. M.; Brisou, B.; Eisinger, J. [Silicon, bone tissue and immunity]. *Rev Rhum Mal Osteoartic* **1979**, *46* (7–9), 483–486.

(178) Spector, T.; Calomme, M.; Anderson, S.; Swaminathan, R.; Jugdaohsingh, R.; Berghe, D.; Powell, J. Effect on Bone Turnover and BMD of Low Dose Oral Silicon as an Adjunct to Calcium/Vitamin D3 in a Randomized, Placebo-Controlled Trial. *Journal of Bone and Mineral Research* **2005**.

(179) Spector, T. D.; Calomme, M. R.; Anderson, S. H.; Clement, G.; Bevan, L.; Demeester, N.; Swaminathan, R.; Jugdaohsingh, R.; Berghe, D. A. V.; Powell, J. J. Choline-Stabilized Orthosilicic Acid Supplementation as an Adjunct to Calcium/Vitamin D3 Stimulates Markers of Bone Formation in Osteopenic Females: A Randomized, Placebo-Controlled Trial. *BMC Musculoskelet Disord* **2008**, *9* (1), 85. https://doi.org/10.1186/1471-2474-9-85.

(180) Schröder, H. C.; Wiens, M.; Wang, X.; Schloßmacher, U.; Müller, W. E. G. Biosilica-Based Strategies for Treatment of Osteoporosis and Other Bone Diseases. In *Molecular Biomineralization*; Müller, W. E. G., Ed.; Progress in Molecular and Subcellular Biology; Springer Berlin Heidelberg: Berlin, Heidelberg, 2011; Vol. 52, pp 283–312. https://doi.org/10.1007/978-3-642-21230-7_10.

(181) Zou, S.; Ireland, D.; Brooks, R. A.; Rushton, N.; Best, S. The Effects of Silicate Ions on Human Osteoblast Adhesion, Proliferation, and Differentiation. *J Biomed Mater Res* **2009**, *90B* (1), 123–130. https://doi.org/10.1002/jbm.b.31262.

(182) Kim, E.-J.; Bu, S.-Y.; Sung, M.-K.; Choi, M.-K. Effects of Silicon on Osteoblast Activity and Bone Mineralization of MC3T3-E1 Cells. *Biol Trace Elem Res* **2013**, *152* (1), 105–112. https://doi.org/10.1007/s12011-012-9593-4.

(183) Reffitt, D. M.; Ogston, N.; Jugdaohsingh, R.; Cheung, H. F. J.; Evans, B. A. J.; Thompson, R. P. H.; Powell, J. J.; Hampson, G. N. Orthosilicic Acid Stimulates Collagen Type 1 Synthesis and Osteoblastic Differentiation in Human Osteoblast-like Cells in Vitro. *Bone* **2003**, *32* (2), 127–135. https://doi.org/10.1016/S8756-3282(02)00950-X.

(184) Arumugam, M. Q.; Ireland, D. C.; Brooks, R. A.; Rushton, N.; Bonfield, W. Orthosilicic Acid Increases Collagen Type I MRNA Expression in Human Bone-Derived Osteoblasts In Vitro. *KEM* **2003**, *254–256*, 869–872. https://doi.org/10.4028/www.scientific.net/KEM.254-256.869.

(185) Dong, M.; Jiao, G.; Liu, H.; Wu, W.; Li, S.; Wang, Q.; Xu, D.; Li, X.; Liu, H.; Chen, Y. Biological Silicon Stimulates Collagen Type 1 and Osteocalcin Synthesis in Human Osteoblast-

Like Cells Through the BMP-2/Smad/RUNX2 Signaling Pathway. *Biol Trace Elem Res* **2016**, *173* (2), 306–315. https://doi.org/10.1007/s12011-016-0686-3.

(186) Han, P.; Wu, C.; Xiao, Y. The Effect of Silicate Ions on Proliferation, Osteogenic Differentiation and Cell Signalling Pathways (WNT and SHH) of Bone Marrow Stromal Cells. *Biomater. Sci.* **2013**, *1* (4), 379–392. https://doi.org/10.1039/C2BM00108J.

(187) Henstock, J. R.; Ruktanonchai, U. R.; Canham, L. T.; Anderson, S. I. Porous Silicon Confers Bioactivity to Polycaprolactone Composites in Vitro. *J Mater Sci: Mater Med* **2014**, *25* (4), 1087–1097. https://doi.org/10.1007/s10856-014-5140-5.

(188) Mladenović, Ž.; Johansson, A.; Willman, B.; Shahabi, K.; Björn, E.; Ransjö, M. Soluble Silica Inhibits Osteoclast Formation and Bone Resorption in Vitro. *Acta Biomaterialia* **2014**, *10* (1), 406–418. https://doi.org/10.1016/j.actbio.2013.08.039.

(189) Zhou, X.; Moussa, F. M.; Mankoci, S.; Ustriyana, P.; Zhang, N.; Abdelmagid, S.; Molenda, J.; Murphy, W. L.; Safadi, F. F.; Sahai, N. Orthosilicic Acid, Si(OH)4, Stimulates Osteoblast Differentiation in Vitro by Upregulating MiR-146a to Antagonize NF-KB Activation. *Acta Biomaterialia* **2016**, *39*, 192–202. https://doi.org/10.1016/j.actbio.2016.05.007.

(190) Beck, G. R.; Ha, S.-W.; Camalier, C. E.; Yamaguchi, M.; Li, Y.; Lee, J.-K.; Weitzmann, M. N. Bioactive Silica-Based Nanoparticles Stimulate Bone-Forming Osteoblasts, Suppress Bone-Resorbing Osteoclasts, and Enhance Bone Mineral Density in Vivo. *Nanomedicine: Nanotechnology, Biology and Medicine* **2012**, *8* (6), 793–803. https://doi.org/10.1016/j.nano.2011.11.003.

(191) Arnst, J.; Jing, Z.; Cohen, C.; Ha, S.-W.; Viggeswarapu, M.; Beck, G. R. Bioactive Silica Nanoparticles Target Autophagy, NF-KB, and MAPK Pathways to Inhibit Osteoclastogenesis. *Biomaterials* **2023**, *301*, 122238. https://doi.org/10.1016/j.biomaterials.2023.122238.

(192) Ha, S.-W.; Viggeswarapu, M.; Habib, M. M.; Beck, G. R. Bioactive Effects of Silica Nanoparticles on Bone Cells Are Size, Surface, and Composition Dependent. *Acta Biomaterialia* **2018**, *82*, 184–196. https://doi.org/10.1016/j.actbio.2018.10.018.

(193) Xynos, I. D.; Edgar, A. J.; Buttery, L. D. K.; Hench, L. L.; Polak, J. M. Ionic Products of Bioactive Glass Dissolution Increase Proliferation of Human Osteoblasts and Induce Insulin-like Growth Factor II MRNA Expression and Protein Synthesis. *Biochemical and Biophysical Research Communications* **2000**, *276* (2), 461–465. https://doi.org/10.1006/bbrc.2000.3503.

(194) Carlisle, E. M. Silicon: A Possible Factor in Bone Calcification. *Science* **1970**, *167* (3916), 279–280. https://doi.org/10.1126/science.167.3916.279.

(195) Landis, W. J.; Lee, D. D.; Brenna, J. T.; Chandra, S.; Morrison, G. H. Detection and Localization of Silicon and Associated Elements in Vertebrate Bone Tissue by Imaging Ion Microscopy. *Calcif Tissue Int* **1986**, *38* (1), 52–59. https://doi.org/10.1007/BF02556595.

(196) Arora, M.; Arora, E. The Promise of Silicon: Bone Regeneration and Increased Bone Density. *Journal of Arthroscopy and Joint Surgery* **2017**, *4* (3), 103–105. https://doi.org/10.1016/j.jajs.2017.10.003.

(197) Schwarz, K. A Bound Form of Silicon in Glycosaminoglycans and Polyuronides. *Proc. Natl. Acad. Sci. U.S.A.* **1973**, *70* (5), 1608–1612. https://doi.org/10.1073/pnas.70.5.1608.

(198) Matsko, N. B.; Žnidaršič, N.; Letofsky-Papst, I.; Dittrich, M.; Grogger, W.; Štrus, J.; Hofer, F. Silicon: The Key Element in Early Stages of Biocalcification. *Journal of Structural Biology* **2011**, *174* (1), 180–186. https://doi.org/10.1016/j.jsb.2010.09.025.

(199) Seaborn, C. D.; Nielsen, F. H. Silicon Deprivation Decreases Collagen Formation in Wounds and Bone, and Ornithine Transaminase Enzyme Activity in Liver. *BTER* **2002**, *89* (3), 251–262. https://doi.org/10.1385/BTER:89:3:251.

(200) Seaborn, C.; Nielsen, F. Dietary Silicon Affects Acid and Alkaline Phosphatase and 45Calcium Uptake in Bone of Rats. *Journal of Trace Elements in Experimental Medicine* **1994**.

(201) Kayongo-Male, H.; Julson, J. L. Effects of High Levels of Dietary Silicon on Bone Development of Growing Rats and Turkeys Fed Semi-Purified Diets. *Biol Trace Elem Res* **2008**, *123* (1–3), 191–201. https://doi.org/10.1007/s12011-008-8102-2.

(202) Huang, Y.; Li, P.; Zhao, R.; Zhao, L.; Liu, J.; Peng, S.; Fu, X.; Wang, X.; Luo, R.; Wang, R.; Zhang, Z. Silica Nanoparticles: Biomedical Applications and Toxicity. *Biomedicine & Pharmacotherapy* **2022**, *151*, 113053. https://doi.org/10.1016/j.biopha.2022.113053.

(203) Yi, G. -R.; Manoharan, V. N.; Michel, E.; Elsesser, M. T.; Yang, S. -M.; Pine, D. J. Colloidal Clusters of Silica or Polymer Microspheres. *Advanced Materials* **2004**, *16* (14), 1204–1208. https://doi.org/10.1002/adma.200306638.

(204) Green, D. L.; Lin, J. S.; Lam, Y.-F.; Hu, M. Z.-C.; Schaefer, D. W.; Harris, M. T. Size, Volume Fraction, and Nucleation of Stober Silica Nanoparticles. *Journal of Colloid and Interface Science* **2003**, *266* (2), 346–358. https://doi.org/10.1016/S0021-9797(03)00610-6.

(205) Fernandes, R. S.; Raimundo, I. M.; Pimentel, M. F. Revising the Synthesis of Stöber Silica Nanoparticles: A Multivariate Assessment Study on the Effects of Reaction Parameters on the Particle Size. *Colloids and Surfaces A: Physicochemical and Engineering Aspects* **2019**, *577*, 1–7. https://doi.org/10.1016/j.colsurfa.2019.05.053.

(206) Stöber, W.; Fink, A.; Bohn, E. Controlled Growth of Monodisperse Silica Spheres in the Micron Size Range. *Journal of Colloid and Interface Science* **1968**, *26* (1), 62–69. https://doi.org/10.1016/0021-9797(68)90272-5.

(207) Murugadoss, S.; Lison, D.; Godderis, L.; Van Den Brule, S.; Mast, J.; Brassinne, F.; Sebaihi, N.; Hoet, P. H. Toxicology of Silica Nanoparticles: An Update. *Arch Toxicol* **2017**, *91* (9), 2967–3010. https://doi.org/10.1007/s00204-017-1993-y.

(208) Ha, S.-W.; Weitzmann, M. N.; Beck, G. R. Bioactive Silica Nanoparticles Promote Osteoblast Differentiation through Stimulation of Autophagy and Direct Association with LC3 and P62. *ACS Nano* **2014**, *8* (6), 5898–5910. https://doi.org/10.1021/nn5009879.

(209) Xu, X.; Zhang, K.; Zhao, L.; Wang, D.; Bu, W.; Zheng, C.; Sun, H. Characteristics of Three Sizes of Silica Nanoparticles in the Osteoblastic Cell Line, MC3T3-E1. *RSC Adv.* **2014**, *4* (87), 46481–46487. https://doi.org/10.1039/C4RA06863G.

(210) Huang, D.; Hung, Y.; Ko, B.; Hsu, S.; Chen, W.; Chien, C.; Tsai, C.; Kuo, C.; Kang, J.; Yang, C.; Mou, C.; Chen, Y. Highly Efficient Cellular Labeling of Mesoporous Nanoparticles in Human Mesenchymal Stem Cells: Implication for Stem Cell Tracking. *FASEB j.* **2005**, *19* (14), 2014–2016. https://doi.org/10.1096/fj.05-4288fje.

(211) Albanese, A.; Tang, P. S.; Chan, W. C. W. The Effect of Nanoparticle Size, Shape, and Surface Chemistry on Biological Systems. *Annu. Rev. Biomed. Eng.* **2012**, *14* (1), 1–16. https://doi.org/10.1146/annurev-bioeng-071811-150124.

(212) Blondeau, M.; Coradin, T. Living Materials from Sol–Gel Chemistry: Current Challenges and Perspectives. *J. Mater. Chem.* **2012**, *22* (42), 22335. https://doi.org/10.1039/c2jm33647b.

(213) Voisin, H.; Aimé, C.; Coradin, T. Understanding and Tuning Bioinorganic Interfaces for the Design of Bionanocomposites. *Eur J Inorg Chem* **2015**, *2015* (27), 4463–4480. https://doi.org/10.1002/ejic.201500403.

(214) Avnir, D.; Coradin, T.; Lev, O.; Livage, J. Recent Bio-Applications of Sol–Gel Materials. *J. Mater. Chem.* **2006**, *16* (11), 1013–1030. https://doi.org/10.1039/B512706H.

(215) Heinemann, S.; Coradin, T.; Desimone, M. F. Bio-Inspired Silica–Collagen Materials: Applications and Perspectives in the Medical Field. *Biomater. Sci.* **2013**, *1* (7), 688. https://doi.org/10.1039/c3bm00014a.

(216) Sarker, B.; Lyer, S.; Arkudas, A.; Boccaccini, A. R. Collagen/Silica Nanocomposites and Hybrids for Bone Tissue Engineering. *Nanotechnology Reviews* **2013**, *2* (4), 427–447. https://doi.org/10.1515/ntrev-2013-0012.

(217) Alvarez Echazú, M.; Renou, S.; Alvarez, G.; Desimone, M.; Olmedo, D. A COLLAGEN-SILICA- Based Biocomposite for Potential Application in Bone Tissue Engineering. *J Biomedical Materials Res* **2022**, *110* (2), 331–340. https://doi.org/10.1002/jbm.a.37291.

(218) Eglin, D.; Maalheem, S.; Livage, J.; Coradin, T. In Vitro Apatite Forming Ability of Type I Collagen Hydrogels Containing Bioactive Glass and Silica Sol-Gel Particles. *J Mater Sci: Mater Med* **2006**, *17* (2), 161–167. https://doi.org/10.1007/s10856-006-6820-6.

(219) Ha, S.-W.; Weitzmann, M. N.; Beck, G. R. Dental and Skeletal Applications of Silica-Based Nanomaterials. In *Nanobiomaterials in Clinical Dentistry*; Elsevier, 2013; pp 69–91. https://doi.org/10.1016/B978-1-4557-3127-5.00004-0.

(220) Lao, J.; Nedelec, J.-M. Verres bioactifs. *Verres et céramiques* **2014**. https://doi.org/10.51257/a-v1-n4955.

(221) Hench, L. L.; Xynos, I. D.; Polak, J. M. Bioactive Glasses for in Situ Tissue Regeneration. *Journal of Biomaterials Science, Polymer Edition* **2004**, *15* (4), 543–562. https://doi.org/10.1163/156856204323005352.

(222) Henstock, J. R.; Canham, L. T.; Anderson, S. I. Silicon: The Evolution of Its Use in Biomaterials. *Acta Biomaterialia* **2015**, *11*, 17–26. https://doi.org/10.1016/j.actbio.2014.09.025.

(223) Rahaman, M. N.; Day, D. E.; Sonny Bal, B.; Fu, Q.; Jung, S. B.; Bonewald, L. F.; Tomsia, A. P. Bioactive Glass in Tissue Engineering. *Acta Biomaterialia* **2011**, *7* (6), 2355–2373. https://doi.org/10.1016/j.actbio.2011.03.016.

(224) Hench, L. L. Bioceramics: From Concept to Clinic. *Journal of the American Ceramic Society* **1991**, *74* (7), 1487–1510. https://doi.org/10.1111/j.1151-2916.1991.tb07132.x.

(225) Kokubo, T. Apatite Formation on Surfaces of Ceramics, Metals and Polymers in Body Environment. *Acta Materialia* **1998**, *46* (7), 2519–2527. https://doi.org/10.1016/S1359-6454(98)80036-0.

(226) Vichery, C.; Nedelec, J.-M. Bioactive Glass Nanoparticles: From Synthesis to Materials Design for Biomedical Applications. *Materials* **2016**, *9* (4), 288. https://doi.org/10.3390/ma9040288.

(227) Sarker, B.; Hum, J.; Nazhat, S. N.; Boccaccini, A. R. Combining Collagen and Bioactive Glasses for Bone Tissue Engineering: A Review. *Adv Healthcare Materials* **2015**, *4* (2), 176–194. https://doi.org/10.1002/adhm.201400302.

(228) Zhou, H.; Luchini, T. J. F.; Bhaduri, S. B.; Deng, L. Silicon (Si) Containing Bone Cements: A Review. *Materials Technology* **2015**, *30* (sup5), 229–236. https://doi.org/10.1179/17535557B15Y.000000005.

(229) Huan, Z.; Chang, J. Novel Bioactive Composite Bone Cements Based on the β-Tricalcium Phosphate–Monocalcium Phosphate Monohydrate Composite Cement System. *Acta Biomaterialia* **2009**, *5* (4), 1253–1264. https://doi.org/10.1016/j.actbio.2008.10.006.

(230) Aparicio, J. L.; Rueda, C.; Manchón, Á.; Ewald, A.; Gbureck, U.; Alkhraisat, M. H.; Jerez, L. B.; Cabarcos, E. L. Effect of Physicochemical Properties of a Cement Based on Silicocarnotite/Calcium Silicate on *in Vitro* Cell Adhesion and *in Vivo* Cement Degradation. *Biomed. Mater.* **2016**, *11* (4), 045005. https://doi.org/10.1088/1748-6041/11/4/045005.

(231) Alsenan, J. Effect of Silicon and Calcium on Human Dental Pulp Cell Cultures. *IJMSA* **2017**, *6* (6), 290. https://doi.org/10.11648/j.ijmsa.20170606.14.

(232) Miyano, Y.; Mikami, M.; Katsuragi, H.; Shinkai, K. Effects of Sr2+, BO33−, and SiO32− on Differentiation of Human Dental Pulp Stem Cells into Odontoblast-Like Cells. *Biol Trace Elem Res* **2023**, *201* (12), 5585–5600. https://doi.org/10.1007/s12011-023-03625-z.

(233) Caliari, S. R.; Burdick, J. A. A Practical Guide to Hydrogels for Cell Culture. *Nat Methods* **2016**, *13* (5), 405–414. https://doi.org/10.1038/nmeth.3839.

(234) Griffanti, G.; Nazhat, S. N. Dense Fibrillar Collagen-Based Hydrogels as Functional Osteoid-Mimicking Scaffolds. *International Materials Reviews* **2020**, *65* (8), 502–521. https://doi.org/10.1080/09506608.2020.1735828.

(235) Helary, C.; Abed, A.; Mosser, G.; Louedec, L.; Letourneur, D.; Coradin, T.; Giraud-Guille, M. M.; Meddahi-Pellé, A. Evaluation of Dense Collagen Matrices as Medicated Wound Dressing for the Treatment of Cutaneous Chronic Wounds. *Biomater. Sci.* **2015**, *3* (2), 373–382. https://doi.org/10.1039/C4BM00370E.

(236) Helary, C.; Bataille, I.; Abed, A.; Illoul, C.; Anglo, A.; Louedec, L.; Letourneur, D.; Meddahi-Pellé, A.; Giraud-Guille, M. M. Concentrated Collagen Hydrogels as Dermal Substitutes. *Biomaterials* **2010**, *31* (3), 481–490. https://doi.org/10.1016/j.biomaterials.2009.09.073.

(237) Li, Y.; Liu, Y.; Li, R.; Bai, H.; Zhu, Z.; Zhu, L.; Zhu, C.; Che, Z.; Liu, H.; Wang, J.; Huang, L. Collagen-Based Biomaterials for Bone Tissue Engineering. *Materials & Design* **2021**, *210*, 110049. https://doi.org/10.1016/j.matdes.2021.110049.

(238) Abou Neel, E. A.; Bozec, L.; Knowles, J. C.; Syed, O.; Mudera, V.; Day, R.; Hyun, J. K. Collagen — Emerging Collagen Based Therapies Hit the Patient. *Advanced Drug Delivery Reviews* **2013**, *65* (4), 429–456. https://doi.org/10.1016/j.addr.2012.08.010.

(239) Brodsky, B.; Ramshaw, J. A. M. The Collagen Triple-Helix Structure. *Matrix Biology* **1997**, *15* (8–9), 545–554. https://doi.org/10.1016/S0945-053X(97)90030-5.

(240) Zhu, S.; Yuan, Q.; Yin, T.; You, J.; Gu, Z.; Xiong, S.; Hu, Y. Self-Assembly of Collagen-Based Biomaterials: Preparation, Characterizations and Biomedical Applications. *J. Mater. Chem. B* **2018**, *6* (18), 2650–2676. https://doi.org/10.1039/C7TB02999C.

(241) Brown, R. A.; Wiseman, M.; Chuo, C. -B.; Cheema, U.; Nazhat, S. N. Ultrarapid Engineering of Biomimetic Materials and Tissues: Fabrication of Nano- and Microstructures by Plastic Compression. *Adv Funct Materials* **2005**, *15* (11), 1762–1770. https://doi.org/10.1002/adfm.200500042.

(242) Cheema, U.; Brown, R. A. Rapid Fabrication of Living Tissue Models by Collagen Plastic Compression: Understanding Three-Dimensional Cell Matrix Repair *In Vitro*. *Advances in Wound Care* **2013**, *2* (4), 176–184. https://doi.org/10.1089/wound.2012.0392.

(243) Marelli, B.; Ghezzi, C. E.; Barralet, J. E.; Nazhat, S. N. Collagen Gel Fibrillar Density Dictates the Extent of Mineralization in Vitro. *Soft Matter* **2011**, *7* (21), 9898. https://doi.org/10.1039/c1sm06027a.

(244) Bitar, M.; Brown, R. A.; Salih, V.; Kidane, A. G.; Knowles, J. C.; Nazhat, S. N. Effect of Cell Density on Osteoblastic Differentiation and Matrix Degradation of Biomimetic Dense Collagen Scaffolds. *Biomacromolecules* **2008**, *9* (1), 129–135. https://doi.org/10.1021/bm701112w.

(245) Coyac, B. R.; Chicatun, F.; Hoac, B.; Nelea, V.; Chaussain, C.; Nazhat, S. N.; McKee, M. D. Mineralization of Dense Collagen Hydrogel Scaffolds by Human Pulp Cells. *J Dent Res* **2013**, *92* (7), 648–654. https://doi.org/10.1177/0022034513488599.

(246) Ruch, J. V. Odontoblast Commitment and Differentiation. *Biochem Cell Biol* **1998**, *76* (6), 923–938.

(247) Fitzgerald, M.; Chiego, D. J.; Heys, D. R. Autoradiographic Analysis of Odontoblast Replacement Following Pulp Exposure in Primate Teeth. *Archives of Oral Biology* **1990**, *35* (9), 707–715. https://doi.org/10.1016/0003-9969(90)90093-P.

(248) Aguilar-Ayala, F. J.; Aguilar-Pérez, F. J.; Nic-Can, G. I.; Rojas-Herrera, R.; Chuc-Gamboa, G.; Aguilar-Pérez, D.; Rodas-Junco, B. A. A Molecular View on Biomaterials and Dental Stem Cells Interactions: Literature Review. *Applied Sciences* **2022**, *12* (12), 5815. https://doi.org/10.3390/app12125815.

(249) Morsczeck, C.; Reichert, T. E. Dental Stem Cells in Tooth Regeneration and Repair in the Future. *Expert Opinion on Biological Therapy* **2018**, *18* (2), 187–196. https://doi.org/10.1080/14712598.2018.1402004.

(250) Shah, P.; Aghazadeh, M.; Rajasingh, S.; Dixon, D.; Jain, V.; Rajasingh, J. Stem Cells in Regenerative Dentistry: Current Understanding and Future Directions. *Journal of Oral Biosciences* **2024**, S1349007924000197. https://doi.org/10.1016/j.job.2024.02.006.

(251) Sharpe, P. T. Dental Mesenchymal Stem Cells. *Development* **2016**, *143* (13), 2273–2280. https://doi.org/10.1242/dev.134189.

(252) Zhang, W.; Walboomers, X. F.; Shi, S.; Fan, M.; Jansen, J. A. Multilineage Differentiation Potential of Stem Cells Derived from Human Dental Pulp after Cryopreservation. *Tissue Engineering* **2006**, *12* (10), 2813–2823. https://doi.org/10.1089/ten.2006.12.2813.

(253) Jo, Y.-Y.; Lee, H.-J.; Kook, S.-Y.; Choung, H.-W.; Park, J.-Y.; Chung, J.-H.; Choung, Y.-H.; Kim, E.-S.; Yang, H.-C.; Choung, P.-H. Isolation and Characterization of Postnatal Stem Cells from Human Dental Tissues. *Tissue Engineering* **2007**, *13* (4), 767–773. https://doi.org/10.1089/ten.2006.0192.

(254) Jin, W.; Wu, H.; Shi, J.; Hu, Z.; Zhou, Y.; Chen, Z.; Shao, C.; Tang, R.; Xie, Z. Biomimetic Mineralized Collagen Scaffolds Enhancing Odontogenic Differentiation of HDPSCs and Dentin Regeneration through Modulating Mechanical Microenvironment. *Chemical Engineering Journal* **2023**, *460*, 141800. https://doi.org/10.1016/j.cej.2023.141800.

(255) Coyac, B. R.; Hoac, B.; Chafey, P.; Falgayrac, G.; Slimani, L.; Rowe, P. S.; Penel, G.; Linglart, A.; McKee, M. D.; Chaussain, C.; Bardet, C. Defective Mineralization in X-Linked Hypophosphatemia Dental Pulp Cell Cultures. *J Dent Res* **2018**, *97* (2), 184–191. https://doi.org/10.1177/0022034517728497.

(256) Chamieh, F.; Collignon, A.-M.; Coyac, B. R.; Lesieur, J.; Ribes, S.; Sadoine, J.; Llorens, A.; Nicoletti, A.; Letourneur, D.; Colombier, M.-L.; Nazhat, S. N.; Bouchard, P.; Chaussain, C.; Rochefort, G. Y. Accelerated Craniofacial Bone Regeneration through Dense Collagen Gel Scaffolds Seeded with Dental Pulp Stem Cells. *Sci Rep* **2016**, *6* (1), 38814. https://doi.org/10.1038/srep38814.

(257) Maillard, S.; Sicard, L.; Andrique, C.; Torrens, C.; Lesieur, J.; Baroukh, B.; Coradin, T.; Poliard, A.; Slimani, L.; Chaussain, C. Combining Sclerostin Neutralization with Tissue Engineering: An Improved Strategy for Craniofacial Bone Repair. *Acta Biomaterialia* **2022**, *140*, 178–189. https://doi.org/10.1016/j.actbio.2021.11.046.

(258) Collignon, A.-M.; Castillo-Dali, G.; Gomez, E.; Guilbert, T.; Lesieur, J.; Nicoletti, A.; Acuna-Mendoza, S.; Letourneur, D.; Chaussain, C.; Rochefort, G. Y.; Poliard, A. Mouse *Wnt1-CRE* -Rosa *Tomato* Dental Pulp Stem Cells Directly Contribute to the Calvarial Bone Regeneration Process. *Stem Cells* **2019**, *37* (5), 701–711. https://doi.org/10.1002/stem.2973.

(259) Novais, A.; Lesieur, J.; Sadoine, J.; Slimani, L.; Baroukh, B.; Saubaméa, B.; Schmitt, A.; Vital, S.; Poliard, A.; Hélary, C.; Rochefort, G. Y.; Chaussain, C.; Gorin, C. Priming Dental Pulp Stem Cells from Human Exfoliated Deciduous Teeth with Fibroblast Growth Factor-2 Enhances Mineralization Within Tissue-Engineered Constructs Implanted in Craniofacial Bone Defects. *Stem Cells Translational Medicine* **2019**, *8* (8), 844–857. https://doi.org/10.1002/sctm.18-0182.

(260) Park, H.; Collignon, A.-M.; Lepry, W. C.; Ramirez-GarciaLuna, J. L.; Rosenzweig, D. H.; Chaussain, C.; Nazhat, S. N. Acellular Dense Collagen-S53P4 Bioactive Glass Hybrid Gel Scaffolds Form More Bone than Stem Cell Delivered Constructs. *Materials Science and Engineering: C* **2021**, *120*, 111743. https://doi.org/10.1016/j.msec.2020.111743.

Chapter II

Study of the impact of fibrillogenesis conditions and cell density on the mineralization of plastically-compressed collagen hydrogels by human dental pulp stem cells

This work has been published as:

Mbitta Akoa, D.; Sicard, L.; Hélary, C.; Torrens, C.; Baroukh, B.; Poliard, A.; Coradin, T. Role of Physico-Chemical and Cellular Conditions on the Bone Repair Potential of Plastically Compressed Collagen Hydrogels. *Gels* **2024**, *10*, 130. https://doi.org/10.3390/gels10020130

II.1. Introduction

At the beginning of our project, we decided to use plastically-compressed collagen hydrogels seeded by dental pulp stem cells as models of the pulp tissue. The first reason for this choice is that the plastic compression process is one of the few available approaches allowing to encapsulate cells in concentrated collagen hydrogels. Indeed, a major challenge in tissue engineering is to immobilize cells in 3D environments whose density and organization resemble somehow the structure of living tissues.[1,2] Two main strategies can be followed: colonization of pre-formed scaffolds or encapsulation where the matrix is formed in the presence of cells.[3] The major advantage of colonization is that the scaffold can be prepared by a variety of processes that may not be cytocompatible. However, achieving homogeneous cellularization of the scaffold can be challenging and time-consuming. In contrast, encapsulation allows cells to fill the scaffold from the very beginning of the culture period. However, this approach faces many challenges, including the cytocompatibility of the starting solutions, reagents and processing conditions.[4]

In the case of type I collagen, host matrices most often consist of hydrogels obtained by neutralization of an acidic solution (pH 2-4).[5–7] Therefore, in encapsulation approaches, the pH of the collagen solution must first be raised near neutral pH before cells suspended in an adequate buffer are included.[8] While this is feasible for collagen concentration up to *ca*. 5 $mg.mL^{-1}$ [9], higher concentrations lead to highly viscous, fast gelling solutions making adequate cell incorporation difficult.[10] More than 15 years ago, Brown and coll. disclosed an original protocol where cells were initially entrapped in a collagen hydrogel at low concentration (*ca*. 2 $mg.mL^{-1}$) followed by densification of this hydrogel, by at least a factor of 10, under plastic compression (PC).[11] Therefore, this process allows for immobilizing cells in dense 3D scaffolds without requiring concentrated collagen solutions.

Initially, the effect of parameters such as loading force and time on the mechanical and morphological properties of the hydrogels, as well as their suitability to host human fibroblasts have been studied.[11] Further on, additional compression steps[12], and different geometries [13–15] have been investigated. Finally, composite and mixed gels were described[16–18] and the range of immobilized cells was extended.[19–23]

A feature of the PC process is its unique ability to create osteoid-like environments in a simple manner that makes it an interesting alternative to additive manufacturing techniques.[24] It has

therefore attracted a large attention to design bone repair materials, either by chemical mineralization of the collagen hydrogels or by immobilization of mineralizing cells.[25] In particular, the team of C. Chaussain showed that PC hydrogels were suitable hosts for encapsulation of stem cells derived from human dental pulp, promoting their osteo/odontogenic differentiation and leading to matrix mineralization *in vitro*.[26] Later on, they also demonstrated that such constructs could efficiently improve bone repair *in vivo* when implanted in critical defects of calvaria in rodents.[27–29] Noticeably, using fluorescent murine Dental Pulp Stem Cells (mDPSCs), it was shown that seeded cells could directly take part in neo-osteogenesis.[30]

On this basis, the PC protocol appeared very-well suited for our objective. However, we realized that, over the years, changes had occurred in the protocol used in the team, especially in terms of buffering conditions.[26,27] The type (i.e. Stem cells from Human Exfoliated Deciduous teeth (SHEDs) or human Dental Pulp Stem Cells (hDPSCs)[31]) and density of the cells were also varied.[26,27] Yet, how such modifications could impact the structural and biological properties of the gels has not been studied. More generally, detailed studies of the influence of PC physico-chemical conditions have been scarcely reported.[32,33] In contrast, it has been repeatedly demonstrated that type I collagen fibrillogenesis is highly dependent on pH, ionic strength and salt type.[7,34–38] SHEDs and hDPSCs also demonstrated different mineralization capabilities in various environments but were never compared within PC collagen hydrogels.[39–41]

On this basis, we decided to study how physico-chemical and cellular conditions could impact the mineralization of PC dense hydrogels by DPSCs. The purpose was two-fold: (1) understand better the role of different parameters on the structure of the gel and on the cellular response (2) identify an optimal protocol for the rest of our study. In particular, we had observed that gels obtained after compression using already-described protocols were very fragile and often crushed during manipulation and we wanted to improve their handling.

II.2. Materials and methods

II.2.1. Materials and cells

Type I collagen was extracted and purified from young rat tail tendon.[36] Young rat tails employed in this investigation were sourced as post-surgical discards from the animal facilities of UR2496 (Université Paris Cité), allowing for the utilization of otherwise discarded biological material in accordance with ethical and responsible laboratory practices. Dental pulps were obtained from exfoliated deciduous teeth of children aged 6–7 years old to isolate SHEDs or from human third molars of young adults (aged 15-20 years) to isolate hDPSCs. Teeth utilized in this study were obtained in the dental department of the AH-HP Bretonneau Hospital under an opt-out consent model, where patients undergoing surgical procedures were informed of the research use of excised tissues, and consent was presumed unless patients explicitly communicated their objection to such usage, in accordance with the ethical guidelines established by the French law on bioethics (agreement IRB 00006477 and n° DC-2009-927, Cellule Bioéthique DGRI/A5). The SHEDs and hDPSCs were isolated and expanded following an established protocol.[31] For all experiments, pulp cells were used at passage 4.

II.2.2. Plastically-compressed collagen hydrogel preparation

In a typical experiment, 2 mL of a solution of type I collagen (4 $mg.mL^{-1}$) in acetic acid (20 mM or 500 mM) was mixed with 0.5, 1 or 1.5 mL of DMEM of concentration varying between 1X and 10 X in a falcon tube. Then, an aqueous solution of NaOH of concentration varying between 0.1 M and 5 M was added until pH 7.4, as monitored by a pH-meter. Finally, DMEM 1X was added so as to obtain a total 5 mL volume and the solution was placed into 24-well plates (2.5 mL/well) and incubated at 37°C under 5% CO_2 atmosphere for 30 min or 24 h. Recovered collagen gels were deposited on a stack of blotting paper, nylon and stainless-steel mesh and compressed/loaded with an unconfined compressive stress of 1 kPa using a calibrated glass plate for 5 min, as previously described (**Figure II.1**).[11,26]

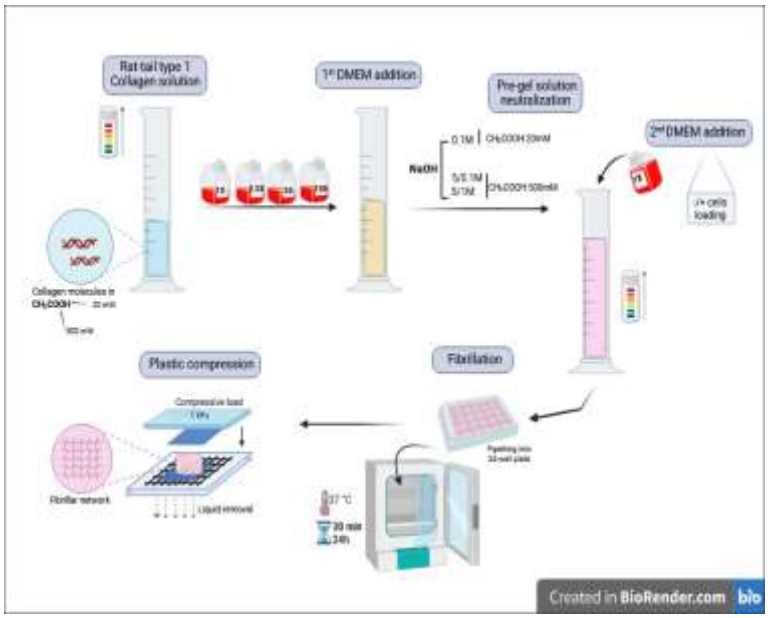

Figure II.1: Schematic overview of the here-studied multi-step preparation of plastically-compressed collagen hydrogels

II.2.3. Cell culture conditions

As previously described, after neutralization of the collagen mixture, two types of dental pulp stem cells at different cell densities were seeded in the collagen mixture prior to incubation: SHEDs: 160,000 cells·mL^{-1} [26], hDPSCs : 0.8 M cell.mL^{-1} and 2 M cells·mL^{-1}. [27] Gelling was followed by the plastic compression procedure described above.

For differentiation/mineralization studies, all cell-laden (with SHEDs or hDPSCs) plastically-compressed dense collagen hydrogels were cultured in an osteo/odontogenic medium made of 300 µM L-ascorbic acid sodium salt, 10 nM dexamethasone, 10 mM β-glycerophosphate, 10% fetal bovine serum, and 1% penicillin/streptomycin for 25 days. Cell-free gels grown in this mineralizing medium were used as negative controls.

II.2.4. Structural and chemical characterizations

II.2.4.1. Scanning electron microscopy (SEM)/Energy-dispersive X-ray (EDX) spectroscopy

Gels were fixed with 4% paraformaldehyde (PFA) in phosphate-buffered saline (PBS) and rinsed with a 0.1 M cacodylate/0.6 M sucrose buffer. They were dehydrated in aqueous

solutions of increasing ethanol content and dried using supercritical CO_2. Dried samples were sputter-coated with a 15 nm gold layer for SEM images and a 20 nm carbon layer for EDX analysis. SEM images were taken at several sites on each sample using a Hitachi S-3400 N microscope operating at 10 kV, while chemical characterization by EDX was performed at 60 kV.

II.2.4.2. Rheological studies

Rheological analysis of collagen hydrogels was carried out using a rheometer (Anton Paar) equipped with parallel, roughened 25 mm diameter stainless steel plate and base. Storage moduli *G'* and loss moduli *G''* were obtained by amplitude sweep with a logarithmic increase in shear strain from 0.01% to 100%. 25 measurement points were recorded for each sample, at a constant angular frequency of 10 $rad.s^{-1}$ and at 20°C. Before each test, a preload of 0.2 N was applied to the gels. All measurements were reproduced three times (n=3).

II.2.4.3. Fourier Transform Infra-Red Spectroscopy (FTIR)

FTIR spectroscopy analysis of acellular and cellularized gels after 25 days of culture was performed on a spectrum 400 spectrometer (PerkinElmer). Freeze-dried samples were deposited on an attenuated total reflectance (ATR) crystal and transmittance spectra were collected with 32 scans at a resolution of 2 cm^{-1}. All the spectra were normalized to type I collagen amide I at 1653 cm^{-1}.

II.2.3. Biological studies

II.2.3.1. Cell viability

Cell viability in cell-seeded dense collagen gels was assessed using a live/dead® assay (Thermofisher, Waltham, MA, USA) on day 24 post-culture. After rinsing twice with PBS, samples were stained with a 2 µM calcein-AM and 4 µM ethidium homodimer-1 solution and incubated at 37˚C for 30 minutes. Then, the gels were rinsed three times with PBS to stop the reaction before imaging. Live cells were viewed by green fluorescence and dead cells by red fluorescence using a fluorescent microscope (Axio Imager D.1, Zeiss, Jena, Germany) or a Leica SP5 upright confocal microscope (Leica DMI6000 Upright TCS SP5) under 10x and 20x magnification, respectively. Three image fields were taken for each scaffold and processed with Image J.

II.2.3.2. Metabolic activity

Cell metabolic activity was assessed using AlamarBlue® Assay (Sigma-Aldrich, St. Louis, MO, USA). Briefly, a 10% FBS supplemented basal medium (without phenol red), 1% (v/v) penicillin–streptomycin and 1% glutamax containing 10% rezazurin was used to replace the culture medium. Samples were incubated at 37° C for 3 h. Media were collected and replaced with fresh medium to prolong the culture. The reduction percentage of Alamar Blue was calculated from the absorbance values at 570 nm and 600 nm of the collected media following the manufacturer instructions.

II.2.3.3. Histological studies

After 24 days of culture, the gels were fixed overnight at room temperature in a 4% PFA solution in PBS, followed by a series of graded dehydrations with ethanol. Dehydrated constructs were then embedded in paraffin and cut into 7 µm thick sections using a manual microtome (Stiassnie, France). Sections were deparaffinized with Toluene, rehydrated in successive baths of increasing water content and stained with Masson's Trichrome (for the presence of cells and collagen), Alizarin red (calcium revelation) and Von Kossa (phosphate revelation). Images were acquired using a light microscope (DMLB, Leica).

II.2.4. Statistical analyses

All quantitative characterizations were performed in triplicate. Data were compared with one-way statistical analysis of variance (ANOVA) tests. *P-value* < 0.05 was considered statistically significant. Data are expressed as mean ± standard deviation (SD).

II.3 Results

II.3.1. Influence of neutralization conditions

In a first step, we qualitatively evaluated the effect of ionic strength and pH of the initial and neutralizing solutions on the structural stability of the hydrogels, before and after PC (**Figure II.1**). For this purpose, the concentration in acetic acid of the starting collagen I solution, the concentration and amount of the Dulbecco's Modified Eagle Medium (DMEM) solution used before neutralization and the concentration of the NaOH solutions used for neutralization were varied. The starting collagen solution volume was kept constant at 2 mL and final DMEM 1X addition was adjusted to reach a total volume of 5 mL. The loading stress and loading time were fixed to 1 kPa and 5 min, respectively, according to the literature.[26]

After 30 min of incubation at 37°C, either no gel was formed, or a weak gel that spread and leached was obtained (**Figure II.2(a)**) or a stable gel was achieved that maintained his shape under its weight (**Figure II.2(b)**). The gel either did not sustain the compression process or led to very thin (**Figure II.2(c)**) or thin gels (**Figure II.2(d)**) that were stable or broke when handled.

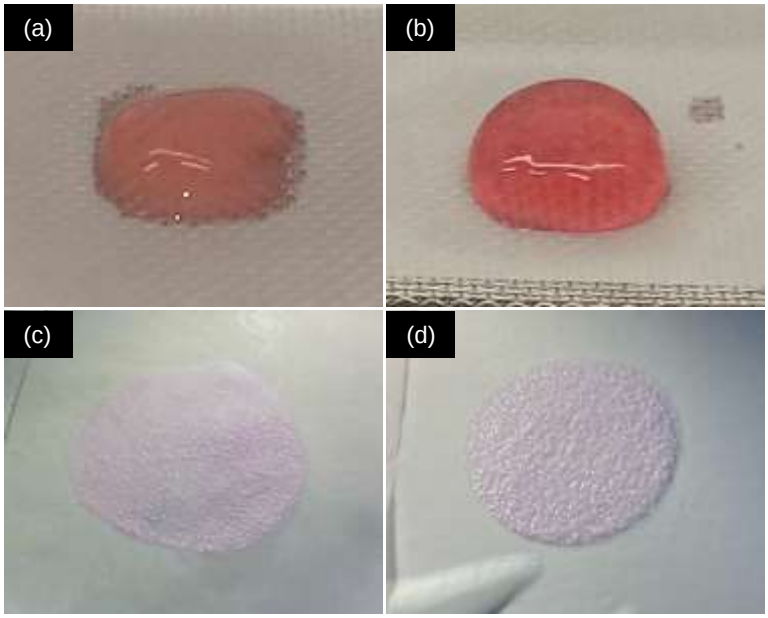

Figure II.2: Macroscopic images of (a) a weak gel before compression; (b) stable gel before compression; (c) very thin gel after compression and (d) thin gel after compression.

Starting from collagen in 20 mM acetic acid at pH 4 and using NaOH 0.1 M, adding 0.5 mL or 1.5 mL of DMEM at 1 X or 2.5 X led to weak gels before compression (**Table II.1**). For a 0.5 mL addition, increasing DMEM concentration up to 10 X led to stable gels before compression but resulting in very thin gels after PC. Addition of 1.5 mL of these concentrated DMEM solutions always yielded weak gels. In contrast, when 1 mL DMEM was added, the gel stability before and after compression increased when DMEM concentration increased from 1 X to 5 X. However, when 1 mL DMEM 10 X was added, no gel was formed.

Table II.1: Influence of DMEM and NaOH volume and concentration on the macroscopic properties of gels before and after compression using 2 mL of an initial collagen solution 4 mg.mL^{-1} in 20 mM acetic acid.

V_{DMEM} (mL)	[DMEM]	pH	[NaOH] (M)	V_{NaOH} (µL)	Final [DMEM]	Gel before compression	Gel after compression
0.5	1X	4.5-5	0.1	350	0.5 X	spread and leak	crush
0.5	2.5 X	4	0.1	450	0.7 X	spread and leak	very thin and fragile
0.5	5 X	3.5	0.1	600	0.9 X	stable	very thin and stable
0.5	10 X	3	0.1	700	1.4 X	stable	very thin and stable
1.0	1 X	6-7	0.1	0	0.6 X	spread and leak	very thin and fragile
1.0	2.5 X	3.5	0.1	600	0.8 X	stable	very thin and stable
1.0	**5 X**	**3**	**0.1**	**700**	**1.3 X**	**stable**	**thin and stable (H)**
1.0	10 X	< 3	0.1	> 1000	-	-	-
1.5	1 X	6-7	0.1	0	0.6 X	spread and leak	crush
1.5	2.5 X	3.5	0.1	700	0.9 X	spread and leak	very thin and fragile
1.5	5 X	3	0.1	800	1.6 X	spread and leak	crush

Table II.2: Influence of DMEM and NaOH volume and concentration on the macroscopic properties of gels before and after compression using 2 mL of an initial collagen solution 4 mg.mL^{-1} in 500 mM acetic acid.

V_{DMEM} (mL)	[DMEM]	pH	[NaOH] (M)	V_{NaOH} (µL)	Final [DMEM]	Gel before compression	Gel after compression
1.0	1 X	3.5-4	5 0.1	200 1000	0.3 X	spread and leak	very thin and stable
1.0	2.5 X	3	5 0.1	205 640	0.7 X	stable	thin and stable
1.0	5 X	2-3	5 0.1	210 700	1.2 X	spread and leak	very thin and fragile
1.0	10 X	2	5 0.1	215 450	2.3 X	no gel formed	-
1.0	1 X	3.5-4	5 1	200 30	0.5 X	spread and leak	very thin and stable
1.0	**2.5 X**	**3**	**5** **1**	**205** **40**	**0.8 X**	**stable**	**thin and stable (I)**
1.0	5 X	2-3	5 1	210 60	1.2 X	spread and leak	very thin and stable

Starting from collagen in 500 mM acetic acid and keeping DMEM volume constant (1 mL), it was found necessary to perform the neutralization step by the successive addition of NaOH 5 M and NaOH 0.1 M (**Table II.2.**). In such conditions, only DMEM 2.5 X yielded to stable gels before and after compression. Again, in optimal conditions, increasing secondary NaOH concentration to 1 M also led to stable gels.

In summary, among all explored conditions, only three led to thin hydrogels that did not break after PC. Condition **H** involve low initial acetic acid concentration (20 mM), intermediate DMEM concentration (5 X) and volume (1 mL) (**Table II.1**). In condition **I**, a higher initial acetic acid concentration (500 mM) and a lower DMEM (2.5 X) concentration were used and both 5 M and 1M NaOH solutions were required to reach neutral pH (**Table II.2**). Note that the use of 0.1 M NaOH as a secondary neutralizing solution was also successful (second condition in **Table II.2**). However, it implies the addition of a large volume of this solution and therefore a low volume of DMEM in the final step, which would require a highly concentrated cell suspension. This condition was therefore not considered further. Altogether, conditions **H** and **I** were the only ones producing hydrogels that could be easily handled without cracking and that were compatible with cell encapsulation.

II.3.2. Influence of gel ageing conditions

In a second stage, the influence of gel ageing before compression was studied for **H** and **I** conditions. Scanning electron microscopy (SEM) imaging of the hydrogels aged for 30 min showed that **H** consist of a porous network of highly intertwined thin fibrils, less than 100 nm in diameter, sometimes assembled as fibrous bundles up to 500 nm in diameter (**Figure II.3(a)**). For sample **I**, a lower occurrence of thin fibrils could be observed and the largest fibers could be up to 1 μm in diameter (**Figure II.3(b)**). No clear modification could be observed for gels aged for 24 h, whatever the condition (**Figure II.3(c,d)**). After compression, a top view image of the gels aged for 30 min showed a decrease of the network porosity (**Figure II.3(e,f)**). The largest bundles seemed partially unraveled, as particularly visible in the condition **I** (**Figure II.3(f)**). These observations were similar for gels aged for 30 min and 24 h (**Figure II.3(g,h)**).

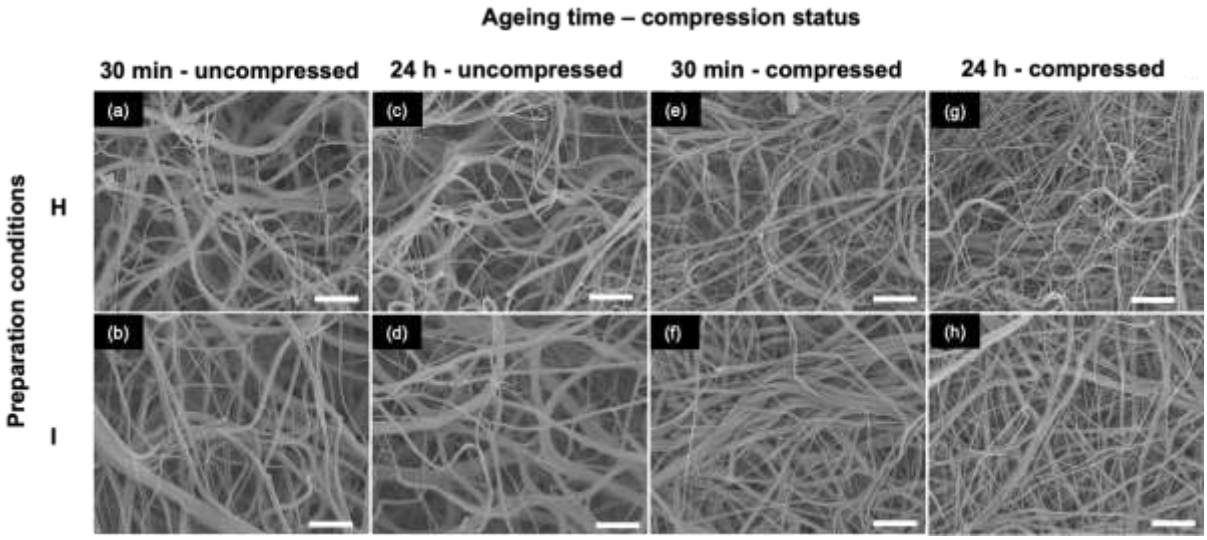

Figure II.3: SEM images of hydrogels prepared in conditions **H** (top row) and **I** (bottom row), aged 30 min (1st column), aged 24 h (2nd column), aged 30 min and compressed (3rd column) and aged 24 h and compressed (4th column). Scale bar: 2 µm.

Compressed gels were also studied by rheology under shear stress. As seen on **Figure II.4(a)**, gels compressed after 30 min or 24 h of ageing exhibited a similar behavior at fixed frequency (10 Hz) and increasing strain, with an initial quasi constant storage modulus *G'* value up to 1 % deformation and then a continuous drop. When *G'* values at a 0.1 % deformation were compared, the storage modulus was comparable for conditions **H** and **I** (**Figure II.4(b)**). Noticeably, there was no significant difference between gels aged for 30 min and 24 h, so the former condition was selected for the rest of the work.

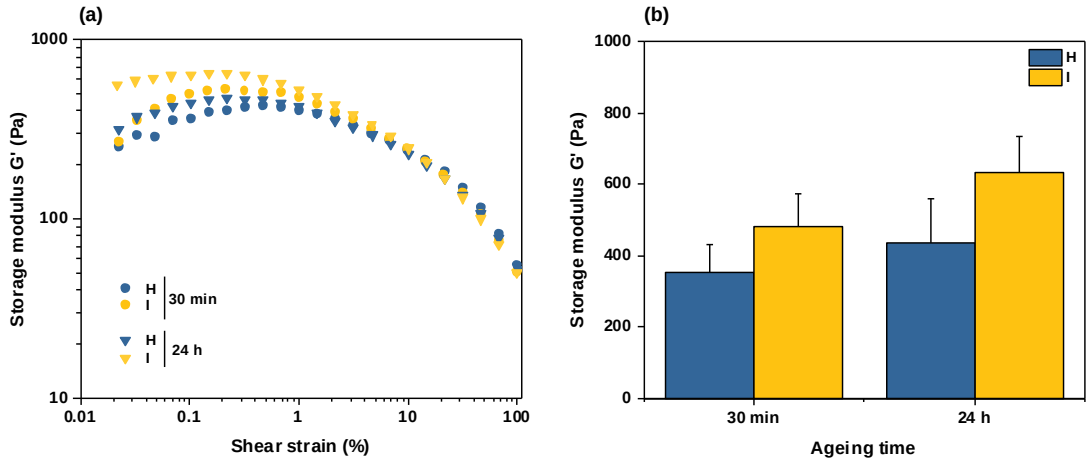

Figure II.4: Rheological properties of hydrogels prepared in conditions **H** and **I** and compressed after 30 min or 24 h ageing. (a) Evolution of storage modulus *G'* as a function of applied shear deformation at fixed frequency (10 Hz). (b) Influence of preparation condition and ageing time on storage modulus *G'* at 0.1 % shear deformation.

II.3.3. Influence of cell density

In a first experiment, SHEDs were encapsulated at a 160,000 cells·mL^{-1} density and the gel was compressed after 30 min. After 25 days of culture, a significant shrinkage of both hydrogels was noticed and, upon recovery, the hydrogel obtained in condition **I** broke into fragments. Study of cell metabolic activity using the Alamar blue test indicated that, in conditions **H**, cell activity remained constant over 25 days of culture (**Figure II.5(a)**). In contrast, in condition **I**, the measured cell activity was small 1 day after compression and rise over the next three weeks to reach the value in **H.** Fluorescence imaging using the live/dead kit after 25 days in culture showed relatively few dead cells in gels obtained in condition **H** (**Figure II.5(b)**) but a higher proportion of these were imaged in condition **I** (**Figure II.5(c)**).

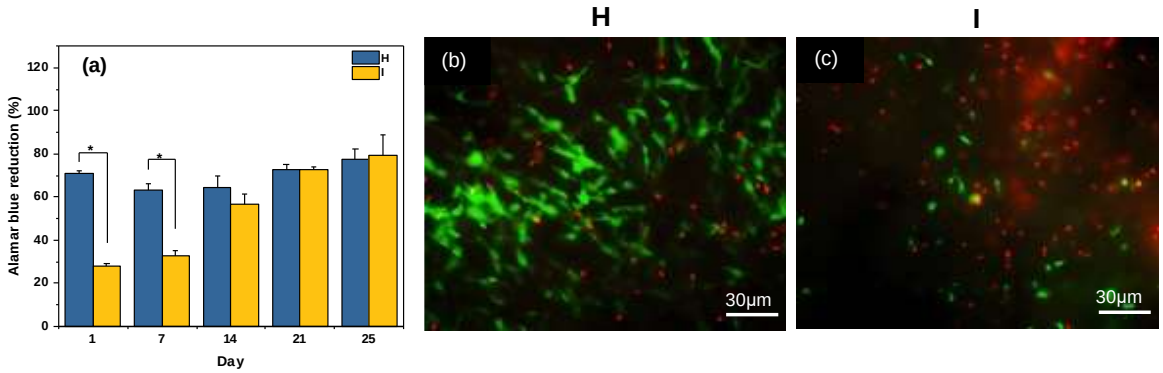

Figure II.5: (a) Evolution of Alamar Blue reduction over 25 days of culture for the two conditions, (b,c) Live/Dead images of SHEDs cells after 25 days of culture. Green and red color are for alive and dead cells, respectively. Scale bar: 30 µm.

Masson's trichrome, that stains both collagen and cells, indicated that **H** consisted of a porous network with few scattered cells (**Figure II.6(a)**). In condition **I**, large cavities were observed, which correlates with the observation of gel breaking into pieces (**Figure II.6(b)**). Finally, staining with Alizarin Red (**Figure II.6(c,d)**) and Von Kossa staining (**Figure II.6(e,f)**) showed no evidence of mineralization in any of the gels.

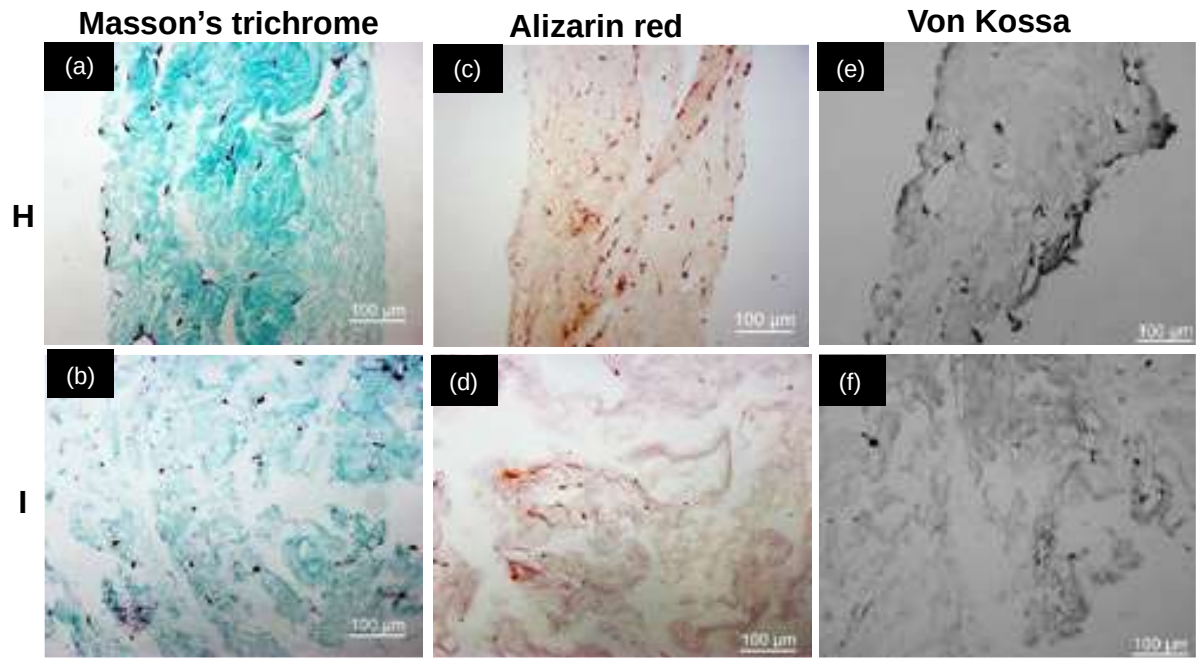

Figure II.6: (a,b) Masson's Trichrome, (c,d) Alizarin Red and (e,f) Von Kossa staining of SHEDs-cellularized hydrogels after 25 days of culture. Scale bar: 100 µm.

Based on this result, condition **H** was selected for the rest of the study as it offers an initial *G'* value comparable to **I** but formed a stable gel after 25 days of culture. Based on the literature[41], hDPSCs were used instead of SHEDs to favor mineralization. We also hypothesized that increasing cell density would increase their mineralization potential [42], so that higher densities of 800,000 cells.mL^{-1} and 2,000,000 cells.mL^{-1} were used.

For both initial cell densities, the Alamar Blue test showed a continuous decrease of cell activity over time (**Figure II.7(a)**). After 25 days, many DPSCs cells could be observed with few dead cells, with no clear effect of the initial cell density (**Figure II.7(b,c)**).

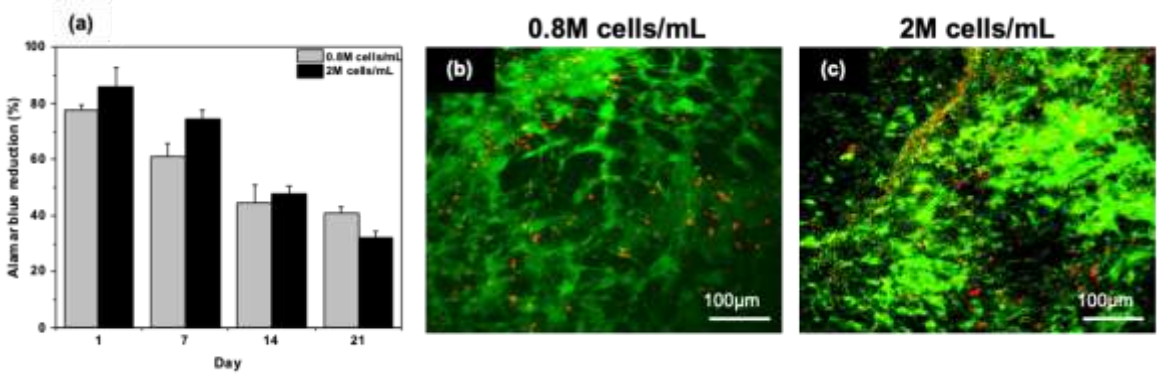

Figure II.7: (a) Evolution of Alamar Blue reduction over 25 days of culture for cell densities, (b,c) Live/Dead images of hDPSCs cells after 25 days of culture. Green and red color are for alive and dead cells, respectively. Scale bar: 100 µm.

For an initial 0.8 $M \cdot mL^{-1}$ content, Masson's Trichrome staining revealed a dense gel with a higher cell density than in the previous conditions, as expected, but, except on the hydrogel edges, cells remained isolated (**Figure II.8(a)**). In contrast, in the initial 2 $M \cdot mL^{-1}$ cell density condition, numerous cell-cell contacts could be evidenced within the dense collagen network (**Figure II.8(b)**). In terms of mineralization, for the lowest cell density, neither Alizarin Red (**Figure II.8(c)**) nor Von Kossa (**Figure II.8(e)**) staining showed significant mineralization. In contrast, with the highest cell content, an important mineral deposit was observed in both stainings (**Figure II.8(d,f)**)

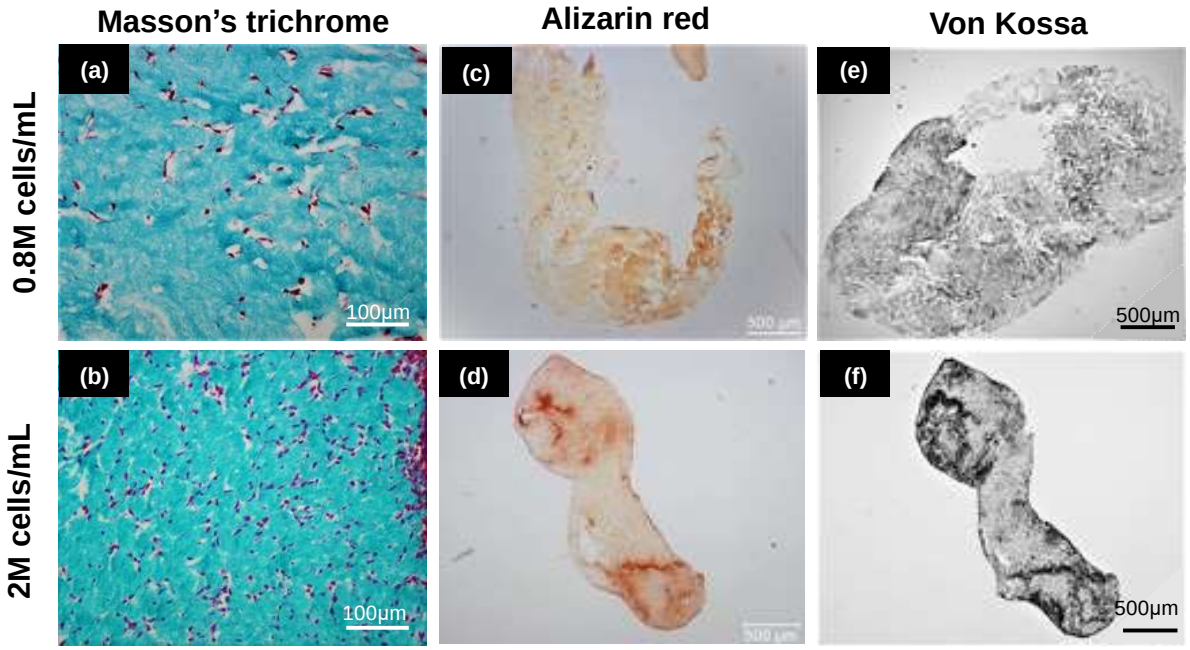

Figure II.8: (a,b) Masson's Trichrome, (c,d) Alizarin Red and (e,f) Von Kossa staining of hDPSCs-cellularized hydrogels after 25 days of culture. Scale bar: (a-b)100 µm; (d-f) 500 µm

Accordingly, at the lowest initial cell density, no mineral deposit could be evidenced on SEM images while Energy-dispersive X-ray (EDX) spectroscopy did not allow for the detection of Calcium (Ca) or Phosphorus (P) (**Figure II.9(a)**). In contrast, a mineral deposit could be observed on SEM images for samples prepared at the highest initial cell density and EDX analyses confirmed that these particles contain Ca and P, with a Ca/P atomic ratio of ca. 1.5, thus close to the expected value for biological hydroxyapatite (**Figure II.9(b)**). The presence of a well-defined vibration band at ca. 1100 cm^{-1} signing for the phosphate group in the hydroxyapatite structure on the Fourier Transform Infra-Red Spectroscopy (FTIR) spectrum of the latter sample only was consistent with our previous observations (**Figure II.9(c)**).

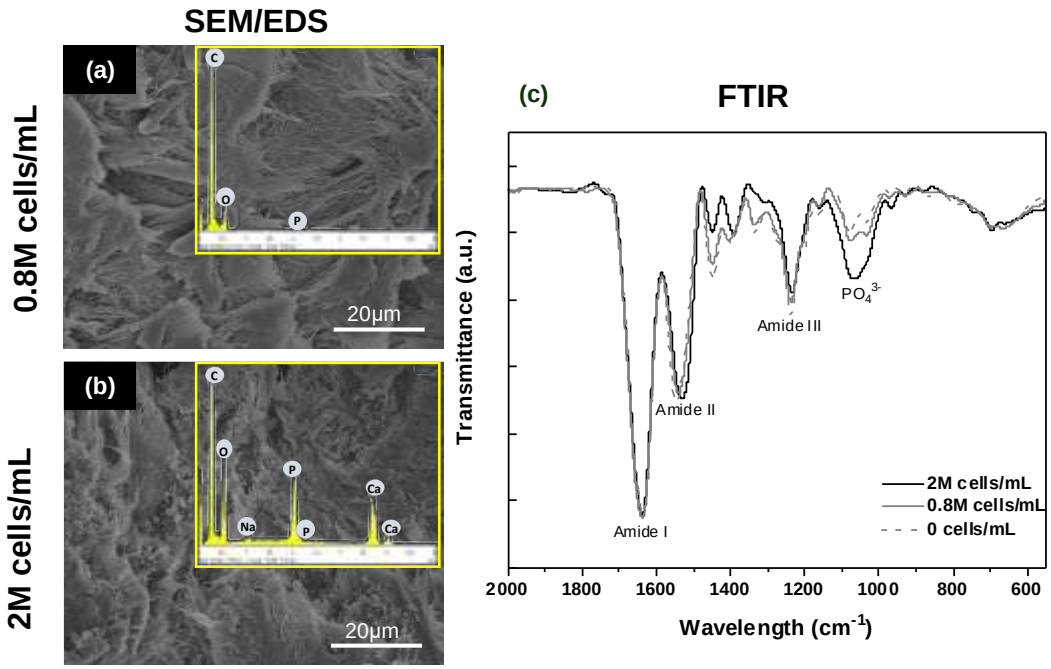

Figure II.9: (a,b) SEM imaging and EDX analysis after 25 days of culture, (c) FTIR spectra of hydrogels after 25 days in culture conditions in the absence of cells and for 0.8 $M.mL^{-1}$ or 2 $M.mL^{-1}$ initial cell density

II.4. Discussion

The aim of this study was to understand how chemical processing conditions and origin/initial density of pulp stem cells could influence the mineralization of plastically-compressed collagen hydrogels.[27] In a first step, some key parameters of the PC process whose influence on final hydrogel structure and properties has not been studied in details so far were selected and varied while keeping collagen initial and final concentrations and total volume constant.

In the pre-compression steps (**Figure II.1**), the initial acetic acid concentration of the collagen solution not only dictates the pH and buffering capacity of the starting solution but it also controls its initial ionic strength. The aim of the first DMEM addition is mainly to provide an adequate inorganic and organic composition favorable to cell survival. However, DMEM also influences the ionic strength and pH of the solution. Further addition of NaOH is required to obtain a precise pH value (7.4) common to all experiments. The last addition of DMEM allows for reaching a final sample volume identical for all conditions, and hence a similar collagen concentration, and also allows for the incorporation of the cell suspension when necessary. Therefore, the concentrations of acetic acid and DMEM are key factors determining the physico-chemical conditions of fibrillogenesis. In the case of the NaOH solution, its concentration determines the volume needed to achieve neutralization, which in turn dictates the volume of DMEM/cell suspension added at the last step, being therefore relevant for both physico-chemical and cellular conditions.

In the PC process, the collagen concentration before compression was fixed to 1.6 $mg.mL^{-1}$, which correspond to the conditions initially described to prepare cellularized soft hydrogels.[11] The starting collagen solution is usually 2 - 2.1 $mg.mL^{-1}$, meaning that only small DMEM and NaOH volumes can be added. Here, a 4 $mg.mL^{-1}$ starting concentration was selected so as to explore a large range of processing conditions. In terms of acetic acid, earlier reports used 20-100 mM concentration.[11,27] Here, to explore in more details the role of ionic strength, a low (20 mM) and a high (500 mM) acetic acid concentration were selected.

Qualitative evaluation of the influence of initial acetic acid concentration, DMEM volume and concentration, and neutralization step on gel formation and compression showed that for 20 mM acetic acid, low DMEM concentration or high DMEM volume led to weak gels. These conditions correspond to the highest pHs before neutralization (**Table II.1**). It has been reported that increasing pH favors fibrillogenesis up to ca. pH 9, corresponding to the isoelectric point

of type I collagen.[37] In acidic conditions, collagen triple helices are highly positively charged and cannot assemble due to electrostatic repulsion. As the pH increases, the positive charge decreases and assembly can proceed. The smaller the charge, the faster triple helices assemble which, according to the nucleation/growth model, results in the formation of numerous small fibrils.[43] The stability of the network is determined by inter-fibrillar interactions and the contact area between two fibrils decreases with the fibril size.[44] Thus, it can be suggested that, in these situations where the pH is already high before the addition of NaOH, small collagen fibrils are rapidly formed, leading to loose networks. In contrast, all gels that were found stable before compression are formed for a pre-neutralization pH of 3 (**Table II.1** and **Table II.2**), i.e. when collagen triple helices do not self-assemble.[45] It is important to note that the pH of DMEM solution decreases with increasing concentration, i.e DMEM 1X has a pH of 8 whereas DMEM 10 X has a pH of 2. This explains why addition of DMEM before neutralization can lead to solutions that are more acidic than the initial collagen solution.

In addition, for similar pHs before neutralization, there seems to be an optimal initial DMEM concentration and volume. For instance, for 20 mM acetic acid, conditions (0.5 mL; 10X) and (1.0 mL; 5X) lead to similar pH (3), same required NaOH volume addition (700 µL) and close final DMEM concentration (1.3-1.4 X) but only the latter yields to thin and stable gels after compression. Thus, the ionic content of these solutions before neutralization also impacts the fibrillogenesis occurring upon NaOH addition, in agreement with the literature.[38] This is because the presence of salts leads to the screening of the positive charges of collagen triple helices, favoring their assembly. When considering 500 mM acetic acid, an optimal initial DMEM concentration (2.5 X) at fixed added volume (1 mL) was found. Importantly, this condition corresponds to a pH value of 3 before neutralization, emphasizing again the key importance of this value, and more globally, of the first addition step. It can be noticed that, although some of the conditions explored here would probably not be suitable for cell survival, the three optimal conditions lead to final DMEM concentration close to 1X, i.e. usual concentration for SHEDs and DPSCs culture.[31]

More detailed investigations of samples **H** (prepared from 20 mM acetic acid) and **I** (prepared from 500 mM acetic acid) provide additional information about the impact of preparation conditions on gel properties. From a structural point of view, the difference between **H** and **I** in terms of fibrillar organization, i.e. thin fibrils with small bundles for the former compared to larger fibers for the latter, points initial acetic acid concentration as a key parameter in the

fibrillogenesis course. This is consistent with previous reports showing that high ionic strength favors collagen fibrils aggregation, by decreasing their repulsive electrostatic interactions via charge screening.[36,37,44] It is important to note that the collagen concentration before final DMEM addition was very close in the two conditions (2.4 $mg.mL^{-1}$ for **H** compared to 2.2 $mg.mL^{-1}$ for **I**) so that the observed structural difference is unlikely to be related to this parameter. Interestingly, these larger fibers appeared significantly disturbed by the compression process, which confirm that they are weak physical aggregates. However, such a structural difference had little impact on the rheological properties of the hydrogels as there was no significant difference in *G'* values found for **H** and **I** samples. Finally, it can be emphasized that neither SEM nor rheology did suggest any modification of interfibrillar interactions when increasing gel ageing before compression. This indicates that a stable structure is already obtained after 30 min in the investigated conditions.

Stem cells isolated from the dental pulp have attracted a large interest in the field of tissue engineering, especially because of their easy access.[46] The difference between SHEDs and hDPSCs originates from the maturity of pulp tissue they are isolated from, i.e. deciduous and permanent teeth, respectively.[31] As a consequence, SHEDs show a higher proliferation capacity whereas DPSCs demonstrate a higher osteogenic/odontogenic differentiation potential.[41] Our initial conditions for mineralization experiments were based on the literature that used the initial PC protocol with SHEDs at a cell density of 150, 000 cells per mL.[26] In this former work, cell activity was not studied and cell viability was reported up to day 16 only, showing a limited number of dead cells via the Live/Dead staining kit. However, high levels of alkaline phosphatase and mineralizing proteins were detected, while the formation of hydroxyapatite was confirmed by FTIR. In our experiments, no significant mineralization could be observed by Von Kossa and Alizarin staining. In condition **H**, we observed that the cell activity was slightly increasing over time while very few dead cells were observed, indicating a slow proliferation of the cells. It is worth pointing out that the matrix average pore size, as estimated from SEM images of the acellular scaffold is below 5 μm. This indicates that cells cannot simply migrate through the porous network but first need to degrade the matrix, explaining the low proliferation rate. In contrast, in condition **I**, the initial cell activity was very low but, with time, a large increase in cell activity was observed, indicating fast proliferation of the SHEDs. Considering that Live/Dead imaging showed a high proportion of dead cells within the gel and that the corresponding gel tends to break into pieces, it can be suggested that such high proliferation correspond to un-encapsulated cells proliferating on plastic walls of the wells

whereas very few survived inside the gels. In other words, in condition **H,** cells remain within the gel and slowly proliferate. The low ratio of dead/live cells suggest that they are undergoing a differentiation stage. In contrast, in condition **I,** the gel breaks and some cells can move to the culture plate. In this situation, cells within the gel pieces die (high dead/live cell ratio) while those outside can freely proliferate (high metabolic activity).

The structural evolution of the gels over the culture period can be related to the cell-mediated remodeling activity, which involves contraction, degradation and extracellular matrix deposition.[47] These processes are highly dependent on the hydrogel composition, structure and mechanical properties, that can also impact stem cells differentiation. In particular, the mechanical properties of the hydrogel are usually considered as a key factor.[48] However, **H** and **I** have similar *G'* values but evolved very differently: **H** became denser, as expected under contraction, whereas **I** broke into pieces. One possible explanation may be related to the difference in structural homogeneity of the starting gels (**Figure II.3**). If the original network is homogenous, contraction will occur similarly within the whole gel, leading to a uniformly-dense network, as observed in **H**. In contrast, if the network is initially heterogeneous, as in **I**, contraction may occur preferentially in some area, creating zones of high and low density, that can lead to local porosity and, ultimately, gel cracking.

On this basis, condition **H** was considered as the most suitable and, in order to achieve mineralization, both cell type and cell density were modified. As pointed out above, hDPSCs were reported to have a lower proliferative but a higher osteogenic differentiation, and hence mineralization, potential compared to SHEDs.[41] The former point is confirmed by our cell activity measurement showing a continuous decrease with culture time whereas few dead cells could be observed by live/dead staining. However, a 0.8 $M.mL^{-1}$ cell density did not allow detection of mineral deposition. In contrast, when cell density was increased to 2 $M.mL^{-1}$, histochemical staining, SEM/EDX and FTIR evidenced mineralization within the gel. At the same time, such an increase in cell density also allowed for cell-cell contact in the gel, that is known to favor differentiation and mineralization.[49] Influence of cell density on mineralization within PC collagen hydrogels has already been studied using a human osteosarcoma cell line (MG63).[50] This work highlighted that cell density influences proliferation, differentiation as well as hydrogel remodeling. Noticeably, the best cell density found here is comparable to the one used when DPSCs-seeded PC collagen hydrogels were found to efficiently promote the repair of calvaria bone critical defects in rodents.[27]

II.5. Conclusions

Here we have demonstrated that the properties of plastically-compressed collagen hydrogels, including their suitability as cellular hosts, are highly sensitive to small modifications of the preparation protocol, especially in the acetic acid concentration of the collagen solution and the amount/concentration of cell culture medium. In addition, we highlighted that cell type and density were critical to achieve mineralization of these dense collagen hydrogels by pulp stem cells *in vitro*.

Coming back to our project, these results indicate that modifications of the protocol should have significantly impacted the collagen structure. For instance, in their initial study, Coyac *et al*. used 100 mM acetic acid collagen solution, DMEM 10X for pre-neutralization, and dropwise addition of 5 M NaOH for neutralization.[26] Chamieh *et al.* used a similar protocol but with 20 mM acetic acid.[27] Novais *et al.* performed pre-neutralization using both DMEM10X and an hydrogenocarbonate buffer and used 0.1 M NaOH solution for neutralization.[28] In all cases, gels that sustained the compression process were reported. This can come as a surprise considering our results demonstrating high sensitivity of the gel stability on experimental conditions.

In fact, discussion with our colleagues indicated that hydrogels obtained with some of the other protocols were sometimes very fragile. Moreover, as our objective was to obtain more easily-handled gels, our criteria for selecting acceptable conditions was probably more demanding. Moreover, with the same purpose, we have worked with larger gels (2.5 mL vs 0.9 mL) which can also impact their mechanical behavior. It is important to note that such modification of hydrogel volume may also have impacted the cell response, especially after contraction when the densification of the network may lead to limitations in oxygen diffusion.

Altogether, this first part of the project has allowed to identify conditions to obtain stable gels allowing hDPSCs survival and efficient mineralization. These systems will now be used to study the effect of silicon on hDPSCs biological behavior.

References

(1) Villalona, G. A.; Udelsman, B.; Duncan, D. R.; McGillicuddy, E.; Sawh-Martinez, R. F.; Hibino, N.; Painter, C.; Mirensky, T.; Erickson, B.; Shinoka, T.; Breuer, C. K. Cell-Seeding Techniques in Vascular Tissue Engineering. *Tissue Engineering Part B: Reviews* **2010**, *16* (3), 341–350. https://doi.org/10.1089/ten.teb.2009.0527.

(2) Maisani, M.; Pezzoli, D.; Chassande, O.; Mantovani, D. Cellularizing Hydrogel-Based Scaffolds to Repair Bone Tissue: How to Create a Physiologically Relevant Micro-Environment? *J Tissue Eng* **2017**, *8*, 204173141771207. https://doi.org/10.1177/2041731417712073.

(3) Parisi, C.; Qin, K.; Fernandes, F. M. Colonization versus Encapsulation in Cell-Laden Materials Design: Porosity and Process Biocompatibility Determine Cellularization Pathways. *Phil. Trans. R. Soc. A.* **2021**, *379* (2206), 20200344. https://doi.org/10.1098/rsta.2020.0344.

(4) Blondeau, M.; Coradin, T. Living Materials from Sol–Gel Chemistry: Current Challenges and Perspectives. *J. Mater. Chem.* **2012**, *22* (42), 22335. https://doi.org/10.1039/c2jm33647b.

(5) Antoine, E. E.; Vlachos, P. P.; Rylander, M. N. Review of Collagen I Hydrogels for Bioengineered Tissue Microenvironments: Characterization of Mechanics, Structure, and Transport. *Tissue Engineering Part B: Reviews* **2014**, *20* (6), 683–696. https://doi.org/10.1089/ten.teb.2014.0086.

(6) Li, Y.; Liu, Y.; Li, R.; Bai, H.; Zhu, Z.; Zhu, L.; Zhu, C.; Che, Z.; Liu, H.; Wang, J.; Huang, L. Collagen-Based Biomaterials for Bone Tissue Engineering. *Materials & Design* **2021**, *210*, 110049. https://doi.org/10.1016/j.matdes.2021.110049.

(7) Zhu, S.; Yuan, Q.; Yin, T.; You, J.; Gu, Z.; Xiong, S.; Hu, Y. Self-Assembly of Collagen-Based Biomaterials: Preparation, Characterizations and Biomedical Applications. *J. Mater. Chem. B* **2018**, *6* (18), 2650–2676. https://doi.org/10.1039/C7TB02999C.

(8) Walters, B. D.; Stegemann, J. P. Strategies for Directing the Structure and Function of Three-Dimensional Collagen Biomaterials across Length Scales. *Acta Biomaterialia* **2014**, *10* (4), 1488–1501. https://doi.org/10.1016/j.actbio.2013.08.038.

(9) Helary, C.; Abed, A.; Mosser, G.; Louedec, L.; Meddahi-Pellé, A.; Giraud-Guille, M. M. Synthesis and in Vivo Integration of Improved Concentrated Collagen Hydrogels. *J Tissue Eng Regen Med* **2011**, *5* (3), 248–252. https://doi.org/10.1002/term.326.

(10) Cross, V. L.; Zheng, Y.; Won Choi, N.; Verbridge, S. S.; Sutermaster, B. A.; Bonassar, L. J.; Fischbach, C.; Stroock, A. D. Dense Type I Collagen Matrices That Support Cellular Remodeling and Microfabrication for Studies of Tumor Angiogenesis and Vasculogenesis in Vitro. *Biomaterials* **2010**, *31* (33), 8596–8607. https://doi.org/10.1016/j.biomaterials.2010.07.072.

(11) Brown, R. A.; Wiseman, M.; Chuo, C. -B.; Cheema, U.; Nazhat, S. N. Ultrarapid Engineering of Biomimetic Materials and Tissues: Fabrication of Nano- and Microstructures by Plastic Compression. *Adv Funct Materials* **2005**, *15* (11), 1762–1770. https://doi.org/10.1002/adfm.200500042.

(12) Abou Neel, E. A.; Cheema, U.; Knowles, J. C.; Brown, R. A.; Nazhat, S. N. Use of Multiple Unconfined Compression for Control of Collagen Gel Scaffold Density and Mechanical Properties. *Soft Matter* **2006**, *2* (11), 986. https://doi.org/10.1039/b609784g.

(13) Braziulis, E.; Diezi, M.; Biedermann, T.; Pontiggia, L.; Schmucki, M.; Hartmann-Fritsch, F.; Luginbühl, J.; Schiestl, C.; Meuli, M.; Reichmann, E. Modified Plastic Compression of Collagen Hydrogels Provides an Ideal Matrix for Clinically Applicable Skin Substitutes. *Tissue Engineering Part C: Methods* **2012**, *18* (6), 464–474. https://doi.org/10.1089/ten.tec.2011.0561.

(14) Ghezzi, C. E.; Marelli, B.; Muja, N.; Nazhat, S. N. Immediate Production of a Tubular Dense Collagen Construct with Bioinspired Mechanical Properties. *Acta Biomaterialia* **2012**, *8* (5), 1813–1825. https://doi.org/10.1016/j.actbio.2012.01.025.

(15) Griffanti, G.; Rezabeigi, E.; Li, J.; Murshed, M.; Nazhat, S. N. Rapid Biofabrication of Printable Dense Collagen Bioinks of Tunable Properties. *Adv Funct Materials* **2020**, *30* (4), 1903874. https://doi.org/10.1002/adfm.201903874.

(16) Marelli, B.; Ghezzi, C. E.; Mohn, D.; Stark, W. J.; Barralet, J. E.; Boccaccini, A. R.; Nazhat, S. N. Accelerated Mineralization of Dense Collagen-Nano Bioactive Glass Hybrid Gels Increases Scaffold Stiffness and Regulates Osteoblastic Function. *Biomaterials* **2011**, *32* (34), 8915–8926. https://doi.org/10.1016/j.biomaterials.2011.08.016.

(17) Chicatun, F.; Pedraza, C. E.; Ghezzi, C. E.; Marelli, B.; Kaartinen, M. T.; McKee, M. D.; Nazhat, S. N. Osteoid-Mimicking Dense Collagen/Chitosan Hybrid Gels. *Biomacromolecules* **2011**, *12* (8), 2946–2956. https://doi.org/10.1021/bm200528z.

(18) Anandagoda, N.; Ezra, D. G.; Cheema, U.; Bailly, M.; Brown, R. A. Hyaluronan Hydration Generates Three-Dimensional Meso-Scale Structure in Engineered Collagen

Tissues. *J. R. Soc. Interface.* **2012**, *9* (75), 2680–2687. https://doi.org/10.1098/rsif.2012.0164.

(19) Buxton, P. G.; Bitar, M.; Gellynck, K.; Parkar, M.; Brown, R. A.; Young, A. M.; Knowles, J. C.; Nazhat, S. N. Dense Collagen Matrix Accelerates Osteogenic Differentiation and Rescues the Apoptotic Response to MMP Inhibition. *Bone* **2008**, *43* (2), 377–385. https://doi.org/10.1016/j.bone.2008.03.028.

(20) East, E.; de Oliveira, D. B.; Golding, J. P.; Phillips, J. B. Alignment of Astrocytes Increases Neuronal Growth in Three-Dimensional Collagen Gels and Is Maintained Following Plastic Compression to Form a Spinal Cord Repair Conduit. *Tissue Engineering Part A* **2010**, *16* (10), 3173–3184. https://doi.org/10.1089/ten.tea.2010.0017.

(21) Levis, H. J.; Brown, R. A.; Daniels, J. T. Plastic Compressed Collagen as a Biomimetic Substrate for Human Limbal Epithelial Cell Culture. *Biomaterials* **2010**, *31* (30), 7726–7737. https://doi.org/10.1016/j.biomaterials.2010.07.012.

(22) Rosenzweig, D. H.; Chicatun, F.; Nazhat, S. N.; Quinn, T. M. Cartilaginous Constructs Using Primary Chondrocytes from Continuous Expansion Culture Seeded in Dense Collagen Gels. *Acta Biomaterialia* **2013**, *9* (12), 9360–9369. https://doi.org/10.1016/j.actbio.2013.07.024.

(23) Vardar, E.; Engelhardt, E.-M.; Larsson, H. M.; Mouloungui, E.; Pinnagoda, K.; Hubbell, J. A.; Frey, P. Tubular Compressed Collagen Scaffolds for Ureteral Tissue Engineering in a Flow Bioreactor System. *Tissue Engineering Part A* **2015**, *21* (17–18), 2334–2345. https://doi.org/10.1089/ten.tea.2015.0048.

(24) Bose, S.; Vahabzadeh, S.; Bandyopadhyay, A. Bone Tissue Engineering Using 3D Printing. *Materials Today* **2013**, *16* (12), 496–504. https://doi.org/10.1016/j.mattod.2013.11.017.

(25) Griffanti, G.; Nazhat, S. N. Dense Fibrillar Collagen-Based Hydrogels as Functional Osteoid-Mimicking Scaffolds. *International Materials Reviews* **2020**, *65* (8), 502–521. https://doi.org/10.1080/09506608.2020.1735828.

(26) Coyac, B. R.; Chicatun, F.; Hoac, B.; Nelea, V.; Chaussain, C.; Nazhat, S. N.; McKee, M. D. Mineralization of Dense Collagen Hydrogel Scaffolds by Human Pulp Cells. *J Dent Res* **2013**, *92* (7), 648–654. https://doi.org/10.1177/0022034513488599.

(27) Chamieh, F.; Collignon, A.-M.; Coyac, B. R.; Lesieur, J.; Ribes, S.; Sadoine, J.; Llorens, A.; Nicoletti, A.; Letourneur, D.; Colombier, M.-L.; Nazhat, S. N.; Bouchard, P.; Chaussain, C.; Rochefort, G. Y. Accelerated Craniofacial Bone Regeneration through

Dense Collagen Gel Scaffolds Seeded with Dental Pulp Stem Cells. *Sci Rep* **2016**, *6* (1), 38814. https://doi.org/10.1038/srep38814.

(28) Novais, A.; Lesieur, J.; Sadoine, J.; Slimani, L.; Baroukh, B.; Saubaméa, B.; Schmitt, A.; Vital, S.; Poliard, A.; Hélary, C.; Rochefort, G. Y.; Chaussain, C.; Gorin, C. Priming Dental Pulp Stem Cells from Human Exfoliated Deciduous Teeth with Fibroblast Growth Factor-2 Enhances Mineralization Within Tissue-Engineered Constructs Implanted in Craniofacial Bone Defects. *Stem Cells Translational Medicine* **2019**, *8* (8), 844–857. https://doi.org/10.1002/sctm.18-0182.

(29) Maillard, S.; Sicard, L.; Andrique, C.; Torrens, C.; Lesieur, J.; Baroukh, B.; Coradin, T.; Poliard, A.; Slimani, L.; Chaussain, C. Combining Sclerostin Neutralization with Tissue Engineering: An Improved Strategy for Craniofacial Bone Repair. *Acta Biomaterialia* **2022**, *140*, 178–189. https://doi.org/10.1016/j.actbio.2021.11.046.

(30) Collignon, A.-M.; Castillo-Dali, G.; Gomez, E.; Guilbert, T.; Lesieur, J.; Nicoletti, A.; Acuna-Mendoza, S.; Letourneur, D.; Chaussain, C.; Rochefort, G. Y.; Poliard, A. Mouse *Wnt1-CRE* -Rosa *Tomato* Dental Pulp Stem Cells Directly Contribute to the Calvarial Bone Regeneration Process. *Stem Cells* **2019**, *37* (5), 701–711. https://doi.org/10.1002/stem.2973.

(31) Gronthos, S.; Mankani, M.; Brahim, J.; Robey, P. G.; Shi, S. Postnatal Human Dental Pulp Stem Cells (DPSCs) *in Vitro* and *in Vivo*. *Proc. Natl. Acad. Sci. U.S.A.* **2000**, *97* (25), 13625–13630. https://doi.org/10.1073/pnas.240309797.

(32) Marelli, B.; Ghezzi, C. E.; Zhang, Y. L.; Rouiller, I.; Barralet, J. E.; Nazhat, S. N. Fibril Formation PH Controls Intrafibrillar Collagen Biomineralization in Vitro and in Vivo. *Biomaterials* **2015**, *37*, 252–259. https://doi.org/10.1016/j.biomaterials.2014.10.008.

(33) Ajalloueian, F.; Nikogeorgos, N.; Ajalloueian, A.; Fossum, M.; Lee, S.; Chronakis, I. S. Compressed Collagen Constructs with Optimized Mechanical Properties and Cell Interactions for Tissue Engineering Applications. *International Journal of Biological Macromolecules* **2018**, *108*, 158–166. https://doi.org/10.1016/j.ijbiomac.2017.11.117.

(34) Williams, B. R.; Gelman, R. A.; Poppke, D. C.; Piez, K. A. Collagen Fibril Formation. Optimal in Vitro Conditions and Preliminary Kinetic Results. *Journal of Biological Chemistry* **1978**, *253* (18), 6578–6585. https://doi.org/10.1016/S0021-9258(19)46970-6.

(35) Roeder, B. A.; Kokini, K.; Sturgis, J. E.; Robinson, J. P.; Voytik-Harbin, S. L. Tensile Mechanical Properties of Three-Dimensional Type I Collagen Extracellular Matrices With Varied Microstructure. *Journal of Biomechanical Engineering* **2002**, *124* (2), 214–222. https://doi.org/10.1115/1.1449904.

(36) Gobeaux, F.; Mosser, G.; Anglo, A.; Panine, P.; Davidson, P.; Giraud-Guille, M.-M.; Belamie, E. Fibrillogenesis in Dense Collagen Solutions: A Physicochemical Study. *Journal of Molecular Biology* **2008**, *376* (5), 1509–1522. https://doi.org/10.1016/j.jmb.2007.12.047.

(37) Li, Y.; Asadi, A.; Monroe, M. R.; Douglas, E. P. PH Effects on Collagen Fibrillogenesis in Vitro: Electrostatic Interactions and Phosphate Binding. *Materials Science and Engineering: C* **2009**, *29* (5), 1643–1649. https://doi.org/10.1016/j.msec.2009.01.001.

(38) Darvish, D. M. Collagen Fibril Formation in Vitro: From Origin to Opportunities. *Materials Today Bio* **2022**, *15*, 100322. https://doi.org/10.1016/j.mtbio.2022.100322.

(39) Hagar, M. N.; Yazid, F.; Luchman, N. A.; Ariffin, S. H. Z.; Wahab, R. M. A. Comparative Evaluation of Osteogenic Differentiation Potential of Stem Cells Derived from Dental Pulp and Exfoliated Deciduous Teeth Cultured over Granular Hydroxyapatite Based Scaffold. *BMC Oral Health* **2021**, *21* (1), 263. https://doi.org/10.1186/s12903-021-01621-0.

(40) Wang, H.; Zhong, Q.; Yang, T.; Qi, Y.; Fu, M.; Yang, X.; Qiao, L.; Ling, Q.; Liu, S.; Zhao, Y. Comparative Characterization of SHED and DPSCs during Extended Cultivation Inï¿½vitro. *Mol Med Report* **2018**. https://doi.org/10.3892/mmr.2018.8725.

(41) Sabbagh, J.; Ghassibe-Sabbagh, M.; Fayyad-Kazan, M.; Al-Nemer, F.; Fahed, J. C.; Berberi, A.; Badran, B. Differences in Osteogenic and Odontogenic Differentiation Potential of DPSCs and SHED. *Journal of Dentistry* **2020**, *101*, 103413. https://doi.org/10.1016/j.jdent.2020.103413.

(42) Goldstein, A. S. Effect of Seeding Osteoprogenitor Cells as Dense Clusters on Cell Growth and Differentiation. *Tissue Engineering* **2001**, *7* (6), 817–827. https://doi.org/10.1089/107632701753337753.

(43) Comper, W. D.; Veis, A. The Mechanism of Nucleation for *in Vitro* Collagen Fibril Formation. *Biopolymers* **1977**, *16* (10), 2113–2131. https://doi.org/10.1002/bip.1977.360161004.

(44) Christiansen, D. L.; Huang, E. K.; Silver, F. H. Assembly of Type I Collagen: Fusion of Fibril Subunits and the Influence of Fibril Diameter on Mechanical Properties. *Matrix Biology* **2000**, *19* (5), 409–420. https://doi.org/10.1016/S0945-053X(00)00089-5.

(45) Harris, J. R.; Soliakov, A.; Lewis, R. J. In Vitro Fibrillogenesis of Collagen Type I in Varying Ionic and PH Conditions. *Micron* **2013**, *49*, 60–68. https://doi.org/10.1016/j.micron.2013.03.004.

(46) Leyendecker Junior, A.; Gomes Pinheiro, C. C.; Lazzaretti Fernandes, T.; Franco Bueno, D. The Use of Human Dental Pulp Stem Cells for in Vivo Bone Tissue Engineering: A Systematic Review. *J Tissue Eng* **2018**, *9*, 204173141775276. https://doi.org/10.1177/2041731417752766.

(47) Ahearne, M. Introduction to Cell–Hydrogel Mechanosensing. *Interface Focus.* **2014**, *4* (2), 20130038. https://doi.org/10.1098/rsfs.2013.0038.

(48) Jagiełło, A.; Castillo, U.; Botvinick, E. Cell Mediated Remodeling of Stiffness Matched Collagen and Fibrin Scaffolds. *Sci Rep* **2022**, *12* (1), 11736. https://doi.org/10.1038/s41598-022-14953-w.

(49) Deegan, A. J.; Aydin, H. M.; Hu, B.; Konduru, S.; Kuiper, J. H.; Yang, Y. A Facile in Vitro Model to Study Rapid Mineralization in Bone Tissues. *BioMed Eng OnLine* **2014**, *13* (1), 136. https://doi.org/10.1186/1475-925X-13-136.

(50) Bitar, M.; Brown, R. A.; Salih, V.; Kidane, A. G.; Knowles, J. C.; Nazhat, S. N. Effect of Cell Density on Osteoblastic Differentiation and Matrix Degradation of Biomimetic Dense Collagen Scaffolds. *Biomacromolecules* **2008**, *9* (1), 129–135. https://doi.org/10.1021/bm701112w.

Chapter III

Effect of soluble silicon on the mineralization of plastically-compressed collagen hydrogels by human dental pulp stem cells

This work has been published as:

Mbitta Akoa, D.; Hélary, C.; Foda, A.; Chaussain, C.; Poliard, A.; Coradin, T. Silicon impacts collagen remodelling and mineralization by human dental pulp stem cells in 3D pulp-like matrices. *Dental Materials* **2024**, 40, 1390-1399. https://doi.org/10.1016/j.dental.2024.06.021

III.1. Introduction

First studies on pulp reactions to silicate-based filling materials date back to the 1940s, suggesting marked degenerative changes in pulp tissue.[1,2] Over the last decades, different calcium silicate (CS) materials exhibiting low toxicity, high biocompatibility and the ability to trigger the formation of mineralized tissue have been developed and launched on the market.[3,4] Their use as pulp-capping materials has become very common in dental clinical practice, as they are able to support dentin repair by promoting differentiation of dental pulp stem cells (DPSCs) into odontoblasts-like cells, as well as mineralization.[5] However, only a limited number of studies have attempted to define the molecular mechanisms mediating the response of DPSCs to these CS materials to form reparative dentin.[6]

Emerging evidence supports that Ca^{2+} ions released by CS biomaterials are mobilized by DPSCs, leading to intracellular transcriptional changes in DPSCs during odontogenic differentiation, with increased mineralization.[7,8] However, studies demonstrated that the viability, proliferation and differentiation of DPSCs were enhanced in CS materials when compared with calcium hydroxide.[9,10] In a clinical study, the success rate of calcium hydroxide was 59% at 2-3 years follow-up; in contrast, calcium silicates showed a success rate of 81-86%.[11] This suggests that the superior effect of calcium silicates over calcium hydroxide might be attributed to the soluble silicon ($Si(OH)_4$, silicic acid) released by CS. When studying the effects of soluble silicon on DPSCs *in vitro*, supernatants obtained from the immersion of CS in the physiological medium were used as a source of silicon (Si).[10,12–14] These solutions stimulated DPSCs proliferation and differentiation more than CH supernatant, suggesting that soluble Si released from CS positively influenced cells. However, CS extracts contain both $Si(OH)_4$ and Ca^{2+} ions, and thus the specific role of soluble Si on DPSC is still not established.

Unlike its role in dentin formation, Si influence on bone formation is well documented, although yet not fully understood.[15–17] It has been advocated that Si promotes bone formation and gene expression involved in cell osteoblastic differentiation, mineralization and type I collagen synthesis.[18–21] The concentration-response is still debated and may vary according to the cell type.[22] For example, increased calcium deposition and type 1 collagen gene expression by human osteosarcoma MG-63 was observed at a supra-physiological concentration of 4 mM Si.[21] Using the same cell line, the largest production of collagen was obtained with the addition of the physiological concentration of 10-20 µM Si in the culture medium, but the researchers

did not find any change in type I collagen RNA level.[18] Similar study with osteoblasts revealed upregulated type I collagen gene expression with 50 µM Si.[19] Using mesenchymal stem cells, Si at a concentration of 625 µM significantly enhanced the proliferation, mineralization nodule formation, bone/tooth-related gene expression (osteocalcin, osteopontin and alkaline phosphatase) and synthesis of mineralization-related proteins (alkaline phosphatase and osteopontin).[23] Such heterogeneity in the cellular response suggests that additional parameters beyond silicic acid concentration play a key role in Si ability to promote mineralization.

Conventionally, the cellular response to soluble silicon has been investigated *in vitro* in 2D cell culture. Although 2D culture research models offer a simple and cost-effective approach to maintaining cell culture, failure to mimic native tissue environment, changes in cell morphology and division, and disruption of interactions between the cells and the extracellular matrix raise the question of their physiological relevance.[24] 3D *in vitro* models have opened up new possibilities for modelling tissue interactions *in vivo*, enabling scientists to explore the biochemical cues underlying tissue formation. Cell-seeded dense, plastically-compressed collagen scaffolds have been validated as 3D cell culture models relevant to dental and bone biology, as they mimic the precursor matrices of tooth and bone mineralization, predentin and osteoid respectively.[25–27] Furthermore, they have the potential to guide DPSC odonto/osteoblastic differentiation and DPSC-mediated matrix mineralization both *in vitro* and *in vivo*.[28–30]

Therefore, a biomimetic 3D dense collagen gel model was used in this study to investigate the effects of soluble silicon on the viability, odonto/osteogenic differentiation, mineralization and matrix remodelling activity of human DPSCs *in vitro*. Physiological (10 µM) and supraphysiological (100 µM) silicic acid concentrations were studied.[31] Results gathered from multiphoton imaging, electron microscopy, viability/metabolic tests, histology and gene expression studies suggest that, in our conditions, hDPSCs may not be influenced by the presence of silicon itself but via silicic acid interactions with the collagen matrix, which in turn modifies the hDPSC-collagen interface. These data also call for a more systematic assessment of possible Si-matrix interactions in studies of silicon-induced biological mineralization together with the design of more biomimetic tissue models.

III.2. Materials and Methods

III.2.1. Cell source

Human DPSCs were isolated from healthy teeth extracted from patients aged 15-20 years for orthodontic reasons at the AH-HP Bretonneau Hospital Dental Department. Teeth were collected according to the ethical guidelines established by French bioethics law (IRB agreement 00006477 and n° DC-2009-927, Cellule Bioéthique DGRI/A5), under an opt-out consent model. Primary DPSC were obtained following the extraction protocol established by Gronthos *et al.*[32] Cells at passage 4 were used in this study.

III.2.2. Preparation of dense collagen hydrogels

Type I collagen was extracted from young rat tail tendons[33] to prepare dense 3D collagen gels using plastic compression, as previously described [28,34]. Briefly, type I collagen (4 $mg.mL^{-1}$) solubilised in a 20 mM acetic acid solution was mixed with DMEM 5X (Dulbecco's Modified Eagle Medium) and adjusted to the physiological pH with 0.1 M NaOH. After neutralization, hDPSCs suspended in a complete medium (DMEM media supplemented with 10% fetal bovine serum and 1% penicillin/streptomycin) were added to the collagen solution to obtain a pre-compression concentration of 2×10^6 $cells.mL^{-1}$.[30] The mixture with a final collagen concentration of 1.6 $mg.mL^{-1}$ was then placed into a 24-well plate and incubated at 37°C/5% CO_2 for 30 minutes. The resulting highly hydrated collagen gels were transferred to a stack of blotting paper, nylon and stainless-steel mesh and loaded with a compressive stress of 1 kPa for 5 min, yielding dense collagen gel scaffolds (> 10% w/v fibrillar collagen density).[34]

III.2.3. Cell culture conditions

The hDPSCs encapsulated in plastically compressed dense collagen hydrogels were grown in a mineralizing induction medium (MIM) made of 300 µM L-ascorbic acid sodium salt, 10 nM dexamethasone, 10 mM β-glycerophosphate, 10% fetal bovine serum, and 1% penicillin/streptomycin, without or with $Si(OH)_4$ at concentrations of 10 µM (Si10) or 100 µM (Si100). Stock solutions of concentrated silicic acid (x100) were previously prepared from a commercial standard solution (Silicon Standard for ICP, 1002 ± 2 $mg.L^{-1}$ in NaOH, Sigma Aldrich) and adjusted to physiological pH with HCl before being diluted in the mineralizing

medium. Cell-laden collagen gels were cultured in 6-well plates using 5 mL of culture medium per well. Acellular gels cultured in MIM alone or supplemented with Si (10-100) were established as controls. Gels were incubated for 24 days, with differentiation media being renewed at 2- or 3-day intervals.

III.2.4. Cell viability, distribution and metabolic activity

Cell viability and distribution within the dense collagen gels were analysed by means of a Leica SP5 upright confocal (Leica DMI6000 Upright TCS SP5) coupled with a multiphoton laser scanning microscopy (Mai Tai multiphoton laser), which enabled the simultaneous acquisition of fluorescence and second-harmonic generation (SHG) signal.[35] Prior to imaging, seeded cells were stained on day 24 post-culture following the live/dead® viability-cytotoxicity assay instructions (Thermofisher, Waltham, MA, USA). Constructs were washed in phosphate buffered saline (PBS) and stained with 2 µM calcein-AM and 4 µM ethidium homodimer-1 solution. Live cells were stained in green and dead cells in red. A hybrid collector with a wavelength of 438 ± 24 nm (initial excitation of 880 nm) was used to detect the SHG signal of the corresponding collagen fibers and a 25x/0.95 water objective with a working distance of 2.5 mm was used to acquire the z-stacks for each sample. Image series were acquired with the Leica Application Suite X software. Live/dead cells volumes and collagen signals were analysed using ImageJ.

Cell metabolic activity in dense collagen gels was analysed by alamarBlue® assay (Sigma-Aldrich, St. Louis, MO, USA) up to day 21 of culture. The cell-laden gels were incubated in a complete culture media containing 10 $\mu g.mL^{-1}$ resazurin at 37°C/5% CO_2 for 3 hours. Absorbances were read at wavelength of 570/600nm with a UV/Vis Uvikon spectrophotometer. The reduction percentage of AlamarBlue was calculated according to the manufacturer's instructions.

III.2.5. Cell-Mediated Gel Contractility Assay

Collagen gel contraction was quantified by measuring gel diameter on days 1, 3, 7, 10 and 14 of culture. The gel size was compared with the initial gel diameter. 4 gels were measured per condition.

III.2.6. Scanning electron microscopy (SEM) / Energy-dispersive x-ray spectroscopy (EDS)

First, gels were fixed with 4% paraformaldehyde (PFA) and washed with 0.1M sodium cacodylate/0.6M sucrose buffer, before being dehydrated in a series of alcohol solutions and dried with supercritical CO_2. Dried samples were mounted on metallic holders and sputter-coated with gold (15 nm layer) for SEM analysis and carbon (20 nm layer) for EDS. Samples were analysed under a Hitachi S-3400 N microscope at accelerating voltage of 10kV for SEM and 70 kV for EDS. Several pictures at different magnifications (1500-10,000x) were taken to examine microstructural features and chemical content.

III.2.7. Histological and Immunohistochemistry staining

After 24 days in culture, gels were fixed in a 4% PFA solution, dehydrated, embedded in paraffin and cut into 7 µm thick sections. Prior to staining, sections were deparaffinized with toluene and rehydrated in ethanol solutions of decreasing concentrations, finishing with water. Cell distribution within the collagen matrix was assessed using Masson's trichrome staining. Calcium and phosphate deposits were detected by alizarin red and Von Kossa, respectively. Micrographs were acquired under a light microscope (DMLB, Leica).

For immunochemistry, sections were rehydrated and permeabilized with 0.05 % Tween 20 (diluted in ethylenediaminetetraacetic acid buffer) at 95 °C for 20 min and blocked with 5 % bovine serum albumin (BSA, ThermoFisher Scientific) in PBS (PBS 1X - BSA 5 %) for 1 h at room temperature. Sections were incubated overnight at 4° C with the following primary antibodies: Nestin (1:200 dilution, 19483-1-AP, Proteintech, USA) and Osteopontin (1:50 dilution, sc-21742, Santa Cruz, USA). The following day, sections were incubated for 1 h with Rhodamine Red™ - X goat anti-mouse IgG secondary antibody (1:200, R6393, Invitrogen, Canada) for OPN and Rhodamine Red™-X goat anti-rabbit IgG secondary antibody (1:200, R6394, Invitrogen, Canada) for Nestin. Nuclei were then counterstained with DAPI (1:1000, Thermo Fisher Scientific) and the multi-exposure images were acquired using bandpass filters appropriate for the red dye and blue DAPI.

III.2.8. qRT-PCR analyses

On days 0, 7, 14, and 21, cell-laden dense collagen gels were digested by collagenase, homogenized using Trizol® (Invitrogen, USA) and stored at -80°C prior to utilization. Total RNA content was extracted using the RNeasy Plus Mini Kit (Qiagen, Hilden, Germany) according to the manufacturer's instructions. For quantitative PCR, single-stranded RNA was transformed into complementary double-stranded DNA (cDNA) by reverse transcription. 1µL of random primers (200uM) (Invitrogen) and 1 µL deoxyribonucleosides triphosphates(10mM) (Invitrogen) were added to 10 µl RNA aliquots (around 300-500 ng). Following denaturation of secondary structure at 65°C and primers binding, 5X reaction buffer, dithiothreitol (0.2 M) and Moloney murine leukemia virus (M-MLV) (Invitrogen) were added. After 60 min at 37°C, the reaction was stopped by heating at 70°C for 10 min. The resulting cDNAs were stored at -20°C until further use.

Table III.1: Primers for real-time PCR (supplied by Roche Diagnostics, GmbH, Germany)

Primer	Sequence (Forward 5'- 3')	Sequence (Reverse 5'- 3')
BGLAP	CAAAGGTGCAGCCTTTGTGTC	TCACAGTCCGGATTGAGCTCA
Col1A1	CCAGTCAGAGTGGCACATCTTGA	GCTCACGATGGTGCCGCTACTA
MMP13	GCCGGTGTAGGTGTAGATAGGAAA	GGAGATGCCCATTTTGATGATGA
IBSP	AACGAACAAGGCATAAACGGCACCA	CTTGCCCTGCCTTCCGGTCT
ALP	GCAGCTTGACCTCCTCGGAAGACACT	TCACCGCCCACCACCTTGTAGCC
GAPDH	TTGATTTTGGAGGGATCTCG	GAGTCAACGGATTTGGTCGT
18S rRNA	TTACAGGGCCTCGAAAGAGT	TGAGAAACGGCTACCACATC

Real-time fluorescence analysis using SYBR Green Master Mix (Roche Diagnostics GmbH, Germany) was used to quantify the expression level of specific genes relative to GAPDH or 18S rRNA housekeeping genes. The primers used in qRT-PCR are listed in the table above (**Table III.1**). The reaction involved a succession of 40 cycles, each cycle including denaturation (95°C, 30 s), annealing (60°C, 30 s) and elongation with Taq polymerase (72°C, 30 s). Target gene quantities were normalized to GAPDH/18S rRNA using the Pfaffl method to determine variations in expression of each target gene under different mineralization conditions. The condition MIM at day 7 was used as calibrator point. Three samples were analysed per group.

III.2.9. Statistical analysis

Statistical analysis was performed on OriginPro 9.4 (OriginLab, Northampton, MA, USA). Data were compared statistically by one-way analysis of variance (ANOVA) tests. Statistical difference was considered at $p < 0.05$. Data are presented as mean ± standard deviation of mean (SD).

III.3 Results

The impact of Si-containing medium on hDPSCs was assessed in cell-seeded plastically compressed 3D dense collagen hydrogels, in terms of cell viability and differentiation, mineral deposition and matrix remodelling. Three mineralization conditions were tested: MIM without silicic acid (control), with 10 µM silicic acid (physiological) and 100 µM silicic acid (supraphysiological).

III.3.1. Influence of silicic acid on hDPSCs viability and metabolic activity

Viability of hDPSCs seeded in collagen hydrogels was assessed using calcein-AM and Ethidium homodimer-1 to stain live and dead cells respectively. Control and silicic acid-treated groups (10 and 100 µM) showed similar high cell viability, with a limited number of dead cells on day 24 of culture (**Figure III.1(a)**). Analysis of the virtual volume occupied by cells in the gels showed a significantly greater volume of living cells than dead cells in each group (**Figure III.1(b)**). In the presence or absence of Si, live/viable cell volumes were not significantly different.

To evaluate the metabolic activity of the cells, the AlamarBlue® test was carried out over 21 days of culture. The hDPSCs showed a similar trend under the three conditions, with a progressive decrease in resazurin reduction over time (**Figure III.1(c)**). Cell metabolic activity was not influenced by silicic acid addition over 2 weeks and was slightly higher in Si10-treated cells after 21 days compared to the two other conditions.

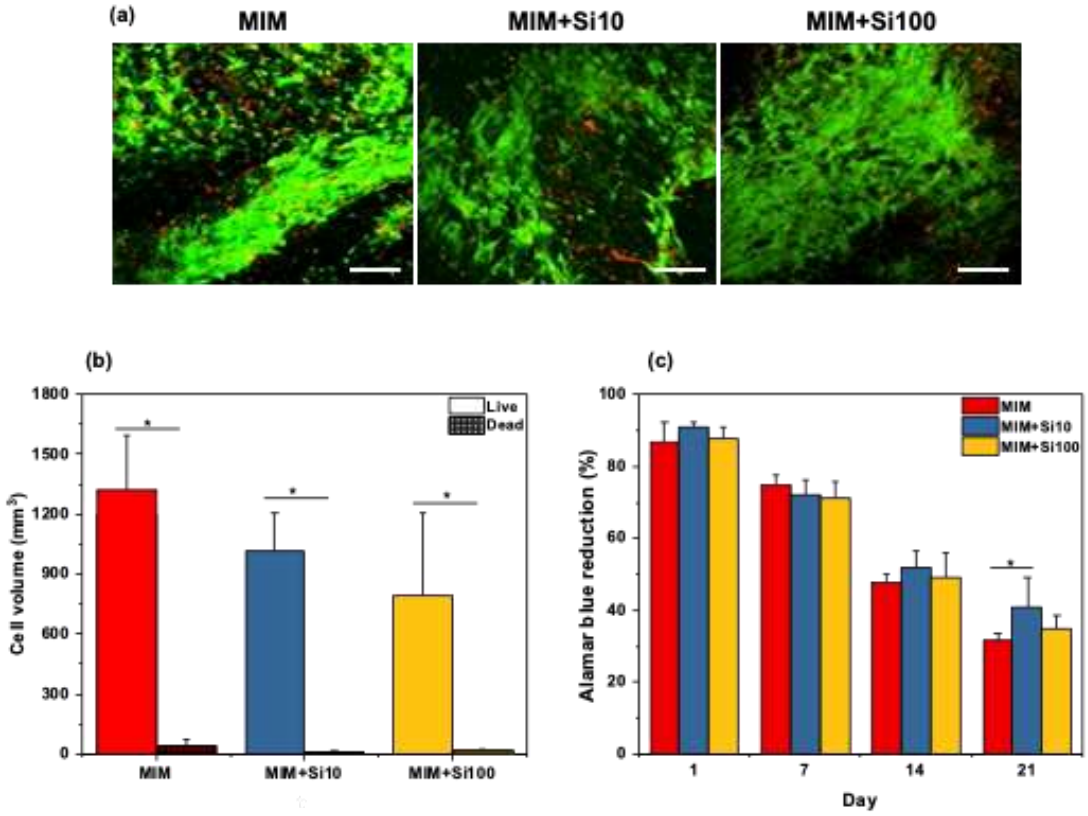

Figure III.1: Viability and metabolic activity of hDPSC seeded in 3D dense collagen gels under mineralizing induction medium (MIM) without or with silicic acid at 10 µM and 100 µM. (a) Confocal images of live/dead stained cells at day 24. Scale bar 100 µm. (b) Quantification of cell volume occupied by live and dead cells in the gels at day 24. (c) Metabolic activity of seeded cells at day 1, 7, 10 and 21 in culture. *p<0.05.

III.3.2. Influence of silicic acid on hDPSCs clustering

The impact of Si on hDPSCs distribution in dense collagen hydrogels was further analysed by SHG and confocal microscopy. On day 24 of differentiation, cells spread out evenly within the collagen matrix cultured in mineralizing medium alone (**Figure III.2(a)**). In contrast, Si10-treated matrix exhibited zones of cell clustering, leaving some hydrogel regions without cells (**Figure III.2(b)**). This trend was even more marked at Si 100 µM where a large cell cluster was observed (**Figure III.2(c)**). Such cell-free areas could be further visualized on hydrogel cross-sections stained with Masson trichrome (**Figures III.2(d-f)**).

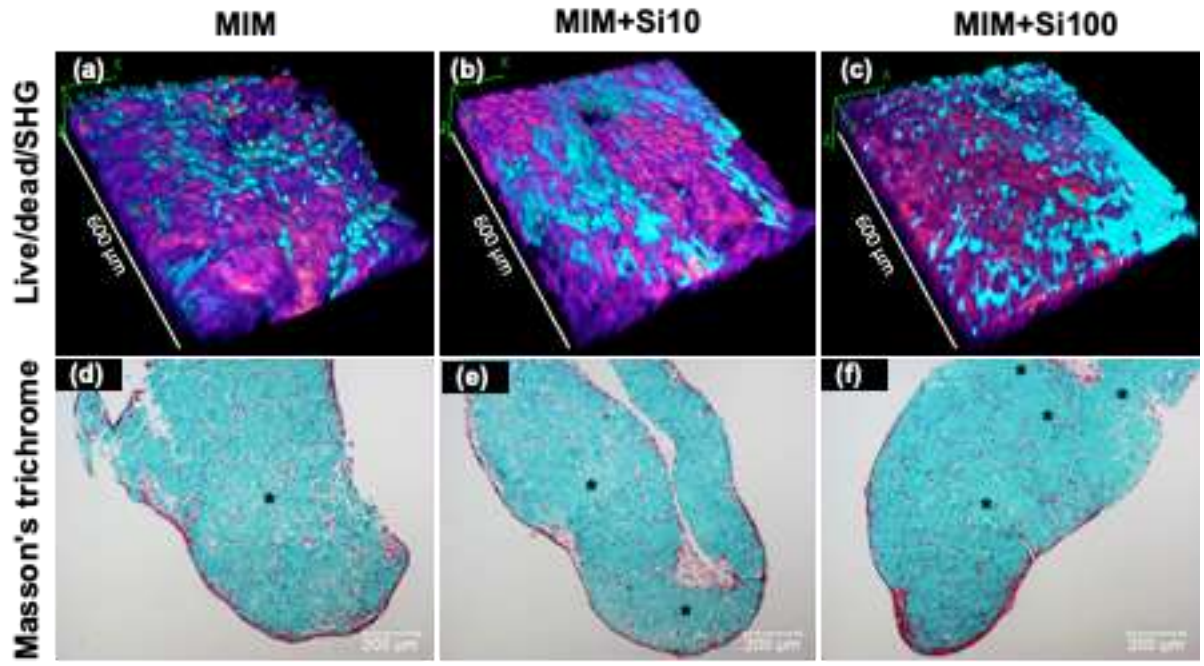

Figure III.2: Cells distribution within the gels on day 24 of growth in absence or presence of Si (10 µM, 100 µM) in Mineralizing Induction Medium (MIM). (a-c) 3D rendering Confocal coupled with SHG images (collagen=purple, live cells=magenta; dead cells=red) and (d-f) Masson's Trichrome staining of scaffolds. Observation of regions without cells (asterisks).

III. 3.3. Influence of silicic acid on hDPSCs proliferation

hDPSC proliferation in dense collagen hydrogels was assessed by analysing RNA content over a 21 days culture in mineralizing media with or without silicic acid. Cell proliferation increased from day 1 to day 7, then decreased in the three groups independently of the presence of Si (**Figure III.3(a)**). A significant difference in RNA content was measured between the Si-100 treated hydrogel and the Si-free group on day 1.

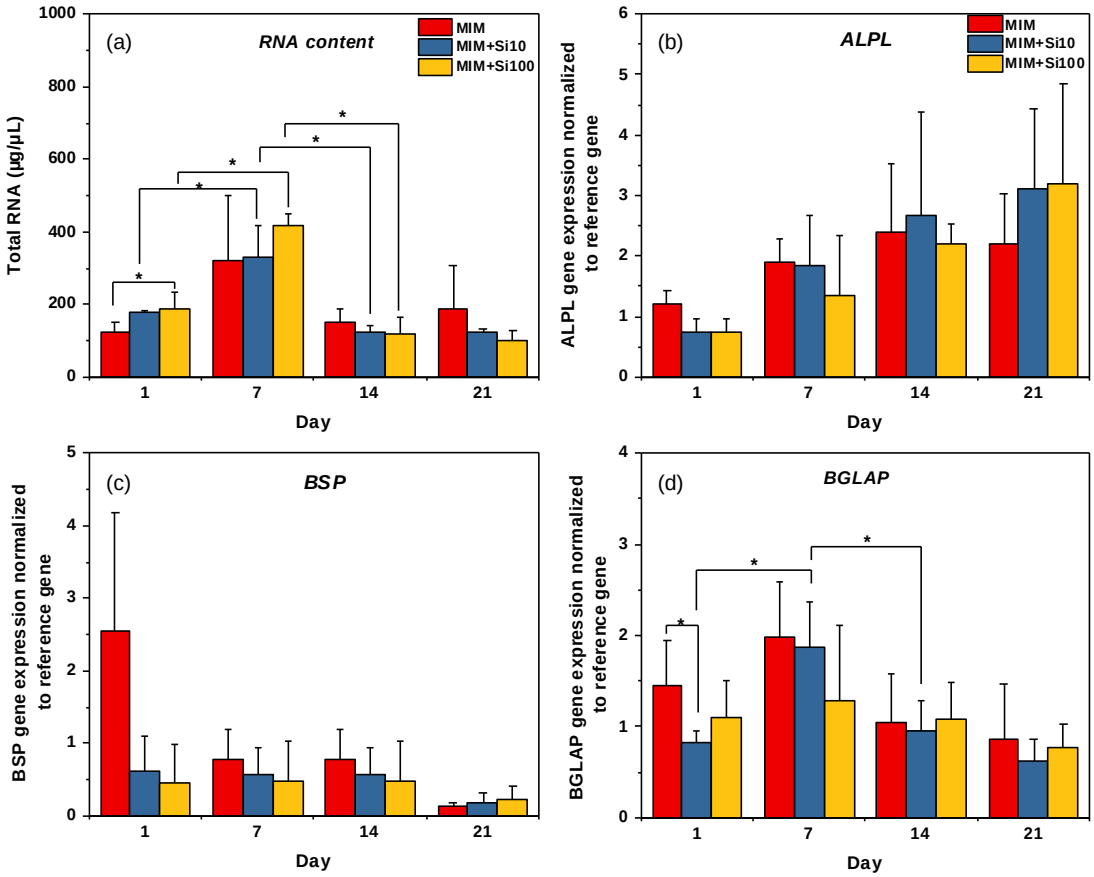

Figure III.3: Influence of Si on hDPSC proliferation and differentiation after culturing dense cells-laden collagen gels in mineralizing media for 1, 7, 14 and 21 days in the absence or presence of Si (10 µM, 100 µM). (a) RNA content/cell proliferation. Gene expression of *ALP* (b), *BSP* (c), *BGLAP* (d) by qRT-PCR analysis. **p*<0.05.

III.3.4. Influence of silicic acid on hDPSCs differentiation

Expression of bone- or tooth-related genes, *i.e.* ALP, BSP and BGLAP (osteocalcin), were investigated by qRT-PCR in the hDPSCs cell-laden gels grown for 1, 7, 14 and 21 days in MIM in the absence or presence of Si (10 and 100µM). All these genes were expressed in both Si- and non-Si-treated groups at all the different time points (**Figures III.3(b-d)**).

ALP gene expression (**Figure III.3(b)**) followed a similar trend in the control and Si groups, with a progressive increase over time. Comparable low levels of BSP expression were detected in the absence or in the presence or Si from day 1 to day 14, even though on day 1, BSP expression in MIM (without Si) was highly expressed without significant difference versus the Si groups (**Figure III.3(c)**). BGLAP expression level (**Figure III.3(d)**) gradually increased in all the groups from day 1 to day 7, when it reached its highest level, and then decreased

dramatically. On day 1, BGLAP was at its lowest level in the Si10 group, and significantly lower compared to the MIM group. Nevertheless, on day 7, BGLAP expression increased up to 2.4-fold in the Si10 group, reaching the same level of expression as in the MIM group. Increasing silicon content (Si100) resulted in a 1.5-fold lower level of BGLAP expression at day 7, albeit no statistically significant difference was observed between the groups.

Complementary immunostaining showed that, at day 24 post-seeding, Nestin, a neural crest mesenchymal stem cells marker [36], was uniformly present throughout the whole width and height of the gels in the three conditions (**Figure III.4(a-c)**). There was a trend of decreasing Nestin-staining intensity with increasing silicon content, but without statistical difference between the three groups (**Figure III.4(g)**)

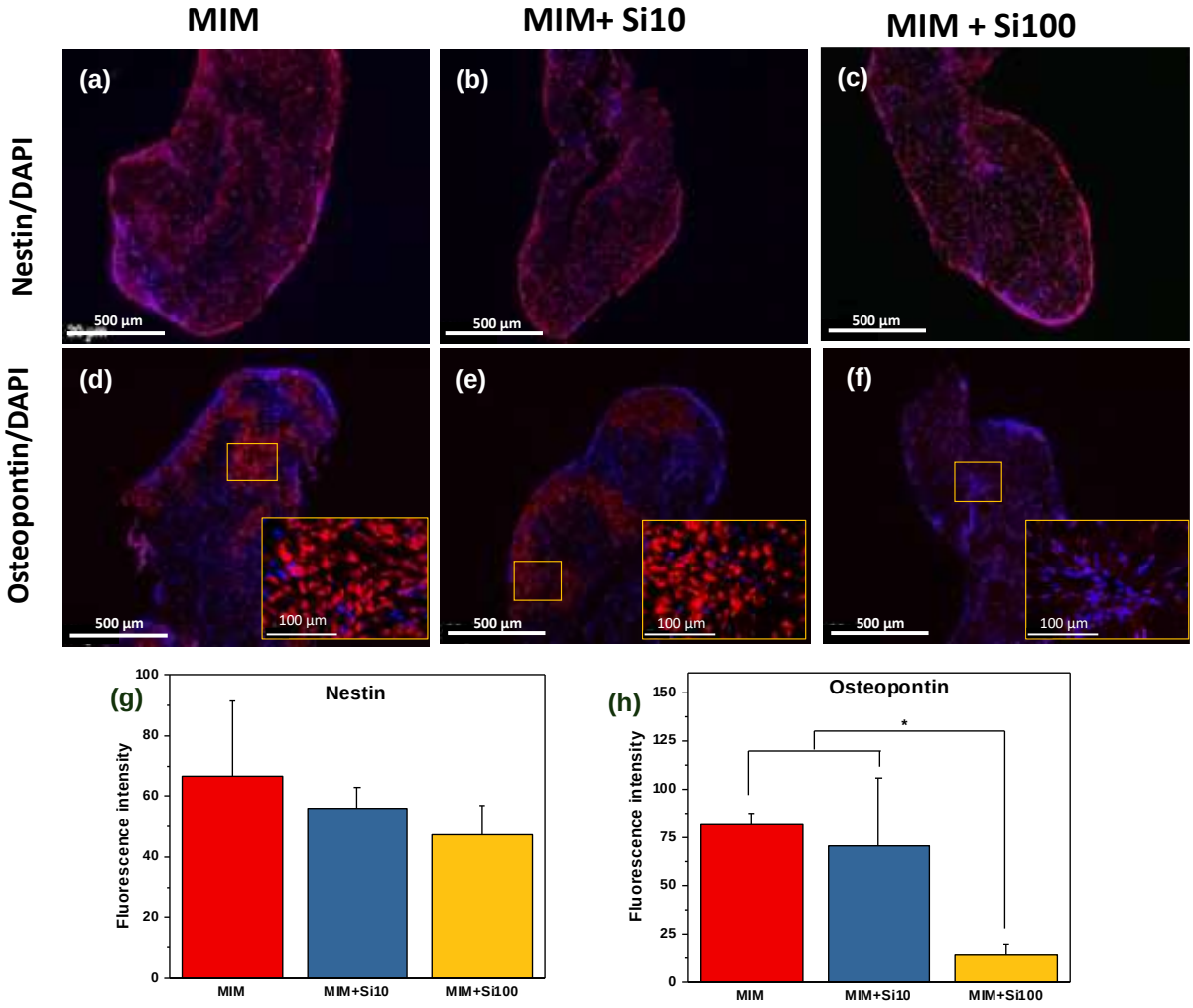

Figure III.4: Immunohistochemically stained sections of hDPSC-seeded scaffolds grown in mineralizing conditions without or with Si (10 µM, 100 µM) for 24 days. (a-c) Nestin/DAPI, (d-f) Osteopontin/DAPI, and quantifications of Nestin (g) and Osteopontin (h) fluorescence at day 24.

In parallel, stronger osteopontin immunolabeling was observed in cell-laden gels grown without Si (**Figure III.4(d)**) and with Si10 (**Figure III.4(e)**), *vs*. gels grown with Si100 (**Figure III.4(f)**). Accordingly, the Si100 group exhibited a significant reduction in the fluorescence intensity of osteopontin (**Figure III.4(h)**).

III.3.5. Mineralization analyses

III.3.5.1. Alizarin red S staining

To determine whether the presence of Si in the hydrogels impacted the extent of mineralization, sections of cellularized hydrogels cultured for 24 days were stained with alizarin red. A comparable calcium red staining was observed in MIM alone (**Figure III.5(a)**) and Si10 conditions (**Figure III.5(b)**), while a fainter and localized staining was observed in Si100 group (**Figure III.5(c)**). Noteworthy, the mineral deposits in the Si10-scaffolds were organized in clusters in some areas of the gel (**Figure III.5(b)**), in line with the cell organization in clusters already observed in the SHG images (**Figure III.2(b)**). In contrast, cross-sectional images of gels grown in MIM alone displayed a uniform distribution of the mineral deposition (**Figure III.5(a)**). The presence of phosphate within the same regions was confirmed by Von Kossa staining (**Figure III.5(d-f)**).

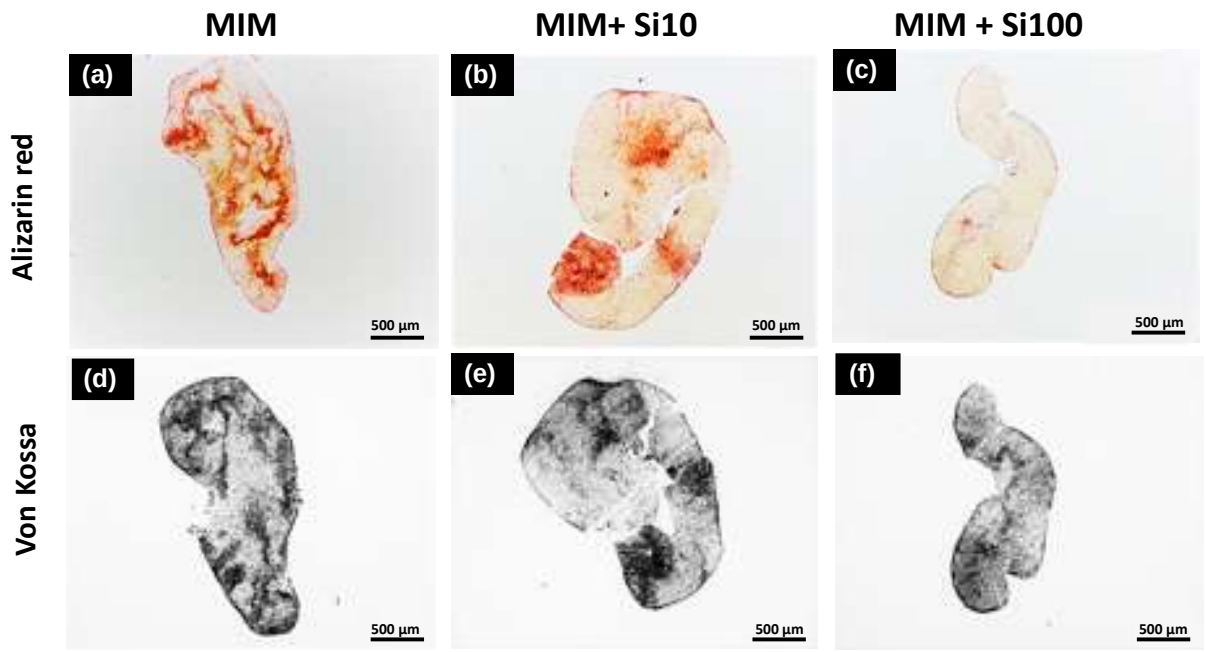

Figure III.5: Histologically stained sections of hDPSC-seeded scaffolds grown in mineralizing conditions without or with Si (10 µM, 100 µM) for 24 days. (a-c) Alizarin Red, (d-f) Von Kossa.

III.3.5.2. SEM imaging and EDS analyses

Cell-mediated matrix mineralization deposition was further analyzed by SEM and EDS, 24 days post-seeding. SEM images clearly indicated that minerals were present along the collagen matrix, and external to the cells, in all the three groups (**Figure III.6(a-c)**). In contrast, similarly-treated acellular collagen gels displayed a fibrillar collagen network with no evidence of mineral deposition **(Figure III.6(d-f)**).

EDS analysis of mineralized regions in the 3 culture conditions revealed the presence of both calcium and phosphorus in addition to oxygen and carbon (**Figure III.6(a-c)**), while only oxygen and carbon were identified in acellular gels (**Figure III.6(d-f)**). The average measured Calcium:Phosphorus ratio was 1.44 ± 0.14 in all samples, confirming the presence of a physiological apatite mineral phase.

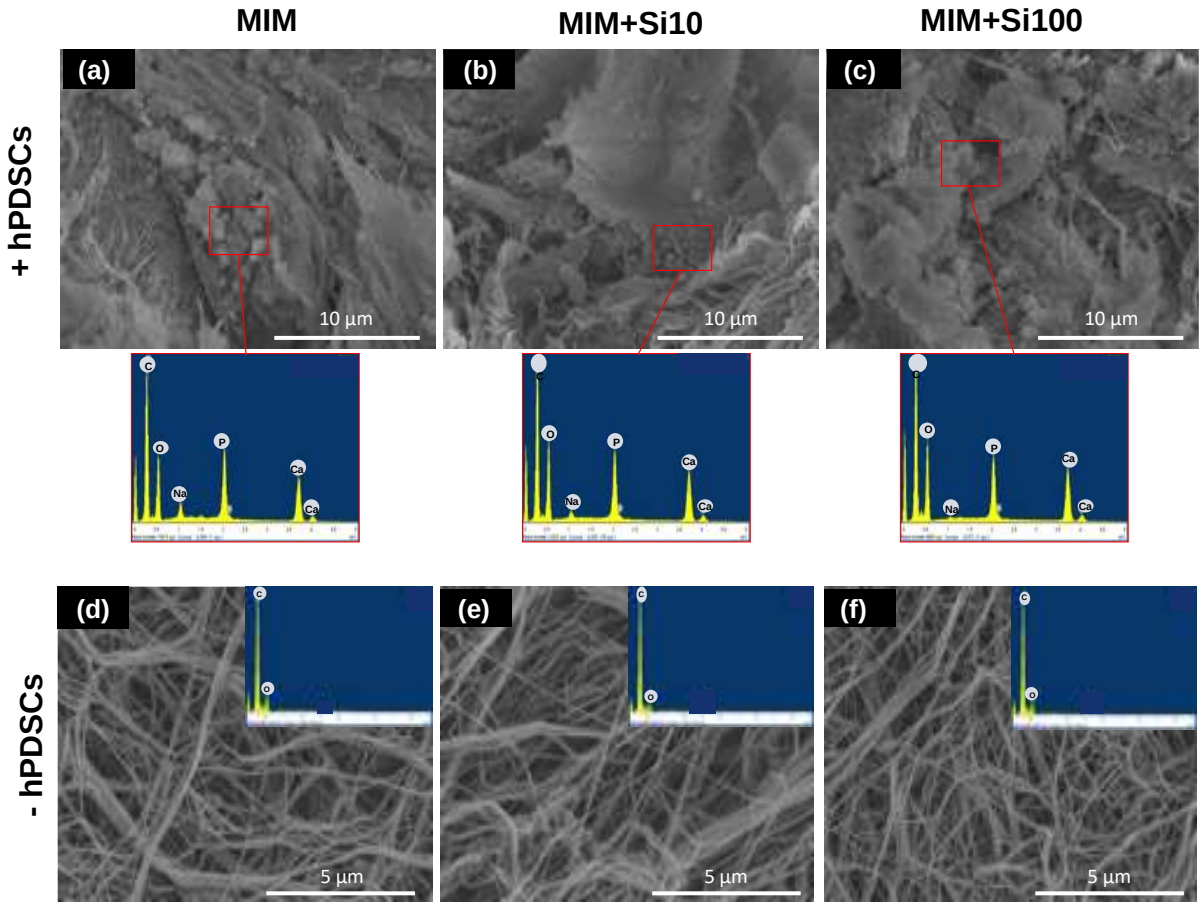

Figure III.6: Mineral formation of dense collagen hydrogels under mineralizing induction medium containing Si (10 µM, 100 µM) or not. (a-c) SEM micrographs and corresponding energy-dispersive x-ray spectra for h-DPSCs seeded hydrogels, (d-f) SEM micrographs and corresponding energy-dispersive x-ray spectra acellular hydrogels

III.3.6. Collagen matrix remodelling

III.3.6.1. Influence of silicic acid on hDPSCs matrix remodelling activity

Expression matrix remodelling-related genes, *i.e.* MMP13 and Col1, were investigated by RT-qPCR in the hDPSCs cell-laden gels grown for 1, 7, 14 and 21 days in MIM in the absence or presence of Si (10 and 100 µM). Treatment with Si at both concentrations resulted in a time-dependent collagen expression increase from day 7 to day 21, while Col1 levels remained constant between days 14 and 21 in the absence of Si (**Figure III.7(a)**). In parallel, MMP 13 expression was low on days 1 and 7 for all groups, with or without Si, and significantly lower for Si10 compared to MIM on day 7 (**Figure III.7(b)**). On day 14, Si10 group showed a higher level of MMP13 gene expression compared to the group with Si100, this difference being significant ($p<0.05$). At day 21, MMP13 gene expression continued to increase only for the Si100 condition, reaching values comparable to the other groups.

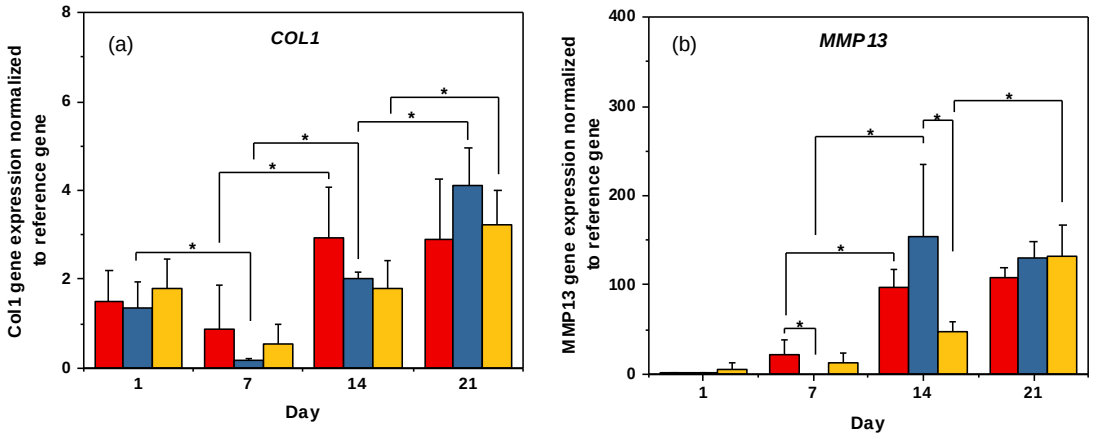

Figure III.7: Influence of Si on hDPSC remodeling activity after culturing dense cells-laden collagen gels in mineralizing media for 1, 7, 14 and 21 days in the absence (in red) or presence of Si (10 µM (in blue), 100 µM (in yellow)). Gene expression of *COL1* (a), *MMP13*(b) by RT-qPCR analysis. **p*<0.05.

III.3.6.2. Gel contraction

Relative extents of remodelling activity of collagen hydrogels by hDPSC were assessed by quantifying gel diameter over 14 days of culture and performing SHG microscopy on day 24. hDPSC-seeded gels grown in media without or with Si (10, 100 µM) showed equivalent decreases in diameter/contraction at the same time points (**Figure III.8(a)**). A reduction in gel diameter of 50% from its original size was measured on day 1, and then contraction remained relatively constant throughout the 14 days of culture (**Figure III.8(b)**). The contraction was completely absent in acellular gels, regardless of the presence or absence of Si (**Figure III.8(c)**).

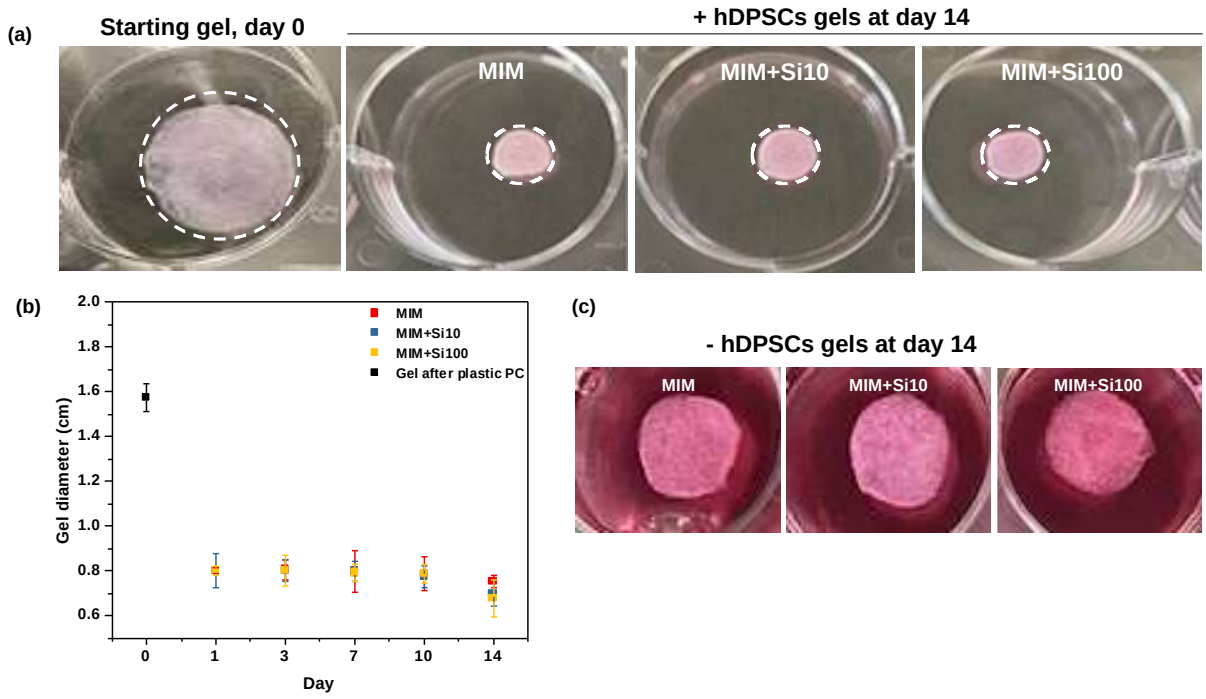

Figure III.8: Contraction of collagen gels by hDPSC in a mineralizing culture medium supplemented with silicon or not. (a) Representative images of collagen gel contraction at day 14, (b) Average collagen gel diameter over 14 days of culture, (c) Representative images of acellular collagen gels at day 14.

III.3.6.3. Collagen network structure

SHG imaging at day 24 of the cell-laden hydrogels grown under the 3 mineralizing conditions (MIM, MIM+Si10, MIM+Si100) highlighted the presence of collagen fibrils, with considerable differences from one condition to the others (**Figure III.9(a)**).

In MIM alone, individual fibrils were difficult to distinguish and seemed to be assembled in dense ball-like aggregates. In the Si10 condition, some individual fibrils, several tens of micrometers in length, can be visualized. At Si100, such fibrils formed most of the matrix, and seemed to exhibit some local orientation. Noticeably, control gels without cells left for 24 days in MIM displayed much thicker and elongated fibers (**Figure III.9(c)**).

Quantitative analysis of collagen fibrils orientation and distribution from SHG images confirmed a more pronounced fiber alignment with increasing Si concentration (**Figure III.9(d)**). SEM images also suggested a significant variation in fiber alignment recorded at the vicinity of the cells in the different conditions. (**Figure III.9(b)**).

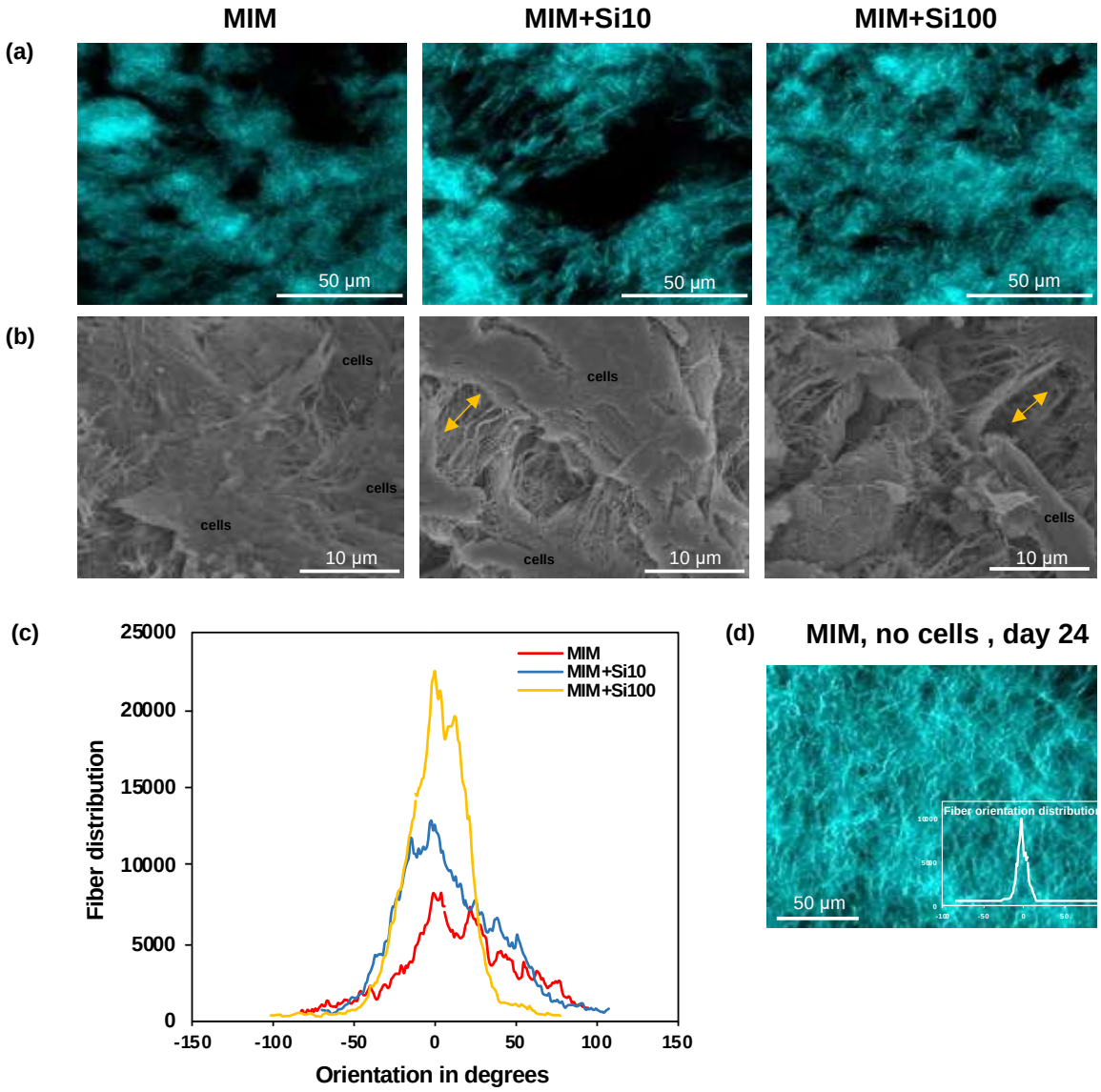

Figure III.9: Matrix structure of hDPSC-seeded dense collagen scaffolds under mineralizing conditions (without and with Si at 10 µM or 100 µM) at 24 days of culture. (a) Second harmonic generation images (individual fibers are highlighted by yellow arrows), (b) SEM micrographs (Fiber alignment is highlighted by yellow arrows) and (c) Quantitative analysis of collagen fiber orientation from SHG. (d) SHG image of a cell-free dense collagen scaffold cultured in MIM alone at day 24 and its analysis of fiber orientation (inset).

II.4. Discussion

The aim of this work was to identify the possible influence of silicic acid on the behavior of human dental pulp stem cells and, in particular, on their mineralization ability. In fact, whereas similar studies have already been performed using other mineralizing cells in a bone repair context, such as Bone Marrow Stem Cells (BMSCs) and osteoblasts, very little attention has been paid to dental stem cells.[22] In addition, most of these investigations were performed in 2D culture conditions. Here, we hypothesized that providing a tissue-like 3D environment to the cells would offer a more representative model of the *in vivo* situation. Specifically, type I collagen-based dense hydrogels appear particularly promising to produce dentin pulp complexes-like environments.[28] For this study, we selected two silicic acid concentrations, 10 μM (0.28 ppm) which is comparable to the physiological $Si(OH)_4$ concentration [15], and 100 μM (2.8 ppm) to check for possible influence of supraphysiological Si content. Importantly, these concentrations remain well-below the solubility of amorphous silica (*ca*. 2 mM) to prevent the occurrence of silica condensation [31], and are also in the lower concentration range used in comparable studies.[22]

Studying the evolution of the metabolic activity of the cells over 3 weeks and evaluating cell viability at the end of the culture time revealed that silicic acid has no toxic effect towards hDPSCs at these concentrations and may even be favorable to cell activity (**Figure III.1(a)**). Total RNA content was similar in all conditions and Nestin, a marker of neural crest stem cells which is present both in undifferentiated DPSCs and in the early stages of their osteogenic differentiation [37], was equally present in all samples. This is consistent with previous studies for other cell types showing that, in such a concentration range, Si usually has no effect on cell metabolic activity.[23]

Considering gene expression of key mineralization-related proteins, there was no significant difference for *alp* and *bsp* at all concentration and time points. *Bglap* expression was slightly down regulated at day 1 for 10 μM Si but was then similar to all other samples in all conditions. This would suggest that Si has only a minor influence on the odonto/osteogenic differentiation of hDPSCs. In the meantime, SEM/EDS indicates that the deposited inorganic phase has a Ca/P ratio similar to the expected value for dentin mineral in all conditions, suggesting that Si has no strong effect on the chemistry of hydroxyapatite formation. However, histological analyses revealed a difference in the mineralization extent as shown by an Alizarin red staining much

weaker for the 100 μM Si condition compared to the two others. This suggests that despite comparable expression of mineralization-related proteins (ALP, BSP and Osteocalcin), and thus a similar differentiation stage of cells towards an osteogenic phenotype, the mineralization process is somehow inhibited in the presence of a non-physiological, albeit relatively low, Si concentration.

One key difference between the various samples is the state of cell dispersion within the collagen matrix. Indeed, the presence of Si favors the grouping of cells in clusters while, in its absence, hDPSCs are homogeneously distributed within the gels. In parallel, Si appears to favor an organization where the collagen fibrils are more aligned than in its absence. Importantly, the contraction occurring during the first week was equivalent in all the conditions, suggesting that Si has no impact on this initial stage of collagen reorganization. During the course of differentiation, Col1 expression level dropped in all conditions between days 1 and 7, and then increased to reach its largest value in the absence of Si at day 14, while it continued to increase up to day 21 in the presence of Si. Noteworthy, the increase in Col1 expression parallels that of MMP13, one of the main enzymes involved in collagen degradation. Taken together, these data suggest that the presence of silicic acid in the mineralization medium delays matrix remodeling by hDPSCs.

The sequence of 3D matrix remodeling involves the local degradation of the environment, cell migration and deposition of a new matrix.[38] Cell clustering can therefore reflect restricted mobility, due to hindered matrix degradation, poor adhesion and/or limited collagen deposition.[39] This is consistent with the observed delayed MMP13 and Col 1 expression. Moreover, OPN has a key role in cell signaling and migration.[40] Thus, low OPN presence in Si 100 μM conditions may also correlate with limited cell migration. However, understanding the low mineralization yield in this condition is not straightforward. Noticeably, it has been shown that DPSCs from MMP13-knockout mice exhibit reduced mineralization potential.[41] Therefore, low mineralization could correlate with delayed MMP13 expression. Alternatively, it has been recently shown that, although cell aggregation favors mineralization in 2D cultures[42], 3D clustering may orient osteoblast precursor cells differentiation towards osteocyte-like cells with a lower mineralization activity.[43]

The next question is to know if this impaired remodeling is due to Si interactions with cells or to a change in the matrix properties leading to unfavorable cell-matrix interactions. Considering the first possibility, it was reported several times that Si promotes the expression of Col1 and

mineralizing proteins in osteogenic cells[18], which is in contradiction with our present observations on hDPSCs. However, it has also been previously shown that silica nanoparticles at a 1 mM concentration decreased the expression of proteins involved in cell adhesion (fibronectin, FAK) in normal human dermal fibroblasts, which hinders cell migration and could delay remodeling.[44] The second possibility is that silicic acid establishes some chemical interactions with the collagen molecules and/or fibrils. In this perspective, it was shown that sodium silicate at *ca*. 150 µM could influence type I collagen fibrillogenesis.[45] Here, silicon was not added at the stage of gel formation so that it was not expected to impact the initial scaffold structure. However, interactions of $Si(OH)_4$ with collagen may occur during remodeling where new collagen molecules are synthesized by the cells and undergo fibrillogenesis. The ability of silicic acid solutions to decrease cell adhesion and/or modify the contraction-induced collagen fiber morphology were also reported several times, albeit at higher silicon concentration.[31] At this stage, it is not possible to know which of these mechanisms, which are not exclusive, is responsible for our observations.

Very few similar studies were performed at such low silicon contents, mostly in 2D environments and, to our knowledge, only once with hDPSCs. This study of Miyano *et al*. tested the effects of 5 µM, 50 µM and 500 µM Si supplementation to culture media on hDPSCs.[46] The largest ALP expression was observed on day 14 of culture for all groups, with highest expression at 5 µM Si, but no difference in ALP activity was found between groups. Meanwhile, alizarin red staining was greater with 5 µM and 500 µM Si compared to 50 µM Si on day 28. The latter result is in line with ours, where mineral deposition was more pronounced for the lowest concentration of 10 µM Si than for the supraphysiological Si dose (100 µM). Another study investigating the effects of high Si concentrations on hDPSCs showed that odontoblastic activity, as monitored by ALP activity, DSP expression and alizarin red staining, was improved by 50 ppm Si (2 mM) treatment.[47] However, at this concentration, Si effects can be attributed not only to the bioavailable form of Si (soluble), but also to polymeric forms of Si. In parallel, no difference in hDPSC mineralization was found between cells grown in odontogenic induction medium (OIM) alone and OIM supplemented with 25 ppm Si (1mM). These data, combined to ours, highlight again the high sensitivity of the hDPSCs response to the silicic acid concentration.

II.5. Conclusions

The aim of this work was to study the effect of silicic acid on hDPSCs immobilized in a dense collagen hydrogel mimicking the pulp matrix. Whereas previous studies devoted to silicic acid interactions with osteogenic cells generally reported either no influence or a beneficial one considering mineralization, our results show no clear effect on mineralization at the gene expression level.

Importantly, and contrary to bone, there is, so far, no evidence of a possible physiological role of silicon on dental tissue formation or repair. This can explain why our study reveals little impact of a physiological silicic acid concentration on DPSCs. In contrast, a supraphysiological concentration may result from the dissolution of biomaterials, such as calcium silicates, at the vicinity of the pulp tissue and have a negative impact on reactive dentine formation. Our findings suggest that the released silicic acid would primarily interact with the extracellular matrix rather than with the cells. So far, the contribution of such interactions to the global cell response to silicon at low concentration (*i.e*. below silica solubility) has never been addressed and constitutes, to our point of view, an important area for further research.

In this context, it is important to point out that collagens (mainly type I and type III) constitute only about one third of the pulp matrix composition.[48] Glycosaminoglycans and proteoglycans are present in major amounts and non-collagenous proteins, especially fibronectin, also play a key role in the organization and mechanical properties of the tissue and in cell-matrix interactions. This calls for the development of more physiological pulp-like 3D environments to improve our understanding of DPSCs response to silicon.[49] More globally, such biomimetic platforms could constitute a useful animal-free alternative to current *in vivo* procedures for testing dental biomaterials.[50]

References

(1) Manley, E. B. Pulp Reactions to Dental Cements. *Proc R Soc Med* **1943**, *36* (9), 488–499.

(2) Zander, H. A. The Reaction of Dental Pulps to Silicate Cements. *The Journal of the American Dental Association* **1946**, *33* (19), 1233–1243. https://doi.org/10.14219/jada.archive.1946.0190.

(3) Prati, C.; Gandolfi, M. G. Calcium Silicate Bioactive Cements: Biological Perspectives and Clinical Applications. *Dental Materials* **2015**, *31* (4), 351–370. https://doi.org/10.1016/j.dental.2015.01.004.

(4) Eskandari, F.; Razavian, A.; Hamidi, R.; Yousefi, K.; Borzou, S. An Updated Review on Properties and Indications of Calcium Silicate-Based Cements in Endodontic Therapy. *International Journal of Dentistry* **2022**, *2022*, 1–19. https://doi.org/10.1155/2022/6858088.

(5) Primus, C. M.; Tay, F. R.; Niu, L. Bioactive Tri/Dicalcium Silicate Cements for Treatment of Pulpal and Periapical Tissues. *Acta Biomaterialia* **2019**, *96*, 35–54. https://doi.org/10.1016/j.actbio.2019.05.050.

(6) Song, W.; Li, S.; Tang, Q.; Chen, L.; Yuan, Z. *In Vitro* Biocompatibility and Bioactivity of Calcium Silicate-based Bioceramics in Endodontics (Review). *Int J Mol Med* **2021**, *48* (1), 128. https://doi.org/10.3892/ijmm.2021.4961.

(7) Kim, J. M.; Choi, S.; Kwack, K. H.; Kim, S.-Y.; Lee, H.-W.; Park, K. G Protein-Coupled Calcium-Sensing Receptor Is a Crucial Mediator of MTA-Induced Biological Activities. *Biomaterials* **2017**, *127*, 107–116. https://doi.org/10.1016/j.biomaterials.2017.02.038.

(8) Rathinam, E.; Govindarajan, S.; Rajasekharan, S.; Declercq, H.; Elewaut, D.; De Coster, P.; Martens, L.; Leybaert, L. The Calcium Dynamics of Human Dental Pulp Stem Cells Stimulated with Tricalcium Silicate-Based Cements Determine Their Differentiation and Mineralization Outcome. *Sci Rep* **2021**, *11* (1), 645. https://doi.org/10.1038/s41598-020-80096-5.

(9) Kim, Y.; Lee, D.; Kim, H.-M.; Kye, M.; Kim, S.-Y. Biological Characteristics and Odontogenic Differentiation Effects of Calcium Silicate-Based Pulp Capping Materials. *Materials* **2021**, *14* (16), 4661. https://doi.org/10.3390/ma14164661.

(10) Peng, W.; Liu, W.; Zhai, W.; Jiang, L.; Li, L.; Chang, J.; Zhu, Y. Effect of Tricalcium Silicate on the Proliferation and Odontogenic Differentiation of Human Dental Pulp Cells.

Journal of Endodontics **2011**, *37* (9), 1240–1246. https://doi.org/10.1016/j.joen.2011.05.035.

(11) Cushley, S.; Duncan, H. F.; Lappin, M. J.; Chua, P.; Elamin, A. D.; Clarke, M.; El-Karim, I. A. Efficacy of Direct Pulp Capping for Management of Cariously Exposed Pulps in Permanent Teeth: A Systematic Review and Meta-analysis. *Int Endodontic J* **2021**, *54* (4), 556–571. https://doi.org/10.1111/iej.13449.

(12) Wu, B.-C.; Kao, C.-T.; Huang, T.-H.; Hung, C.-J.; Shie, M.-Y.; Chung, H.-Y. Effect of Verapamil, a Calcium Channel Blocker, on the Odontogenic Activity of Human Dental Pulp Cells Cultured with Silicate-Based Materials. *Journal of Endodontics* **2014**, *40* (8), 1105–1111. https://doi.org/10.1016/j.joen.2013.12.019.

(13) Wu, T.; Xu, C.; Du, R.; Wen, Y.; Chang, J.; Huan, Z.; Zhu, Y. Effects of Silicate-Based Composite Material on the Proliferation and Mineralization Behaviors of Human Dental Pulp Cells: An *in Vitro* Assessment. *Dental Materials Journal* **2018**, *37* (6), 889–896. https://doi.org/10.4012/dmj.2017-328.

(14) Peng, W.; Huan, Z.; Pei, G.; Li, J.; Cao, Y.; Jiang, L.; Zhu, Y. Silicate Bioceramics Elicit Proliferation and Odonto-Genic Differentiation of Human Dental Pulp Cells. *Dent. Mater. J.* **2022**, *41* (1), 27–36. https://doi.org/10.4012/dmj.2021-042.

(15) Jugdaohsingh, R. Silicon and Bone Health. *J Nutr Health Aging* **2007**, *11* (2), 99–110.

(16) Götz, W.; Tobiasch, E.; Witzleben, S.; Schulze, M. Effects of Silicon Compounds on Biomineralization, Osteogenesis, and Hard Tissue Formation. *Pharmaceutics* **2019**, *11* (3), 117. https://doi.org/10.3390/pharmaceutics11030117.

(17) Henstock, J. R.; Canham, L. T.; Anderson, S. I. Silicon: The Evolution of Its Use in Biomaterials. *Acta Biomaterialia* **2015**, *11*, 17–26. https://doi.org/10.1016/j.actbio.2014.09.025.

(18) Reffitt, D. M.; Ogston, N.; Jugdaohsingh, R.; Cheung, H. F. J.; Evans, B. A. J.; Thompson, R. P. H.; Powell, J. J.; Hampson, G. N. Orthosilicic Acid Stimulates Collagen Type 1 Synthesis and Osteoblastic Differentiation in Human Osteoblast-like Cells in Vitro. *Bone* **2003**, *32* (2), 127–135. https://doi.org/10.1016/S8756-3282(02)00950-X.

(19) Kim, E.-J.; Bu, S.-Y.; Sung, M.-K.; Choi, M.-K. Effects of Silicon on Osteoblast Activity and Bone Mineralization of MC3T3-E1 Cells. *Biol Trace Elem Res* **2013**, *152* (1), 105–112. https://doi.org/10.1007/s12011-012-9593-4.

(20) Zhou, X.; Moussa, F. M.; Mankoci, S.; Ustriyana, P.; Zhang, N.; Abdelmagid, S.; Molenda, J.; Murphy, W. L.; Safadi, F. F.; Sahai, N. Orthosilicic Acid, Si(OH)4, Stimulates Osteoblast Differentiation in Vitro by Upregulating MiR-146a to Antagonize

NF-KB Activation. *Acta Biomaterialia* **2016**, *39*, 192–202. https://doi.org/10.1016/j.actbio.2016.05.007.

(21) Shie, M.-Y.; Ding, S.-J.; Chang, H.-C. The Role of Silicon in Osteoblast-like Cell Proliferation and Apoptosis. *Acta Biomaterialia* **2011**, *7* (6), 2604–2614. https://doi.org/10.1016/j.actbio.2011.02.023.

(22) Turner, J.; Nandakumar, A.; Anilbhai, N.; Boccaccini, A. R.; Jones, J. R.; Jell, G. The Effect of Si Species Released from Bioactive Glasses on Cell Behaviour: A Quantitative Review. *Acta Biomaterialia* **2023**, *170*, 39–52. https://doi.org/10.1016/j.actbio.2023.09.012.

(23) Han, P.; Wu, C.; Xiao, Y. The Effect of Silicate Ions on Proliferation, Osteogenic Differentiation and Cell Signalling Pathways (WNT and SHH) of Bone Marrow Stromal Cells. *Biomater. Sci.* **2013**, *1* (4), 379–392. https://doi.org/10.1039/C2BM00108J.

(24) Duval, K.; Grover, H.; Han, L.-H.; Mou, Y.; Pegoraro, A. F.; Fredberg, J.; Chen, Z. Modeling Physiological Events in 2D vs. 3D Cell Culture. *Physiology* **2017**, *32* (4), 266–277. https://doi.org/10.1152/physiol.00036.2016.

(25) Griffanti, G.; Nazhat, S. N. Dense Fibrillar Collagen-Based Hydrogels as Functional Osteoid-Mimicking Scaffolds. *International Materials Reviews* **2020**, *65* (8), 502–521. https://doi.org/10.1080/09506608.2020.1735828.

(26) Coyac, B. R.; Hoac, B.; Chafey, P.; Falgayrac, G.; Slimani, L.; Rowe, P. S.; Penel, G.; Linglart, A.; McKee, M. D.; Chaussain, C.; Bardet, C. Defective Mineralization in X-Linked Hypophosphatemia Dental Pulp Cell Cultures. *J Dent Res* **2018**, *97* (2), 184–191. https://doi.org/10.1177/0022034517728497.

(27) Troka, I.; Griffanti, G.; Canaff, L.; Hendy, G.; Goltzman, D.; Nazhat, S. Effect of Menin Deletion in Early Osteoblast Lineage on the Mineralization of an In Vitro 3D Osteoid-like Dense Collagen Gel Matrix. *Biomimetics* **2022**, *7* (3), 101. https://doi.org/10.3390/biomimetics7030101.

(28) Coyac, B. R.; Chicatun, F.; Hoac, B.; Nelea, V.; Chaussain, C.; Nazhat, S. N.; McKee, M. D. Mineralization of Dense Collagen Hydrogel Scaffolds by Human Pulp Cells. *J Dent Res* **2013**, *92* (7), 648–654. https://doi.org/10.1177/0022034513488599.

(29) Chamieh, F.; Collignon, A.-M.; Coyac, B. R.; Lesieur, J.; Ribes, S.; Sadoine, J.; Llorens, A.; Nicoletti, A.; Letourneur, D.; Colombier, M.-L.; Nazhat, S. N.; Bouchard, P.; Chaussain, C.; Rochefort, G. Y. Accelerated Craniofacial Bone Regeneration through Dense Collagen Gel Scaffolds Seeded with Dental Pulp Stem Cells. *Sci Rep* **2016**, *6* (1), 38814. https://doi.org/10.1038/srep38814.

(30) Mbitta Akoa, D.; Sicard, L.; Hélary, C.; Torrens, C.; Baroukh, B.; Poliard, A.; Coradin, T. Role of Physico-Chemical and Cellular Conditions on the Bone Repair Potential of Plastically Compressed Collagen Hydrogels. *Gels* **2024**, *10* (2), 130. https://doi.org/10.3390/gels10020130.

(31) Heinemann, S.; Coradin, T.; Desimone, M. F. Bio-Inspired Silica–Collagen Materials: Applications and Perspectives in the Medical Field. *Biomater. Sci.* **2013**, *1* (7), 688. https://doi.org/10.1039/c3bm00014a.

(32) Gronthos, S.; Mankani, M.; Brahim, J.; Robey, P. G.; Shi, S. Postnatal Human Dental Pulp Stem Cells (DPSCs) *in Vitro* and *in Vivo*. *Proc. Natl. Acad. Sci. U.S.A.* **2000**, *97* (25), 13625–13630. https://doi.org/10.1073/pnas.240309797.

(33) Gobeaux, F.; Mosser, G.; Anglo, A.; Panine, P.; Davidson, P.; Giraud-Guille, M.-M.; Belamie, E. Fibrillogenesis in Dense Collagen Solutions: A Physicochemical Study. *Journal of Molecular Biology* **2008**, *376* (5), 1509–1522. https://doi.org/10.1016/j.jmb.2007.12.047.

(34) Brown, R. A.; Wiseman, M.; Chuo, C. -B.; Cheema, U.; Nazhat, S. N. Ultrarapid Engineering of Biomimetic Materials and Tissues: Fabrication of Nano- and Microstructures by Plastic Compression. *Adv Funct Materials* **2005**, *15* (11), 1762–1770. https://doi.org/10.1002/adfm.200500042.

(35) Bancelin, S.; Decencière, E.; Machairas, V.; Albert, C.; Coradin, T.; Schanne-Klein, M.-C.; Aimé, C. Fibrillogenesis from Nanosurfaces: Multiphoton Imaging and Stereological Analysis of Collagen 3D Self-Assembly Dynamics. *Soft Matter* **2014**, *10* (35), 6651–6657. https://doi.org/10.1039/C4SM00819G.

(36) Lendahl, U.; Zimmerman, L. B.; McKay, R. D. G. CNS Stem Cells Express a New Class of Intermediate Filament Protein. *Cell* **1990**, *60* (4), 585–595. https://doi.org/10.1016/0092-8674(90)90662-X.

(37) Di Benedetto, A.; Posa, F.; Carbone, C.; Cantore, S.; Brunetti, G.; Centonze, M.; Grano, M.; Lo Muzio, L.; Cavalcanti-Adam, E. A.; Mori, G. NURR1 Downregulation Favors Osteoblastic Differentiation of MSCs. *Stem Cells Int* **2017**, *2017*, 7617048. https://doi.org/10.1155/2017/7617048.

(38) Harjanto, D.; Zaman, M. H. Modeling Extracellular Matrix Reorganization in 3D Environments. *PLoS One* **2013**, *8* (1), e52509. https://doi.org/10.1371/journal.pone.0052509.

(39) Schultz, K. M.; Kyburz, K. A.; Anseth, K. S. Measuring Dynamic Cell–Material Interactions and Remodeling during 3D Human Mesenchymal Stem Cell Migration in

Hydrogels. *Proc. Natl. Acad. Sci. U.S.A.* **2015**, *112* (29). https://doi.org/10.1073/pnas.1511304112.

(40) Sodek, J.; Ganss, B.; McKee, M. D. Osteopontin. *Critical Reviews in Oral Biology & Medicine* **2000**, *11* (3), 279–303. https://doi.org/10.1177/10454411000110030101.

(41) Duncan, H. F.; Kobayashi, Y.; Yamauchi, Y.; Quispe-Salcedo, A.; Chao Feng, Z.; Huang, J.; Partridge, N. C.; Nakatani, T.; D'Armiento, J.; Shimizu, E. The Critical Role of MMP13 in Regulating Tooth Development and Reactionary Dentinogenesis Repair Through the Wnt Signaling Pathway. *Front. Cell Dev. Biol.* **2022**, *10*, 883266. https://doi.org/10.3389/fcell.2022.883266.

(42) Deegan, A. J.; Aydin, H. M.; Hu, B.; Konduru, S.; Kuiper, J. H.; Yang, Y. A Facile in Vitro Model to Study Rapid Mineralization in Bone Tissues. *BioMed Eng OnLine* **2014**, *13* (1), 136. https://doi.org/10.1186/1475-925X-13-136.

(43) Kim, J.; Adachi, T. Cell Condensation Triggers the Differentiation of Osteoblast Precursor Cells to Osteocyte-Like Cells. *Front Bioeng Biotechnol* **2019**, *7*, 288. https://doi.org/10.3389/fbioe.2019.00288.

(44) Zhang, Y.; Hu, L.; Yu, D.; Gao, C. Influence of Silica Particle Internalization on Adhesion and Migration of Human Dermal Fibroblasts. *Biomaterials* **2010**, *31* (32), 8465–8474. https://doi.org/10.1016/j.biomaterials.2010.07.060.

(45) Eglin, D.; Shafran, K. L.; Livage, J.; Coradin, T.; Perry, C. C. Comparative Study of the Influence of Several Silica Precursors on Collagen Self-Assembly and of Collagen on 'Si' Speciation and Condensation. *J. Mater. Chem.* **2006**, *16* (43), 4220–4230. https://doi.org/10.1039/B606270A.

(46) Miyano, Y.; Mikami, M.; Katsuragi, H.; Shinkai, K. Effects of Sr2+, BO33−, and SiO32− on Differentiation of Human Dental Pulp Stem Cells into Odontoblast-Like Cells. *Biol Trace Elem Res* **2023**, *201* (12), 5585–5600. https://doi.org/10.1007/s12011-023-03625-z.

(47) Alsenan, J. Effect of Silicon and Calcium on Human Dental Pulp Cell Cultures. *IJMSA* **2017**, *6* (6), 290. https://doi.org/10.11648/j.ijmsa.20170606.14.

(48) Linde, A. Session II: Cells and Extracellular Matrices of the Dental Pulp — C.T. Hanks, Chairman: The Extracellular Matrix of the Dental Pulp and Dentin. *J Dent Res* **1985**, *64* (4), 523–529. https://doi.org/10.1177/00220345850640040S.

(49) Hadjichristou, C.; Papachristou, E.; Bonovolias, I.; Bakopoulou, A. Three-Dimensional Tissue Engineering-Based Dentin/Pulp Tissue Analogue as Advanced Biocompatibility

Evaluation Tool of Dental Restorative Materials. *Dental Materials* **2020**, *36* (2), 229–248. https://doi.org/10.1016/j.dental.2019.11.013.

(50) Tran, X. V.; Gorin, C.; Willig, C.; Baroukh, B.; Pellat, B.; Decup, F.; Opsahl Vital, S.; Chaussain, C.; Boukpessi, T. Effect of a Calcium-Silicate-Based Restorative Cement on Pulp Repair. *J Dent Res* **2012**, *91* (12), 1166–1171. https://doi.org/10.1177/0022034512460833.

Chapter IV

Effect of silicon-releasing nanoparticles on the mineralization of plastically-compressed collagen hydrogels by human dental pulp stem cells

IV.1. Introduction

Building on the foundations laid in previous chapters, which relied on the optimization of collagen hydrogel formulation and the effects of exogenous silicic acid supplementation on human dental pulp stem cells (hDPSCs) encapsulated in the collagenous hydrogel, this chapter addresses the effects of silicon-delivering materials incorporated into cellularized collagen hydrogels on the behaviour of DPSCs. In the clinical situation, the pulp capping materials are in direct contact with the tissues and release silicic acid in a progressive rather than continuous manner, both of which could impact the cell response. To model this situation, we have used silica-based nanoparticles that were incorporated within the collagen gels in the presence of hDPSCs. Such an approach is motivated by the prevalence of silica-based nanoparticles in dental materials, thus necessitating a comprehensive examination of their direct impact on DPSC behavior within a biomimetic scaffold.[1,2] In addition, silicon-based nanoparticles offer an alternative means of delivering silicon in a localized, controlled, and long-term/sustainable manner.[3–5]

The two distinct nanoparticle types were investigated: silica and bioglass nanoparticles. Silica nanoparticles, with their high surface area and tunable physicochemical properties, are a common component of various dental formulations.[1,6] Bioglass nanoparticles, characterized by their bioactive properties and ability to promote mineralization, offer an alternative route for silicon delivery, with potential implications for improving tissue regeneration.[5,7] This dual approach allows for a comprehensive evaluation of the influence of nanoparticle concentration and composition on cellular behavior and mineralization dynamics within the collagen hydrogel matrix. Hereafter, we will describe cell viability assessments, matrix characterization and mineral deposition studies, as a first step towards the elucidation of the complex mechanisms underlying the bioactivity of silicon-loaded collagen hydrogel nanocomposites.

IV.2. Materials and Methods

IV.2.1. Synthesis of nanoparticles

IV.2.1.1. Silica nanoparticles

Silica nanoparticles (NPs) were synthesized by hydrolysis of tetraethylorthosilicate (TEOS 98%, Sigma-Aldrich) in an alcoholic medium, in the presence of water and ammonia, according to a methodology previously established.[8] In the standard synthesis protocol, 0.5 mL TEOS was rapidly mixed with 2 mL ethanol. Next, this TEOS/ethanol mixture was introduced into a solution comprising 100 mL ethanol and 20 mL NH_4OH (28±30%, Merck), and stirred for 2 h at room temperature. The resulting NPs were collected by centrifugation, dispersed by ultrasonication and alternately centrifuged three times with ethanol and deionized water to remove any unreacted precursors. Then, silica NPs (Si) were dried in a freeze-dryer for 24 hours.

IV.2.1.2. Bioglasses

The synthesis of bioactive glass nanoparticles (BGs) was conducted via a modified Stöber route, adapted from a previously established methodology.[9] Initially, two distinct solutions were prepared at ambient temperature. Solution 1 was formulated by swiftly adding 2.34 mL of tetraethyl orthosilicate (TEOS) to 20 mL of absolute ethanol, while solution 2 was composed of 11.7 mL of deionized water, 17.5 mL of absolute ethanol, and 1.7 mL of ammonium hydroxide. Following 30 minutes of mechanical stirring, solution 1 was introduced into solution 2 and allowed to amalgamate for 2 hours. Subsequently, a 5 g of calcium nitrate, ($(Ca(NO_3)_2).4H_2O$) was incorporated into the resulting turbid mixture and subjected to stirring for the duration of 22 hours. The resultant white suspension was centrifuged and subjected to sequential washing steps involving ethanol and water to eliminate residual reagents. The resulting white solid was then subjected to overnight drying at 60°C, followed by a heat treatment at 650°C for 3 hours.

IV.2.1.3. Nanoparticles characterization

Nanoparticle size was measured by Dynamic Light Scattering on a Zetasizer nano-ZS90 and morphology were studied by SEM using a Hitachi S-3400 N microscope operating at 60 kV.

The particles were deposited on a carbon film and observed without being metallized. Particle size distribution was determined by measuring the diameter of more than 50 particles from SEM micrographs using ImageJ processing software. Chemical composition was determined using an ATR-FTIR spectrometer. Wavelength-dispersive X-ray fluorescence (WDXRF) was used to determine the % silicon and calcium atoms in the BGs.

Nanoparticle synthesis and part of the characterizations were performed by Anthony Avril during his M2 internship.

IV.2.2. Formation of hydrogels composite gels

Dense collagen gels (DC) encapsulating silica nanoparticles have been synthesized, as hybrid gels with or without hDPSCs. The protocol of gel preparation was the same as in the previous chapters, with the addition of nanoparticles after neutralization. Gels containing three concentrations of nanoparticles were prepared: 10, 100 et 1000 μM (of silicon). Cellularization and growth conditions were similar to those described in the previous chapter.

IV.2.3. Study of nanoparticle dissolution in collagen gels

Culture media from cellularized nanocomposite gel environments were collected and analyzed at days 3, 7, 14 and 21 to measure the released silicon concentration in solution. Samples of growth media from cellularized gels (without NPs) were used as controls. Analysis was performed by inductively coupled plasma atomic emission spectrometry (ICP-AES) at the Institut de Physique du Globe de Paris.

ICP-AES was performed by Pierre Burckel at the Institute de Physique du Globe de Paris.

Viability, metabolic activity and mineralization of the hDPSC in the gels were assessed using the same techniques described in the previous sections.

IV.3 Results

IV.3.1. Morphology, composition, and dissolution of nanoparticles

The sol-gel synthesis used here produces spherical particles.[8] Electron microscopy confirmed the spherical shape of the particles and allowed to determine their size (**Figure IV.1(a)**). Silica particles were 170 ± 50 nm in diameter, and bioglasses 140 ± 55 nm. Homogeneous particles were observed on the SEM images in both types of nanoparticles. The FTIR spectra of silica showed the presence of a band around 1600 cm^{-1} corresponding to the vibration of the OH bonds of the adosrbed water, an intense band around 1100 cm^{-1} which corresponds to the stretching vibrations of the Si-O-Si bonds in the SiO_4 tetrahedron, a band around 950 cm^{-1} which corresponds to the Si-O bond of the silanols and a band around 800 cm^{-1} which corresponds to inter-tetrahedral Si-O-Si bending vibration mode. For the bioglass particles, the band at 950 cm^{-1} has almost disappeared, as a result of the heating treatment yielding to the condensation of the silicate network (**Figure IV.1(b)**). WDXRF indicated that the bioglass particles displayed a Ca:Si atomic ratio of 0.05.

Once the particles have been characterized, the next step was to examine their dissolution in the conditions of the biological experiments, i.e. within hDPSCs-seeded collagen hydrogels (DC). Three concentrations of silica (Si) and bioglass (BG) nanoparticles in the collagen gels were studied: 10, 100, and 1000 μM. As expected, the gels containing the highest concentrations of nanoparticles exhibited the highest release of silicon, with different kinetic behaviour between silica and bioglass particles (**Figure IV.1(c)**). The release of silicon was the highest on day 3 in all the conditions, with mean release of concentrations of 100, 40, 10 and 10 μM in culture medium for DC-Si 1000, DC-BG 1000, DC-Si 100 and DC-BG 100, respectively, far below the toxic level (1mM).[10] The dissolution curves for 10 and 100 μM showed similar trends over time, with a steady release of 10 μM silicon throughout cell culture. This observation suggests that at very low nanoparticle concentrations (10 μM) in the gels, dissolved silicon concentrations are very low and below the detection limits of the technique. Therefore, only gels containing concentrations of 100 and 1000 μM were studied in the rest of the project.

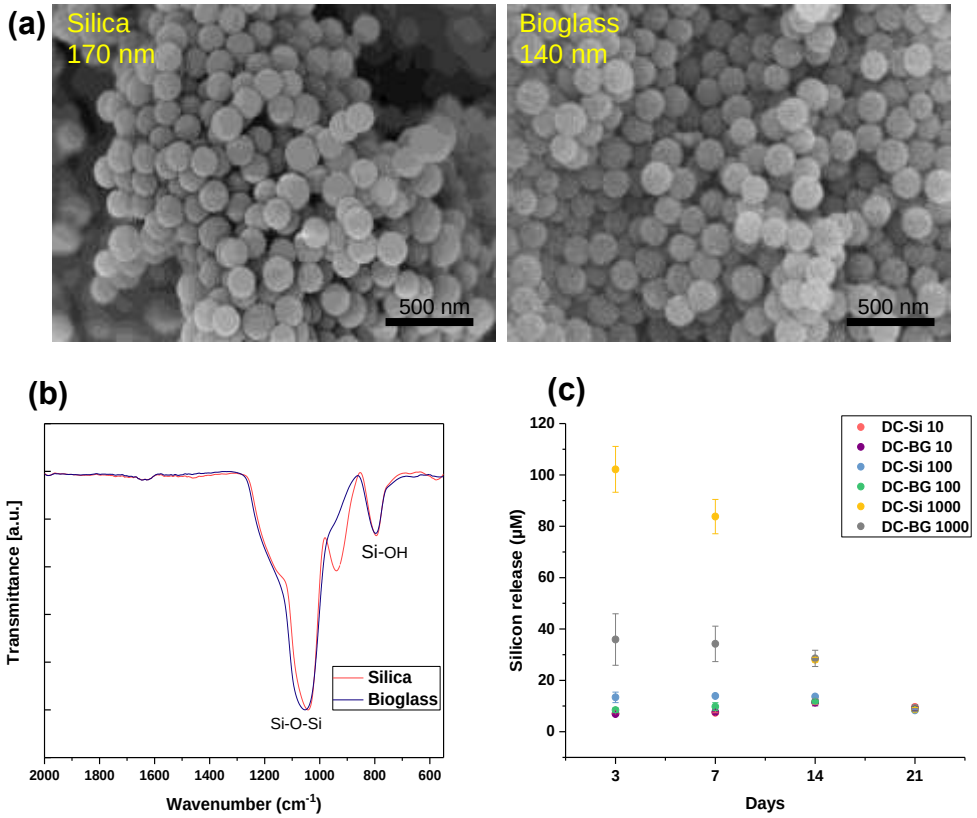

Figure IV.1: Morphology, composition and dissolution of synthetised silica and bioglasses nanoparticles. (a) SEM images of nanoparticles. Scale bar 500 nm. (b) ATR-FTIR of dried powder. (c) Follow up of the release of silicon in culture media from cellularized collagen gels with initial concentration of 10 µM, 100 µM and 1000 µM of nanoparticles at days 3, 7, 14 and 21 in culture.

IV.3.2. Viability, metabolic activity of hDPSCs in hybrid gels

To validate the cellular response to and odontogenic potential of the DC-Si and DC-BG hydrogels, seeded hDPSCs were cultured in the scaffolds for up to 28 days in mineralizing media. Live/Dead staining of hDPSCs seeded within plastically compressed collagen hydrogels was performed after incubation for 28 days in mineralizing medium. As shown in **Figure IV.2(a)**, most hDPSCs were viable in the presence of low (100 µM) and high (1000 µM) concentrations of silica or bioglass nanoparticles, indicating the cytocompatibility of these silica-based nanocomposite collagen scaffolds. The metabolic activity of hDPSCs seeded in DC, DC-Si and DC-BG decreased with culture time (**Figure IV.2(b)**). However, cells in DC-BG (100 and 1000) displayed significantly higher metabolic activity than cells in DC alone and DC-Si (100 and 1000).

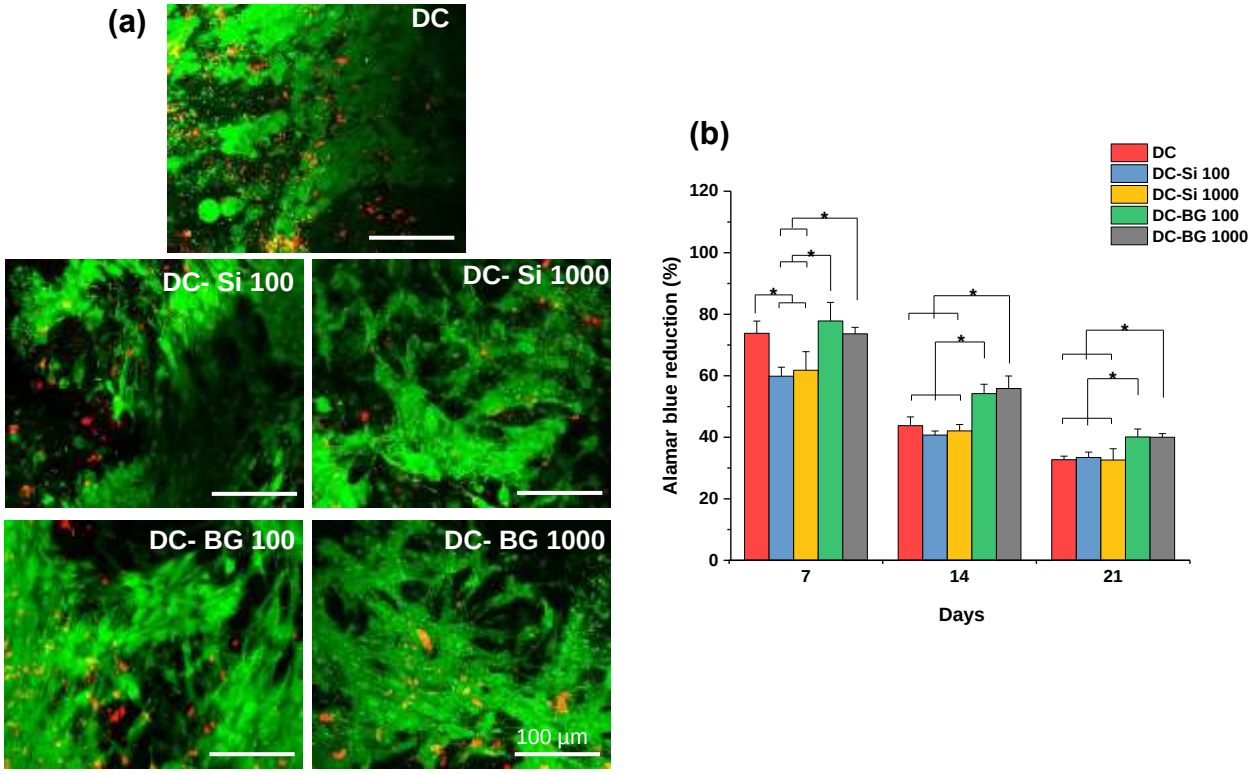

Figure IV.2: Viability and metabolic activity of hDPSCs within collagen gels without nanoparticles and containing 100 µM and 1000 µM silica or bioglases nanoparticles, grown in mineralizing medium. (a) Live/dead confocal images on day 28 of growth with cells in green and dead cells in red, and (b) Metabolic activity assessed with alamarblue reduction test up to day 21 of culture.

IV. 3.3. Distribution of hDPSCs in hybrid gels

Cell distribution within the collagen scaffolds was evaluated through Masson's trichrome histological staining of gels cross-sections and SHG imaging coupled with confocal microscopy on day 28 of culture. Masson's trichrome staining revealed distinct patterns of cell distribution within the gels (**Figure IV.3(a)**). In DC and DC-BG 100 gels, clusters of cells were observed both inside and outside the gel, while they were predominantly located at the edges of DC-Si 100 and DC-Si1000 gels. Conversely, uniform distribution of cells was observed throughout the DC-BG 1000 gel. The SHG/confocal 3D images in the xy- and xz-directions further illustrate this uniform distribution of cells within the nano-composite gel loaded with 1000 µM bioglasses nanoparticles (**Figure IV.3(b)**).

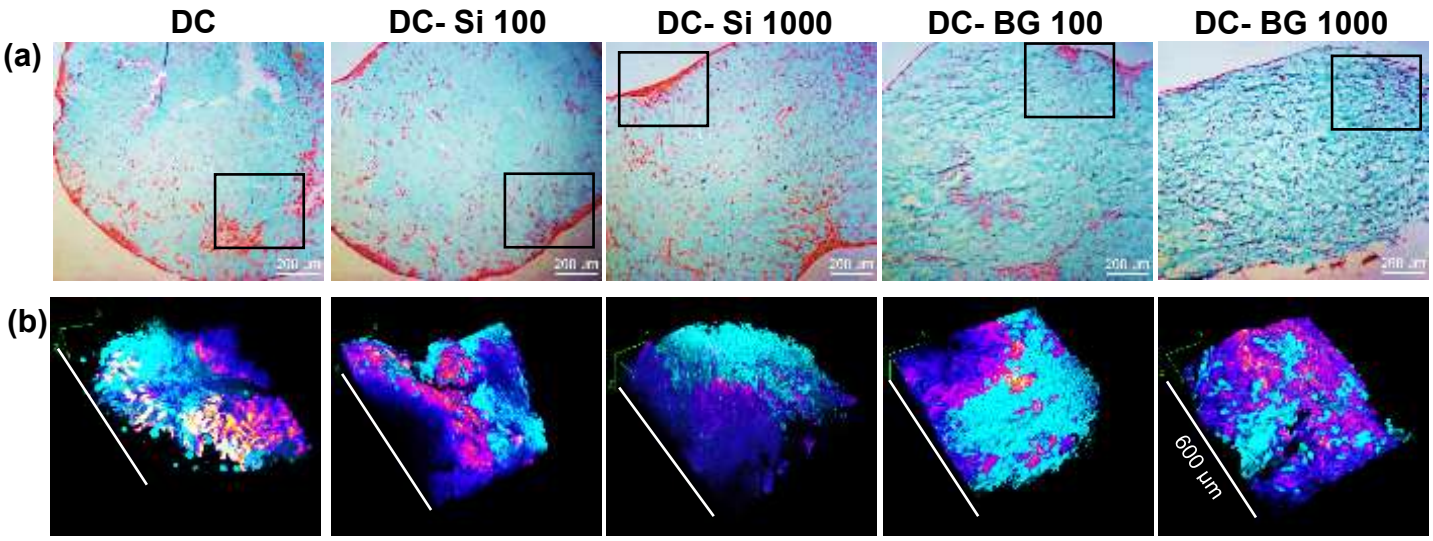

Figure IV.3: Distribution of hDPSC cells in the plastically compressed collagen hydrogels, without or with 100 and 1000 µM silica or bioglass nanoparticles. (a) Masson's trichrome histological staining of cross-sections of the gels after 28 days of culture, scale bar=200 µm. (b) SHG images coupled with confocal live-cells imaging on day 28 of culture, illustrating the specific areas indicated in the inset in (a).

IV.3.4. Collagen network organization

Collagen fibers organization was observed using Second-harmonic generation (SHG) microscopy. On day 28 of culture, the matrix showed collagen fibers organized in globules in all the 5 types of gel. No qualitative differences were observed between images (**Figure IV.4**).

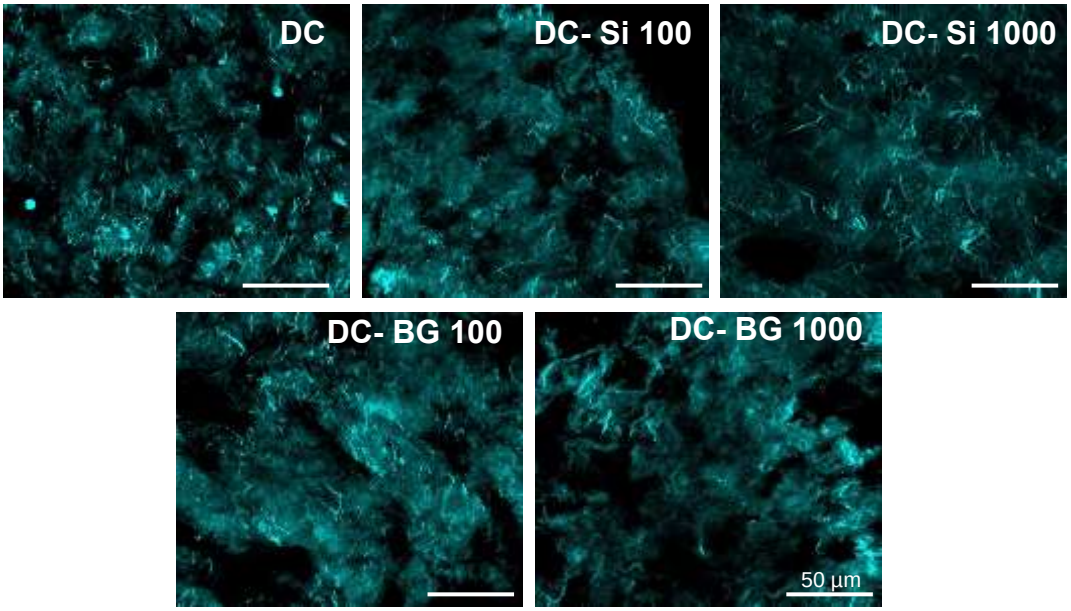

Figure IV.4: SHG imaging of dense collagenous matrix loaded with hDPSC without and with 100 and 1000 µM silica or bioglass nanoparticles after 28 days in culture.

IV.3.5. Mineralization analyses

IV.3.5.1. Von Kossa staining

Von Kossa staining was used to detect calcium deposits in the gel sections, evidenced by dark coloration. All five types of cell-laden gels, with and without nanoparticles, were positive to Von Kossa staining after 28 days of culture, indicating successful mineralization. However, the distribution of mineral deposits varied between gels. Like the distribution of cells revealed by Masson's trichrome staining (**Figure IV.3(a)**), mineral deposits occurred in clusters, corresponding to areas of cell aggregation, particularly evident with clustered minerals within DC gels and at the periphery of DC-Si 100 and DC-Si 1000 gels (**Figure IV.5**). Interestingly, the mineral deposit was slightly more uniform in the presence of 100 µM bioglasses and even more uniform in the presence of 1000 µM.

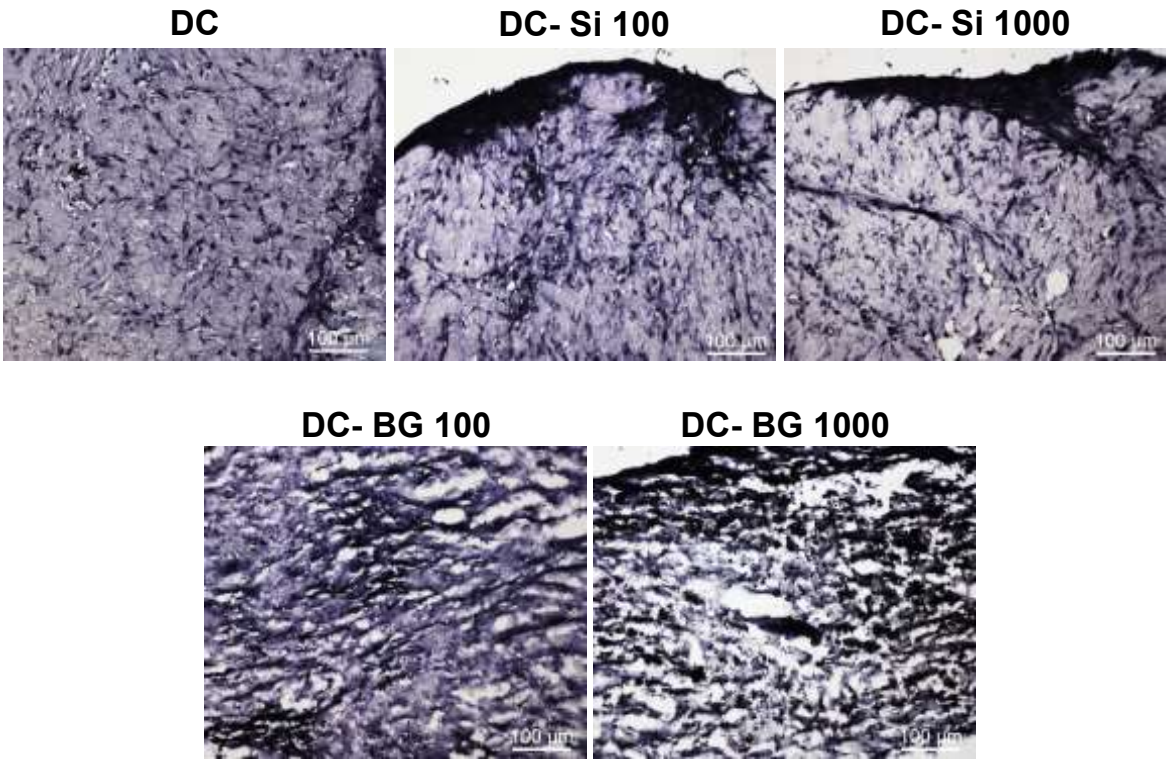

Figure IV.5: Histological von kossa staining of cross-sections of scaffolds seeded with hDPSCs grown in mineralizing medium for 28 days. Scale bar = 100 µm.

IV.3.5.1. Nestin immunostaining

Nestin expression was studied in hDPSCs cultured in collagen hydrogels for 28 days to assess the impact of nanoparticle incorporation into the gel on neural crest-related features of hDPSCs. As shown in **Figure IV.6**, the presence of bioglass nanoparticles did not affect nestin expression or localization, with comparable expression in DC and DC-BG gels. However, nestin expression was less pronounced in the presence of silica particles (DC-Si).

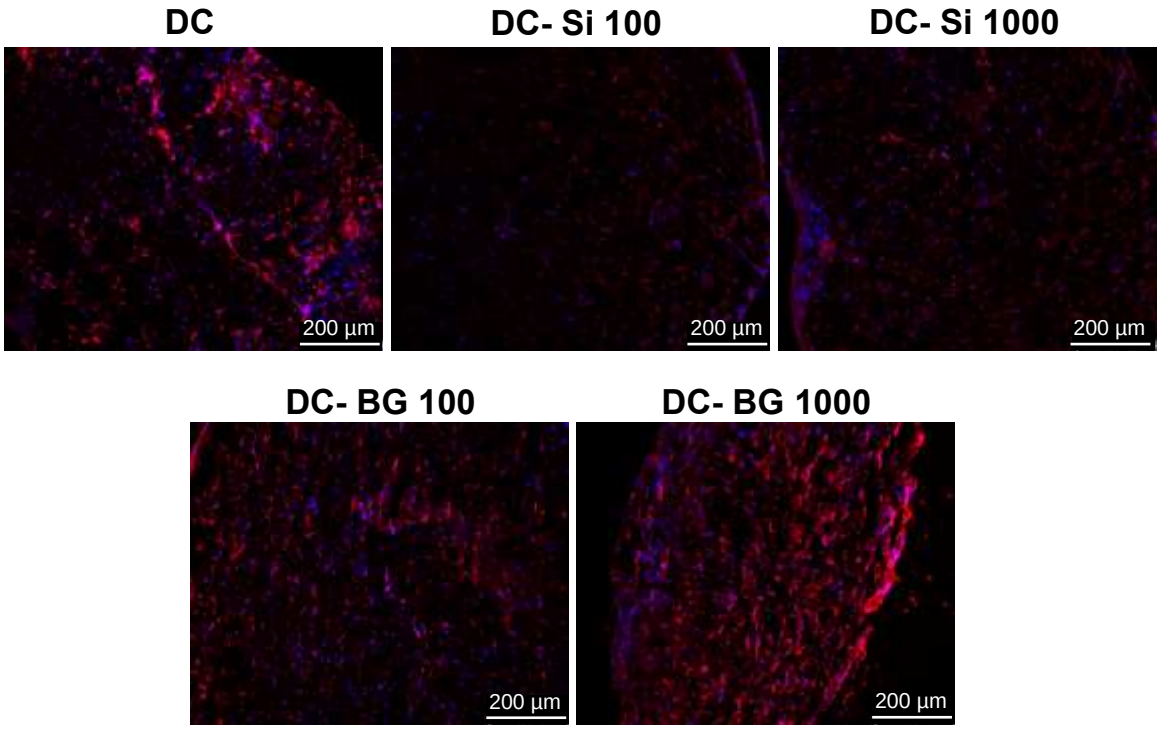

Figure IV.6: Immunofluorescence analysis of the nestin expression (red) in hDPSC-laden dense collagen gels on day 28 of culture without or with silica or bioglasses nanoparticles.

IV.3.5.2. SEM and EDS imaging analyses

SEM images of gels with and without particles revealed a similar, dense, and random collagen fibril network, suggesting that nanoparticle presence (at the studied concentrations) does not disrupt fibril formation (**Figure IV.7**). Bioactivity of acellular hybrid DC-Si and DC-BG gels was assessed on day 21, with only DC-BG gels exhibiting mineral formation, evidenced by mineral deposits along collagen fibrils (**Figure IV.7**). EDS analysis of deposited particles identified the presence of both calcium and phosphorus, indicating hydroxyapatite-like minerals (**Figure IV.8**).

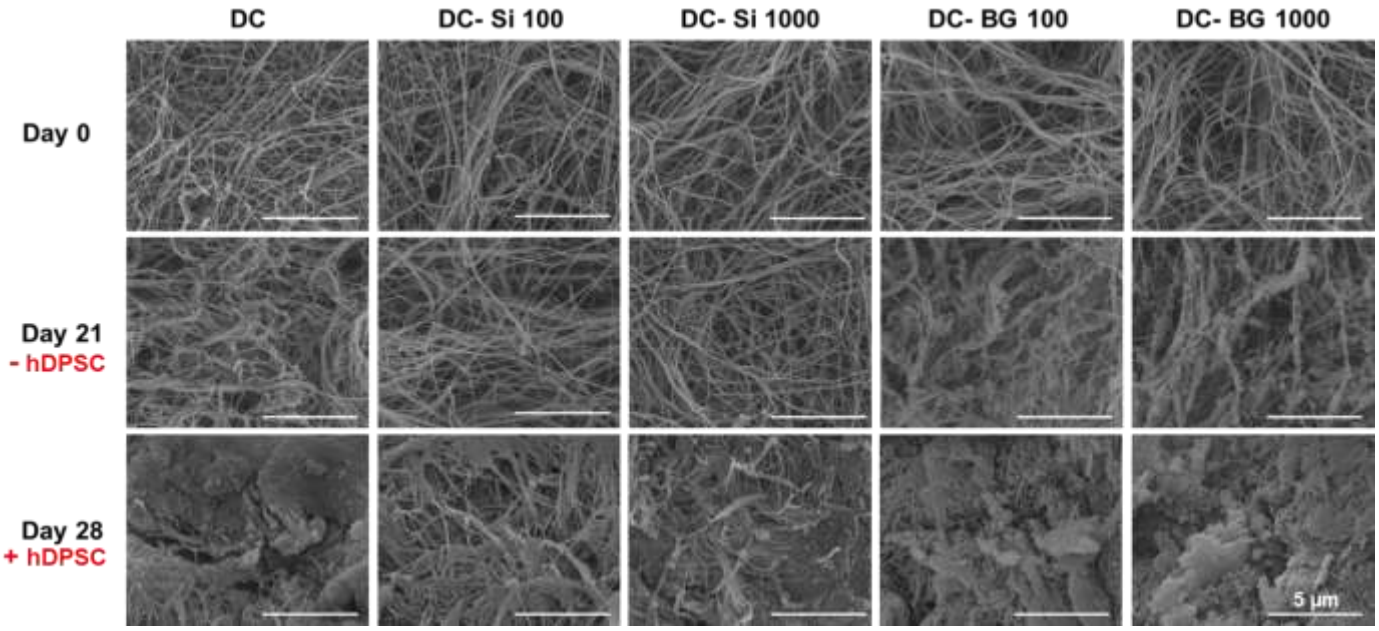

Figure IV.7: SEM images of dense collagen gels with and without silica or bioglass nanoparticles immediately after gel preparation (1st line), acellular dense collagen hydrogels with and without silica or bioglass nanoparticles on day 21 of culture in mineralizing medium (2nd line), and cellular dense collagen hydrogels with and without silica or bioglass nanoparticles on day 28 of culture (3rd line).

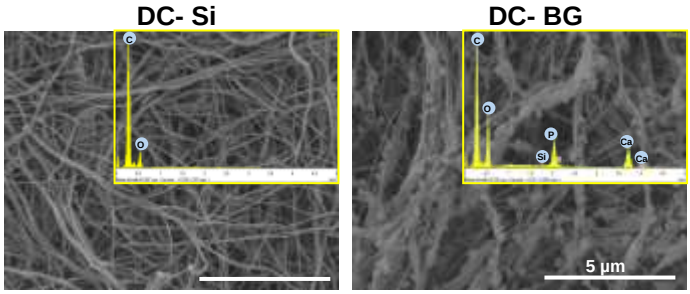

Figure IV.8: SEM micrographs of acellular DC-Si (left) and DC-BG (right) gels placed in mineralizing medium for 21 days and corresponding EDS analysis in inset.

Qualitative SEM evaluation of cellularized gels on day 28 showed matrix mineralization across all gel types, with mineral deposition observed in front of cells and along collagen fibrils, indicative of cell-mediated mineralization **(Figure IV.7**). However, mineral deposition in cell-seeded gels appeared qualitatively less pronounced compared to non-cell-seeded gels.

IV.3.5.3. ATR-FTIR

ATR-FTIR spectra of as-made DC scaffolds exhibited characteristic collagen triple helix signals via amide I, II, and III bands at 1643, 1550, and 1243 cm^{-1}, respectively. While the inclusion of 1000 µM bioactive glass in the gels showed slight indications of Si-O-Si groups on the spectra, other nanoparticle-containing conditions did not, likely due to their low concentrations in the gels (below the detection limit). On day 21, only spectra of acellular gels DC-BG (100 and 1000) revealed phosphate bands (between 1100 and 900 cm^{-1}), confirming mineral phase formation as observed by SEM. On the other hand, all cell-seeded gels, regardless of the presence of nanoparticles (silica or bioglass) in the gels, exhibited phosphate bands (between 1100 and 900 cm^{-1}) after 28 days of culture, albeit at lower intensity compared to acellular DC-BG on day 21. No noticeable difference in cell-mediated matrix mineralization was observed among the five groups, as the extent of phosphate band intensity was the same.

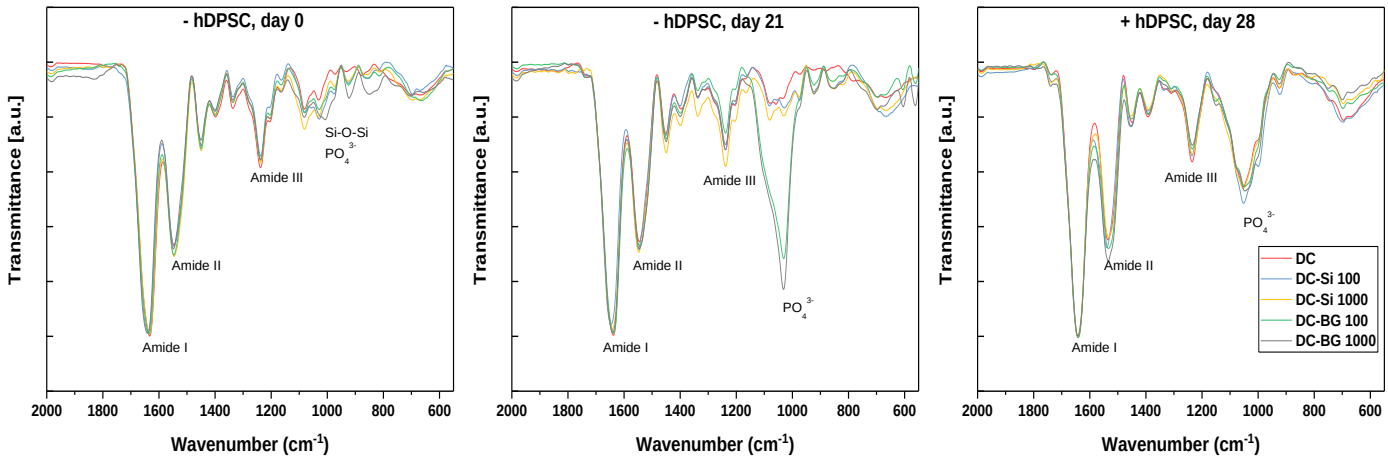

Figure IV.9: ATR-FTIR spectroscopy of dense collagen gels with and without silica or bioglass nanoparticles directly after gel preparation (left panel), acellular dense collagen gels with and without silica or bioglass nanoparticles after 21 days in mineralizing medium (middle), and cellularized dense collagen gels with and without silica or bioglass nanoparticles directly after 28 days in mineralizing medium (right).

IV.4. Discussion

In dentistry, silicon-based materials have shown great potential for dentin repair, although the specific impact of silicon on the stem cells of the dental pulp is still poorly understood. In the previous chapter, we had studied how the continuous addition of silicon at constant concentration could influence the viability and mineralization of human dental pulp stem cells (hDPSCs) within compressed 3D dense collagen hydrogels. However, in the clinical situation, silicon is released as the result of the dissolution of the applied biomaterial, which is in contact with the dental tissue. To mimic this situation, we have incorporated silicon-releasing particles within the collagen hydrogels. Two types of nanoparticles, silica and bioglass, were studied at concentrations of 100 and 1000 µM in the collagen gels.

Collagen self-assembly follows a nucleation/growth mechanism.[11] The nucleation or "lag" phase involves conformational changes in the protein and/or the formation of microfibrils from the initial triple helices, while the growth phase sees the assembly of collagen microfibrils and helices into fibrils. The subsequent association of these fibrils can lead to gel formation. This process is sensitive to pH, ionic strength, and additives. In the present study, silica-based NPs were added to the collagenous solution before gelation. However, the presence of nanoparticles had no clear impact on the collagen network, and fibers morphology was identical in all gel compositions, indicating that fibrillogenesis proceeded without hindrance. Indeed, NPs were introduced post-neutralization of the acidic collagen solution, i.e after the nucleation phase, and at very low concentrations. Previous research revealed that silica NPs can disrupt or even inhibit fibrillogenesis at higher concentrations (>1mM) if added before nucleation phase.[12] However, when added after nucleation, as in this study, no fibrillogenesis inhibition was observed, indicating that NPs can interact with triple helices but not with assembled fibrils. Similar findings were noted in the interaction between silica particles and another self-assembling protein, fibrin.[13]

The sol-gel method was employed for the preparation of silica and bioglass NPs, as this technique offers several advantages like their simplicity, reproducibility and effectiveness.[8,14,15] However, sol-gel derived particles are known to exhibit a rapid release of ions products upon exposure to liquid environments.[7,16] Such a release can lead to a sudden increase in pH levels in the surrounding area, potentially resulting in cell and tissue death. Here, the maximal silicon concentration of 100 µM was released by particles, which is considerably below a possible

toxic level (1mM).[10] Our findings showed that both types of NPs in the gels are cytocompatible towards hDPSCs within the dense collagen gels. Cells cultured in the presence of bioglass NPs exhibited a superior metabolic activity compared to pure silica, likely due to their bioactive properties that create a favorable microenvironment for cell attachment and proliferation.[5,7,17] On the other hand, it has been shown that silica NPs can be taken up by cells and, depending on their size, influence cellular functions.[18–20] For example, a study showed that 80 nm SiO_2 nanoparticles internalized by cells induced a significant loss of mitochondrial membrane integrity and a decrease in mitochondrial dehydrogenase activity compared to 500 nm nanoparticles.[21] Considering the central role of mitochondria in regulating cellular metabolism[22,23], these dysfunctions could be linked to the reduction in cellular metabolic activity observed in the early stages of our study.

The differences observed in cell distribution within the collagen matrix, as revealed by Masson's trichrome staining and SHG imaging coupled with confocal microscopy, provide valuable insights into the impact of nanoparticles on cellular behavior. First, cells clusters appeared both inside and outside DC while cells were mainly located at the edges of DC-Si 100 and DC-Si1000 gels. This suggests that silica nanoparticles may influence cell migration and distribution within collagen scaffolds, consistent with previous research showing that nanoparticles uptake by fibroblasts could impair their adhesion and migration.[21] Cell adhesion is well-known to regulate many cellular functions such as growth, migration, differentiation, survival and tissue organization, and its alteration can therefore have a negative impact on these functions.[24,25] The second hypothesis is that silicic acid released by the silica NPs chemically interacted with the collagen molecules during matrix remodelling, as proposed in the previous chapter. This interaction could have modified the matrix at certain points, thereby affecting cell adhesion to the gels. Interestingly, these results on cell distribution within collagen gels incorporating silica NPs and locally releasing silicic are in line with the previous chapter's findings using exogenous silicic acid supplementation. In the case of BG NPs, the cell distribution was dependent on their concentration, with DC-BG100 being similar to DC whereas DC-BG1000 showed a more homogeneous cell dispersion over the whole gel volume. Remembering that bioglasses release both silicic acid and calcium ions, one possible explanation is that the cell behavior results from the combination of the opposite effects of these two species: while silicic acid would hinder cell adhesion and favor cell clustering, the presence of calcium ions can promote hDPSCs proliferation and mineralization activity.

Regarding mineral deposition, the addition of bioglass in the acellular collagen gels led to the formation of hydroxyapatite. A fundamental characteristic of bioactive glasses is their ability to dissolve and re-precipitate in contact with physiological aqueous media. The presence of network-modifying oxides, such as alkali and alkaline-earth oxides, generates non-bridging oxygens that facilitate glass degradation in aqueous environments. This alters the chemical composition and pH, creating favorable conditions for the nucleation of calcium phosphates on the glass surface.[5,17,26] This unique characteristic of bioglass explains why, in the absence of cells, only hybrid gels containing BG underwent mineralization, regardless of their concentration in the gels.

In the presence of hDPSC, all gel groups were mineralized by the end of the culture time. Despite the bioactive nature of bioglass compared to silica, the extent of mineralization was similar across all groups. However, the distribution of mineral deposits matched/mirrored the observed distribution of cells in the gels. Mineral deposits were mainly located at the periphery of nanocomposite gels containing pure silica, while a more homogeneous distribution was observed in hybrid gels containing bioglass. This demonstrates that in hDPSC-seeded collagen gels, hybrid or not, mineralization is cell-mediated.

In contrast to this study, several studies in literature support the superior odonto/osteogenic potential of silica and bioglass NPs in various cell types and tissue engineering applications.[2,7] For instance, a study by Di Tinco *et al*. reported increased cell proliferation and odonto/osteogenic differentiation of hDPSC cells when cultured with BGs nanoparticles.[27] Some studies attributed these effects to the degradation of NPs, which release species such as $Si(OH)_4$ and Ca^{2+}, inducing a positive cellular response depending on ion concentration.[28–30] A systematic study[31] quantitatively compared the *in vitro* responses of cells to soluble BGs dissolution products, focusing on the concentration of Si and its effects on cellular outcomes such as metabolic activity, angiogenesis, and osteogenesis. The results indicated no significant differences in odontoblast/osteoblast differentiation markers (osteocalcin and ALP activity), biomineralization (using alizarin red) and VEGF production across varying Si levels. Similarly, there was no effect of Si on stem cell differentiation into osteogenic or angiogenic lineages.

While all cellularized gels showed similar levels of mineral deposition, ATR-FTIR analysis revealed a higher phosphate band peak in acellular DC-BG gels, suggesting that cell-free constructs may outperform cell-seeded ones in dental/bone mineralization. The same findings were observed in the study of Park *et al.*[32], where the acellular DC-BG collagen gel implanted

in critical-sized murine calvarial defect resulted in a greater bone volume than the cellular DC-BG collagen gel. This suggests that the bioactive properties of bioglass may be sufficient to promote mineralization, or that cells could interfere with the mineralization process facilitated by bioglass. Thus, it may not always be necessary to add cells to bioglass-containing scaffolds, as bioglass are intrinsically bioactive and can promote tissue regeneration.

IV.5. Conclusions

In summary, the impact of silica and bioglass nanoparticles on hDPSCs was investigated in this study. The results showed that both types of nanoparticles were not toxic and did not disrupt the metabolic activity of hDPSCs in dense collagen hydrogels at the studied concentrations. In the previous chapter, our results showed that silicic acid impacts collagen matrix remodeling. Here collagen organization did not change between conditions and we found no clear difference in cell-mediated matrix mineralization in the presence of silicon. But, similarly to the previous studies, we found that the cell organization within the gels was highly impacted by the presence of the nanoparticles. Strikingly, silica nanoparticles seemed to favor cell clustering at the surface of the gels, which would fit with our previous hypothesis that released silicic acid has a negative impact on the cell-matrix interactions. Noticeably, despite the low amount of calcium present in the bioglass particles, homogeneous cell dispersion could be obtained in their presence, suggesting that they are able to overcome the negative effect of silicic acid. To further understand these results, it is necessary to study the expression of genes related to mineralization and collagen matrix remodeling. PCR experiments are in due course to address this point.

This study highlights that the physical and chemical form from which silicon is released have a huge impact on its biological effect. Here, while concentrations of $Si(OH)_4$ present in the medium upon dissolution was comparable to the ones used in the previous chapter, the results we have gathered are clearly different. Therefore, whereas we have previously mentioned that more “biomimetic” gels must be used to better reproduce the *in vivo* processes, this chapter also suggest that using “real” biomaterials used by dentists as source of silicon, such as Biodentine, would also be interesting to study. In fact, during this PhD work, some preliminary attempts were made to prepare Biodentine/collagen composites but these could not be investigated further due to the lack of time. However, using more chemically-complex systems would make difficult to identify the specific role of Si. This is clearly illustrated here as the influence of calcium, even in small amounts, in the bioglass particles appears to prevail over the effect of silicon.

References

(1) Lührs, A.-K.; Geurtsen, W. The Application of Silicon and Silicates in Dentistry: A Review. In *Biosilica in Evolution, Morphogenesis, and Nanobiotechnology*; Müller, W. E. G., Grachev, M. A., Eds.; Progress in Molecular and Subcellular Biology; Springer Berlin Heidelberg: Berlin, Heidelberg, 2009; Vol. 47, pp 359–380. https://doi.org/10.1007/978-3-540-88552-8_16.

(2) Ha, S.-W.; Weitzmann, M. N.; Beck, G. R. Dental and Skeletal Applications of Silica-Based Nanomaterials. In *Nanobiomaterials in Clinical Dentistry*; Elsevier, 2013; pp 69–91. https://doi.org/10.1016/B978-1-4557-3127-5.00004-0.

(3) Yang, Y.; Zhang, M.; Song, H.; Yu, C. Silica-Based Nanoparticles for Biomedical Applications: From Nanocarriers to Biomodulators. *Acc. Chem. Res.* **2020**, *53* (8), 1545–1556. https://doi.org/10.1021/acs.accounts.0c00280.

(4) Huang, Y.; Li, P.; Zhao, R.; Zhao, L.; Liu, J.; Peng, S.; Fu, X.; Wang, X.; Luo, R.; Wang, R.; Zhang, Z. Silica Nanoparticles: Biomedical Applications and Toxicity. *Biomedicine & Pharmacotherapy* **2022**, *151*, 113053. https://doi.org/10.1016/j.biopha.2022.113053.

(5) Hench, L. L.; Xynos, I. D.; Polak, J. M. Bioactive Glasses for in Situ Tissue Regeneration. *Journal of Biomaterials Science, Polymer Edition* **2004**, *15* (4), 543–562. https://doi.org/10.1163/156856204323005352.

(6) Zych, Ł.; Osyczka, A. M.; Łacz, A.; Różycka, A.; Niemiec, W.; Rapacz-Kmita, A.; Dzierzkowska, E.; Stodolak-Zych, E. How Surface Properties of Silica Nanoparticles Influence Structural, Microstructural and Biological Properties of Polymer Nanocomposites. *Materials (Basel)* **2021**, *14* (4), 843. https://doi.org/10.3390/ma14040843.

(7) Rahaman, M. N.; Day, D. E.; Sonny Bal, B.; Fu, Q.; Jung, S. B.; Bonewald, L. F.; Tomsia, A. P. Bioactive Glass in Tissue Engineering. *Acta Biomaterialia* **2011**, *7* (6), 2355–2373. https://doi.org/10.1016/j.actbio.2011.03.016.

(8) Stöber, W.; Fink, A.; Bohn, E. Controlled Growth of Monodisperse Silica Spheres in the Micron Size Range. *Journal of Colloid and Interface Science* **1968**, *26* (1), 62–69. https://doi.org/10.1016/0021-9797(68)90272-5.

(9) Kesse, X.; Vichery, C.; Nedelec, J.-M. Deeper Insights into a Bioactive Glass Nanoparticle Synthesis Protocol To Control Its Morphology, Dispersibility, and

Composition. *ACS Omega* **2019**, *4* (3), 5768–5775. https://doi.org/10.1021/acsomega.8b03598.

(10) Murugadoss, S.; Lison, D.; Godderis, L.; Van Den Brule, S.; Mast, J.; Brassinne, F.; Sebaihi, N.; Hoet, P. H. Toxicology of Silica Nanoparticles: An Update. *Arch Toxicol* **2017**, *91* (9), 2967–3010. https://doi.org/10.1007/s00204-017-1993-y.

(11) Kadler, K. E.; Holmes, D. F.; Trotter, J. A.; Chapman, J. A. Collagen Fibril Formation. *Biochemical Journal* **1996**, *316* (1), 1–11. https://doi.org/10.1042/bj3160001.

(12) Eglin, D.; Shafran, K. L.; Livage, J.; Coradin, T.; Perry, C. C. Comparative Study of the Influence of Several Silica Precursors on Collagen Self-Assembly and of Collagen on 'Si' Speciation and Condensation. *J. Mater. Chem.* **2006**, *16* (43), 4220–4230. https://doi.org/10.1039/B606270A.

(13) Wang, K.; Albert, K.; Mosser, G.; Haye, B.; Percot, A.; Paris, C.; Peccate, C.; Trichet, L.; Coradin, T. Self-Assembly/Condensation Interplay in Nano-to-Microfibrillar Silicified Fibrin Hydrogels. *International Journal of Biological Macromolecules* **2020**, *164*, 1422–1431. https://doi.org/10.1016/j.ijbiomac.2020.07.220.

(14) Zhang, J. H.; Zhan, P.; Wang, Z. L.; Zhang, W. Y.; Ming, N. B. Preparation of Monodisperse Silica Particles with Controllable Size and Shape. *J. Mater. Res.* **2003**, *18* (3), 649–653. https://doi.org/10.1557/JMR.2003.0085.

(15) Green, D. L.; Lin, J. S.; Lam, Y.-F.; Hu, M. Z.-C.; Schaefer, D. W.; Harris, M. T. Size, Volume Fraction, and Nucleation of Stober Silica Nanoparticles. *Journal of Colloid and Interface Science* **2003**, *266* (2), 346–358. https://doi.org/10.1016/S0021-9797(03)00610-6.

(16) Siekkinen, M.; Karlström, O.; Hupa, L. Effect of Local Ion Concentrations on the in Vitro Reactions of Bioactive Glass 45S5 Particles. *Int J of Appl Glass Sci* **2022**, *13* (4), 695–707. https://doi.org/10.1111/ijag.16579.

(17) Henstock, J. R.; Canham, L. T.; Anderson, S. I. Silicon: The Evolution of Its Use in Biomaterials. *Acta Biomaterialia* **2015**, *11*, 17–26. https://doi.org/10.1016/j.actbio.2014.09.025.

(18) Ha, S.-W.; Viggeswarapu, M.; Habib, M. M.; Beck, G. R. Bioactive Effects of Silica Nanoparticles on Bone Cells Are Size, Surface, and Composition Dependent. *Acta Biomaterialia* **2018**, *82*, 184–196. https://doi.org/10.1016/j.actbio.2018.10.018.

(19) Xu, X.; Zhang, K.; Zhao, L.; Wang, D.; Bu, W.; Zheng, C.; Sun, H. Characteristics of Three Sizes of Silica Nanoparticles in the Osteoblastic Cell Line, MC3T3-E1. *RSC Adv.* **2014**, *4* (87), 46481–46487. https://doi.org/10.1039/C4RA06863G.

(20) Peters, K.; Unger, R. E.; Kirkpatrick, C. J.; Gatti, A. M.; Monari, E. Effects of Nano-Scaled Particles on Endothelial Cell Function in Vitro: Studies on Viability, Proliferation and Inflammation. *Journal of Materials Science: Materials in Medicine* **2004**, *15* (4), 321–325. https://doi.org/10.1023/B:JMSM.0000021095.36878.1b.

(21) Zhang, Y.; Hu, L.; Yu, D.; Gao, C. Influence of Silica Particle Internalization on Adhesion and Migration of Human Dermal Fibroblasts. *Biomaterials* **2010**, *31* (32), 8465–8474. https://doi.org/10.1016/j.biomaterials.2010.07.060.

(22) Vakifahmetoglu-Norberg, H.; Ouchida, A. T.; Norberg, E. The Role of Mitochondria in Metabolism and Cell Death. *Biochemical and Biophysical Research Communications* **2017**, *482* (3), 426–431. https://doi.org/10.1016/j.bbrc.2016.11.088.

(23) Spinelli, J. B.; Haigis, M. C. The Multifaceted Contributions of Mitochondria to Cellular Metabolism. *Nat Cell Biol* **2018**, *20* (7), 745–754. https://doi.org/10.1038/s41556-018-0124-1.

(24) Huang, S.; Ingber, D. E. The Structural and Mechanical Complexity of Cell-Growth Control. *Nat Cell Biol* **1999**, *1* (5), E131–E138. https://doi.org/10.1038/13043.

(25) Khalili, A.; Ahmad, M. A Review of Cell Adhesion Studies for Biomedical and Biological Applications. *IJMS* **2015**, *16* (8), 18149–18184. https://doi.org/10.3390/ijms160818149.

(26) Lao, J.; Nedelec, J.-M. Verres bioactifs. *Verres et céramiques* **2014**. https://doi.org/10.51257/a-v1-n4955.

(27) Di Tinco, R.; Sergi, R.; Bertani, G.; Pisciotta, A.; Bellucci, D.; Carnevale, G.; Cannillo, V.; Bertoni, L. Effects of a Novel Bioactive Glass Composition on Biological Properties of Human Dental Pulp Stem Cells. *Materials* **2020**, *13* (18), 4049. https://doi.org/10.3390/ma13184049.

(28) Hoppe, A.; Güldal, N. S.; Boccaccini, A. R. A Review of the Biological Response to Ionic Dissolution Products from Bioactive Glasses and Glass-Ceramics. *Biomaterials* **2011**, *32* (11), 2757–2774. https://doi.org/10.1016/j.biomaterials.2011.01.004.

(29) Li, H.-W.; Sun, J.-Y. Effects of Dicalcium Silicate Coating Ionic Dissolution Products on Human Mesenchymal Stem-Cell Proliferation and Osteogenic Differentiation. *J Int Med Res* **2011**, *39* (1), 112–128. https://doi.org/10.1177/147323001103900114.

(30) Xynos, I. D.; Edgar, A. J.; Buttery, L. D. K.; Hench, L. L.; Polak, J. M. Ionic Products of Bioactive Glass Dissolution Increase Proliferation of Human Osteoblasts and Induce Insulin-like Growth Factor II mRNA Expression and Protein Synthesis. *Biochemical and Biophysical Research Communications* **2000**, *276* (2), 461–465. https://doi.org/10.1006/bbrc.2000.3503.

(31) Turner, J.; Nandakumar, A.; Anilbhai, N.; Boccaccini, A. R.; Jones, J. R.; Jell, G. The Effect of Si Species Released from Bioactive Glasses on Cell Behaviour: A Quantitative Review. *Acta Biomaterialia* **2023**, *170*, 39–52. https://doi.org/10.1016/j.actbio.2023.09.012.

(32) Park, H.; Collignon, A.-M.; Lepry, W. C.; Ramirez-GarciaLuna, J. L.; Rosenzweig, D. H.; Chaussain, C.; Nazhat, S. N. Acellular Dense Collagen-S53P4 Bioactive Glass Hybrid Gel Scaffolds Form More Bone than Stem Cell Delivered Constructs. *Materials Science and Engineering: C* **2021**, *120*, 111743. https://doi.org/10.1016/j.msec.2020.111743.

General conclusions and perpectives

Understanding the biological role of silicon in dentin repair materials, particularly pulp capping materials, is essential for improving dental repair and/or regenerative treatments and optimising the biomaterials used to maintain pulp vitality and promote the formation of reparative dentin. As demonstrated in the first chapter devoted to the state of the art on the subject, silicon is suggested to be essential for the formation and repair of bone tissue, which is known to have similarities with dentin, particularly in terms of the composition of the extracellular matrix and the bone formation process. The initial steps in the development/formation of these mineralized tissue involve the synthesis of a fibrillar collagenous extracellular matrix by differentiated odonto/osteogenic cells, infiltrated with non-collagenous proteins and additional proteoglycans, thus providing a molecular environment to guide the mineralisation process. Reproducing such a three-dimensional (3D) extracellular matrix is therefore essential for studying cell differentiation in relation to matrix mineralisation, and plastic compression technique provides a valuable means of achieving this goal. In this context, using such cell culture models was appropriate for our project. Our objectives were multiple, starting with the preparation of a three-dimensional (3D) plastically-compressed collagen matrix and then examining the effects of silicon on dental pulp stem cells in this environment.

To achieve this, we focused on using physicochemical characterisation, molecular biology and histology techniques to study the fate of pulp stem cells in collagen matrices in the presence of silicon. This approach, which combines materials chemistry, biology and tissue engineering, has led to a better understanding of:

(1) The effects of different formulations of collagen hydrogels on their structure, fibrillar organisation and rheological properties,

(2) The viability, differentiation and mineralisation of pulp stem cells in the presence of silicon, and the factors governing them,

(3) Interactions of the collagen matrix with silicon in the presence or absence of cells.

In our first study, we tested different gel formulations to obtain stable gels suitable for plastic compression. Our results highlighted the sensitivity of collagen hydrogels to the small modifications of the preparation protocol, especially the initial acetic acid concentration of the collagen solution that not only dictates the pH and buffering capacity of the starting solution but also controls its initial ionic strength. The hydrogels produced using collagen molecules in a 500 mM acetic acid buffer demonstrated a lower degree of uniformity compared to those prepared at with a concentration of 20 mM, leading to their degradation during cell culture time. In addition, our findings demonstrate that the mineralizing potential of hDPSCs is influenced

by their initial density within the gel. Particularly, we observed a lack of mineral deposition at a cell density of 0.8 $M.mL^{-1}$, while a higher density of 2 $M.mL^{-1}$ resulted in successful mineralization. From a wider perspective, these results indicate that both collagen hydrogel preparation protocols and cell culture conditions dictate gel properties as well as mineralization success.

The next phase of our study focused on investigating the impact of silicon on dental pulp stem cells immobilized in dense collagen hydrogels. First, this was achieved by enriching the culture medium in which the cellularized gels were cultured with exogenous silicic acid. While previous research on the interactions between silicic acid and bone cells has shown either no or positive impact in terms osteoblastic differentiation, our findings indicate that there is no distinct effect on odontoblast differentiation at the genetic expression level. However, it is important to note that in this study, the presence of silicic acid at physiological levels did not affect the deposition minerals in the gels, in contrast to supraphysiological concentrations that hindered mineral deposition. Furthermore, when mineralization occurred in the presence of silicic acid, the mineral deposits were typically aggregated, similar to what was observed in the cellular organization within the collagen matrix. This brings forth significant inquiries regarding the biological function of silicon in hDPSCs, indicating that silicon may possibly interact with the extracellular matrix rather than the cells themselves. This interaction could potentially impede/impair the process of mineralization, with higher concentrations of silicon resulting in decreased mineralization.

The final aspect of this investigation focused on the impact of silicon-based particles, silica (SiO_2) and bioglass (SiO_2-CaO), on dental pulp stem cells when incorporated into a collagen matrix. Despite their similar sizes, these nanoparticles (NPs) were found to release varying concentrations of silicon into the culture medium. Notably, the behaviour of the cells in the gels was more influenced by the type of NPs rather than the amounts of particles in the gels or the concentrations of silicon released. The findings of this study demonstrate that the incorporation of SiO_2 in collagen gels resulted in cell clustering along the periphery of the gel. Furthermore, this clustering also coincided with a preferential deposition of minerals in these regions. As in the previous study, this suggests a potential interaction between silicon and the collagen matrix that may hinder matrix mineralization. In contrast, when bioglass NP were present in collagen gels, the distribution of both cells and mineral deposits was more uniform throughout the matrix. This may be attributed to the presence of calcium in the bioglass, which potentially

counteracted the adverse effects of silicon in the cellularized collagen gels, albeit at a low atomic mass percentage of 3%.

Regarding acellular gels, only the ones containing bioglasss exhibited mineralization, thus confirming their inherent bioactive nature. Conversely, there was no significant difference in mineralization between the different types of cellularized gels, irrespective of the presence of nanoparticles in the gels. All this suggests that mineralization in cellularized gels is mediated by the cells. The enhanced mineralization of acellular gels containing bioglass compared to their cellularized equivalents observed here raises the question of the value of adding cells to bioglass-containing constructs for the regeneration of mineralized tissue. Further investigation into the necessity of incorporating cells into such constructs could provide valuable insight into the most effective approach in both dental and bone tissue engineering.

In summary, this project successfully demonstrates the utility of utilizing plastically compressed collagen hydrogels, which replicate the 3D characteristics of the native dentin extracellular matrix, for investigating the effects of silicon on dental pulp stem cells within these matrices. This approach offers physiological relevance as it closely resembles the *in vivo* environment, compared to conventional 2D models frequently used in literature. However, our findings highlight that soluble silica supplied in its free form or released by silica-based nanoparticles primarily affects the extracellular matrix rather than the cellular functions, indicating that silicon may have minimal impact on these cells. This calls for the development of new matrices whose biochemical and cellular composition would be even closer to the native tissue.

Another important outcome of our work is that the additional presence of calcium, even at very low concentration, has a huge impact on the cell response to the presence of silicon when released from nanoparticles. In particular, it seems to mitigate the potential detrimental effects of silicic acid. The question is raised whether this is due to the combination of the effects of the two elements acting independently or if some interactions between calcium ions and silicic acid occur. More globally, these findings highlight the crucial role played by the physical and chemical properties of silicon in conjunction with other chemical elements/molecules in determining its biological effects. Thus, further investigations into clinically-used biomaterials such as Biodentine, typically employed for pulp capping, are warranted to gain a deeper understanding of the specific contributions of silicon to the process of dental tissue regeneration.

Finally, it is important to remember that this project was based on the reported enhanced repair ability of calcium silicates pulp capping materials compared to calcium salts. This led us to hypothesize that silicon could play a role and/or influence dental tissue mineralization, all the more as it was repeatedly shown to do so in bone mineralization. Our first results could question this hypothesis, or at least suggest that there is not direct interaction between silicon and dental stem cells. However, the effect of silicon on bone-derived stem cells has never been studied in dense collagen hydrogels. Therefore, it would be important to perform a series of systematic studies where both bone and dental pulp stem cells are exposed to silicon in the same conditions and, especially, matrices to address this intriguing question.

Abbreviations

ALP	Alkaline phosphatase
ANOVA	Analysis of variance
ATR -FTIR	Attenuated total reflectance- fourier transform infra-red spectroscopy
BG	Bioglass
BGLAP	Bone gamma-carboxyglutamate protein
BMD	Bone mineral density
BMP	Bone morphogenetic Protein
BSP	Bone sialoprotein
DEJ	Dentino-enamel junction
CFD	Collagen fibrillar density
Col1	Collagen type 1
CS	Calcium silicate
DC	Dense collagen
DMEM	Dulbecco's modified eagle medium
DMP1	Dentin matrix protein-1
DSPP	Dentin sialophosphoprotein
DSP	Dentin sialoprotein
ECM	Extracellular matrix
EDX	Energy-dispersive X-ray
FAK	Focal adhesion kinase
FGF	Fibroblast growth factor
ICP-AES	Inductively coupled plasma atomic emission spectrometry
GAG	Glycosaminoglycans
GAPDH	Glyceraldehyde 3-phosphate dehydrogenase
HAP	Hydroxyapatite
DPSC	Dental pulp stem cells
MEPE	Matrix extracellular phosphoglycoprotein
MIM	Mineralizing induction medium
MMP	Metalloproteinases
MSC	Mesenchymal stem cells
MTA	Mineral trioxide aggregate
NCPs	Non-collagenous proteins

NP	Nanoparticles
OCN	Osteocalcin
OPN	Osteopontin
PBS	Phosphate-buffered saline
PC	Plastic compression
qRT-PCR	Quantitative real time -polymerase chain reaction
RNA	Ribonucleid acid
PFA	Paraformaldehyde
SD	Standard deviation
SEM	Scanning electron microscopy
SHG	Second-harmonic generation
SiNP	Silica nanoparticle
SLRP	Small leucine-rich proteoglycans
SHED	Human exfoliated deciduous teeth stem cells
TEOS	Tetraethyl orthosilicate
TGF-β	Transforming growth factor-beta
TNF-α	Tumor necrosis factor-alpha
WDXRF	Wavelength-dispersive X-ray fluorescence
2D	Two dimensional
3D	Three dimensional

Résumé en français

Biomatériaux cellularisés pour l'étude de l'effet du silicium sur la régénération dentaire

I. Introduction

Le silicium est le deuxième élément le plus abondant sur terre après l'oxygène, et le troisième oligo-élément le plus abondant dans le corps humain. Plusieurs études ont démontré que le silicium est un oligo-élément essentiel pour les processus métaboliques associés au développement des os. Dès lors, le Si a été intégré dans la conception de nombreux biomatériaux pour la réparation/régénération des os. À cette fin, les bioverres sont l'un des matériaux les plus efficaces. Il a été démontré que le silicium contenu dans ces composés est bioactif et favorise la formation spontanée d'une couche biologiquement active de type apatite à leur surface. Des composés à base de silicium sont également fréquemment utilisés en odontologie pour la réparation dentaire. Ceux-ci sont principalement utilisés comme matériaux d'obturation dentaire, pour le traitement des caries et/ou comme matériau endodontique. La bioactivité de ces matériaux dentaires à base de silice ou de silicate de calcium est attribuée à leur capacité à libérer l'ion calcium pour former des précipités cristallins de type apatite au contact des fluides physiologiques contenant du phosphate. A ce jour, le silicium dans ces composés est considéré comme bio inerte dans le processus de minéralisation. Aucune étude n'a montré que le silicium pouvait avoir un impact sur la formation des tissus dentaires, en particulier l'émail et la dentine. Le rôle du silicium dans la formation des os ayant été identifié, la question est de savoir quel est son rôle dans la formation de la dentine.

Dans ce contexte, ce projet visait à préparer de nouveaux matériaux, combinant le collagène, la principale protéine de la pulpe et de la dentine, et des cellules souches de la pulpe dentaire, afin d'étudier le rôle du silicium sur la réparation des tissus dentaires.

II. Impact des conditions de fibrillogenèse et de la densité cellulaire sur la minéralisation des hydrogels de collagène plastiquement comprimés par les cellules souches de la pulpe dentaire humaine

Dans cette première partie, nous avons décidé d'étudier comment les conditions physico-chimiques et cellulaires pourraient impacter la minéralisation d'hydrogels denses obtenus par compression plastique (PC) par les cellules souches de la pulpe dentaire. L'objectif était double: (1) mieux comprendre le rôle des différents paramètres sur la structure du gel et sur la réponse cellulaire (2) identifier un protocole optimal pour la suite de notre étude.

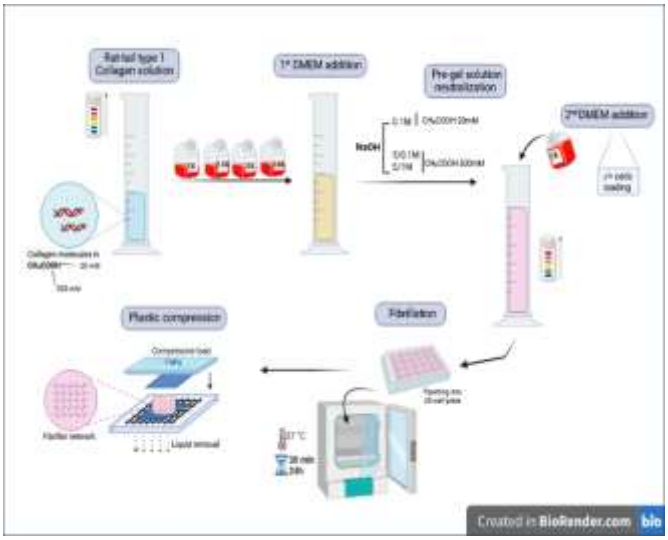

Figure 1. Protocole de préparation d'hydrogels denses de collagène par compression plastique

Dans un premier temps, certains paramètres clés du procédé PC (**Figure 1**) ont été sélectionnés et variés tout en maintenant les concentrations initiales et finales de collagène et le volume total constants. L'évaluation qualitative de l'influence de la concentration initiale d'acide acétique, du volume et de la concentration de DMEM, ainsi que de l'étape de neutralisation sur la formation et la compression du gel, a montré qu'une faible concentration de DMEM ou un volume de DMEM élevé conduisaient à des gels faibles. Ces conditions correspondent aux pH les plus élevés avant neutralisation. On peut suggérer que, dans ces situations où le pH est déjà élevé avant l'ajout de NaOH, de petites fibrilles de collagène se forment rapidement, conduisant à des réseaux lâches. En revanche, tous les gels jugés stables avant compression se forment pour un pH de pré-neutralisation de 3, c'est-à-dire lorsque les triples hélices de collagène ne s'auto-assemblent pas. Des analyses plus détaillées (SEM, rhéologie) des échantillons fournissent des informations supplémentaires (**Figure 2).** D'un point de vue structurel, les

différences en termes d'organisation fibrillaire fait ressortir la concentration initiale d'acide acétique comme un paramètre clé dans l'évolution de la fibrillogenèse. Cependant, une telle différence structurelle a eu peu d'impact sur les propriétés rhéologiques des hydrogels.

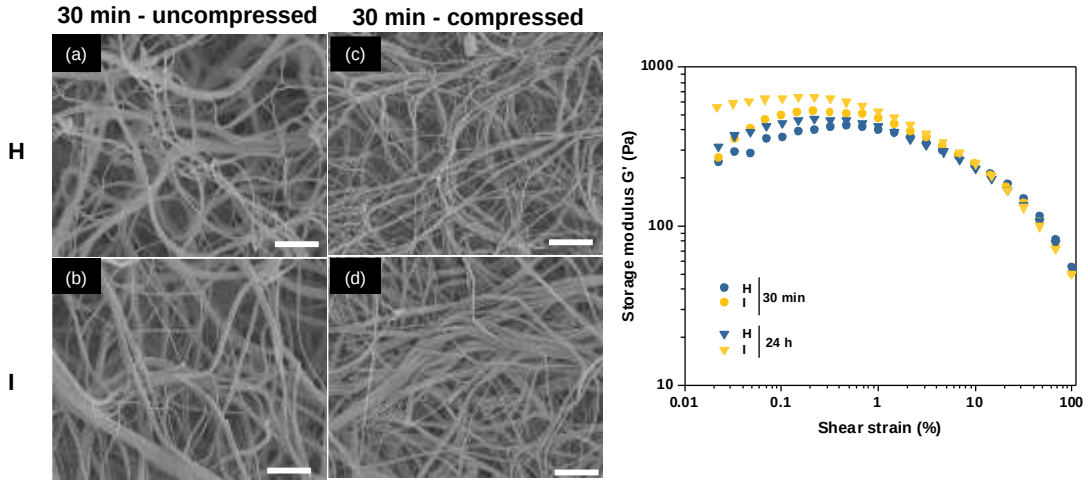

Figure 2. Etude par MEB et rhéologie de gels préparés à partir d'une solution d'acide acétique à 20 mM (H) et 500 mM (I).

Dans un deuxième temps, des cellules souches de la pulpe dentaire humaines, SHEDs et hDPSCs, ont été encapsulées dans les hydrogels. Nos conditions initiales étaient basées sur la littérature qui utilisait des SHED à une densité cellulaire de 150 000 cellules par mL. Dans nos expériences, aucune minéralisation significative n'a pu être observée. Afin d'obtenir la minéralisation, le type cellulaire et la densité cellulaire ont été modifiés. La présence de DPSCs à 0.8 M cellules.mL^{-1} n'a pas permis la détection de dépôts minéraux. En revanche, à 2 M cellules.mL^{-1}, la coloration histochimique, SEM/EDX et FTIR ont mis en évidence une minéralisation dans le gel (**Figure 3**). Dans le même temps, une telle augmentation de la densité cellulaire a également permis le contact cellule-cellule dans le gel, connu pour favoriser la différenciation et la minéralisation. Il est à noter que la densité cellulaire trouvée ici est comparable à celle utilisée lorsque les hydrogels de collagène PC ensemencés par DPSC favorisent efficacement la réparation des défauts critiques des os de la calvaria chez les rongeurs.

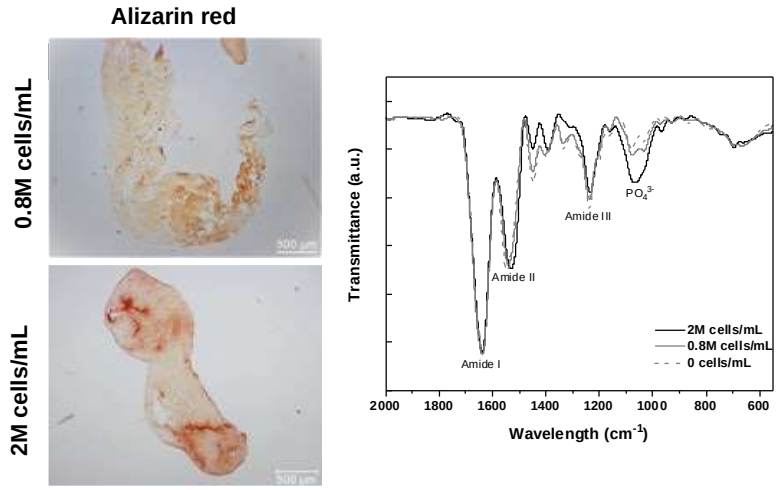

Figure 3. Effet de la densité cellulaire sur la minéralisation, étudiée par histologie et spectroscopie infra-rouge

Nous avons donc démontré que les propriétés des hydrogels de collagène densifiés par compression plastiques, y compris leur pertinence en tant qu'hôtes cellulaires, sont très sensibles à de petites modifications du protocole de préparation, notamment en termes de concentration en acide acétique de la solution de collagène et de quantité/concentration de milieu de culture cellulaire. De plus, nous avons souligné que le type et la densité cellulaires étaient essentiels pour parvenir à la minéralisation par les cellules souches pulpaires in vitro. Au total, cette première partie du projet a permis d'identifier les conditions pour obtenir des gels stables permettant la survie des hDPSC et une minéralisation efficace. Ces systèmes ont ensuite été utilisés pour étudier l'effet du silicium sur le comportement biologique des hDPSCs.

III. Effet du silicium soluble sur la minéralisation des hydrogels de collagène plastiquement comprimés par les cellules souches de la pulpe dentaire humaine

Le but de cette partie était d'identifier l'influence possible de l'acide silicique sur le comportement des cellules souches de la pulpe dentaire humaine et, en particulier, sur leur capacité de minéralisation en environnement de collagène dense 3D. Pour cette étude, nous avons sélectionné deux concentrations d'acide silicique, 10 μM (0,28 ppm), comparable à la concentration physiologique de $Si(OH)_4$, et 100 μM (2,8 ppm) pour vérifier l'influence possible du Si supraphysiologique.

L'étude de l'évolution de l'activité métabolique des cellules sur 3 semaines et l'évaluation de la viabilité cellulaire à la fin du temps de culture ont révélé que l'acide silicique n'a aucun effet toxique envers les hDPSC à ces concentrations et peut même être favorable à l'activité cellulaire

(**Figure 4**). Ceci est cohérent avec des études antérieures sur d'autres types de cellules montrant que, dans une telle plage de concentrations, le Si n'a généralement aucun effet sur l'activité métabolique cellulaire.

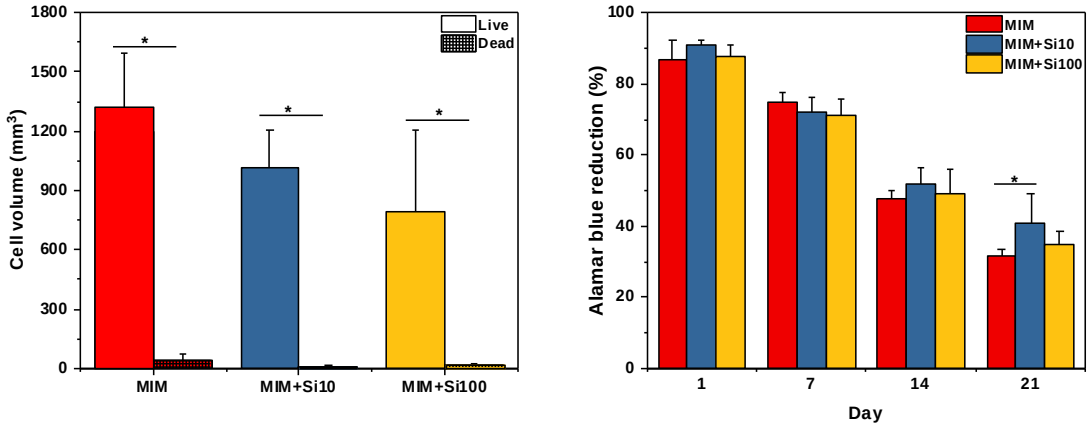

Figure 4. Influence de l'acide silicique à 10 et 100 mm sur la viabilité et l'activité cellulaire des hDPSCs

En ce qui concerne l'expression génique des protéines liées à la minéralisation, il n'y avait aucune différence significative à toutes les concentrations et à tous les moments. Cela suggère que le Si n'a qu'une influence mineure sur la différenciation odonto/ostéogénique des hDPSCs. Le SEM/EDS indique que la phase inorganique déposée a un rapport Ca/P similaire à la valeur attendue pour la dentine dans toutes les conditions, ce qui suggère que le Si n'a pas d'effet important sur la chimie de la formation d'hydroxyapatite. Cependant, les analyses histologiques ont révélé une différence dans l'étendue de la minéralisation, beaucoup plus faible pour la condition 100 μM Si par rapport aux deux autres (**Figure 5**). Ceci suggère que malgré une expression comparable de protéines liées à la minéralisation, et donc un stade de différenciation cellulaire similaire vers un phénotype ostéogénique, le processus de minéralisation est inhibé en présence d'une concentration non physiologique, bien que relativement faible, de Si.

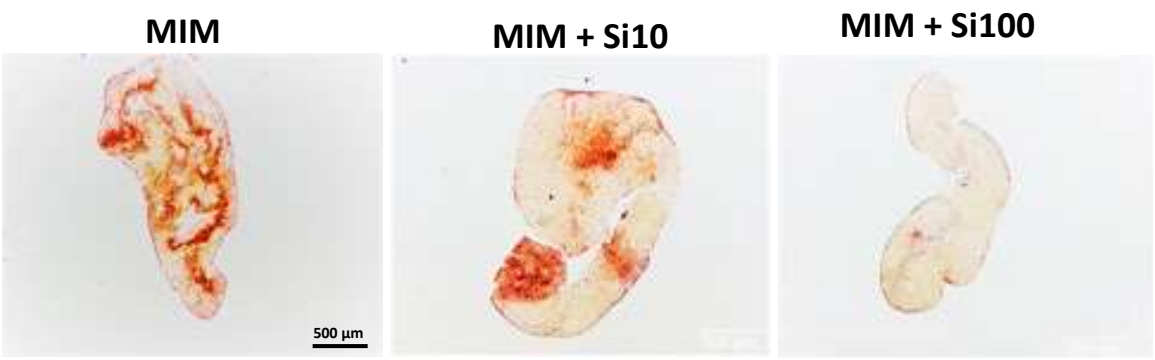

Figure 5. Influence de l'acide silicique à 10 et 100 mm sur la minéralisation d'hydrogels de collagène par les hDPSCs

L'une des principales différences entre les différents échantillons réside dans l'état de dispersion cellulaire au sein de la matrice de collagène (**Figure 6**). En effet, la présence de Si favorise le regroupement des cellules en clusters alors qu'en son absence, les hDPSC sont réparties de manière homogène au sein des gels. Parallèlement, le Si semble favoriser une organisation où les fibrilles de collagène sont plus alignées qu'en son absence. En outre, au cours de la différenciation, le niveau d'expression de Col1 a chuté dans toutes les conditions entre les jours 1 et 7, puis a augmenté pour atteindre sa valeur la plus élevée en l'absence de Si au jour 14, alors qu'il a continué à augmenter jusqu'au jour 21 en présence de Si. Il convient de noter que l'augmentation de l'expression de Col1 est parallèle à celle de MMP13, l'une des principales enzymes impliquées dans la dégradation du collagène. Prises ensemble, ces données suggèrent que la présence d'acide silicique dans le milieu de minéralisation retarde le remodelage matriciel par les hDPSC.

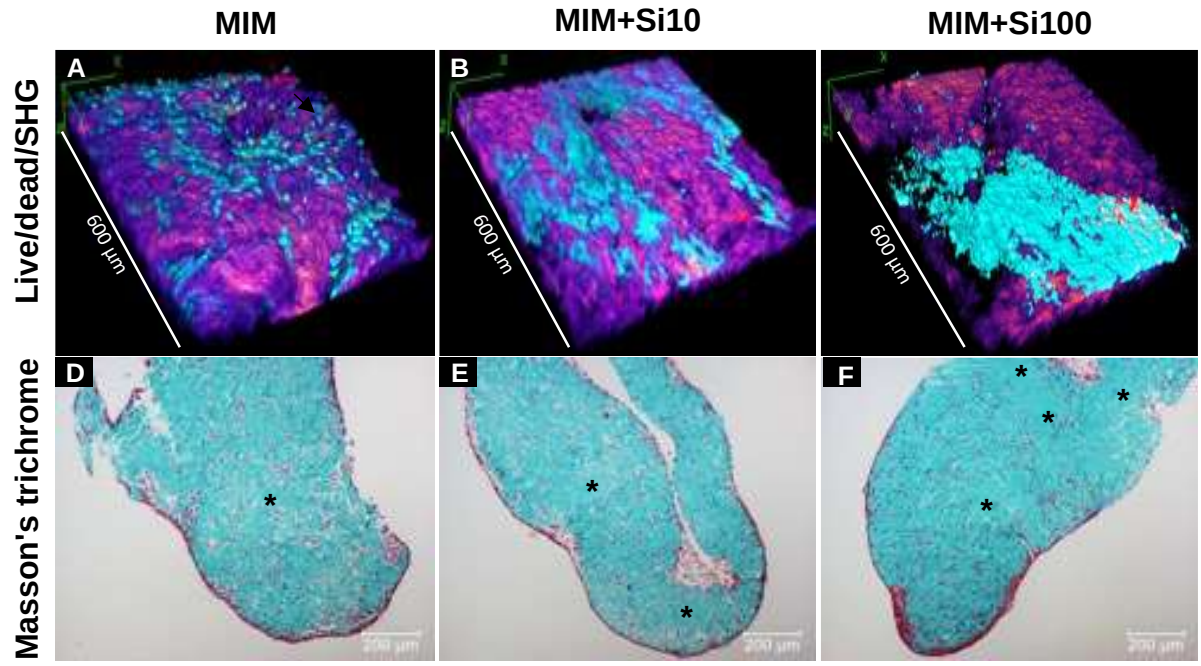

Figure 6. Effet de l'acide silicique sur la répartition des hDPSCs dans des matrices de collagène

Le regroupement cellulaire peut refléter une mobilité restreinte, due à une dégradation entravée de la matrice, une mauvaise adhésion et/ou un dépôt limité de collagène. Ceci est cohérent avec l'expression retardée observée de MMP13 et Col 1. Une faible minéralisation pourrait être en corrélation avec une expression retardée de MMP13. Alternativement, il a été récemment montré que le regroupement 3D peut orienter la différenciation des cellules précurseurs des ostéoblastes vers des cellules de type ostéocyte avec une activité de minéralisation plus faible. La question suivante est de savoir si ce remodelage altéré est dû à des interactions du Si avec les cellules ou à une modification des propriétés de la matrice conduisant à des interactions cellule-matrice défavorables. Il a été rapporté à plusieurs reprises que Si favorisait l'expression de Col1 et des protéines minéralisantes dans les cellules ostéogéniques, ce qui est en contradiction avec nos observations. Il a également été démontré que les nanoparticules de silice diminuaient l'expression de protéines impliquées dans l'adhésion cellulaire. La deuxième possibilité est que l'acide silicique établisse des interactions chimiques avec les molécules de collagène et/ou les fibrilles. Des interactions de $Si(OH)_4$ avec le collagène pourraient se produire lors du remodelage.

Très peu d'études similaires ont été réalisées avec des teneurs en silicium aussi faibles, principalement dans des environnements 2D et, à notre connaissance, une seule fois avec des hDPSC. Cette étude de Miyano et ses collègues a testé les effets d'une supplémentation en Si de 5 µM, 50 µM et 500 µM dans les milieux de culture sur les hDPSC. L'expression la plus

importante de l'ALP a été observée au jour 14 de la culture pour tous les groupes, avec l'expression la plus élevée à 5 µM de Si, mais aucune différence dans l'activité de l'ALP n'a été trouvée entre les groupes. Pendant ce temps, la coloration au rouge d'alizarine était plus importante avec 5 µM et 500 µM de Si qu'avec 50 µM de Si au jour 28. Ce dernier résultat est conforme au nôtre, où le dépôt minéral était plus prononcé pour la concentration la plus faible de 10 µM de Si que pour la concentration supraphysiologique. Si dose (100 µM).

Il est important de noter que, contrairement aux os, il n'existe jusqu'à présent aucune preuve d'un éventuel rôle physiologique du silicium dans la formation ou la réparation des tissus dentaires. Cela peut expliquer pourquoi notre étude révèle peu d'impact d'une concentration physiologique d'acide silicique sur les DPSC. En revanche, une concentration supraphysiologique peut résulter de la dissolution de biomatériaux, tels que les silicates de calcium, à proximité du tissu pulpaire et avoir un impact négatif sur la formation de dentine réactive. Nos résultats suggèrent que l'acide silicique libéré interagirait principalement avec la matrice extracellulaire plutôt qu'avec les cellules.

IV. Effet de nanomatériaux libérant de l'acide silicique sur la minéralisation des hydrogels de collagène plastiquement comprimés par les cellules souches de la pulpe dentaire humaine

Dans cette dernière partie, nous avons cherché à nous rapprocher de la situation thérapeutique dans laquelle le matériau délivrant de l'acide silicique est en contact avec les tissus. Pour cela nous avons élaboré des nanoparticules de silice et de bioverre que nous avons encapsulées dans les hydrogels de collagène à des concentrations de 100 mM et 1 mM. L'étude de leur solubilisation a montré un relargage de l'acide silicique sur 2 semaines, avec une concentration maximale de 100 mM au bout de 3 jours et une valeur seuil de 10 mm, en bon accord avec les expériences précédentes (**Figure 7**).

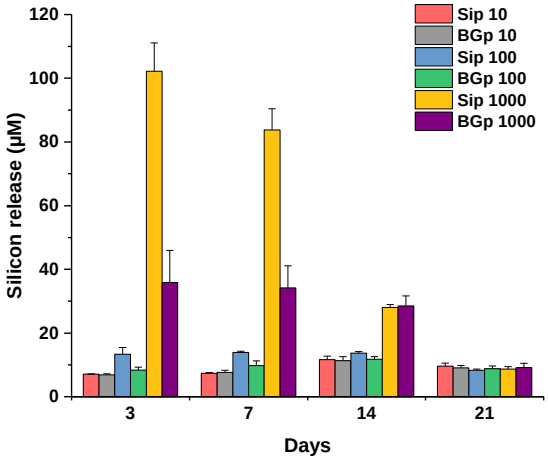

Figure 7. Cinétique de relargage du silicium par des nanoparticules de silice et de bioverres au sein d'hydrogels de collagène

Les études d'activité métaboliques ont montré l'absence de toxicité et même une amélioration en présence des particules de bioverre. L'analyse de la répartition des cellules a montré une grande hétérogénéité en présence des particules, avec la formation d'amas cellulaires locaux.

L'analyse de la minéralisation par histologie a montré le rôle favorable des bioverres. Dans le cas des particules de silice, une minéralisation importante a été notée mais elle semble concentrée à la surface des hydrogels.

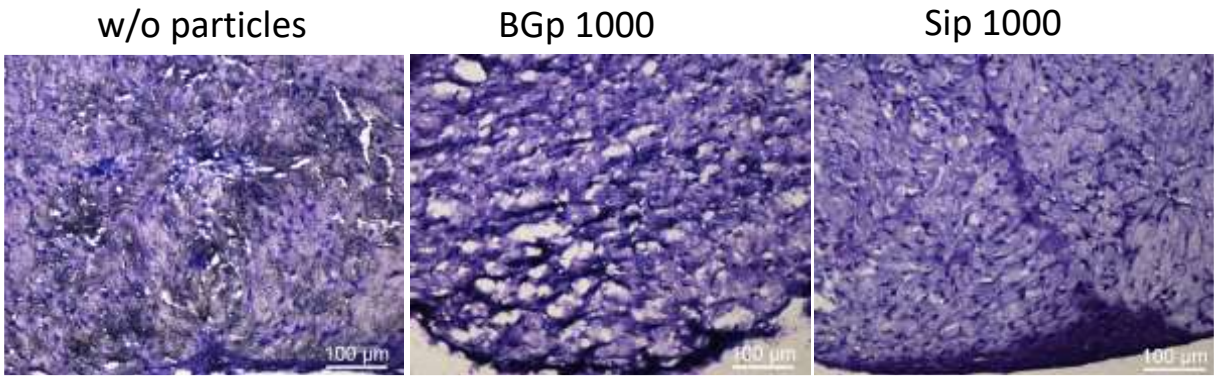

Figure 8. Minéralisation d'hydrogels de collagène par les DPSCs, sans, avec 1 mM de bioverre et 1 mM de silice

L'étude par MEB indique qu'en absence de cellules les nanoparticules de bioverres conduisent à la précipitation d'une nouvelle phase minérale. En présence de cellules, toutes les conditions permettent d'observer des dépôts minéraux. L'étude par FTIR confirme ce résultat et indique

qu'en absence de cellules, c'est principalement de la silice qui précipite alors qu'en présence de cellules, il y a formation de phosphates de calcium.

Ces premiers résultats suggèrent que la présence de nanoparticules, indépendamment de leur composition chimique, a un effet important sur le comportement cellulaire. Elle pourrait en particulier favoriser l'agrégation locale des hDPSCs. En outre, les deux types de particules mènent à une quantité de minéral déposé équivalente. Cependant, nous n'avons pas observé d'effet spécifique attribuable au silicium alors qu'une faible incorporation de calcium a un effet notable. Des études par RT-PCR devraient nous permettre de mieux comprendre ces observations.

V. Conclusions et perspectives

L'objectif de ce projet était d'évaluer l'effet du silicium, tel qu'il peut être relargué de matériaux comme les ciments utilisés pour le coiffage pulpaire, sur la minéralisation par les cellules souches de la pulpe dentaire. Nous avons d'abord cherché à mieux comprendre les paramètres importants pour obtenir des hydrogels de collagène denses qui pouvaient servir d'hôtes à ces cellules souches et favoriser leur minéralisation. Ces matériaux ont ensuite permis de tester l'effet du silicium soluble, l'acide silicique, sur les cellules souches. Nos résultats suggèrent que l'acide silicique, dans ces conditions, n'interagit pas directement avec les cellules mais plutôt avec la matrice qui, en retour, influence l'activité cellulaire. Enfin, en élaborant des nanocomposites capables de délivrer localement l'acide silicique, nous avons pu observer une forte hétérogénéité dans la répartition et la réponse des cellules, qui suggère à nouveau l'influence majeur de la structure du matériau sur le comportement cellulaire.

Cette forte dépendance de la réponse cellulaire à son environnement n'est pas inattendue mais n'a jamais été discutée dans le contexte de l'étude du rôle du silicium sur des cellules minéralisantes. Elle explique probablement que les effets rapportés dans la littérature divergent souvent en termes de dose réponse. Elle souligne aussi la nécessité d'améliorer le caractère « biomimétique » des modèles d'étude, et en particulier de la matrice de collagène. Cela inclus par exemple l'augmentation de la concentration ainsi que l'incorporation d'autres éléments de la matrice extracellulaire, qu'ils soient moléculaires (fibronectine, GAGs,..) ou cellulaires (fibroblastes, cellules endothéliales,...).

ABSTRACT

Silicon is present in low but non-negligible amounts in biological fluids and has been shown to be beneficial for bone formation. In parallel, many silica-based materials are used in bone repair. In sharp contrast, although silica-based materials are used in dentistry as pulp capping materials for dentin repair, very few studies to date have demonstrated that silicon can have an impact on dentin formation. In this context, the present project aims at preparing materials that allow for studying the role of silicon on dentin tissue formation. These materials combined collagen, the main protein in dentin, and human dental pulp stem cells.

In a first step, dense collagen hydrogels were prepared using plastic compression method, and fully characterized in terms of structure and mechanical properties. Then they were used as hosts for dental pulp stem cells to study the behaviour of the cells within the matrix. Results showed that this method was sensitive to small differences in protocol preparation and cell culture conditions. Successful mineralization was achieved with a cell density of 2 $M.mL^{-1}$ within the gels. In a second step, we analyzed the effects of soluble silicon (silicic acid) on dental pulp stem cells in the collagenous matrix. Our results revealed that silicic acid at supraphysiological doses (100 µM), although subtoxic (< 1mM), reduce mineral formation.

Finally, nanocomposites hydrogels combining collagen and silicon-releasing nanoparticles (silica and bioglasses) were prepared. As in the 2^{nd} step, the impact these silica-based nanoparticles on the dental pulp stem cells was assessed. Our findings showed that the extent of mineral deposition was comparable in all gels. While cell distribution and mineral deposition in the matrix with silica nanoparticles were not uniform, gels containing bioglasses showed homogeneous cell distribution and mineralization. A proposed mechanism is that silicon interacts with collagenous matrix, rather than cells themselves, and this may be detrimental to the cell mineralization function. These results offer valuable insight into the biological importance of silicon in dental applications and may contribute to the improvement of these materials as part of mineralized tissue engineering strategies.

Keywords: silicon, collagen hydrogels, human dental pulp stem cells, dentin repair/regeneration

RESUME

Le silicium est présent en quantités faibles mais non négligeables dans les fluides biologiques et il a été démontré qu'il était bénéfique pour la formation des os. Parallèlement, de nombreux matériaux à base de silice sont utilisés dans la réparation osseuse. En revanche, bien que les matériaux à base de silice soient utilisés en dentisterie comme matériaux de coiffage pulpaire pour la réparation de la dentine, très peu d'études ont démontré jusqu'à présent que le silicium peut avoir un impact sur la formation de la dentine. Dans ce contexte, le présent projet vise à préparer des matériaux qui permettent d'étudier le rôle du silicium sur la formation de la dentine. Ces matériaux combinent le collagène, la principale protéine de la dentine, et les cellules souches de la pulpe dentaire humaine.

Dans un premier temps, des hydrogels de collagène denses ont été préparés par compression plastique et entièrement caractérisés en termes de structure et de propriétés mécaniques. Ils ont ensuite été utilisés comme hôtes pour les cellules souches de la pulpe dentaire afin d' étudier le comportement des cellules dans la matrice. Les résultats ont montré que cette méthode était sensible à de petites variations du protocole de préparation et des conditions de culture cellulaire. Une minéralisation effective a été obtenue avec une densité cellulaire de 2 $M.mL^{-1}$ dans les gels. Dans un deuxième temps, nous avons analysé les effets du silicium soluble (acide silicique) sur les cellules souches de la pulpe dentaire dans la matrice collagénique. Nos résultats ont révélé que l'acide silicique à des doses supraphysiologiques (100 µM), bien que subtoxiques (< 1mM), réduit la formation minérale.

Enfin, des hydrogels nanocomposites associant collagène et nanoparticules (silice et bioverres) relarguant du silicium ont été préparés. Comme dans l'étape 2, l'impact de ces nanoparticules sur les cellules souches de la pulpe dentaire a été évalué. Nos résultats ont montré un dépôt minéral comparable dans tous les gels. Alors que la distribution des cellules et le dépôt minéral dans la matrice contenant des nanoparticules de silice n'étaient pas uniformes, les gels contenant des bioverres présentaient une distribution cellulaire et une minéralisation homogènes. L'un des mécanismes proposés est que le silicium interagit avec la matrice de collagène, plutôt qu'avec les cellules, ce qui peut entraver la fonction minéralisatrice des cellules. Ces résultats offrent un aperçu précieux de la place biologique du silicium dans les applications dentaires et peuvent contribuer à l' amélioration de ces matériaux dans le cadre de l'ingénierie des tissus minéralisés.

Mots clés: silicium, hydrogels de collagène, cellules souches de la pulpe dentaire humaine, réparation/régénération de la dentine